LNCIS
Lecture Notes in Control and Information Sciences
284

Mikael Johansson

Piecewise Linear Control Systems

Springer

Lecture Notes
in Control and Information Sciences 284

Editors: M. Thoma · M. Morari

Springer

Berlin
Heidelberg
New York
Hong Kong
London
Milan
Paris
Tokyo

Mikael Johansson

Piecewise Linear Control Systems

A Computational Approach

With 69 Figures

Springer

Author

Dr. Mikael Johansson
Information Systems Laboratory
Packard Building 243
94305 Stanford, CA
USA

Cataloging-in-Publication Data applied for
Die Deutsche Bibliothek – CIP-Einheitsaufnahme
Piecewise linear control systems / Mikael Johansson. - Berlin ; Heidelberg ; New York ; Hong Kong ; London ; Milan ; Paris ; Tokyo : Springer, 2003

(Lecture notes in control and information sciences ; 284)
(Engineering online library)
ISBN 3-540-44124-7

ISBN 3-540-44124-7 Springer-Verlag Berlin Heidelberg New York

Springer-Verlag Berlin Heidelberg New York
a member of BertelsmannSpringer Science + Business Media GmbH

http://www.springer.de

Typesetting: Digital data supplied by author. Data-conversion by PTP-Berlin, Stefan Sossna e.K.
Cover-Design: design & production GmbH, Heidelberg
Printed on acid-free paper SPIN 10890960 62/3020Rw - 5 4 3 2 1 0

To Laurence and Axel

Acknowledgments

This book is an extended version of my PhD thesis from Lund Institute of Technology, which was written in the spring of 1999. My thesis advisors were Anders Rantzer and Karl-Erik Årzén and significant parts of this book is based on joint work with them. In addition, Andrey Ghulchak and Karl Johan Åström had a strong influence on the organization and content of the thesis. Its a pleasure and honor to acknowledge their contributions.

I am also grateful to Anders Rantzer for suggesting me to transform the thesis into this book, to Stephen Boyd for enthusiastically encouraging me to do so, and to Laurent El Ghaoui for keenly supporting this project and providing the funding that made it happen.

Several people have read and commented parts of this manuscript. In particular, Karl-Henrik Johansson, Haitham Hindi and Lin Xiao provided many constructive comments on a late draft that greatly enhanced the quality of this book. All the remaining errors are now, I fear, my own.

Berkeley, California, May 30, 2002 MIKAEL JOHANSSON

Financial Support

The work resulting in this book has been funded by a number of sources over the years. The support from National Science Foundation under contract ECS-9983874, the Swedish Foundation for International Cooperation in Research and Higher Education, the Blanceflor Foundation, Volvo, ABB and the Institute of Applied Mathematics (ITM), the Swedish Research Council for Engineering Sciences (TFR) under grant 95-759 and the Esprit LTR project FAMIMO is gratefully acknowledged.

Contents

1

Introduction

Computer control systems are becoming an increasingly competitive factor in a wide range of industries. Many products now achieve their competitive edge due to the complex functionality provided in algorithms and software. As more and more product value is invested in software, there is a strong desire to formally verify its correctness. System analysis, which many engineers may previously have regarded as an academic exercise, is becoming instrumental for coping with complexity and guaranteeing correctness of advanced software. At the same time, increased performance demands over wide operating ranges force control engineers to move from linear to nonlinear controllers, for which linear analysis techniques often fail.

Competition also forces faster and more effective product development. Today, more and more control designs are based on mathematical process models, and their performance is thoroughly tested in simulations before full-scale trials. This reduces expensive and time-consuming experimentation and tuning on prototype products. Working with mathematical models, however, always involves uncertainty: there is always a mismatch between what is predicted by mathematical models and what can be observed in reality. It then becomes important to account for uncertainty in the analysis, in order to grant that the results are valid also in reality.

The amazing advances in computer technology have made high performance computers broadly available. Toaday's control engineers are skilled users of advanced software, and most control designs are today performed using sophisticated CAD tools. This makes it very attractive to develop analysis and design methods that are based on numerical computations.

This book presents a computational approach for analysis of nonlinear and uncertain systems. We focus on systems with piecewise linear dynamics and extend some aspects of the celebrated theory for linear systems and quadratic criteria to piecewise linear systems and piecewise quadratic criteria. The analysis tools are easily accessible (as user-friendly computer programs) and computationally efficient (relying on convex optimization).

M. Johansson: Piecewise Linear Control Systems, LNCIS 284, pp. 1-8, 2003.

Piecewise Linear Systems

In this book, we consider piecewise linear systems on the form

$$\dot{x} = A_i x + a_i \qquad \text{for } x \in X_i.$$

Here $\{X_i\}$ is a partition of the state space into operating regimes. The dynamics in each region is described by a system of linear (or, rather, affine) differential equations. Piecewise linear systems have a wide applicability in a range of engineering sciences. Some of the most common nonlinear components encountered in control systems, such as relays and saturations, are piecewise linear. Switches also occur naturally, *e.g.*, when a plant operates in different modes or under physical constraints. Diodes and transistors, key components in even the simplest electronic circuits, are naturally modeled as piecewise linear. Many advanced controllers, notably gain-scheduled flight control systems, are based on piecewise linear ideas. The construction of a globally valid nonlinear model from locally valid linearizations is easy to understand and widely accepted among engineers.

Some of the first investigations of piecewise linear systems in the control literature can be traced back to Andronov who used tools from Poincaré to investigate oscillations in nonlinear systems [3]. The practical benefits of moving from linear to piecewise linear servomechanisms were also noticed early on [184]. An interesting early attempt to develop a qualitative understanding of piecewise linear systems were made by Kalman [111]. He considered a saturated system as a series of polyhedral regions in the state space, separated by switching boundaries (this is also the view of piecewise linear systems that we will adopt in this book). By identifying the singular points of the dynamics in the different regions he could then make qualitative statements about the global dynamics. It would take several decades before these ideas were refined and developed into more complete analysis tools. In the meantime, developments on piecewise linear systems appeared almost exclusively as work on linear systems interconnected with static nonlinearities such as relays, saturations and friction. Since these systems turned out to be very challenging to analyze, these directions have remained very active areas of research. Many theoretical results with broad applications, such as the work on optimal control [58] absolute stability [164], and differential equations with discontinuous right-hand sides [57], have their roots in this research.

It is fair to say that it was the circuit theory community that first recognized piecewise linear systems as an interesting system class in its own right. Driven by the need for efficient simulation and analysis of large-scale circuits with diodes and other piecewise linear elements, a considerable research effort has focused on efficient representation of piecewise linear systems [42, 198, 107]. The research has focused almost exclusively on static problems, while analysis of the more complicated dynamical behaviors has remained largely unattended.

Triggered by the recent increase in the use of switched and hybrid controllers, two conceptually different approaches to analysis of general piecewise linear dynamical systems have emerged. For discrete-time dynamics, Sontag has proposed to exploit properties of affine mappings and polyhedral sets to formulate decision procedures for answering basic analysis questions, see [191]. This approach captures some unique features of discrete-time piecewise linear systems but is computationally demanding to implement in practice (see the work by Kantner [113] who used similar techniques for set-valued simulation of piecewise linear systems). For piecewise linear systems with continuous-time dynamics, Pettit has developed a qualitative analysis method based on vector field considerations [159]. The approach can be seen as a multidimensional extension of phase portrait techniques and gives a qualitative picture of the overall dynamics, indicating sliding modes, probable limit cycles, and instabilities. More recently, Jirstrand [92] and Einarsson [51] have developed alternative analysis methods that combine local analysis of the systems dynamics within the operating region with graph-theoretic ideas to describe the global dynamics.

This book focuses on *quantitative* analysis of piecewise linear dynamic systems. Stability and gain computations are typical examples. Up until very recently, such results existed almost exclusively for particular classes of piecewise linear systems (such as linear systems with saturation). The research presented in this book has its roots in computational Lyapunov theory, which we will describe next.

Computational Analysis of Dynamical Systems

Stability analysis of dynamical systems was pioneered by Lyapunov [133, 134]. The intuition behind his results came from energy considerations: if every motion of a system has the property that its energy decreases with time, the system must come to rest irrespectively of its initial state. To make the argument more rigorous, Lyapunov required that the energy measure $V(x(t))$ of a motion $x(t)$ should be proper in the sense that $V(0) = 0$,

$$V(x) > 0 \qquad \forall x \neq 0$$

and $V(x) \to \infty$ as $\|x\| \to \infty$. The requirement that V should be decreasing along all trajectories of the system $\dot{x} = f(x)$ takes the form

$$\dot{V}(x) = \frac{\partial V(x)}{\partial x} f(x) < 0 \qquad \forall x \neq 0.$$

These are the well-known Lyapunov conditions for asymptotic stability. A function $V(x)$ that satisfies these conditions is called a Lyapunov function for the system, and can be seen as an abstract measure of the system energy. Physical insight may sometimes hint at the appropriate energy function, but in most cases the choice is far from obvious. To this day, the main obstacle in the use of Lyapunov's method is the nontrivial step of finding an appropriate Lyapunov function.

In essence, Lyapunov function construction is only simple for linear systems. Already Lyapunov showed that a linear system is asymptotically stable if and only if it admits a quadratic Lyapunov function $V(x) = x^T Px$. The conditions that such a function be proper and decreasing along all motions of a continuous-time linear system $\dot{x} = Ax$ lead to the well-known Lyapunov inequalities

$$P > 0, \qquad\qquad A^T P + PA < 0.$$

With today's terminology, we would say that these conditions are linear matrix inequalities (LMIs) in P. Since the inequalities admit an explicit solution, this view was not be adopted until almost a century later. Indeed, by picking an arbitrary positive definite matrix Q, stability can be assessed from the solution P to the system of linear equalities

$$A^T P + PA = -Q.$$

The system is asymptotically stable if and only if P is positive definite.

Encouraged by these results, several researchers tried to find results of similar elegance for nonlinear systems. In particular, much research was focused on the absolute stability problem which considers a linear system interconnected with a static memoryless nonlinearity. The absolute stability problem nurtured several important theoretical developments. Two beautiful examples are the circle criteria [215] and the Popov criteria [163]. These results give frequency domain conditions on the transfer function of the linear system that are sufficient for existence of certain Lyapunov functions for the interconnection. Such frequency domain criteria give valuable insight and were particularly important before the computer era, since they allowed for simple geometrical verification rather than solving difficult matrix inequalities in the time domain.

Automatic control went through a drastic change in the 1960's with the advent of state space theory. The development was fueled by demanding applications (the space race), new technology (computers), and a strong influence of mathematics. This led to the development of optimal control, where the merit of a control law is often expressed as some integral criteria

$$\int_0^\infty L(x(t), u(t))\, dt.$$

Bellman [13] showed that controls u for the system $\dot{x} = f(x,u)$ that are optimal with respect to the above criterion can be characterized in terms of solutions V to the Hamilton-Jacobi-Bellman equation

$$\inf_u \left(\frac{\partial V(x)}{\partial x} f(x) + L(x,u) \right) = 0.$$

Notice that for the optimal solutions we have $\dot{V} = -L(x,u)$ which is typically negative. Hence $V(x)$ may serve as a Lyapunov function for the closed loop system. However, the Hamilton-Jacobi-Bellman equation is notoriously hard to solve in general. Many numerical methods have been devised for the solution of optimal control problems but they tend to suffer from combinatorial explosion. This limits practical applications of optimal control theory to systems of low state dimension or to the optimization of trajectories rather than feedback laws.

An important exception is the combination of linear systems and quadratic criteria. In this case, the dynamics is on the form $\dot{x} = Ax + Bu$, and the criterion takes the form

$$\int_0^\infty x^T Q x + 2u^T C x + u^T R u \, dt.$$

The first solution to this problem was due to Kalman [112] who showed that the optimal controller is a linear state feedback. In the early 1970's, Willems gave several equivalent characterizations of the optimal solution [211]. One of these characterizations is that there exists a symmetric matrix $P = P^T$ that satisfies the linear matrix inequality condition

$$\begin{bmatrix} A^T P + PA + Q & PB + C^T \\ B^T P + C & R \end{bmatrix} \geq 0.$$

However, the numerical methods at hand made it more attractive to consider an alternative characterization in terms of an algebraic matrix equation which could be solved using numerical linear algebra. Willems also showed that many other questions involving quadratic criteria, such as computations of induced gains, can be characterized by Lyapunov-like functions (called storage functions) [212]. For linear systems the existence conditions for such functions take the form of linear matrix inequalities.

A decade later, numerical methods for convex optimization started to get widely available. In their 1982 study of the absolute stability problem (now extended to multiple nonlinearities) Pyatnitskii and Skorodinskii derived a solution in terms of LMIs and gave a numerical algorithm that is guaranteed to find a solution when it exists [166].

The early methods for convex optimization had high complexity. A breakthrough came in 1984 when Karmarkar proposed an interior point method for linear programming [114]. This method had polynomial complexity and worked well in practice. The method was later extended to general convex programming by Nesterov and Nemirovski [146]. Promoted by efficient software [62, 214, 206], strong theoretical developments and excellent tutorial texts [27, 180], researchers have started to accept a linear matrix inequality condition as a solution of similar value to an analytical result. Moreover, linear matrix inequalities have turned out to be convenient for the formulation of a wide range of important control problems and the interest in these methods has soared.

Since the mid-90's, there has been a strong activity in trying to extend computational results for linear uncertain systems to piecewise linear and hybrid systems using non-quadratic Lyapunov functions (see, *e.g.*, [190, 97, 158, 71, 67]). The combined effort of a large number of researchers has now produced a relatively complete set of analysis tools for general piecewise linear systems. A key contribution in this book is to show how the search for *piecewise quadratic Lyapunov functions*

$$V(x) = \begin{bmatrix} x \\ 1 \end{bmatrix}^T \bar{P}_i \begin{bmatrix} x \\ 1 \end{bmatrix} \qquad \text{for } x \in X_i$$

for piecewise linear systems can be cast as a convex optimization problem in terms of linear matrix inequalities. Based on this result, we extend some aspects of the successful theory of linear systems and quadratic constraints to *piecewise linear systems* and *piecewise quadratic constraints*. We describe numerical procedures for assessing stability, computing induced gains and solving optimal control problems for piecewise linear systems. These developments enable analysis of a large and practically important class of control systems that are not easily dealt with using other techniques. The analysis tools are easily accessible (as user-friendly computer programs [77]) and computationally efficient (relying on convex optimization).

Philosophy of this Book

The class of piecewise linear systems studied in this book have nonlinear (possibly discontinuous) dynamics and allow switching rules that incorporate memory and logic. These systems may exhibit astonishingly complex behaviors (including limit cycles, multiple equilibrium points, chaos, etc.) and an exact analysis of piecewise linear systems should be expected to be hard. In fact, it has been shown that even the problem of establishing stability for very simple piecewise linear systems (such as linear systems with saturated feedback) is undecidable, see [26].

In light of such results, we cannot hope to find a computationally efficient (polynomial-time) method for stability analysis of piecewise linear systems that is guaranteed to work for all problem instances. Rather, the aim of this book is to develop analysis methods that are computationally efficient, work for *most* practical problems, and produce guaranteed results (when they work). The methods are based on searching for Lyapunov function in a fixed, yet flexible, finite-dimensional Lyapunov function class. The search is formulated as a convex optimization problem that can be solved globally and efficiently using a wide variety of publically available software. If the optimization problem is feasible it returns a Lyapunov function that *guarantees* a certain system performance. If the optimization problem is infeasible, on the other hand, our methods are inconclusive. Infeasibility happens when the system does not admit a Lyapunov function within the fixed class (this does not necessarily mean that the system is unstable!) or when no such Lyapunov function can be found due to conservatism in the computations. The approach can be illustrated graphically as in Figure 1.1.

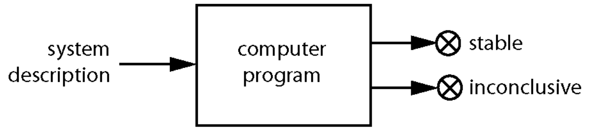

Figure 1.1 Computer implementation of approximate stability analysis (from [71]).

Although the methods are not guaranteed to work for all problem instances they appear to work very well in practice. They give strict performance improvements over approaches that use quadratic or Luré-type Lyapunov functions, and allow analysis of a wide range of systems that cannot be analyzed (or are not easily dealt with) using alternative techniques.

Finally, this book focuses exclusively on continuous-time piecewise linear systems. Many results developed in this book have direct analogues for systems where the dynamics in each mode is described by affine difference equations, see, *e.g.*, [141, 56]. Other aspects of the theory, on the other hand, are quite different (see, *e.g.*, [191, 15, 16]).

About This Manuscript

This book is based on the author's Ph.D. thesis [97]. Although this book remains faithful to the original at large it has been revised and extended in many respects. Several sections have been re-written and many results have been improved compared to the original version: issues related to sliding modes now receive more attention and an alternative analysis method based on C^1 Lyapunov functions has been introduced in Chapter 4; Chapter 7 contains significantly improved analysis procedures for systems with limited regions of attraction as well as a converse Lyapunov theorem for smooth nonlinear systems. The chapters on control design and analysis of hybrid systems have been extended and new results have been added. This book also contains a chapter on convex sets and convex optimization. In addition, many chapters include short descriptions of parallel or more recent work that complement the original content: Chapter 4 shows how Lyapunov function computations can be carried out using optimization software that supports equality constraints [72]; Chapter 6 describes a procedure for quadratic stabilization of piecewise linear systems using globally linear control laws [72] and illustrates how design of piecewise linear control laws can solved as a bilinear matrix optimization problem (*cf.* [171]); Chapter 8 contains a description of an alternative analysis procedure for hybrid systems that uses Lyapunov functionals [73] and discusses robustness issues in hybrid systems [158]. The Comments and References sections of all chapters have also been revised to reflect recent progress.

2

Piecewise Linear Modeling

This book treats analysis and design of piecewise linear control systems. In this chapter, we lay the foundation for the analysis by presenting the mathematical model on which the subsequent developments will be based. We derive an explicit matrix representation of the model and discuss solution concepts. We extend modeling techniques for uncertain linear systems to piecewise linear systems and show how norm-bound uncertainties and smooth nonlinearities can be treated rigorously in this framework. Finally, we note that piecewise linear systems enjoy important interconnection properties that allow complex systems to be constructed from the interconnection of simpler subsystems, and discuss memory-efficient model representations.

2.1 Model Representation

A piecewise linear dynamical system is a nonlinear system

$$\begin{cases} \dot{x} = f(x, u, t) \\ y = g(x, u, t) \end{cases}$$

whose right-hand side is a piecewise linear function of its arguments. For example, a linear system with saturated input results in system equations that are piecewise linear in the input variable u. Linear systems with abrupt changes in parameter values (such as jump-linear systems [193]) are piecewise linear systems in time t. The most common situation, however, is when the system equations are piecewise linear in the system state x. Such a model can, for example, arise from linearizations of a nonlinear system around different operating points, or from interconnections of linear systems and static piecewise linear components.

We will understand the term piecewise linear as piecewise linear in the system state. With this interpretation, piecewise linear indicates that the

M. Johansson: Piecewise Linear Control Systems, LNCIS 284, pp. 9-31, 2003.

state space can be partitioned into a set of regions, X_i, such that the dynamics within each region is affine in x

$$\begin{cases} \dot{x} = A_i x + a_i + B_i u \\ y = C_i x + c_i + D_i u \end{cases} \qquad \text{for } x \in X_i.$$

When written in this way, it is clear that a piecewise linear system has two important components: the partition $\{X_i\}$ of the state space into regions, and the equations describing the dynamics within each region. To obtain a good understanding of the global dynamics of such systems one needs to account for both. Although the term piecewise linear does not impose any restriction on the geometry of the regions, such restrictions are often necessary in order to arrive at useful results. In this book we restrict our attention to ***polyhedral piecewise linear dynamical systems***, where the state space is partitioned into convex polyhedra.

Introductory Examples

Before stating a precise model definition it is useful to develop a basic understanding of piecewise linear systems by studying some examples. We will begin with one of the simplest piecewise linear systems:a linear system under saturated feedback control.

EXAMPLE 2.1—ACTUATOR SATURATION IN LINEAR SYSTEMS
Consider a linear system under bounded linear state feedback,

$$\dot{x} = Ax + b\,\mathsf{sat}(v), \qquad v = k^T x.$$

As illustrated in Figure 2.1, the saturation nonlinearity induces a partition of the state space into three polyhedral cells corresponding to negative saturation (X_1), linear operation (X_2), and positive saturation (X_3), respectively. The dynamics is piecewise linear

$$\dot{x} = \begin{cases} Ax - b & x \in X_1 \\ (A + bk^T)x & x \in X_2 \\ Ax + b & x \in X_3 \end{cases} \tag{2.1}$$

In this example, it is natural to let the cells be closed (but unbounded) polyhedra that only share their common boundaries. The presence of offset terms makes the dynamics in each cell affine rather than linear in the state x. □

Note that the interconnection of a linear system with any other static piecewise linear component (such as a relay, dead-zone, minimum or maximum

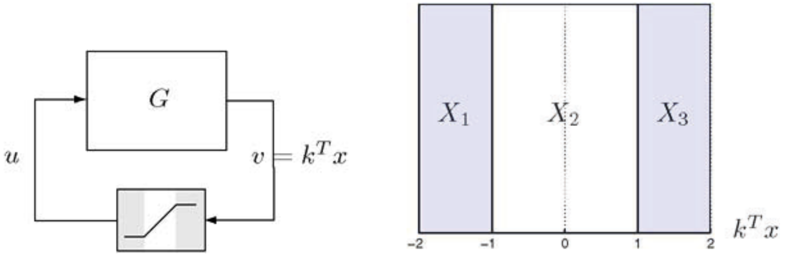

Figure 2.1 A saturated linear feedback (left) induces a piecewise linear system with a polyhedral partition of the state space (right).

function, piecewise linear spline, etc.) or linear combinations of such components would also result in a system with piecewise linear dynamics.

The initial motivation for using piecewise linear models in circuits and systems was to approximate nonlinear components in a way that allows for tractable computations. This is also a key idea in gain-scheduling approaches to modeling and control of dynamic systems. A simple approach for constructing a piecewise linear approximation to a smooth function is to evaluate the function at a number of grid points and use linear interpolation between these points to construct the approximant. We illustrate this approach by the following example.

EXAMPLE 2.2—APPROXIMATION OF SMOOTH SYSTEMS

The following differential equations describe a mechanical system with a nonlinear spring and damper.

$$\begin{cases} \dot{x}_1 = f_1(x) = x_2 \\ \dot{x}_2 = f_2(x) = -x_2|x_2| - x_1(1 + x_1^2) \end{cases} \tag{2.2}$$

A piecewise linear approximation of the system equations can be obtained by evaluating the right-hand side of (2.2) on the grid shown in Figure 2.2 (left) and then use linear interpolation between these points. The function $f_2(x)$ and the piecewise linear approximation $\hat{f}_2(x)$ obtained in this way are shown in Figure 2.2 (right). □

Several other methods for constructing piecewise linear models from data have been suggested in the literature, see the Comments and References at the end of this chapter.

With the basic intuition for piecewise linear systems developed in the examples, we are now ready to state a more precise mathematical model.

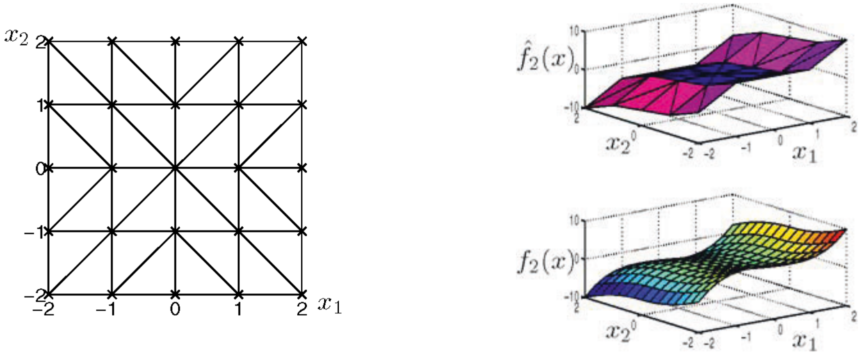

Figure 2.2 Partition (left) induced by the grid points marked with $\times$, piecewise linear approximation (top right), and actual nonlinear function (bottom right).

Model Definition

A *polyhedral piecewise linear system* consists of a subdivision of the state space into polyhedral regions and the specification of the dynamics valid within each region. We will write the system dynamics as

$$\begin{cases} \dot{x}(t) = A_i x(t) + a_i + B_i u(t) \\ y(t) = C_i x(t) + c_i + D_i u(t) \end{cases} \qquad \text{for } x(t) \in X_i \quad i \in I \tag{2.3}$$

Here, $x \in \mathbb{R}^n$ is the continuous state vector, $u \in \mathbb{R}^m$ is the input vector and $y \in \mathbb{R}^p$ is the output vector. The matrices $A_i, a_i, B_i, C_i, c_i, D_i$ are constant and of compatible dimensions.

The regions $X_i \subseteq \mathbb{R}^n$ are assumed to be closed (possibly unbounded) n-dimensional convex polyhedra which we will call *cells*. The set of cell indices is denoted I and the union of all cells, $X = \cup_{i \in I} X_i$, will be referred to as the *partition*. We assume that the cells have disjoint interior so that any two cells may only share their common boundary. Depending on the system matrices, the right-hand side of (2.3) may or may not be unique on cell boundaries.

Many results in this book are concerned with the analysis of equilibria. Unless stated otherwise, we will assume that the equilibrium point of interest is located at $x = 0$. It is then convenient to let $I_0 \subseteq I$ be the set of indices for cells that contain the origin and $I_1 \subseteq I$ be the set of indices for cells that do not contain the origin. It is assumed that $a_i = c_i = 0$ for $i \in I_0$.

Since the cells are closed convex polyhedra, they can be represented as the intersection of a finite number of closed halfspaces. In other words, for each cell X_i, there exists a matrix G_i and a vector g_i such that

$$X_i = \{G_i x + g_i \succeq 0\} \tag{2.4}$$

Here, the inequality $z \succeq 0$ means that all entries of the vector z are non-negative. The following example demonstrates the notation on the piecewise linear system from Example 2.1.

EXAMPLE 2.3—DESCRIBING THE SATURATED LINEAR SYSTEM
Consider the linear system with actuator saturation used in Example 2.1. The cells can be represented as in (2.4) with

$$G_1 = -k^T,\ g_1 = -1, \quad G_2 = \begin{bmatrix} k^T \\ -k^T \end{bmatrix},\ g_2 = \begin{bmatrix} 1 \\ 1 \end{bmatrix}, \quad G_3 = k^T,\ g_3 = -1,$$

The index sets are $I_0 = \{2\}$ and $I_1 = \{1, 3\}$, and from (2.1) we can verify that $a_i = c_i = 0$ for $i \in I_0$. □

A Matrix Parameterization

For convenient treatment of affine terms, we define

$$\bar{x}(t) = \begin{bmatrix} x(t) \\ 1 \end{bmatrix}.$$

Throughout this book, a bar over a signal vector denotes the augmentation of the vector with the unit element 1. Somewhat informally, a bar over a matrix indicates that it has been modified to be compatible with the augmented signal vector, *e.g.*,

$$\dot{\bar{x}} = \begin{bmatrix} \dot{x} \\ 0 \end{bmatrix} = \begin{bmatrix} A_i & a_i \\ 0_{1\times n} & 0 \end{bmatrix} \bar{x} := \bar{A}_i \bar{x}$$

This allows us to introduce the compact notation

$$\bar{S}_i = \left[\begin{array}{c|c} \bar{A}_i & \bar{B}_i \\ \hline \bar{C}_i & \bar{D}_i \end{array}\right] = \left[\begin{array}{cc|c} A_i & a_i & B_i \\ 0_{1\times n} & 0 & 0_{1\times m} \\ \hline C_i & c_i & D_i \end{array}\right] \tag{2.5}$$

$$\bar{G}_i = \begin{bmatrix} G_i & g_i \end{bmatrix}. \tag{2.6}$$

The matrices $\bar{S}_i$ will be called ***system matrices***, and $\bar{G}_i$ will be called ***cell identifiers***. With this notation, the dynamics (2.3) can be re-written as

$$\begin{bmatrix} \dot{\bar{x}}(t) \\ y(t) \end{bmatrix} = \bar{S}_i \begin{bmatrix} \bar{x}(t) \\ u(t) \end{bmatrix} \qquad \text{for } \{x \mid \bar{G}_i \bar{x} \succeq 0\} \tag{2.7}$$

and the system (2.3) can be represented by a set of matrix pairs,

$$\left\{(\bar{S}_i, \bar{G}_i)\right\}_{i\in I}.$$

specifying the local dynamics and state space partitioning, respectively.

2.2 Solution Concepts

A dynamic model can not be fully understood without specifying what we mean by a solution to the system equations. One way of defining solutions is to specify how to generate the future behavior $x(t)$ of the system from any initial state. This approach, closely related to providing a simulation algorithm, is easy to pursue for piecewise linear systems with continuous right-hand side: in the interior of a cell, integration of the equation (2.3) gives unique solutions; when we detect that the solution hits a cell boundary we simply determine what cell the state is entering, revise the right-hand side of (2.3) accordingly, and continue the integration.

As we will demonstrate shortly, this approach is not easily extended to general piecewise linear systems. For systems with discontinuous right-hand side, it it possible that trajectories that enter a cell boundary cannot be continued into any of the neighboring regions, or that trajectories can be continued into several regions. The following definition of a trajectory allows us to restrict our attention to the case when the non-smooth dynamics does not create any problem for our analysis.

DEFINITION 2.1—TRAJECTORY
Let $x(t) \in \cup_{i\in I} X_i$ be an absolutely continuous function. We say that $x(t)$ is a ***trajectory*** of the system (2.3) on $[t_0, t_f]$ if, for almost all $t \in [t_0, t_f]$, the equation $\dot{x}(t) = A_i x(t) + a_i + B_i u(t)$ holds for all i with $x(t) \in X_i$. □

Note that this definition of a trajectory does not require that the system has continuous right-hand side. If $x(t)$ at some time t_k passes through a cell boundary where the vector fields in the neighboring regions do not match, the model (2.3) does not provide a well-defined time derivative. If there are sufficiently few crossing times (technically speaking, if the set of times of discontinuity have measure zero [175]), however, these time instants can be removed without disqualifying $x(t)$ from being a trajectory, see Figure 2.3. Trajectories are allowed to remain on cell boundaries only if the vector field in the neighboring regions match.

As illustrated by the following example, trajectories in the sense of Definition 2.1 might be non-unique or not even exist.

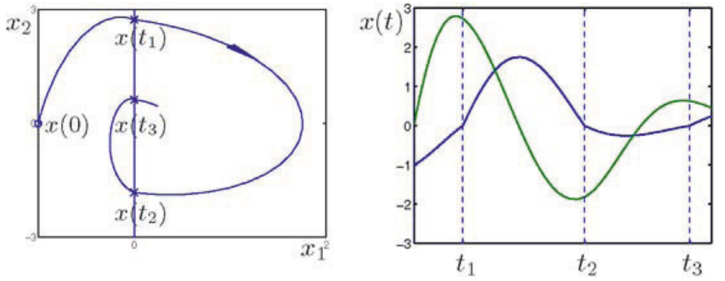

Figure 2.3 Phase plane plot (left) and time plots (right) of a trajectory of a piecewise linear system. The times t_k, marked with dashed lines in the time plot, are the times where $x(t) \in X_1 \cap X_2$ and the time derivative of (2.3) is not defined. As the number of switches is countable, $x(t)$ still qualifies as a trajectory.

Example 2.4—Non-existence & Non-uniqueness of Trajectories
Consider the piecewise linear system[1]

$$\begin{cases} \dot{x}_1 = -2x_1 - 2x_2 \operatorname{sgn}(x_1) \\ \dot{x}_2 = x_2 + 4x_1 \operatorname{sgn}(x_1) \end{cases} \tag{2.8}$$

The state-space partition and the vector field in the interior of the two cells is shown in Figure 2.4. We see that trajectories with initial values $x(0) \in \mathcal{S}_1^- =$

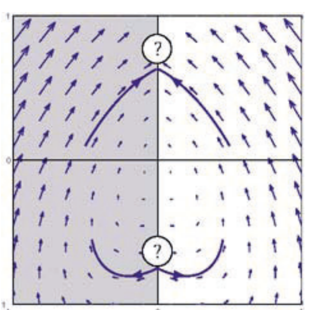

Figure 2.4 Simple piecewise linear system illustrates that trajectories in the sense of Definition 2.1 need not be unique or even exist.

$\{x \mid x_1 = 0 \wedge x_2 \leq 0\}$ are not unique since they can be continued into either cell. Trajectories that reach the manifold $\mathcal{S}_1^+ = \{x \mid x_1 = 0 \wedge x_2 \geq 0\}$, on the other hand, cannot be continued into any of the regions (the vector fields in both cells point toward $\mathcal{S}_1^+$). In fact, the only trajectory for this system on $[0, \infty)$ is the trivial $x \equiv 0$. □

[1] Here, $\operatorname{sgn}(\cdot)$ denotes the set-valued function $\operatorname{sgn}(z) = 1$ if $z \geq 0$ and $\operatorname{sgn}(z) = -1$ if $z \leq 0$.

Non-uniquness and non-existence of trajectories are discomforting from a model validation point-of-view. These phenomena indicate that important characteristics of the underlying physical system have been neglected and raise questions about how to interpret the model equations (see the Comments and Reference section at the end of this chapter for more details). From an analysis point-of-view, however, the main obstacle will be the cases when no continuation of a trajectory in the sense of Definition 2.1 is possible. The following definition allow us to single out such situations.

DEFINITION 2.2—ATTRACTIVE SLIDING MODE
The system (2.3) is said to have an ***attractive sliding mode*** at x_s if there exists a trajectory with final state x_s but no trajectory with initial state x_s. □

For sake of clarity, we will present the main results in this book for systems without attractive sliding modes. Solution concepts for systems with sliding modes are discussed below and a method for detecting sliding modes will be described in Section 3.3. The general analysis procedures will be developed for systems without attractive sliding modes and a technique for extending these results to systems with attractive sliding modes is given in Section 4.8.

Generalized Solutions

It is still possible to define meaningful solution concepts for systems with attractive sliding modes if we consider functions $x(t)$ that remain on the cell boundaries for some time interval. The most well-known solution concepts are due to Filippov [57] and Utkin [197]. Typically, solutions are defined by some limiting process, such as introducing a small hysteresis around cell boundaries and letting the hysteresis parameter tend to zero; see Figure 2.5. In this way, the behavior on the surface of discontinuity is defined by averaging the dynamics in the neighboring regions. The following definition specializes the approach of Filippov to piecewise linear systems.

DEFINITION 2.3—FILIPPOV SOLUTION
Let $x(t) \in \cup_{i\in I} X_i$ be an absolutely continuous function. We say that $x(t)$ is a ***Filippov solution*** of the system (2.3) on $[t_0, t_f]$ if, for almost all $t \in [t_0, t_f]$,

$$\dot{x}(t) \in \overline{\mathrm{co}}_{k\in K(t)} \{A_k x(t) + a_k + B_k u(t)\}$$

where $K(t)$ is the set of cell indices k such that $x(t) \in X_k$. □

In the above definition, $\overline{\mathrm{co}}$ denotes convex closure. In other words, $x(t)$ is a Filippov solution of (2.3) if and only if there exist positive scalars $\alpha_k(t) \geq 0$

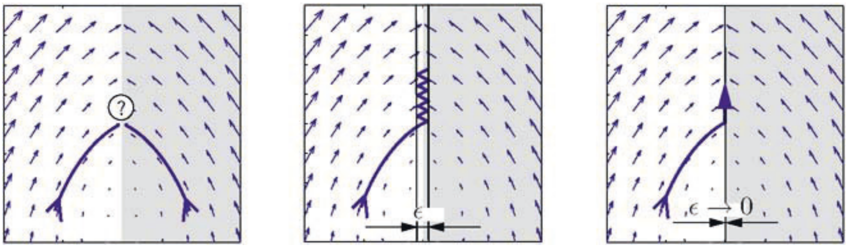

Figure 2.5 Filippov solutions may remain on cell boundaries following dynamics generated by averaging the dynamics in the neighboring regions.

with $\sum \alpha_k(t) = 1$ such that

$$\dot{x}(t) = \sum_{k \in K(t)} \alpha_k(t) \{A_k x(t) + a_k + B_k u(t)\} \tag{2.9}$$

for almost all $t \in [t_0, t_f]$. In the interior of cells, the differential inclusion contains only one element and Filippov solutions coincide with the trajectory concept defined above. Time functions $x(t)$ that remain on a cell boundary for some time are also accpeted as Filippov solutions if they can be constructed from *some* convex combination of the dynamics in the neighboring regions. As illustrated in the following example, the additional information that $x(t)$ remains on the boundary can be used to narrow down the admissible behaviors and sometimes even derive unique dynamics on the sliding mode.

EXAMPLE 2.5—SLIDING MODE DYNAMICS ON SIMPLE BOUNDARIES
Consider again the piecewise linear system (2.8) on the set $\mathcal{S}_1^+ = \{x \mid x_1 = 0 \wedge x_2 \geq 0\}$. Filippov's definition gives

$$\dot{x}(t) \in \overline{\text{co}}\,\{A_1 x(t), A_2 x_2(t)\} = \alpha_1(t) A_1 x(t) + \alpha_2(t) A_2 x(t)$$

where the weights satisfy $\alpha_1(t) \geq 0$, $\alpha_2(t) \geq 0$ and $\alpha_1(t) + \alpha_2(t) = 1$. However, not all such weights give rise to solutions that stay on $\mathcal{S}_1^+$. In order for $x(t)$ to stay on $\mathcal{S}_1^+$ we must have $\dot{x}_1(t) = 0$, *i.e.*,

$$\alpha_1(t)\,[-2x_1(t) - 2x_2(t)] + \alpha_2(t)\,[-2x_1(t) + 2x_2(t)] = 0 \qquad x(t) \in \mathcal{S}_1^+$$

Combining this requirement with $\alpha_1(t) + \alpha_2(t) = 1$, we find

$$\alpha_1(t) = \alpha_2(t) = 1/2$$

Hence, the unique dynamics on the sliding mode is

$$\dot{x}_1(t) = 0 \qquad \dot{x}_2(t) = x_2(t) \qquad x(t) \in \mathcal{S}_1^+$$

□

On simple boundaries of piecewise linear systems, it is always possible to derive a unique (but not necessarily linear) sliding mode dynamics by balancing the vector fields as above. However, sliding modes do not only occur on simple cell boundaries but can also arise on the intersection of multiple boundaries. As demonstrated by the following example, the sliding mode dynamics on intersecting boundaries is in general not unique.

EXAMPLE 2.6—NON-UNIQUE SLIDING MODE DYNAMICS
Consider the piecewise linear system

$$\begin{aligned}
\dot{x}_1 &= x_2 - \operatorname{sgn}(x_1) \\
\dot{x}_2 &= x_3 - \operatorname{sgn}(x_2) \\
\dot{x}_3 &= -2x_1 - 4x_2 - 4x_3 - x_3\operatorname{sgn}(x_2)\operatorname{sgn}(x_1 + 1)
\end{aligned}$$

The two first state equations reveal that sliding occurs on the sets

$$\mathcal{S}_1 = \{x \mid x_1 = 0 \,\wedge\, |x_2| \leq 1\} \qquad \mathcal{S}_2 = \{x \mid x_2 = 0 \,\wedge\, |x_3| \leq 1\}$$

As indicated in the simulation shown in Figure 2.6, sliding can also occur on the intersection of these surfaces,

$$\mathcal{S}_{12} = \{x \mid x_1 = 0 \,\wedge\, x_2 = 0 \,\wedge\, |x_3| \leq 1\}$$

To study the sliding motion on $\mathcal{S}_{12}$ in more detail, note that the sign functions induce a partition of the state space into four cells, being the four quadrants in the $x_1 - x_2$ plane (see Figure 2.6, right). The vector fields in the four regions point toward the set $\mathcal{S}_{12}$ so the sliding mode is attractive (solutions reaching $\mathcal{S}_{12}$ cannot be continued into any cell). Filippov solutions satisfy

$$\dot{x} = \sum_{k=1}^{4} \alpha_k \{A_k x + a_k\} \tag{2.10}$$

Here, the weights α_k should be non-negative, sum to one

$$\alpha_1 + \alpha_2 + \alpha_3 + \alpha_4 = 1$$

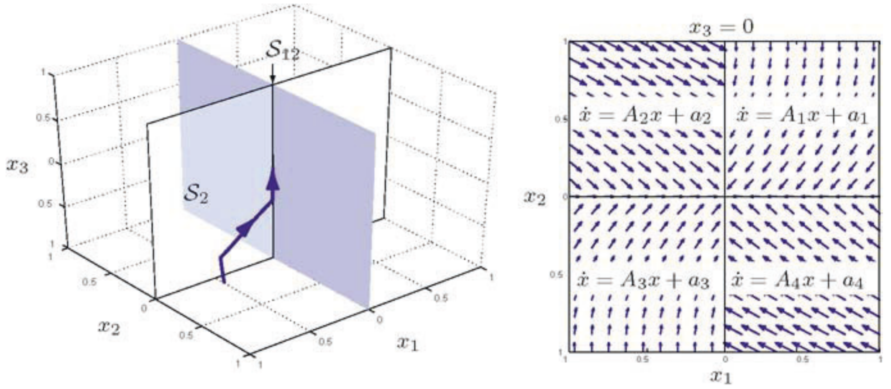

Figure 2.6 A Filippov solution enters $\mathcal{S}_2$ and slides into the set $\mathcal{S}_{12}$ where a new sliding motion can be sustained (left). The rightmost figure shows the vector fields on the subspace $\{x \mid x_3 = 0\}$: the vector fields in the four cells point toward $\mathcal{S}_{12}$.

and guarantee sliding on $\mathcal{S}_{12}$, *i.e.*, that $\dot{x}_1 = \dot{x}_2 = 0$ when $x_1 = x_2 = 0$:

$$\begin{aligned} \dot{x}_1 = 0 \Rightarrow \qquad & -\alpha_1 + \alpha_2 + \alpha_3 - \alpha_4 = 0 \\ \dot{x}_2 = 0 \Rightarrow \qquad & x_3 - \alpha_1 - \alpha_2 + \alpha_3 + \alpha_4 = 0 \end{aligned}$$

Since there are four vector fields to balance but only three constraints, one might suspect that the dynamics in the sliding mode is not unique. Indeed, it is straightforward to verify that one solution is given by

$$\alpha_1 = \frac{1 + \operatorname{sgn}(x_3)}{4}, \quad \alpha_2 = \frac{1 + x_3}{2} - \alpha_1, \quad \alpha_3 = -\frac{x_3}{2} + \alpha_1, \quad \alpha_4 = \frac{1}{2} - \alpha_1$$

while another solution is

$$\alpha_1' = \alpha_2 \qquad \alpha_2' = \alpha_1 \qquad \alpha_3' = \alpha_4 \qquad \alpha_4' = \alpha_3$$

In fact, these weights define the Filippov solutions with the minimal and maximal velocity for x_3 on $\mathcal{S}_{12}$. The time responses shown in Figure 2.7 reveal that the two definitions give rise to drastically different sliding mode dynamics, with settling times differing by at least a factor of four. □

Non-uniqueness of the sliding mode dynamics indicates that some important characteristics of the underlying physical system has been neglected, and that one needs to review the assumptions made when deriving the model. A unique sliding dynamics can sometimes be recovered by modeling salient features of the switching mechanisms, such as the relative speed of relay components (see, *e.g.*, [136]).

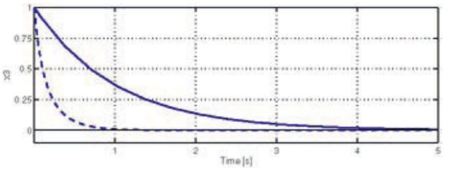

Figure 2.7 Filippov's definition yields non-unique velocities along the sliding mode.

The fact that sliding modes can occur on intersections of multiple boundaries makes it hard to verify that a given model is free from attractive sliding modes. Not only is there an exponential number of surfaces that need to be checked for potential sliding modes, but it is also much harder to verify that sliding modes on intersecting surfaces are attractive (*i.e.*, that solutions starting close to an intersection converge to it). In essence, one then needs to do a complete stability analysis of the potential sliding manifold, which quickly becomes prohibitively expensive. The following example, taken from [201, 197], illustrates this point.

EXAMPLE 2.7—ESTABLISHING ATTRACTIVITY OF SLIDING MODES
Consider the following piecewise linear system

$$\begin{aligned} \dot{x}_1 &= -\text{sgn}(x_1) + 2\text{sgn}(x_2) \\ \dot{x}_2 &= -2\text{sgn}(x_1) - \text{sgn}(x_2) \end{aligned}$$

The sign-functions induce a partition into four cells, each being one of the quadrants in $\mathbb{R}^2$. The vector field is constant in each cell and it is strongly suggested that solutions should behave as shown in Figure 2.8: solutions spiral toward the origin, which is reached in finite time, and remain there. Since the vector fields within the four cells do not match, the origin is a sliding mode, and the Fillipov solution $x(t) \equiv 0$ can be constructed by giving the system matrices in the four cells equal weights in (2.9).

It is far from trivial to prove that the origin is attractive. Vector field considerations are not easily used since no vector field points towards the origin. For this particular system, convergence to the origin can be proved by noting that $d/dt(|x_1(t)| + |x_2(t)|) = -2$, which means that solutions with initial state $(x_1(0), x_2(0))$ cannot stay away from the origin for longer than $(|x_1(0)| + |x_2(0)|)/2$ units of time. □

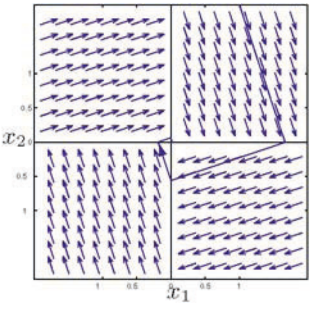

Figure 2.8 Piecewise linear system with non-traversal sliding.

2.3 Uncertainty Models

Uncertainty and robustness are central themes in modeling and analysis of feedback systems. One of the most important reasons for using feedback is to guarantee that system specifications are met despite variations in system components and exogenous disturbances. Furthermore, since there is always a mismatch between the model used in the mathematical analysis and the actual physical system, it is important to account for this uncertainty to ensure that the results derived from the model will hold in reality. In this section, we will extend the standard uncertainty models for linear uncertain systems (see, *e.g*, [220]) to systems that are piecewise linear. These uncertainty models will enable us to extend analysis procedures for piecewise linear systems to yield rigorous results for smooth nonlinear systems.

To verify robustness we have to specify the sets of admissible uncertainties and disturbances. We will consider two main classes of uncertainties. The first deals with systems on the form

$$\dot{x} = f(x)$$

and considers the effects of uncertainties in the function $f(x)$. This situation may occur when $f(x)$ is a piecewise linear approximation of some smooth function. If the uncertainty is due to unknown or time-varying parameters, this is usually called *parametric uncertainty*. The second class of uncertainty descriptions considers systems on the form

$$\begin{aligned}\dot{x} &= f(x, y)\\ \dot{y} &= g(x, y)\end{aligned}$$

where $g(x, y)$ is uncertain or lacks a description with appropriate structure. This type of uncertainty is usually called *dynamic uncertainty*, and may occur when y represents an exogenous disturbance or a neglected component.

Piecewise Linear Differential Inclusions

One way to embed more general nonlinear systems in the piecewise linear framework is to allow systems with time-varying system matrices

$$\begin{cases} \dot{x}(t) = A_i(t)x(t) + a_i(t) + B_i(t)u(t) \\ y(t) = C_i(t)x(t) + c_i(t) + D_i(t)u(t) \end{cases} \qquad \text{for } x \in X_i$$

We will consider the case when the system matrices $\bar{S}_i$ for each cell can be written as a convex combination of matrices $\bar{S}_i^1, \dots, \bar{S}_i^K$. In other words, we assume that for every t there exist scalars $\alpha_k(t) \geq 0$ with $\sum_k \alpha_k(t) = 1$ such that $\bar{S}_i(t)$ can be written as

$$\bar{S}_i(t) = \sum_{k=1}^{K} \alpha_k(t)\bar{S}_i^k. \tag{2.11}$$

We will then consider the family of models obtained by considering all admissible $\alpha_k(t)$. For notational convenience, we will to each cell X_i associate an index set $K(i)$ that specifies the matrices that are used in the inclusion. We will then write (2.11) as

$$\bar{S}_i(t) \in \underset{k \in K(i)}{\overline{\mathrm{co}}} \left\{ \bar{S}_i^k \right\}. \tag{2.12}$$

We will call these models *piecewise linear differential inclusions, pwLDIs.*

An absolutely continuous function $x(t)$ is called a *solution* of the inclusion on $[t_0, t_f]$ if, for almost all $t \in [t_0, t_f]$, it satisfies

$$\begin{bmatrix} \dot{\bar{x}}(t) \\ y(t) \end{bmatrix} \in \underset{k \in K(i)}{\overline{\mathrm{co}}} \left\{ \bar{S}_i^k \begin{bmatrix} \bar{x}(t) \\ u(t) \end{bmatrix} \right\} \qquad \text{for } x(t) \in X_i \tag{2.13}$$

Linear differential inclusions have been used to model parametric uncertainty in linear systems. One of the most well-known examples is the sector conditions that have been used in the work on absolute stability [132, 215, 163]. In this context, the extension to piecewise linear differential inclusions allows us to use *piecewise linear sector bounds* to embed smooth nonlinearities into the piecewise linear framework.

EXAMPLE 2.8—SECTOR BOUND NONLINEARITY

Consider an integrator in a negative feedback loop with static nonlinearity

$$\begin{cases} \dot{x}(t) = -\varphi(x(t)) \\ y(t) = x(t) \end{cases}$$

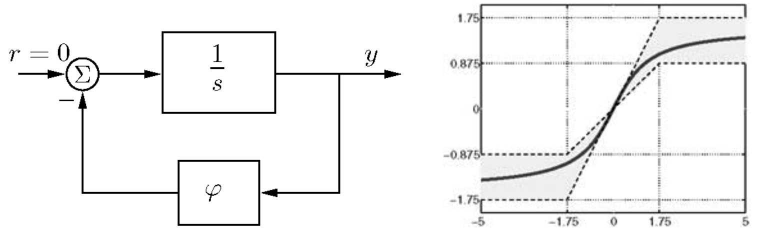

Figure 2.9 Analysis of smooth nonlinear system (left) via piecewise linear sector bounds on the nonlinearity (right).

Assume that the nonlinearity $\varphi(x(t))$ can be bounded by "piecewise linear sectors", see Figure 2.9. In other words, assume that there exist vectors $\bar{l}_i$ and $\bar{u}_i$, describing upper and lower bounds respectively, such that

$$\varphi(x(t)) \in \overline{\mathrm{co}}\left\{\bar{l}_i^T \bar{x}(t), \bar{u}_i^T \bar{x}(t)\right\} \qquad \text{for } x \in X_i.$$

The closed loop system can then be described by the piecewise linear differential inclusion

$$\bar{S}_i(t) \in \overline{\mathrm{co}}\left\{\bar{S}_i^+, \bar{S}_i^-\right\}$$

with

$$\bar{S}_i^+ = \left[\begin{array}{c|c} -\bar{l}_i & 1 \\ \mathbf{0} & 0 \\ \hline 1 & 0 \end{array}\right], \qquad \bar{S}_i^- = \left[\begin{array}{c|c} -\bar{u}_i & 1 \\ \mathbf{0} & 0 \\ \hline 1 & 0 \end{array}\right].$$

Notice that the integrator system could be replaced with a general piecewise linear system, and all results would follow similarly. □

Methods for obtaining upper and lower piecewise linear bounds on scalar functions can be found in [129] and a procedure for identifying tight upper and lower bounds from data has been proposed in [107]. We will use the piecewise linear sector bounds to analyse smooth nonlinear systems in Sections 4.7 and fuzzy control systems in Section 7.4.

Norm-Bound Approximation Errors

One problem with uncertainty descriptions in terms of differential inclusions is that the analysis conditions must consider every extreme dynamics in each region. A careless application of pwLDIs in the modeling phase can generate a large number of extreme systems which may render the analysis computations intractable.

If the piecewise linear system is obtained by approximating a smooth system, it is natural to use a norm bound on the error

$$\|f(x) - A_i x - a_i\| \leq \epsilon_i \|x\| \qquad \text{for } x \in X_i, i \in I.$$

between the right-hand side of $\dot{x} = f(x)$ and its piecewise linear approximation. Now, rather than specifying several extreme dynamics for each cell we only have to provide a single norm bound ϵ_i. Moreover, if $f(x)$ is smooth, the bounds on the approximation error will decrease as the partition is refined. In Chapter 7, we will use this observation to establish a converse theorem for analysis of smooth nonlinear systems using piecewise linear techniques.

Dynamic Uncertainties and Dissipation Inequalities

The standard approach to account for dynamic uncertainties is to consider norm-bound uncertainties in a feedback interconnection, as shown in Figure 2.10. In robust control literature, the nominal system Σ is assumed to be

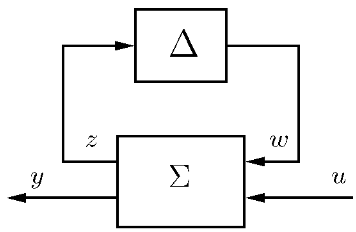

Figure 2.10 Piecewise linear system with uncertainty feedback.

linear time invariant, while system nonlinearities and uncertainties are confined to the uncertainty block Δ. In contrast, we will allow Σ to be piecewise linear. This allows us to choose whether to describe system nonlinearities explicitly in the piecewise linear subsystem or to model them as uncertainties in the Δ subsystem. This additional freedom can be used to trade off computational complexity against conservatism in the analysis.

The operator Δ that specifies the feedback $w = \Delta z$ may be linear time varying or nonlinear, but is assumed to satisfy the dissipation inequality

$$\int_0^t \begin{bmatrix} z(s) \\ w(s) \end{bmatrix}^T M \begin{bmatrix} z(s) \\ w(s) \end{bmatrix} ds \geq 0 \qquad \text{for all } t \geq 0 \tag{2.14}$$

for some real symmetric matrix M. This includes, for example, passive components and elements with bounded $\mathcal{L}_2$-induced gain. After establishing gain and passivity properties of Σ and Δ using, for example, the techniques in Chapter 5, we may try to use small gain or passivity results to establish stability of the closed loop system [116].

A Modeling Trade-Off: Uncertainty versus Complexity

The piecewise linear sector bounds allow stepwise refinements of a global sector bounds to improve a nonlinearity description. In the end, such refinements allow arbitrarily tight inclusions of any continuous function. However, each such refinement comes at the price of increased memory requirements for the model representation and increased computational cost for the analysis. It is thus natural to look for the simplest model that gives a sufficiently accurate answer in the analysis. The following example illustrates this idea.

EXAMPLE 2.9—PIECEWISE LINEAR MODELING AND COMPLEXITY
In Chapter 5 we will encounter a system on the form

$$\dot{x}(t) = Ax(t) - B\varphi(Cx(t))$$

where the nonlinearity $\varphi(\cdot)$ is a spring with the piecewise linear characteristic shown in Figure 2.11 (left). Nonlinear spring arrangements of this type can be found in engine control systems (see, *e.g.*, [120]). The exact description has many segments and results in relatively demanding analysis computations. It is therefore attractive to base the analysis on an approximate model that requires less computations. The piecewise linear sector bounds give many possibilities. For the specific example in Chapter 5, the piecewise linear sector bounds shown in Figure 2.11 (middle) can be used to asses stability while an analysis based on global sector bounds (right) fails. □

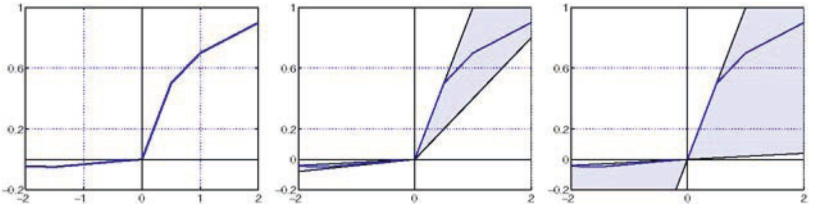

Figure 2.11 From exact description to global sector bounds. Piecewise linear sector bounds allow us to trade precision of the model against simplicity of the computations.

Although the principle of refinements using piecewise linear sector bounds has been illustrated on a scalar nonlinearity the methods applies also to multivariable nonlinearities.

2.4 Modularity and Interconnections

Modularity and structure-preserving interconnections are attractive features in modeling and analysis of dynamic systems. Modularity allows complex systems to be represented as the interconnection of simpler subsystems. Important model components can be stored in a library and recalled and interconnected as needed. Structure-preserving interconnections are also very useful since they grant that the interconnected system shares important structural properties with its components. For example, series, parallel and feedback interconnections of linear systems are themselves linear systems. This allows the full systems and its components to be analyzed using the same tools. We can choose whether to analyze the full system directly, or to first analyze its subcomponents and then invoke interconnection results, such as small gain and passivity theorems.

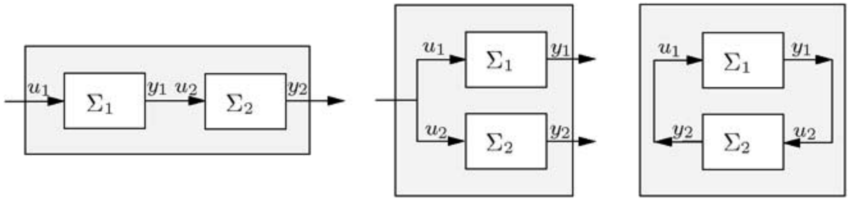

Figure 2.12 Series, parallel, and feedback interconnection of dynamical systems.

The following proposition states that the most common interconnection structures preserve the piecewise linearity of its components (*cf.* [198, 159]).

PROPOSITION 2.1—STRUCTURE-PRESERVING INTERCONNECTIONS
Series, parallel and feedback interconnections (without algebraic loops) of polyhedral piecewise linear systems are themselves polyhedral piecewise linear systems. Moreover, a matrix representation $\{\bar{S}_i, \bar{G}_i\}_{i\in I}$ for the total system is obtained directly from the matrix representations of its components. □

Proof: The result follows by direct computations, see Section B.1.

The proof of Proposition 2.1 reveals that the interconnection of two piecewise linear systems results in a combinatorial growth in the number of cells. Consider the interconnection of the system Σ_1 with state vector x and partition $\{X_i\}_{i\in I}$ and the system Σ_2 with state vector z and partition $\{Z_j\}_{j\in J}$. The partition of the interconnected system is obtained by considering all combinations of (i, j) such that $x \in X_i$ and $z \in Z_j$. Hence, if Σ_1 has a partition of p_1 cells and Σ_2 has a partition of p_2 cells, the interconnected system may have $p_1 \times p_2$ cells. This illustrates the usefulness of an input-output

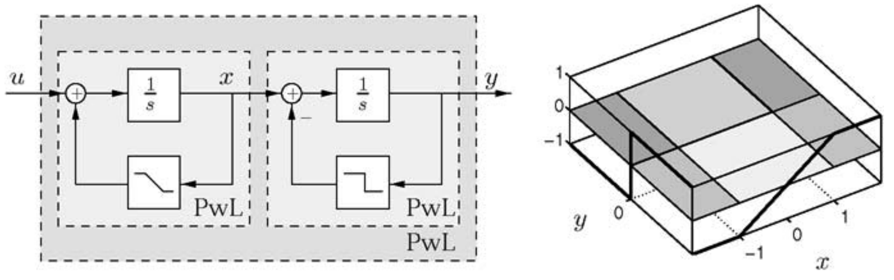

Figure 2.13 Series connection of two piecewise linear systems is piecewise linear (left). The interconnected system has the partition shown to the right.

analysis for piecewise linear systems: if analysis of the interconnected system is too computationally demanding, we can try to analyze the simpler subsystems and apply small gain or passivity arguments.

Proposition 2.1 allows descriptions of standard piecewise linear components, such as relays and saturations, to be stored in a library and recalled when needed. In this context, it is useful to allow partitioning in the product space of the input space and the state space, *i.e.*, to let

$$\widetilde{X}_i = \left\{ \begin{bmatrix} x \\ u \end{bmatrix} \middle| \widetilde{G}_i \begin{bmatrix} \bar{x} \\ u \end{bmatrix} \succeq 0 \right\}.$$

Although this route will not be pursued here we note that a similar result to Proposition 2.1 holds also in this case. The following example illustrates the interconnection properties of piecewise linear systems.

EXAMPLE 2.10—INTERCONNECTION PRESERVES STRUCTURE
Consider the series connection of two piecewise linear systems

$$\begin{aligned} \dot{x} &= -\mathrm{sat}(x) + u \\ \dot{y} &= -\mathrm{sgn}(y) - x \end{aligned}$$

illustrated in Figure 2.13 (left). The interconnection is itself piecewise linear in accordance with Proposition 2.1. The individual subsystems have two and three cells, respectively, while the interconnected system has six. Although the combinatorial growth is not so pronounced in this example, it can be significant in more complex systems. □

Unfortunately, the modular approach does not extend directly to the case when the systems are uncertain in the pwLDI-sense, since this may introduce uncertainty in the state space partitioning. Analysis of piecewise linear systems with uncertain partitions will be discussed in Chapter 8.

2.5 Piecewise Linear Function Representations

We have proposed to represent piecewise linear systems using the matrix parameterization (2.7). This representation is easy to understand and convenient to use for analysis. However, if the piecewise linear system (2.3) has continuous right-hand side, the representation contains a lot of redundant information and is not very memory efficient.

Modeling and simulation of piecewise linear systems has attracted a large interest in the circuits and systems community during the last decades. Driven by the need to simulate large-scale circuits with piecewise linear components, a large research effort has been devoted to deriving memory efficient representations for piecewise linear systems [42, 126, 107]. More compact descriptions than the matrix representation (2.7) can be obtained when the vector field of the system is continuous across cell boundaries. To see this, consider the situation in Figure 2.14. To obtain continuity on the cell

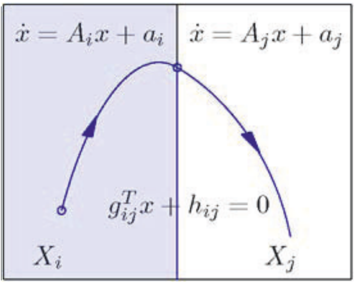

Figure 2.14 Continuity of vector fields allows parameter savings.

boundary $\partial X_{ij} = \{x \mid g_{ij}^T x + h_{ij} = 0\}$, the system matrices must satisfy

$$\begin{aligned} A_j &= A_i + c_{ij} g_{ij}^T \\ a_j &= a_i + c_{ij} h_{ij} \end{aligned}$$

for some $c_{ij} \in \mathbb{R}^n$. Since the boundary equations of the cells re-appear in the description of feasible changes in the mapping, there is a certain redundancy in the data given by the simple model (2.7). The argument above indicates that it should be sufficient to store one linear system description, the boundary equations, and the update vectors c_{ij}.

The first compact parameterization of that appeared was the *canonical piecewise linear function description* introduced in [42]. For piecewise linear dynamic systems, it takes the form

$$\dot{x} = Ax + a + \sum_{i=1}^{p} c_i |g_i^T x + h_i|. \tag{2.15}$$

This representation stores only a single affine system description, the boundary hyperplane equations and the update vectors. It has also eliminated the need for explicit storage of cell identifiers and no cell identification is necessary to evaluate the mapping. The representation (2.15) is very efficient compared to the simple matrix parameterization (2.7), but it can only represent a subset of the continuous piecewise linear mappings (*cf.* [109, 115]). To overcome this problems, various higher order basis function expressions have been suggested. These are much more complicated than the simple model (2.15), but can be put in the general form

$$\dot{x} = Ax + a + \sum_{i=1}^{q} c_i \varphi_i(x)$$

Here, the $\varphi_i(x)$ are piecewise linear functions constructed from nested absolute or maximum functions, see [109, 70, 115, 107].

An alternative formulation, which is closely related to the matrix representation (2.7), is the ***implicit piecewise linear function description*** [198, 115]

$$\begin{cases} \dot{x} = Ax + a + Bu \\ i = Gx + g + Cu \\ 0 = u^T i \qquad u \succeq 0,\ i \succeq 0 \end{cases} \tag{2.16}$$

This representation was derived from a static linear network where some ports have been terminated by negative ideal diodes. The variables i and u correspond to currents and voltages respectively, and the last equation of (2.16) describes the characteristic of an ideal negative diode. Vectors u and i that satisfy this equation are called ***complementary***. To see the close connection to our matrix parameterization, consider the region where $u = 0$. Then, the above model reduces to

$$\dot{x} = Ax + a \qquad\qquad \text{for } x \text{ such that } Gx + g \succeq 0.$$

Given x, an evaluation of the mapping needs the associated diode voltages u. These can be computed by solving the linear complementary problem of finding i and u that satisfy the last two equations of (2.16). In principle, a solution to this problem can be obtained through a sequence of pivoting operations around the C-matrix. Each such pivoting step forces one entry of the vectors u or i to zero while the corresponding entry in the other vector is allowed to be non-zero. The second equation in (2.16) implies that the zero entries of i and u force the corresponding entries of the other vector to be affine expressions of x. Hence, every configuration of u and i into zero and non-zero entries define a polyhedron in the state space (via the conditions $i \succeq 0$ and $u \succeq 0$). In each polyhedron, the affine expressions for u describe the changes in the local dynamics via the first equation of (2.16). In this way, the matrix C encodes the changes in the cell descriptions while the matrix B encodes the changes in the affine dynamics. For more details, see [198, 38, 159, 107].

One drawback with the implicit model (2.16) is that a solution to the linear complementary problem may require a number of pivoting operations that is exponential in the number of entries of the vectors u and i. As we have seen above, solving the linear complementary problem plays the role of performing a cell identification in our framework. The exponential complexity is related to the fact that we may have to check membership of all cells when evaluating the piecewise linear mapping. However, once a feasible set of complementary vectors u and i has been found only one pivoting operation is needed in order to determine the new set-up when a single constraint has been violated. This has allowed the development of fast and memory efficient simulation programs based on this model [38].

2.6 Comments and References

Many important remarks can be made to the developments described so far. Rather than obstructing the general presentation with long discussions, we have chosen to collect such remarks in a special section at the end of each chapter. Some of the material presented in these sections are small remarks, while other material discusses related work, gives alternative perspectives on the material or presents issues that are not otherwise covered in the book.

Piecewise Linear or Piecewise Affine?

The term piecewise linear may at first appear inappropriate for the system (2.3) since the dynamics is in fact affine in the state. However, since the name is generally accepted, we have chosen not to make a stronger point out of this. One may motivate the name piecewise linear by the fact that around any trajectory inside a cell, the dynamics will behave linearly.

Special Classes of Piecewise Linear Systems

Systems with piecewise linear dynamics have been studied for a long time in science and engineering, and many particular classes of piecewise linear systems have been introduced.

Linear systems with saturation and relay nonlinearities probably have the longest tradition (see, *e.g.*, [75, 153, 3]). They are practically relevant and serve as excellent prototype systems for understanding more general piecewise linear systems. However, even these apparently simple systems can exhibit astonishingly complex behaviours, and the set of analysis and synthesis tools is still not complete (see [67, 95] for recent developments).

More general classes of piecewise linear systems, notably the systems described on the implicit form (2.16), have been studied in the circuits and systems community [198, 127]. Complementarity conditions also occur in the modeling of impulse and contact forces in mechanics leading to dynamical systems that are conveniently described by the implicit model (2.16) (see, *e.g.*, [131]). Recently, a number of important system-theoretic results have been developed for systems on the form (2.16) under the name ***linear complementarity systems*** [202, 79].

Several additional piecewise linear models have been suggested for systems with discrete-time dynamics, notably the min-max-plus-scaling systems [183] and the mixed logical dynamical systems [15]. A nice exposition of the different system models and their relationships can be found in [80].

Well-Posedness of Piecewise Linear Systems

We have defined trajectories of piecewise linear systems as absolutely continuous functions that satisfy the model equations at all times. Although any reasonable model of a physical system should produce solutions with this property, we have seen how model simplifications can result in systems with attractive sliding modes. It is thus natural to ask if a given piecewise linear system is well-posed in the sense that it produces unique trajectories from every initial state. Conditions for well-posedness of bi-modal piecewise linear systems (without affine terms) have been derived in [87]. Further results have been developed for particular classes of piecewise linear systems such as relay systems or linear complementarity systems, see *e.g.*, [95, 200, 78]. As we have illustrated by several examples, conditions for well-posedness of general piecewise linear systems appears to be very hard to establish.

Constructing Piecewise Linear System Models from Data

In one of the motivating examples, we constructed a piecewise linear approximation of a smooth nonlinear system by evaluating the right-hand-side of the smooth differential equation at a number of points and using linear interpolation between these points. This is also how piecewise linear circuit models were constructed in [88, 149, 40]. In many cases, however, we do not have access to an explicit system model, but need to estimate our model from data. Methods for estimating piecewise linear models from data have been developed in, for example, [22, 145, 188, 35, 128, 108, 173]. Methods for identifying piecewise linear sector bounds from data are described in [107].

3

Structural Analysis

In this chapter, we will present some basic tools for analysis of piecewise linear dynamical systems. We will treat equilibrium computations and static gain analysis as well as verification of affine state constraints and detection of attractive sliding modes. These results are useful for ruling out degeneracies in piecewise linear models, provide critical engineering insight, and are valuable complements to the Lyapunov-based methods developed in the subsequent chapters.

3.1 Equilibrium Points and the Steady-State Characteristic

An initial problem in the study of a nonlinear system is to determine its equilibrium points. We will understand the term *equilibrium point* as a constant trajectory (in the sense of Definition 2.1). Contrary to a linear system, which always has an equilibrium at the origin, a general nonlinear system

$$\begin{aligned}\dot{x} &= f(x,u)\\ y &= g(x,u)\end{aligned}$$

may have any number of isolated equilibrium points. To compute the equilibrium points, we pick a constant input $u = u_{\text{eq}}$ and find the solutions x_{eq} to the equation $f(x_{\text{eq}}, u_{\text{eq}}) = 0$. By repeating the computations for a range of inputs and recording the stationary outputs $y_{\text{eq}} = g(x_{\text{eq}}, u_{\text{eq}})$ we obtain the *steady-state characteristic*.

Equilibrium Point Computations

Computing the equilibrium points of a piecewise linear system is straightforward: we simply have to check if each affine subsystem has any equilibrium points within its operating regime. Hence, for given u_{eq}, we need to

M. Johansson: Piecewise Linear Control Systems, LNCIS 284, pp. 32-40, 2003.

check if there exists any solutions $x_{\text{eq}} \in X_i$ to

$$0 = A_i x_{\text{eq}} + a_i + B_i u_{\text{eq}}$$

The following result shows how the equilibrium point computations can be conveniently formulated as a linear programming problem.

PROPOSITION 3.1—EQUILIBRIUM POINTS

The set of equilibrium points of the piecewise linear system (2.3) in the interior of cell X_i is given by

$$Q_i = \{x \mid A_i x + a_i + B_i u_{\text{eq}} = 0,\; G_i x + g_i \succ 0\}$$

Finding a feasible equilibrium point $x_{\text{eq}} \in Q_i$, or verifying that no such point exists, is a linear programming problem. □

The computations can be simplified when the matrices A_i are invertible. In this case the potential equilibrium point $x_{\text{eq}} = -A_i^{-1}(a_i + B_i u_{\text{eq}})$ lies in the interior of X_i if and only if

$$-G_i A_i^{-1}(a_i + B_i u_{\text{eq}}) + g_i \succ 0.$$

The above approach is still computationally intensive since all cells have to be considered one-by-one. More efficient algorithms have been developed for piecewise linear systems with continuous right-hand side, see [44, 207, 155]. The following example demonstrates the analysis.

EXAMPLE 3.1—A BISTABLE ELECTRICAL CIRCUIT

Consider the tunnel diode circuit in Figure 3.1. The circuit equations are

$$\begin{cases} C\dfrac{d}{dt}v_c = i_L - g_R(v_c) \\ L\dfrac{d}{dt}i_L = u - Ri_L - v_c \end{cases}$$

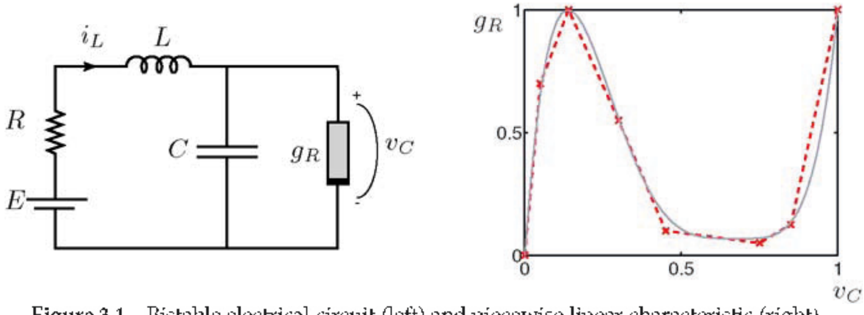

Figure 3.1 Bistable electrical circuit (left) and piecewise linear characteristic (right).

Here, $g_R(v_c)$ denotes the conductance of the nonlinear element. We use the parameters R $= 1.5$kΩ, $C = 2$pF, $L = 5\mu H$ (taken from [116, 43]). By measuring time in nanoseconds and currents in mA, we obtain

$$\begin{cases} \dfrac{d}{dt}v_c = 0.5[-g_R(v_c) + i_L] \\ \dfrac{d}{dt}i_L = 0.2[-v_c - Ri_L + u] \end{cases}$$

A piecewise linear approximation of the system is constructed by approximating $g_R(v_c)$ by a seven-segment piecewise linear function, see Figure 3.1 (right). Letting $u_{\text{eq}} = 1.2$, we run the computations of Proposition 3.1 to find the three equilibrium points

$$x_1^* = \begin{bmatrix} 0.07 \\ 0.76 \end{bmatrix}, \qquad x_2^* = \begin{bmatrix} 0.28 \\ 0.62 \end{bmatrix}, \qquad x_3^* = \begin{bmatrix} 0.87 \\ 0.22 \end{bmatrix}.$$

which have good correspondence with the computations in [116]. □

The value of an equilibrium point computation is significantly increased if it is combined with a local analysis of the properties of the equilibria. The local analysis, which can be done by eigenvalue inspection of the matrices A_i, might reveal important qualitative properties of the overall system. For example, if the system has no sliding modes and no stable equilibrium points then the state vector either tends to infinity or towards some non-stationary behavior (possibly a limit cycle).

The Steady-State Characteristic

The extension to computation of the steady-state characteristic is now immediate. For each admissible input u_{eq}, we simply compute the associated equilibrium points x_{eq} (as we have seen above, there might be many) and record the corresponding outputs

$$y_{\text{eq}} = C_i x_{\text{eq}} + c_i + D_i u_{\text{eq}}$$

This results in a steady-state characteristic $\{u_{\text{eq}}, \{y_{\text{eq}}\}\}$.

EXAMPLE 3.2—STEADY-STATE CHARACTERISTIC OF BISTABLE CIRCUIT
As shown in Example 3.1, the bistable electrical circuit exhibits multiple equilibrium points for $u_{\text{eq}} = 1.2$V. By considering the capacitor voltage v_c as an output and performing the static analysis above with $u_{\text{eq}} \in [0, 2]$, we obtain the characteristic shown in Figure 3.2. We see that the system has three equilibrium points for $0.6V \leq u_{\text{eq}} \leq 1.6V$, while it has unique equilibria for

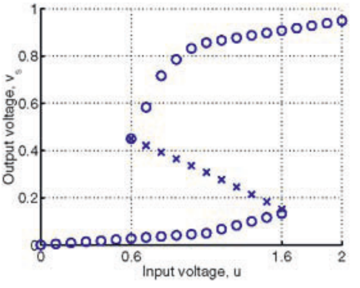

Figure 3.2 Steady-state characteristic showing multiple equilibria for $0.6V \leq u \leq 1.6V$. Local stability of the equilibria is marked by $\circ$, instability marked by $\times$.

other inputs. One equilibrium point is locally unstable (marked $\times$) while the others are locally stable (marked $\circ$). Indeed, the circuit has been used as a computer memory, exploiting the fact that a change in the input voltage can shift the system state from one equilibrium to the other. □

State Transformations

When analyzing the global properties of an equilibrium point, it is often convenient to make a state transformation so that this point is the origin in the transformed coordinates. This transformation is then given by

$$\bar{z} = \begin{bmatrix} x - x_{\mathrm{eq}} \\ 1 \end{bmatrix} = \begin{bmatrix} I & -x_{\mathrm{eq}} \\ 0 & 1 \end{bmatrix} \bar{x} := \mathcal{T}\bar{x}.$$

By applying the state transformation $\bar{x} \mapsto \mathcal{T}^{-1}\bar{z}$, one obtains a piecewise linear system with an equilibrium point at the origin.

3.2 Constraint Verification and Invariance

In practice, it is often desirable to verify that a system satisfies safety constraints in the presence of exogenous disturbances. In this section we will show how a variation of this problem can be studied using vector field considerations and resolved using linear programming.

To this end, consider the piecewise linear system (2.3) and assume that $u(t)$ is an exogenous disturbance that satisfies the magnitude constraint

$$\underline{u} \leq u(t) \leq \overline{u} \qquad \text{for all } t \geq 0 \tag{3.1}$$

but is otherwise arbitrary. Let the set of safe operation be given by

$$\mathcal{O} = \{x \mid Rx + s \succeq 0\} = \{x \mid r_k^T x + s_k \geq 0 \quad k = 1, \ldots, m\} \tag{3.2}$$

We are interested in verifying that all trajectories that originate in $\mathcal{O}$ remain in the set for all future times. We then say that the set $\mathcal{O}$ is *positively invariant* with respect to the dynamics (2.3) (see, *e.g.*, [116, 24]).

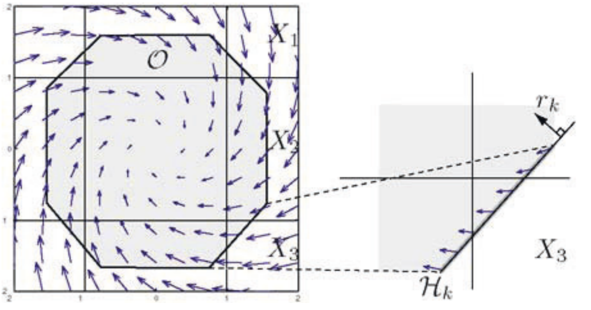

Figure 3.3 Desired invariant set $\mathcal{O}$ (left). Invariance of the individual constraints $r_k^T x + s_k \geq 0$ requires that the vector field is inward at the constraint hyperplane.

Invariance of $\mathcal{O}$ can be addressed by establishing invariance of each individual constraint separately. For each constraint

$$r_k^T x + s_k \geq 0 \tag{3.3}$$

in (3.2), define the associated set of constrained states $\mathcal{H}_k$ as

$$\mathcal{H}_k = \{x \in \mathcal{O} \mid r_k^T x + s_k = 0\}$$

Then, the constraint (3.3) is invariant if and only if

$$\frac{d}{dt}(r_k^T x(t) + s_k) \geq 0 \qquad \text{for all } x(t) \in \mathcal{H}_k \tag{3.4}$$

This condition ensures that if a trajectory approaches the constraint set from within $\mathcal{O}$, the quantity $r_k^T x(t) + s_k$ will increase in value, and the constraint (3.3) will remain being satisfied.

To express the invariance condition (3.4) for a piecewise linear system, define I_k as the set of indices for the cells that intersect the constraint set,

$$I_k = \{i \mid X_i \cap \mathcal{H}_k \neq \emptyset\}.$$

For ease-of-computation, we will require the inequality in (3.4) to be strict. Then, to verify (3.4), we need to verify that

$$r_k^T(A_i x + a_i + B_i u) > 0 \qquad \text{for all } x \in X_i \cap \mathcal{H}_k,\ i \in I_k, \tag{3.5}$$

and all $u \in [\underline{u}, \overline{u}]$. The geometrical interpretation is that the vector field should be inward at $\mathcal{H}_k$, see Figure 3.3. Condition (3.5) is equivalent to establishing that there is no solution x to the inequalities

$$\bar{S}_{ik}(u)\bar{x} := \left[\begin{array}{c|c} S_{ik} & s_{ik}(u) \end{array}\right]\bar{x} = \left[\begin{array}{c|c} -r_k^T A_i & -r_k^T(a_i + B_i u) \\ r_k^T & s_k \\ -r_k^T & -s_k \\ C_s & d_s \\ G_i & g_i \end{array}\right]\bar{x} \succeq 0 \tag{3.6}$$

A direct application of Farkas' lemma now yields the following result.

Proposition 3.2—Constraint Verification
Consider the system (2.3) whose input satisfies the constraint (3.1). If there exists vectors $v_{ik} \succeq 0$ and $w_{ik} \succeq 0$ that satisfy

$$\begin{aligned} v_{ik}^T S_{ik} &= 0 & \qquad v_{ik}^T s_{ik}(\underline{u}) &> 0 \\ w_{ik}^T S_{ik} &= 0 & \qquad w_{ik}^T s_{ik}(\overline{u}) &> 0 \end{aligned}$$

for every $i \in I_s$ and $k \in \{1, \ldots, m\}$, then $\mathcal{O}$ is positively invariant. □

For related results on invariance in piecewise linear systems, see *e.g.*, [39, 49, 92, 173] and the Comments and References section at the end of this chapter.

3.3 Detecting Attractive Sliding Modes on Cell Boundaries

As discussed in Chapter 2, piecewise linear systems with discontinuous right-hand side may exhibit sliding modes on the boundaries between two or more cells. Since the presence of sliding modes complicates the system analysis and challenges the assumptions made in the modeling process, it is important to have tools that detect the presence of attractive sliding modes in a given model. A complete, yet computationally efficient, solution to this problem appears to be out of reach. We have seen how sliding modes can occur on the intersection of multiple boundaries even if the vector fields are not traversal, in which case one needs to do a full stability analysis to assess if the sliding mode is attractive. We will therefore limit our ambition and only consider attractive sliding modes on the $n-1$ dimensional boundaries between two cells. Initially, we consider the case of a ***regular sliding mode***, where the vector fields in both cells point toward the common boundary as in Figure 3.4. The following definition is then natural.

DEFINITION 3.1—REGULAR SLIDING SET
Let $\partial X_{ij} = X_i \cap X_j \subseteq \{x \mid h_{ij}^T x + g_{ij} = 0\}$ be the boundary between cells X_i and X_j, defined such that $h_{ij}^T x + g_{ij} \geq 0$ for $x \in X_i$. The set

$$\mathcal{S}_{ij} = \{x \in \operatorname{int} \partial X_{ij} \mid h_{ij}^T (A_i x + a_i) < 0 \;\wedge\; h_{ij}^T (A_j x + a_j) > 0\}$$

is called the ***regular sliding set*** for (2.3) on ∂X_{ij}. If the set is non-empty, then the system (2.3) has an attractive sliding mode on $\mathcal{S}_{ij}$. □

The following proposition, which shows how attractive sliding modes can be detected by solving a simple linear program, is now immediate.

PROPOSITION 3.3
If the optimal solution $(x^\star, t^\star)$ to the linear programming problem

$$\begin{aligned} &\text{maximize} \quad t \\ &\text{subject to} \quad \begin{bmatrix} G_i \\ G_j \\ -h_{ij}^T A_i \\ h_{ij}^T A_j \end{bmatrix} x + \begin{bmatrix} g_i \\ g_j \\ -h_{ij}^T a_i \\ h_{ij}^T a_j \end{bmatrix} \succeq \begin{bmatrix} 0 \\ 0 \\ t \\ t \end{bmatrix} \end{aligned}$$

has $t^\star > 0$, then (2.3) has a non-empty regular sliding set on ∂X_{ij}. □

A regular sliding mode occurs when the vector fields in both cells point toward the common boundary $\partial X_{ij} = \{x \in X_i \cap X_j \mid h_{ij}^T x + g_{ij} = 0\}$. Sliding modes can also arise when the vector fields are tangent to the boundary, which gives rise to so called ***higher-order sliding modes*** [60]. For example, a second-order sliding mode occurs when the first time-derivative of $h_{ij}^T x$ vanishes on some point on the boundary

$$h_{ij}^T (A_i x + a_i) = h_{ij}^T (A_j x + a_j) = 0 \qquad \text{for some } x \in \partial X_{ij}$$

while the second derivative of $h_{ij}^T x$ is negative for the dynamics in X_i and positive for the dynamics in X_j. A third-order sliding mode occur when the first two derivatives of $h_{ij}^T x$ vanish, *etc.* Similarly to above, these conditions can be used to define higher-order sliding sets and the existence of such a sets on cell boundaries can be verified using linear programming. The resulting conditions are closely related to the well-posedness test for bimodal piecewise linear systems proposed in [87].

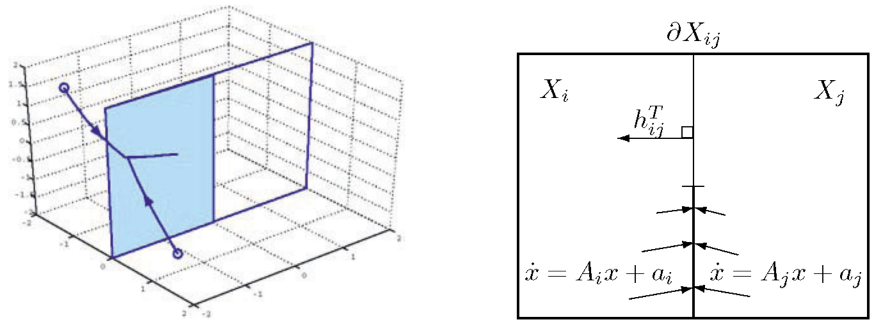

Figure 3.4 Vector fields in neighboring cells point towards the regular sliding set $\mathcal{S}_{ij}$.

3.4 Comments and References

From Signals to Symbols

Vector field considerations are useful for obtaining simplified pictures of the dynamics of piecewise linear systems. By examining the behavior of trajectories on the surfaces of the cells it is sometimes possible to limit the system behavior to a finite number of alternatives. For example, in some cases one may be able to establish that no trajectory that start inside a cell can exit through a certain cell face. Such an analysis gives a natural aggregation of solutions that makes it possible to abstract away detailed information about solutions in order to obtain a simple picture of the global dynamics. This idea has been used in [159] for the construction of "phase-portraits" for high-dimensional piecewise linear systems. Similar ideas have been used in [92] for verification of piecewise linear hybrid systems. Related is also the concept of cell-to-cell mappings, see [84].

Controllability and Observability of Piecewise Linear Systems

The treatment of static gain analysis touches upon the concepts of observability and controllability of piecewise linear systems. These issues have not been investigated within this book. Controllability of a certain class of piecewise linear systems has been treated in [208, 125]. Related is also the more recent work [203].

Constraints and Invariance

Invariant sets is a useful notion in the analysis and design of control systems. Their history in control dates back to the early work of Lyapunov: as any level set of a proper Lyapunov function is invariant, Lyapunov functions can be used to establish invariance of state and control constraints [24, 117, 27]. More recently, invariance have been used in the design of controllers that minimize the peak-to-peak gain (l_∞-induced gain) see [25, 186] and the references therein. These approaches are often based on the same ideas that were used in Section 3.2. Note, however, that the problem of *computing* an invariant set is much more involved than simply verifying that a given polyhedral set is invariant. An efficient approach for computing invariant sets of piecewise linear systems has been developed in [92].

4

Lyapunov Stability

The main contribution of this book is the development of a Lyapunov-based analysis method for piecewise linear systems. The key component of such an analysis, namely methods for Lyapunov function construction, will be presented in this chapter. We will show how piecewise quadratic and piecewise linear Lyapunov functions can be computed via convex optimization. These approaches are substantially more powerful than analysis based on quadratic Lyapunov functions, yet allow the analysis to be be carried out using efficient numerical computations. The application to system analysis and design of optimal control laws is described in the subsequent chapters.

As always, it is a good idea to use "simple things first". After determining the equilibrium points of a piecewise linear system it is advisable to verify local stability properties first. For locally stable equilibrium points, one may invoke the tools developed in this chapter to try to extend the domain of analysis and in many cases establish global results.

4.1 Exponential Stability

Stability is one of the most fundamental properties of dynamical systems. Intuitively, stability is the property that a system does not "blow up". In many control systems, stability alone is not satisfactory but one seeks to achieve asymptotic stability, which ensures that the system state comes to rest after an initial transient. We will focus on the particular case of exponential stability, which guarantees that the convergence of the system state to its equilibrium point can be bounded by an exponential function of time (see, *e.g.*, [116] for precise definitions).

There are certainly many asymptotically stable systems whose convergence is not exponential. Still the framework of exponential stability is particularly attractive for Lyapunov-based analysis of piecewise linear systems. For smooth nonlinear systems, an equilibrium point is locally exponentially

M. Johansson: Piecewise Linear Control Systems, LNCIS 284, pp. 41-84, 2003.

stable if and only if its linearization around this point is exponentially stable ([116, Theorem 3.13]). In other words, the linearization provides necessary and sufficient information about local exponential stability. Moreover, a smooth nonlinear system is globally exponentially stable if and only if there exists a Lyapunov function that proves it ([116, Theorem 3.12]).

The following result, which combines a number of standard results from Lyapunov theory, will be the main tool throughout this chapter.

LEMMA 4.1
Let $x(t) : [0, \infty) \longrightarrow \mathbb{R}^n$ and let and let $V(t) : [0, \infty) \longrightarrow \mathbb{R}$ be a non-increasing and piecewise $\mathcal{C}^1$ function satisfying

$$\frac{d}{dt} V(t) \leq -\gamma \|x(t)\|^p \tag{4.1}$$

for some $\gamma > 0$ and some $p > 0$, almost everywhere on $[0, \infty)$.
If there exists $\alpha > 0$ such that

$$\alpha \|x(t)\|^p \leq V(t) \leq \beta \|x(t)\|^p \tag{4.2}$$

then $\|x(t)\|$ tends to zero exponentially. If the maximal α that satisfies (4.2) is negative, then $\|x(t)\| \to \infty$ as $t \to \infty$. □

Proof: See Section B.2.

Note that the above result allows both verification of exponential stability and detection of instabilities. Moreover, the formulation does not require that $V(t)$ be continuous as long as the value of $V(t)$ decreases at the points of discontinuity.

4.2 Quadratic Stability

The term *quadratic stability* refers to stability that can be established using a quadratic Lyapunov function. Quadratic stability dates back to the pioneering work of Lyapunov [133, 134] who established that the existence of a quadratic Lyapunov function is a necessary and sufficient condition for asymptotic stability of a linear system. Quadratic Lyapunov functions are often the first resort also in the analysis of nonlinear systems and much work on absolute stability is based on quadratic Lyapunov functions (see, *e.g.*, [45, 27]).

Quadratic Stability for Local Linear Analysis

To verify exponential stability of a nonlinear system one may start by establishing stability of its linearization. This is often done by eigenvalue inspection. One drawback of this approach is that one has no idea about the domain of validity of the analysis and exponential convergence can only be guaranteed for trajectories starting very close to the equilibrium. A useful addition to a local stability analysis is to also have an estimate of the ***domain of attraction*** of the equilibrium point, *i.e.*, the set of initial values from which trajectories are guaranteed to converge to the equilibrium. In the piecewise linear framework the domain of validity of the linearization is incorporated in the model. By using Lyapunov function computations rather than eigenvalue inspection it is then possible to compute a guaranteed domain of attraction. The following theorem establishes exponential stability of an equilibrium point and also returns the largest domain of attraction that can be guaranteed by a local analysis using quadratic Lyapunov functions.

PROPOSITION 4.1—[27]
Let $\dot{x} = Ax$ be valid in the polyhedron $X_0 = \{x \mid g_k^T x \leq 1, \quad k = 1, \dots, p\}$. The origin is exponentially stable if and only if the convex optimization problem

$$\begin{array}{ll} \text{minimize} & \log\det Q^{-1} \\ \text{subject to} & 0 < Q \\ & 0 > QA^T + AQ \\ & 1 \geq g_k^T Q^T g_k \qquad k = 1, \dots, p. \end{array}$$

has a solution. Moreover, the ellipsoid $\mathcal{E}_{\mathrm{roa}} = \{x \mid x^T Q^{-1} x \leq 1\}$ is the domain of attraction with largest volume in X_0 that can be estimated using any quadratic Lyapunov function. □

Proof: See [27, Section 5.2.2].

The strength of this result is that the computations, in addition to verifying exponential stability, return the largest region of attraction that can be estimated using *any* quadratic Lyapunov function. In most cases, this domain is substantially larger than what may be obtained by simply solving the Lyapunov equation

$$A^T P + PA = -R \tag{4.3}$$

for some arbitrary chosen positive definite matrix R. This is illustrated in the following example.

EXAMPLE 4.1—LOCAL ANALYSIS OF SATURATED SYSTEM
Consider the saturated linear system of Example 2.1,

$$\dot{x} = Ax + b\text{sat}(k^T x)$$

and let

$$A = \begin{bmatrix} 0 & 1 \\ 0 & 0 \end{bmatrix}, \qquad b = \begin{bmatrix} 0 \\ 1 \end{bmatrix}, \qquad k = \begin{bmatrix} -2 \\ -3 \end{bmatrix}.$$

By restricting the analysis to the unsaturated region, the polyhedron $|k^T x| \leq 1$, we can use Proposition 4.1 to verify exponential stability of the origin. The analysis returns the region of attraction shown in dashed lines in Figure 4.1. If we simply solve the Lyapunov equation (4.3) with $R = I$, we can only guarantee exponential stability of trajectories starting within the (much smaller) domain shown as the filled ellipsoid in Figure 4.1. □

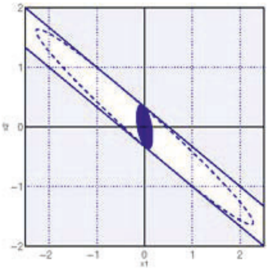

Figure 4.1 Linear (white) and saturated (shaded) regions in the state space. The larger region of attraction is computed via Proposition 4.1, while the smaller (filled) ellipsoid is the stability domain obtained by solving the Lyapunov equation (4.3) with $R = I$.

Although Proposition 4.1 guarantees a much larger region of attraction than the Lyapunov equation approach, the result is still very weak. In fact, the saturated system is globally asymptotically stable (we will prove this in Chapter 7, where we also develop specialized methods for estimating regions of attraction for linear systems with saturation). One of the reasons for the disappointing performance is that we have only analyzed the behaviour in the unsaturated region. It is possible that the computed Lyapunov function would be able to verify stability also for the saturated regions, but since these have not been accounted for in the analysis no such conclusion can be drawn. This situation will appear repeatedly when we compute Lyapunov functions on a restricted domain: stability can only be granted for trajectories whose initial values lie within the largest level set of the computed Lyapunov function that is fully contained in the analysis region.

Quadratic Stability for Global Nonlinear Analysis

Quadratic Lyapunov functions are often the first resort also for analysis of nonlinear systems. Many of these methods are somehow related to the analysis of the ***linear differential inclusion***

$$\dot{x} \in \overline{\mathrm{co}}\{A_1 x, \ldots, A_L x\}. \tag{4.4}$$

In other words, they are related to the analysis of the family of linear time-varying systems that can be written as

$$\dot{x} = A(t)x = \sum_{i=1}^{L} \alpha_i(t) A_i x(t) \tag{4.5}$$

where $\alpha_i(t)$ are arbitrarily time-varying weights that satisfy $\alpha_i(t) \geq 0$ and $\sum_{i=1}^{L} \alpha_i(t) = 1$. The following result is central [83, 30].

PROPOSITION 4.2
Consider the system (4.4). If the convex optimization problem

$$\begin{cases} 0 < P = P^T \\ 0 > A_i^T P + P A_i \qquad i = 1, \ldots, L \end{cases} \tag{4.6}$$

has a solution, then the origin is globally exponentially stable. □

Proof: See Section B.2.

Note that Proposition 4.2 only gives sufficient conditions for stability. Since the Lyapunov function search in Proposition 4.2 is a convex optimization problem a solution P can always be found if it exists. The conservatism comes from the fact that quadratic Lyapunov functions are only sufficient for establishing stability of linear differential inclusions [142].

The main advantage of Proposition 4.2 is that the search for a quadratic Lyapunov function has been formulated as a convex optimization problem. The computational complexity for solving the inequalities in Proposition 4.2 grows gracefully with the number of extreme systems L, and solving the multiple Lyapunov inequalities is not much more demanding than solving a single Lyapunov equation, see [205, 27]

There have been many applications of the above results to systems with piecewise linear dynamics, see for example the work on fuzzy systems [195, 219] which can be embedded in the linear time varying formulation (4.5) by the appropriate restrictions. The application to piecewise linear systems typically takes the following form.

COROLLARY 4.1
Consider the system (2.3), and assume that $a_i = 0$ for every $i \in I$. If the convex optimization problem (4.6) has a solution, then every trajectory $x(t) \in \cup_{i \in I} X_i$ of (2.3) with $u \equiv 0$ tends to zero exponentially. □

Proof: See Section B.2.

In some cases, it is of interest to verify that no common solution P to the conditions of Proposition 4.2 exists. This verification can be done by solving the following dual problem (*cf.* [14]).

PROPOSITION 4.3
If there exists positive definite matrices R_i satisfying

$$\begin{cases} 0 < R_i = R_i^T \\ 0 < \displaystyle\sum_{i=1}^{L} (R_i A_i^T + A_i R_i) \end{cases} \qquad \text{for } i = 1, \ldots, L \tag{4.7}$$

then there exists no solution to the LMIs of Proposition 4.2. □

Proof: See Section B.2.

4.3 Conservatism of Quadratic Stability

Although computationally attractive, several issues make the quadratic stability analysis of piecewise linear systems given in Corollary 4.1 very conservative. A first limitation is that no affine terms are permitted in the dynamics so that a simple system such as the saturated control system in Example 4.1 can not be analyzed as it stands. A second issue is that no information about the partition is used in the analysis. Rather than exploiting that each system of differential equations only describes the system dynamics in a restricted part of the state space, the piecewise linear dynamics is embedded in a global differential inclusion. The following example illustrates the limitations of this approach.

EXAMPLE 4.2—THE NEED FOR USING PARTITION INFORMATION
Consider the piecewise linear system

$$\dot{x} = \begin{cases} \begin{bmatrix} -0.1 & 1 \\ -10 & -0.1 \end{bmatrix} x & x_1 x_2 \geq 0 \\ \begin{bmatrix} -0.1 & 10 \\ -1 & -0.1 \end{bmatrix} x & x_1 x_2 < 0 \end{cases} \tag{4.8}$$

The system matrices are stable and have the same eigenvalues. The simulation shown in Figure 4.2 indicates that the system is stable.

It is straightforward to verify that $V(x) = x^T x$ is a Lyapunov function for the system. Still, an application of Proposition 4.2 fails. Since the matrices

$$R_1 = \begin{bmatrix} 2 & -1 \\ -1 & 2 \end{bmatrix} \qquad R_2 = \begin{bmatrix} 2 & 1 \\ 1 & 2 \end{bmatrix}$$

satisfy the conditions in Proposition 4.2 this failure is fundamental (and not an artifact of numerical optimization). We can understand the reason for this failure by interchanging the system matrices in the model (4.8). Simulating this system yields unbounded trajectories, see Figure 4.2. Since stability depends on the partition, Proposition 4.2 cannot be used to establish stability. At the end of this chapter we will return to this example with a more powerful tool set and prove stability of the initial setup. □

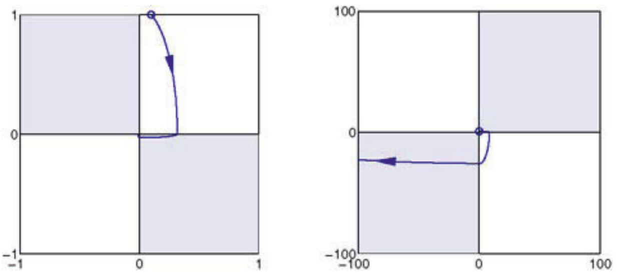

Figure 4.2 The original setup (left) is exponentially stable, while interchanging the two system matrices gives an unstable system (right; note the different scalings!). Thus, stability can not be proved without taking the structural information into account.

A third limitation is of course that many systems do not admit a quadratic Lyapunov function. The following example illustrates a simple system that cannot be analyzed using quadratic Lyapunov functions.

EXAMPLE 4.3—THE NEED FOR NON-QUADRATIC LYAPUNOV FUNCTIONS
Consider the piecewise linear system $\dot{x}(t) = A_i x(t)$ with the cell partition shown in Figure 4.3 and system matrices

$$A_1 = A_3 = \begin{bmatrix} -\epsilon & \omega \\ -\alpha\omega & -\epsilon \end{bmatrix}, \qquad A_2 = A_4 = \begin{bmatrix} -\epsilon & \alpha\omega \\ -\omega & -\epsilon \end{bmatrix}.$$

Letting $\alpha = 5$, $\omega = 1$ and $\epsilon = 0.1$, a simulation with initial value $x_0 = (-2,\ 0)$ generates the trajectory shown in Figure 4.3. Clearly, no quadratic Lyapunov function can generate level sets with the property that once a trajectory enters a level set, it remains in this set for all future times. Hence, there is no obvious quadratic Lyapunov function that can establish asymptotic stability.

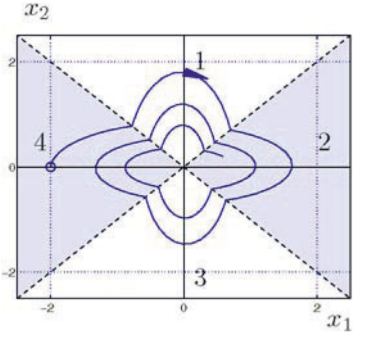

Figure 4.3 Simulated trajectory (full) and cell boundaries (dashed) in Example 4.3.

□

As illustrated above, the computational convenience of quadratic stability analysis of piecewise linear systems is out-weighted by its many limitations. The analysis conditions do not permit affine terms in the dynamics, and even very basic piecewise linear systems cannot be treated as they stand. The use of partition information can be critical for establishing stability, yet it is completely disregarded in Corollary 4.1. Finally, it can be very conservative to only consider quadratic Lyapunov functions.

In the remaining parts of this chapter we will develop an approach that does not suffer from these shortcomings. The method will be based on non-quadratic Lyapunov functions, exploit partition information and allow for affine terms in the dynamics. All analysis conditions will be formulated as convex optimization problems, allowing complex piecewise linear systems to be analyzed using efficient numerical computations.

4.4 From Quadratic to Piecewise Quadratic

To find inspiration for alternatives to the globally quadratic Lyapunov functions, we will analyze the simple selector control system shown in Figure 4.4. Selector control is a common strategy for constraint handling in the process industry (see, *e.g.*, [8, 59, 31]) that often results in closed-loop systems with piecewise linear dynamics.

Consider the set-up shown in Figure 4.4 (left) and assume that G_0 is a linear system described by the state-space equations $\dot{x} = A_0 x + Bu$. The

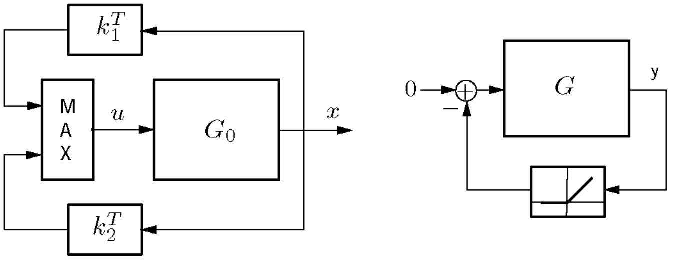

Figure 4.4 Selector control system (left) transformed into feedback form (right).

closed-loop dynamics can then be written as

$$\dot{x} = A_0 x + B \max\left(k_1^T x, k_2^T x\right) = (A_0 + Bk_2^T)x + B \max\left((k_1 - k_2)^T x, 0\right)$$

Letting $A = A_0 + Bk_2^T$ and $k = k_1 - k_2$, we can re-write the dynamics as

$$\dot{x} = Ax + B \max\left(k^T x, 0\right) \tag{4.9}$$

The system is clearly piecewise linear, and can be written as

$$\dot{x} = \begin{cases} Ax & \text{if} \quad k^T x \le 0 \\ (A + Bk^T)x & \text{if} \quad k^T x \ge 0 \end{cases}$$

Now, consider the specific system defined by

$$A = \begin{bmatrix} -5 & -4 \\ -1 & -2 \end{bmatrix}, \qquad B = \begin{bmatrix} 3 \\ 21 \end{bmatrix}, \qquad k = \begin{bmatrix} 1 \\ 0 \end{bmatrix}.$$

By solving the dual problem stated in Proposition 4.3 one can verify that there is no globally quadratic Lyapunov function $V(x) = x^T Px$ that verifies stability of the system. Still, the simulations shown in Figure 4.5 indicate that the system is stable.

As an alternative to a globally quadratic Lyapunov function it is natural to consider the following Lyapunov function candidate

$$V(x) = \begin{cases} x^T Px, & \text{if } k^T x \le 0 \\ x^T Px + \eta(k^T x)^2, & \text{if } k^T x \ge 0 \end{cases} \tag{4.10}$$

where P and $\eta \in \mathbb{R}$ are chosen so that both quadratic forms are positive definite. Note that the Lyapunov function candidate is constructed to be continuous and piecewise quadratic. The search for appropriate values of η and

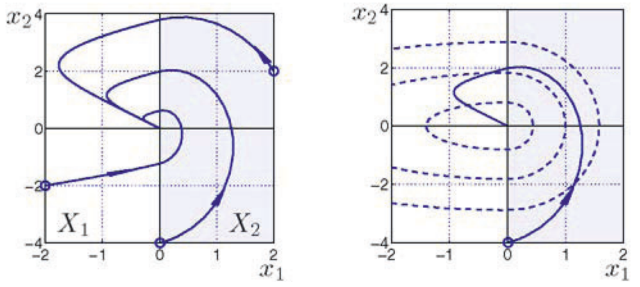

Figure 4.5 Trajectories in the phase plane of the selector control system.

P can be done by solving the following linear matrix inequalities

$$
\begin{aligned}
P = P^T &> 0, & P + \eta k k^T &> 0, \\
A^T P + PA &< 0 & (A + Bk^T)^T (P + \eta k k^T) + (P + \eta k k^T)(A + Bk^T) &< 0.
\end{aligned}
$$

One feasible solution is given by $P = \text{diag}\{1, 3\}$ and $\eta = 9$, which establishes exponential stability of the system. The level surfaces of the computed Lyapunov function are indicated in Figure 4.5.

Relation to Frequency Domain Criteria

It is instructive to compare this solution with what can be achieved using frequency domain methods such as the circle and Popov criteria. In order to put the system in negative feedback form, we re-write (4.9) as

$$
\dot{x} = Ax - (-B)\max\left(k^T x, 0\right) \tag{4.11}
$$

Defining $G(s) = -k^T(sI - A)^{-1}B$, we obtain the frequency condition

$$
\text{Re } G(i\omega) > -1, \qquad \forall \omega \in [0, \infty]
$$

for the circle criterion and

$$
\text{Re } [(1 + i\omega\eta)G(i\omega)] > -1, \qquad \forall \omega \in [0, \infty]
$$

for the Popov criterion. Inspection of the Nyquist and Popov plots of Figure 4.6 reveals that stability follows from the Popov criterion but not from the circle criterion.

The failure of the circle criterion comes as no surprise, since it relies on the existence of a common quadratic Lyapunov function (see, *e.g.*, [116])

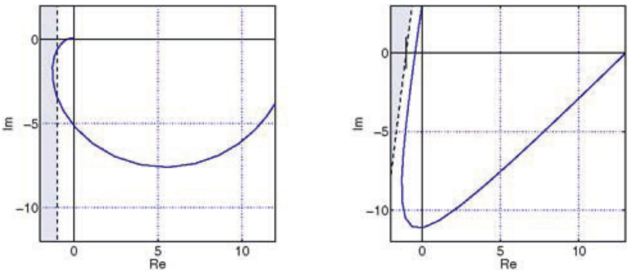

Figure 4.6 The circle criterion (left) fails to prove stability. The Popov plot (right) is separated from -1 by a straight line of slope $1/\eta$. Hence stability follows.

which we know does not exist. The Popov criteria, on the other hand, is based on the Lyapunov function

$$V(x) = x^T P x + 2\eta \int_0^z \varphi(\sigma)\, d\sigma. \tag{4.12}$$

By evaluating this function for $\varphi(\sigma) = \max(\sigma, 0)$ and $z = k^T x$, one recovers the Lyapunov function candidate (4.10) used in the optimization above.

It is not hard to establish that all Lyapunov function of Lure-type

$$V(x) = x^T P x + \int_0^z \varphi(\sigma)\, d\sigma$$

constructed from piecewise linear functions $\varphi(\sigma)$ are continuous and piecewise quadratic. However, rather than tailoring the analysis to linear systems interconnected with scalar nonlinearities we will aim for results that are applicable to general piecewise linear systems. Motivated by the examples above, we will employ Lyapunov functions that are continuous and piecewise quadratic.

4.5 Interlude: Describing Partition Properties

In order to generalize the ideas used in the motivating example we need to be able to construct continuous piecewise quadratic functions on general polyhedral partitions and we need to be able to enforce positivity (and negativity) of such functions. In this section, we will introduce a matrix parameterization of continuous piecewise quadratic functions and describe a computational procedure for enforcing positivity.

A Parameterization of Continuous Piecewise Quadratic Functions

Our analysis will be based on Lyapunov functions that are continuous and piecewise quadratic. A fundamental problem in the search for such functions is how the continuity constraint should be enforced on the Lyapunov function candidate. One potential solution would be to patch together piecewise quadratics "by hand", as was done in the analysis of the selector system. If we only require continuity of the piecewise quadratics, we can allow less restrictive updates in the quadratic forms than $\eta k k^T$ used above. To illustrate this, let

$$V(x,i) = x^T P_i x + 2q_i^T x_i + r_i = \begin{bmatrix} x \\ 1 \end{bmatrix}^T \begin{bmatrix} P_i & q_i \\ q_i^T & r_i \end{bmatrix} \begin{bmatrix} x \\ 1 \end{bmatrix} := \bar{x}^T \bar{P}_i \bar{x}$$

be the quadratic expression used to describe $V(x)$ for $x \in X_i$. Consider two cells X_i and X_j with boundary hyperplane $\partial\mathcal{H}_{ij} = \{x \mid h_{ij}^T x + g_{ij} = 0\}$. To obtain continuity across the boundary hyperplane

$$V(x,j) = V(x,i) \qquad\qquad \forall x \in \partial\mathcal{H}_{ij}$$

there must exist $t_{ij} \in \mathbb{R}^n$ and $s_{ij} \in \mathbb{R}$ such that

$$V(x,j) = V(x,i) + 2(h_{ij}^T x + g_{ij})(t_{ij}^T x + s_{ij}).$$

Letting $\bar{h}_{ij} = \begin{bmatrix} h_{ij}^T & g_{ij} \end{bmatrix}^T$ and $\bar{t}_{ij} = \begin{bmatrix} t_{ij}^T & s_{ij} \end{bmatrix}^T$ this condition reads

$$\bar{P}_j = \bar{P}_i + \bar{h}_{ij}\bar{t}_{ij}^T + \bar{t}_{ij}\bar{h}_{ij}^T. \tag{4.13}$$

Since each cell boundary induces a new equality constraint on the form (4.13) it is very cumbersome to construct explicit expressions for the matrices $\bar{P}_i$ other than in very simple examples. An alternative is to simply view (4.13) as an equality constraint in the variables $\bar{P}_i$, $\bar{P}_j$ and $\bar{t}_{ij}$ that the optimization software should deal with. However, as of today, very few SDP solvers treat equality constraints (see the Comments and References section at the end of this chapter for more details).

We will therefore introduce a compact matrix parameterization of continuous piecewise quadratic functions on polyhedral partitions. This will allow our analysis procedures to be implemented in widely available SDP solvers. The parameterization is based on continuity matrices, defined as follows:

Definition 4.1—Continuity Matrix
A matrix $\bar{F}_i = [F_i \quad f_i]$ is a *continuity matrix* for cell X_i if

$$\bar{F}_i \bar{x}(t) = \bar{F}_j \bar{x}(t) \qquad \text{for } x(t) \in X_i \cap X_j. \tag{4.14}$$

Furthermore, we say that $\{\bar{F}_i\}$ have the *zero interpolation property* if

$$f_i = 0 \qquad \text{for } i \in I_0. \tag{4.15}$$

□

A compact matrix parameterization of continuous piecewise quadratic functions can now be obtained as follows.

LEMMA 4.2—PWQ PARAMETERIZATION
Let $\{X_i\}_{i\in I}$ be a polyhedral partition, and let $\bar{F}_i \in \mathbb{R}^{p\times(n+1)}$ be continuity matrices that satisfy (4.14). Then, for each $T \in \mathbb{R}^{p\times p}$, the scalar function

$$V(x) = \bar{x}^T \bar{F}_i^T T \bar{F}_i \bar{x} := \bar{x}^T \bar{P}_i \bar{x} \qquad \text{for } x \in X_i. \tag{4.16}$$

is continuous and piecewise quadratic. Moreover, if $\{\bar{F}_i\}$ have the zero interpolation property, then there exist α and β such that

$$\alpha \|x\|_2^2 \le V(x) \le \beta \|x\|_2^2. \tag{4.17}$$

□

Proof: See Section B.2.

Note that the continuity matrices for a given partition are not unique. For example, if we use the following continuity matrix in all regions

$$\bar{F}_i = \begin{bmatrix} I_{n\times n} & 0_{n\times 1} \end{bmatrix} \qquad\qquad i \in I.$$

the parameterization suggested in Lemma 4.2 results in a Lyapunov function candidate that is globally quadratic. Clearly, one would like a way of constructing the continuity matrices that gives maximal freedom in the Lyapunov function search. Procedures for computing continuity matrices for a given piecewise linear system are described in Appendix A. The following example illustrates one choice of continuity matrices for the saturated system from Example 2.1.

EXAMPLE 4.4—CONTINUITY MATRICES FOR SATURATED SYSTEM
The following matrices are natural continuity matrices for the saturated feedback system in Example 2.1.

$$\bar{F}_1 = \begin{bmatrix} -k^T & -1 \\ 0_{1\times n} & 0 \\ I_{2\times 2} & 0 \end{bmatrix}, \qquad \bar{F}_2 = \begin{bmatrix} 0_{1\times n} & 0 \\ 0_{1\times n} & 0 \\ I_{2\times 2} & 0 \end{bmatrix}, \qquad \bar{F}_3 = \begin{bmatrix} 0_{1\times n} & 0 \\ k^T & -1 \\ I_{2\times 2} & 0 \end{bmatrix}.$$

Note that the matrices have the zero interpolation property and that a Lyapunov function candidate constructed as in Lemma 4.2 has no affine terms in the region that contains the origin. □

Verifying Positivity of a Quadratic Function on a Polyhedron

In order for a function to satisfy the conditions of Lemma 4.1, we need to enforce that the function is positive and that its time-derivative is negative. For piecewise quadratic functions, the positivity condition reads

$$\bar{x}^T \bar{P}_i \bar{x} > \alpha \|x\|_2^2 \qquad \forall x \in X_i, \quad i \in I \tag{4.18}$$

Hence, for each i we need to verify that there exists a positive scalar α such that $\bar{x}^T \bar{P}_i \bar{x} - \alpha x^T x$ is positive on X_i. We know from Example 4.2 that it is critical to exploit the partition information and that it is too restrictive to require that the expression is positive for all $x \in \mathbb{R}^n$. To support the computations, we define polyhedral cell boundings as follows.

Definition 4.2—Polyhedral Cell Bounding
A matrix $\bar{E}_i = [E_i \quad e_i]$ is called a ***polyhedral cell bounding*** if it satisfies

$$\bar{E}_i \bar{x}(t) \succeq 0 \qquad \text{for } x(t) \in X_i. \tag{4.19}$$

Furthermore, we say that $\{\bar{E}_i\}$ have the zero interpolation property if

$$e_i = 0 \qquad \text{for } i \in I_0. \tag{4.20}$$

□

Verifying positivity of a piecewise quadratic function on a polyhedral partition can now be done using the following result.

Lemma 4.3
Consider the piecewise quadratic function

$$V(x) = \begin{cases} x^T P_i x & x \in X_i,\ i \in I_0 \\ \bar{x}^T \bar{P}_i \bar{x} & x \in X_i,\ i \in I_1 \end{cases} \tag{4.21}$$

with $P_i = P_i^T$, $\bar{P}_i = \bar{P}_i^T$, and let $\bar{E}_i$ be cell boundings satisfying (4.19) and (4.20). If there exist matrices W_i with nonnegative entries such that

$$P_i - E_i^T W_i E_i > 0 \qquad i \in I_0 \tag{4.22}$$

$$\bar{P}_i - \bar{E}_i^T W_i \bar{E}_i > 0 \qquad i \in I_1 \tag{4.23}$$

then there exists $\alpha > 0$ such that $V(x) > \alpha \|x\|_2^2$ for all $x \in X$. □

Proof: See Section B.2.

The technique used in Lemma 4.3 is known as the S-procedure and is treated in more detail in Appendix A. The method is conservative in general, but appears to work very well in practice.

There is a direct relationship between cell identifiers and cell boundings. The key difference is that cell boundings use linear forms for bounding cells that contain the origin. This will be critical for formulating analysis procedures using strict LMIs. In Appendix A we give a simple algorithm for translating cell identifiers to cell boundings and show that this step does not introduce any conservatism in the Lyapunov function search. The following example illustrates cell boundings for the saturated system.

EXAMPLE 4.5—CELL BOUNDINGS FOR SATURATED SYSTEM

The following matrices are cell boundings for the saturated system

$$\bar{E}_1 = \begin{bmatrix} -k^T & -1 \\ 0_{1\times n} & 1 \end{bmatrix}, \qquad \bar{E}_2 = \begin{bmatrix} 0_{1\times n} & 0 \\ 0_{1\times n} & 0 \end{bmatrix}, \qquad \bar{E}_3 = \begin{bmatrix} k^T & -1 \\ 0_{1\times n} & 1 \end{bmatrix}.$$

Moreover, these cell boundings have the zero interpolation property. □

4.6 Piecewise Quadratic Lyapunov Functions

The previous section has laid the grounds for analysis of piecewise linear systems using piecewise quadratic Lyapunov functions. In Lemma 4.2 we proposed a matrix parameterization of continuous piecewise quadratic functions and in n Lemma 4.3 we showed how it is possible to express the condition that the function be positive on the partition using linear matrix inequalities. We will now combine these results to formulate the search for piecewise quadratic Lyapunov functions on the form

$$V(x) = \begin{cases} x^T P_i x & \text{for } x \in X_i, i \in I_0 \\ \begin{bmatrix} x \\ 1 \end{bmatrix}^T \bar{P}_i \begin{bmatrix} x \\ 1 \end{bmatrix} = x^T P_i x + 2q_i^T x + r_i & \text{for } x \in X_i, i \in I_1. \end{cases} \tag{4.24}$$

We have the following result.

THEOREM 4.1—PIECEWISE QUADRATIC STABILITY
Consider symmetric matrices T, U_i and W_i such that U_i and W_i have non-negative entries, while

$$\begin{aligned} P_i &= F_i^T T F_i, && i \in I_0 \\ \bar{P}_i &= \bar{F}_i^T T \bar{F}_i, && i \in I_1 \end{aligned}$$

satisfy

$$\begin{cases} 0 > A_i^T P_i + P_i A_i + E_i^T U_i E_i \\ 0 < P_i - E_i^T W_i E_i \end{cases} \qquad i \in I_0$$

$$\begin{cases} 0 > \bar{A}_i^T \bar{P}_i + \bar{P}_i \bar{A}_i + \bar{E}_i^T U_i \bar{E}_i \\ 0 < \bar{P}_i - \bar{E}_i^T W_i \bar{E}_i \end{cases} \qquad i \in I_1$$

Then every trajectory $x(t) \in \cup_{i \in I} X_i$ satisfying (2.3) with $u \equiv 0$ for all $t \geq 0$ tends to zero exponentially. □

Proof: See Section B.2.

In the absence of attractive sliding modes, the above conditions ensure that (4.24) is a Lyapunov function for the system. If the partition X is positively invariant then every trajectory that starts in X tends to zero exponentially. In particular, if the partition covers the whole state space then the system is globally exponentially stable. Even if invariance of X cannot be established, any level set of $V(x)$ that is fully contained in the partition is a region of attraction for the equilibrium point $x = 0$.

With the piecewise quadratic stability theorem at hand we can now return to the motivating examples where the standard LMI conditions for quadratic stability fail.

EXAMPLE 4.6—PIECEWISE QUADRATIC WHERE QUADRATIC FAILS – I
Consider the system (4.8) in Example 4.2. Let E_i denote the cell bounding used in quadrant i. Letting

$$E_1 = -E_3 = \begin{bmatrix} 1 & 0 \\ 0 & 1 \end{bmatrix}, \qquad E_2 = -E_4 = \begin{bmatrix} -1 & 0 \\ 0 & 1 \end{bmatrix},$$

and $F_i = \begin{bmatrix} E_i^T & I_n \end{bmatrix}^T$ we invoke Theorem 4.1 and find a feasible solution

$$V(x) = x^T x \qquad\qquad x \in X_i, i \in I.$$

Hence, stability can indeed be established using a quadratic Lyapunov function but it is critical to use partition information in the Lyapunov function search. The level curves of the computed Lyapunov function are shown together with a simulation in Figure 4.7(left). □

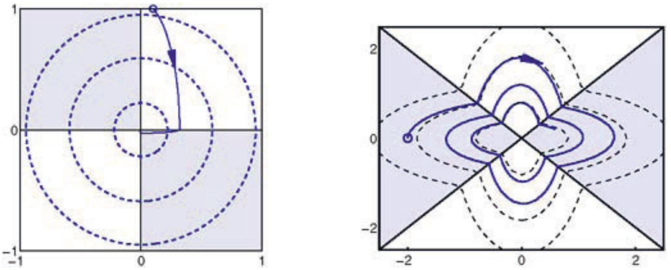

Figure 4.7 Level surfaces (dashed) for the systems in Example 4.2 and Example 4.3 computed using Theorem 4.1. In both cases, the standard conditions for quadratic stability fail while Theorem 4.1 verifies stability.

EXAMPLE 4.7—PIECEWISE QUADRATIC WHERE QUADRATIC FAILS – II
As a second example, consider the system with flower-like trajectories used in Example 4.3. Similarly as above, we let

$$E_1 = -E_3 = \begin{bmatrix} -1 & 1 \\ -1 & -1 \end{bmatrix}, \qquad E_2 = -E_4 = \begin{bmatrix} -1 & 1 \\ 1 & 1 \end{bmatrix},$$

and $F_i = \begin{bmatrix} E_i^T & I_n \end{bmatrix}^T$. From the conditions of Theorem 4.1 we find the piecewise quadratic Lyapunov function $V(x) = x^T P_i x$ with

$$P_1 = P_3 = \begin{bmatrix} 5 & 0 \\ 0 & 1 \end{bmatrix}, \qquad P_2 = P_4 = \begin{bmatrix} 1 & 0 \\ 0 & 5 \end{bmatrix}.$$

As seen in Figure 4.7(right), the level surfaces of the computed Lyapunov function are neatly tailored to the system trajectories. □

Analysis of a Min-Max Selector System

The examples analyzed so far have been small examples in two dimensions, constructed to illustrate the shortcomings of quadratic and merits of piecewise quadratic Lyapunov functions. Our next example is motivated by industrial applications, has higher state dimension (seven continuous states), and a nonlinearity that is not easily dealt with using alternative techniques.

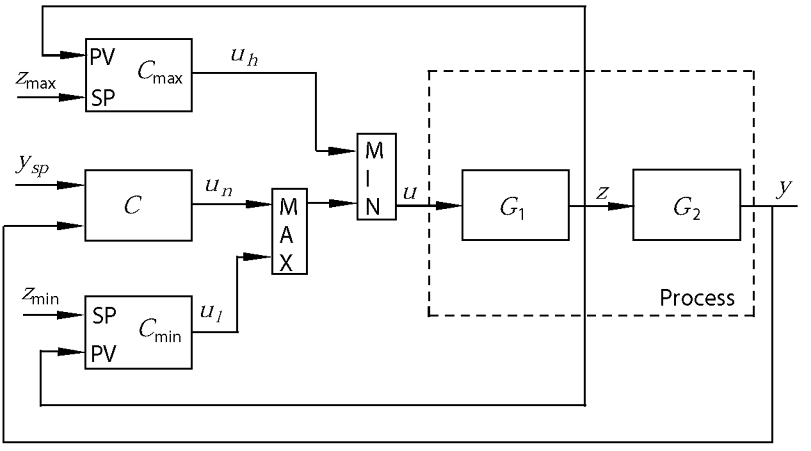

Figure 4.8 Control system with min/max selectors, from [8].

The example is the min-max selector control system shown in Figure 4.8. This scheme is common in situations where several process variables have to be taken into account using a single control signal. In Figure 4.8, y is the primary variable and z is a process variable that must remain within given ranges. The controller C is designed to control the primary variable while the controllers $C_{\max}$ and $C_{\min}$ are designed to keep the critical variable z within certain bounds. Designed correctly, the min-max selector chooses the controller that is most appropriate for the situation and allows good control of the primary variable while respecting the constraints.

Consider a system characterized by

$$G_1(s) = \frac{40}{0.05s^3 + 2s^2 + 22s + 40},$$
$$G_2(s) = \frac{5}{s^2 + 7s + 5}.$$

To control the primary variable, we design a lead-lag controller

$$C(s) = \frac{s^2 + 3s + 3}{0.02s^2 + s + 0.01},$$

while $C_{\min}$ and $C_{\max}$ are proportional controllers

$$u_h = K_h(z_{\max} - z),$$
$$u_l = K_l(z_{\min} - z).$$

The plots in Figure 4.9 show a simulation of the system without constraint controllers. The tracking of the primary variable is quite good, but the critical variable z exceeds it constraint limits (shown in dashed lines). The plots in Figure 4.10 show a simulation of the min-max selector strategy. The constraints are now respected while the tracking of the primary variable remains satisfactory.

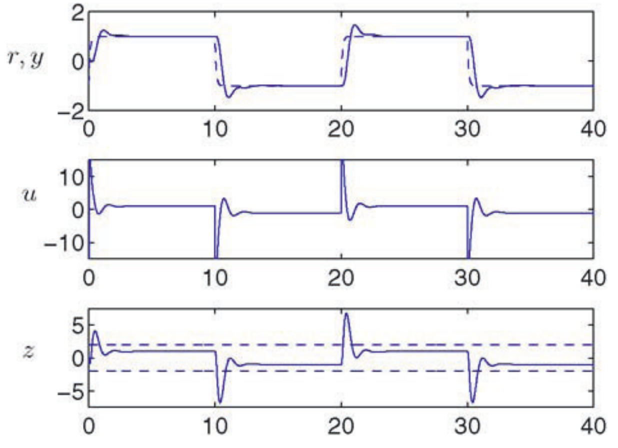

Figure 4.9 Simulation of the control system in Figure 4.8 without constraint handling. The tracking of the primary variable is quite good (top), but the critical variable exceeds it limits (bottom).

We will apply Theorem 4.1 to stability analysis of the system for a constant set-point y_{sp} and constant constraint limits z_{min}, z_{max}. Different values of y_{sp}, z_{min} and z_{max} result in different equilibrium points. For sake of simplicity, we will let $y_{sp} = z_{max} = z_{min} = 0$, but the technique would apply similarly to any choice of constant inputs.

For analysis purposes, it is convenient to re-write the system equations as a linear system interconnected with the static nonlinearity

$$u = \min\left(u_h, \max\left(u_n, u_l\right)\right).$$

The selector nonlinearity has three input signals u_h, u_n, u_l and one output, u. Similarly to the selector system used as motivating example in Section 4.4, we can reduce the number of inputs by one using a simple loop transformation. This results in the system shown in Figure 4.11. The transformed system has two outputs, v_{hl} and v_{nl}, and the selector nonlinearity is now reduced to the two-dimensional mapping $\varphi(v_{hl}, v_{nl})$ shown in Figure 4.12.

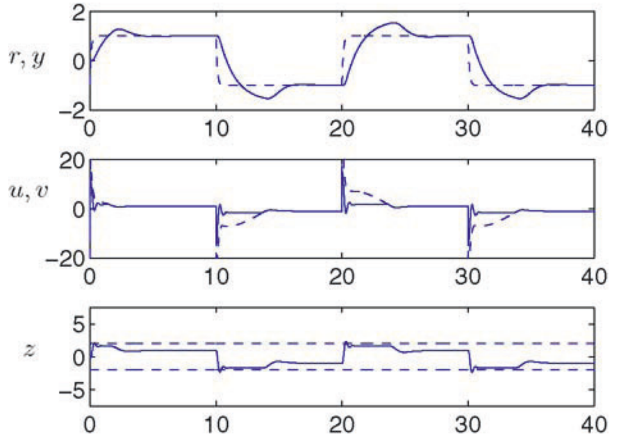

Figure 4.10 Simulation of the min-max selector system. The constraint limits are respected (bottom), while the tracking of the primary variable is still satisfactory (top). The middle plot shows how the constraint controllers override the primary control signal (dashed) resulting in a control (full) that respects the constraints.

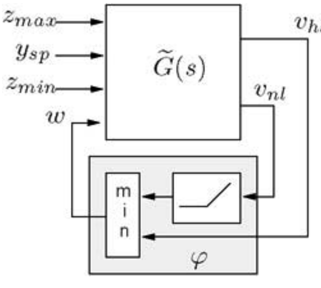

Figure 4.11 Selector control system rewritten as linear system interconnected with a static multi-variable nonlinearity.

The nonlinearity φ is piecewise linear and has the explicit expression

$$\varphi = \begin{cases} 0 & \text{if } (v_{hl} \geq 0) \wedge (v_{nl} \leq 0) \\ v_{nl} & \text{if } (v_{nl} \geq 0) \wedge (v_{hl} \geq v_{nl}) \\ v_{hl} & \text{otherwise} \end{cases}$$

Since the region where $\varphi(v_{hl}, v_{nl}) = v_{hl}$ is not convex, we have to introduce an additional region, see Figure 4.12(right).

While this nonlinearity fits directly in the piecewise linear framework, it is not easily dealt with using other techniques. It is easy to verify that the

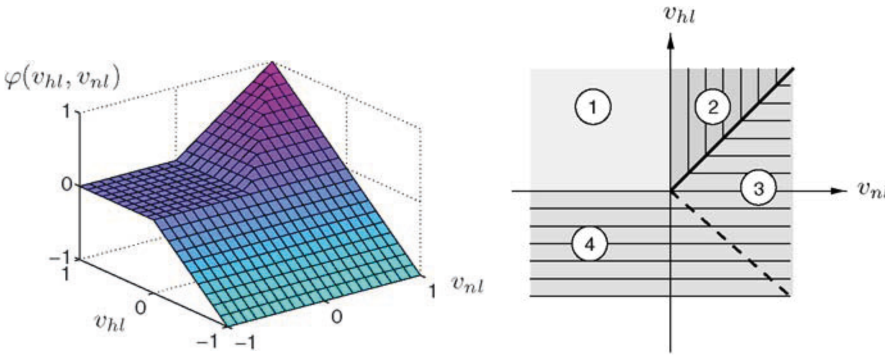

Figure 4.12 Static nonlinearity (left). The corresponding non-convex state partition (right) is rendered convex by splitting one cell in two (the dashed line in rightmost figure).

nonlinearity has gain less than one, which motivates an attempt to apply the small gain theorem. However, the $\mathcal{L}_2$-induced gain of the linear system is 15.8, and the small gain can not verify stability. An approach based on linear differential inclusions (Corollary 4.1) also fails.

In contrast, a numerical stability analysis using Theorem 4.1 verifies system stability. In this case, the optimization returns a Lyapunov function which is globally quadratic. Since Corollary 4.1 fails to establish stability, this example shows the importance of using partition information in the analysis.

4.7 Analysis of Piecewise Linear Differential Inclusions

The LMI computations of Theorem 4.1 are readily extended to systems described by piecewise linear differential inclusions (pwLDIs),

$$\dot{x}(t) \in \overline{\mathrm{co}}_{k \in K(i)} \{A_k x(t) + a_k\} \qquad\qquad x(t) \in X_i.$$

In order to guarantee that the Lyapunov function is decreasing along all possible solutions of the pwLDI, we must require that the Lyapunov function is decreasing with respect to every extreme dynamics $\dot{x} = A_k x + a_k$ that defines the inclusion in each cell. This leads to multiple decreasing conditions in each region (one for each extreme dynamics) and the following result.

THEOREM 4.2—PWQ STABILITY OF PWLDIS
Consider symmetric matrices T, U_{ik} and W_{ik} such that U_{ik} and W_{ik} have

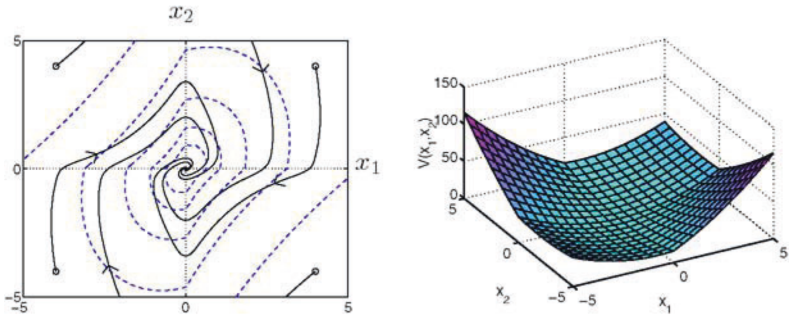

Figure 4.13 The left figure shows simulations (full) and Lyapunov function level surfaces (dashed) obtained in Example 4.8. The right figure shows the computed Lyapunov function.

nonnegative entries, while

$$P_i = F_i^T T F_i, \qquad i \in I_0$$
$$\bar{P}_i = \bar{F}_i^T T \bar{F}_i, \qquad i \in I_1$$

satisfy

$$\begin{cases} 0 > A_k^T P_i + P_i A_k + E_i^T U_{ik} E_i \\ 0 < P_i - E_i^T W_{ik} E_i \end{cases} \qquad i \in I_0, \quad k \in K(i)$$

$$\begin{cases} 0 > \bar{A}_k^T \bar{P}_i + \bar{P}_i \bar{A}_k + \bar{E}_i^T U_{ik} \bar{E}_i \\ 0 < \bar{P}_i - \bar{E}_i^T W_{ik} \bar{E}_i \end{cases} \qquad i \in I_1, \quad k \in K(i)$$

Then every solution $x(t) \in \cup_{i \in I} X_i$ of the inclusion (2.12) with $u \equiv 0$ for $t \geq 0$ tends to zero exponentially. □

Proof: Follows similarly to Theorem 4.1 and Proposition 4.2.

Theorem 4.2 enables the use of the piecewise quadratic machinery for rigorous stability analysis of smooth nonlinear systems. The following example demonstrates the ideas.

EXAMPLE 4.8—EMBEDDING SMOOTH SYSTEMS IN PWLDIS
Simulations indicate that the following nonlinear system is stable

$$\dot{x}_1 = -2x_1 + 2x_2 + \text{sat}(x_1 x_2) x_1$$
$$\dot{x}_2 = -2x_1 - \text{sat}(x_1 x_2)(x_1 + 4x_2).$$

We would like to verify global exponential stability of the origin by computing a piecewise quadratic Lyapunov function for the system. A simple technique for rigorous analysis of the system is to explore the bounds

$$p_{min} \leq \text{sat}(x_1 x_2) \leq p_{max}$$

and re-write the model as the differential inclusion

$$\dot{x} = \begin{bmatrix} -2 & 2 \\ -2 & 0 \end{bmatrix} x + p(t) \begin{bmatrix} 1 & 0 \\ -1 & -4 \end{bmatrix} x \tag{4.25}$$

with $p_{min} \leq p(t) \leq p_{max}$. By using information about the nonlinearity $p(t) = \text{sat}(x_1 x_2)$ we can obtain pwLDIs of different accuracy. First, notice that analysis using a global model based on the bound $-1 \leq p(t) \leq 1$ is futile since $p(t) = -1$ gives an unstable extreme dynamics. Taking the step from linear analysis to piecewise linear analysis, we can obtain a refined model by exploring the fact that

$$0 \leq \text{sat}(x_1 x_2) \leq 1$$

in the first and third quadrant, and

$$-1 \leq \text{sat}(x_1 x_2) \leq 0$$

in the second and fourth quadrant. This observation motivates a model with four regions, each region covering one quadrant. The dynamics in each region is given by a linear differential inclusion on the form (2.12). To verify stability, we apply Theorem 4.2 and find the Lyapunov function with the level curves indicated in Figure 4.8. This proves global exponential stability. Note that the level surfaces are non-convex sets and that the system is not easily dealt with using absolute stability results due to the multi-variable nature of the nonlinearity $\text{sat}(x_1 x_2)$. □

4.8 Analysis of Systems with Attractive Sliding Modes

The analysis procedures developed so far are only concerned with systems that do not have any attractive sliding modes. As demonstrated by the following example, however, attractive sliding modes can play a critical role for system stability and must be accounted for in the analysis.

EXAMPLE 4.9—SLIDING MODES AND STABILITY
Consider again the piecewise linear system from Example 2.4:

$$\dot{x} = \begin{cases} A_1 x = \begin{bmatrix} -2 & -2 \\ 4 & 1 \end{bmatrix} x & x_1 \geq 0 \\ A_2 x = \begin{bmatrix} -2 & 2 \\ -4 & 1 \end{bmatrix} x & x_1 \leq 0 \end{cases} \tag{4.26}$$

Since both system matrices are stable, and the system admits a solution to the LMIs in Theorem 4.1, it is easy to be misled to believe that this would imply exponential stability of (4.26). However, we know from Example 2.5 that the system does not have any non-trivial trajectories, so Theorem 4.1 does not apply. In fact, we also know that the dynamics on the sliding mode is unstable, $\dot{x}_2 = x_2$, so once Filippov solutions reach the attractive sliding mode, they tend to infinity along the positive x_2-axis, see Figure 4.14. □

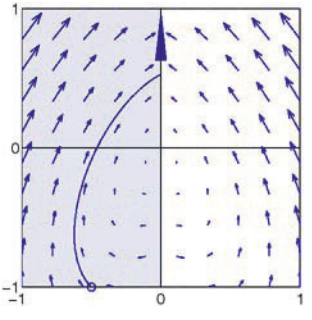

Figure 4.14 The behavior on attractive sliding modes is critical for system stability. The Filippov solution reaches the sliding mode and tends to infinity.

For systems with attractive sliding modes, it is natural to look for conditions that ensure stability of Filippov solutions. To this end, let

$$\mathcal{S} = \{x \mid \bar{G}\bar{x} \succeq 0 \wedge \bar{H}\bar{x} = 0\} \tag{4.27}$$

be a set on which there is an attractive sliding mode (this might be a regular sliding set on the boundary between two cells, a higher-order sliding set, or a sliding set on the intersection of multiple boundaries) and define

$$K_s = \{k \mid X_k \cap \mathcal{S} \neq \emptyset\}.$$

Thus, any Filippov solution that remains in $\mathcal{S}$ satisfies

$$\dot{x}(t) \in \underset{k \in K_s}{\overline{\text{co}}} \{A_k x(t) + a_k\}$$

Let $V(x,i) = \bar{x}^T \bar{P}_i \bar{x}$ be the expression used for defining the Lyapunov function candidate in cell X_i. If, for some $i \in K_s$,

$$\frac{\partial V(x,i)}{\partial x} \{A_k x + a_k\} < 0 \qquad \forall x \in \mathcal{S}\backslash\{0\}, \quad \forall k \in K_s \tag{4.28}$$

then $V(x)$ is decreasing along Filippov solutions on $\mathcal{S}$. This condition can be reformulated as the LMI

$$\bar{A}_k^T \bar{P}_i + \bar{P}_i \bar{A}_k + \bar{G}_s^T W_{ik} \bar{G}_s + \bar{H}_s^T N_{ik} + N_{ik}^T \bar{H}_s < 0 \qquad \forall k \in K_s \tag{4.29}$$

where $W_{ik} \succeq 0$ and N_{ik} are matrix variables of appropriate dimensions. Thus, the piecewise quadratic analysis can be extended to systems with attractive sliding modes by first identifying sliding sets on the form (4.27) and then augmenting the conditions of Theorem 4.1 with constraint of the type (4.29). Due to continuity of $V(x)$, we only need to enforce the above conditions for one $i \in K_s$ (if $V(x,i)$ is decreasing then so is $V(x,j)$ for all $j \in K_s$). The following example illustrates the approach.

EXAMPLE 4.10—EXPONENTIAL STABILITY OF SLIDING MODE SYSTEM
Consider the following slight modification of Example 4.9

$$\dot{x} = \begin{cases} A_1 x & x_2 \geq 0 \\ A_2 x & x_2 \leq 0 \end{cases}$$

Here, A_1 and A_2 are the system matrices defined in Example 4.9. Also this system has an attractive sliding mode as illustrated by the Filippov solution shown in Figure 4.15 (left). To verify exponential stability of all Filippov solutions, we apply the above technique and find the LMI conditions

$$\begin{aligned} A_1^T P_1 + P_1 A_1 &< 0 & \qquad P_1 > 0 \\ A_2^T P_2 + P_2 A_2 &< 0 & \qquad P_2 > 0 \\ A_1^T P_2 + P_2 A_1 + \begin{bmatrix} 0 & 1 \end{bmatrix}^T N + N \begin{bmatrix} 0 & 1 \end{bmatrix} &< 0 \end{aligned}$$

where $P_i = F_i^T T F_i$ for $i = 1, 2$. The conditions have a feasible solution which guarantees that all Filippov solutions converge exponentially to zero. Time responses of a Filippov solution and the corresponding value of the computed Lyapunov function are shown in Figure 4.15. □

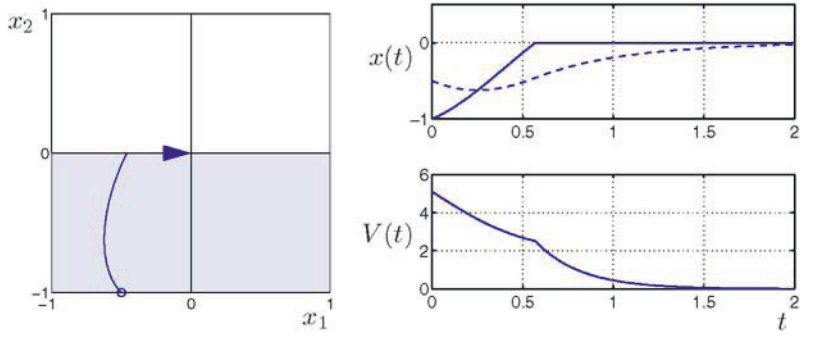

Figure 4.15 The extended stability conditions verify stability also in the presence of attractive sliding modes. The computed Lyapunov function decreases also on the attractive sliding mode (right).

Attractive sliding modes give a significant increase in the analysis computations since we need to analyze a differential inclusion on every sliding set, and sliding sets can potentially appear on every cell boundary and intersection of boundaries. Hence, if sliding modes can be ruled out a priori one should use theorems that only considers trajectories. For systems with sliding modes it is advised to first rule out attractive sliding modes on as many boundaries as possible before applying the methodology described above.

4.9 Improving Computational Efficiency

We have seen how the piecewise quadratic analysis is much more powerful than the classical approach based on quadratic Lyapunov functions and how it allows us to analyze many systems where other methods fail or are hard to apply. However, the piecewise quadratic approach is computationally more demanding and a straightforward implementation of the LMI conditions in Theorem 4.1 may result in very large optimization problems (this is especially true when the state space partitioning is performed in many dimensions). It is therefore of interest to develop methods that decrease the computational burden without introducing excessive conservatism. This section will describe two such approaches.

Stability Analysis in Two Steps

The LMI conditions in Theorem 4.1 incorporate the positivity condition in the Lyapunov function search. Looking back at Lemma 4.1, however, we see that there is little reason for doing so. The result suggests that any function which is decreasing along system trajectories contain all information about system stability. If the function is positive definite, stability follows analogously to Theorem 4.1. If we find some point where the computed function is non-positive, on the other hand, then no trajectory passing through this point can approach the origin as $t \to \infty$. We give the following result.

PROPOSITION 4.4—STABILITY ANALYSIS IN TWO STEPS
Consider a symmetric matrix T and symmetric matrices $U_i \succeq 0$ with non-negative entries, while $P_i = F_i^T T F_i$ and $\bar{P}_i = \bar{F}_i^T T \bar{F}_i$ satisfy

$$\begin{aligned} 0 >& A_i^T P_i + P_i A_i + E_i^T U_i E_i && i \in I_0 \\ 0 >& \bar{A}_i^T \bar{P}_i + \bar{P}_i \bar{A}_i + \bar{E}_i^T U_i \bar{E}_i && i \in I_1 \end{aligned}$$

Let $x(t) \in \cup_{i \in I} X_i$ be a trajectory of (2.3) with $u \equiv 0$ for $t \geq 0$, and define

$$V(x) = \bar{x}^T \bar{P}_i \bar{x} \qquad \text{for } x \in X_i, i \in I.$$

If there exists $\alpha > 0$ such that $V(x) > \alpha \|x\|_2^2$, then every trajectory $x(t)$ tends to zero exponentially. If $V(x_0) \leq 0$ for some $x_0 \in X \backslash \{0\}$, then no trajectory $x(t)$ with $x(0) = x_0$ can tend to zero as $t \to \infty$. □

Proof: Follows from Lemma 4.1 along the lines of the proof of Theorem 4.1.

Proposition 4.4 implies that the large LMI problem in Theorem 4.1 can be split into several smaller problems. By disregarding the positivity constraints in the Lyapunov function search we reduce the number of constraints by roughly 50% and eliminate the need for the variables W_i. This problem can be solved in a fraction of the time needed to solve the original problem. Moreover, if the LMI conditions in Proposition 4.4 do not admit a solution, then neither do the analysis conditions in Theorem 4.1.

Once a Lyapunov function candidate is found we can use Lemma 4.3 to check if this function is positive on the partition. Verifying positivity then amounts to solving a single LMI problem for each region. Since the Lyapunov function is now fixed, each such problem has only one constraint in one free matrix variable and can be solved very efficiently. We will illustrate the savings obtained by Proposition 4.4 in the end of this section.

Quadratic Cell Boundings – Computational Savings at a Price

It is often the number of free parameters in the S-procedure relaxation (the entries of the matrices U_i and W_i) that adds the most parameters to the Lyapunov function search. A second approach for reducing the computational burden is therefore to limit the number of parameters in the S-procedure. Returning to Lemma 4.3 we see that for given $\bar{P}_i$ a solution to the inequality

$$\bar{P}_i - \bar{E}_i^T U_i \bar{E}_i > 0$$

implies that $V(x)$ is positive for all x in the quadratic set

$$\mathcal{E}_i = \{x \mid \bar{x}^T \bar{E}_i^T U_i \bar{E}_i \bar{x} \geq 0\}.$$

Since $X_i \subseteq \mathcal{E}_i$, we may view $\mathcal{E}_i$ as a quadratic cell bounding, see Figure 4.16. From this perspective, the free parameters in U_i are used to form a quadratic set that separates X_i from the set $V^- = \{x \mid V(x) \leq 0\}$. One way to reduce

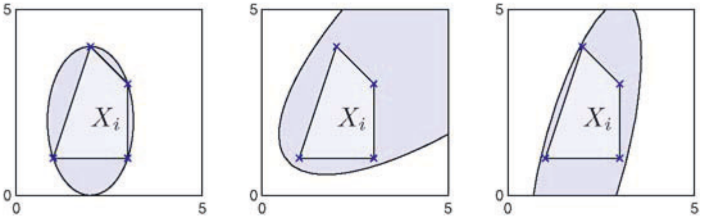

Figure 4.16 Several quadratic boundings $\mathcal{E}_i(\bar{E}_i)$ (dark) of the cell X_i (light) can be derived by varying the entries in the matrix U_i.

the number of search variables is to *fix* a quadratic cell bounding before the Lyapunov function search. Procedures for computing optimal ellipsoidal approximations of polyhedra are described in Appendix A. To pursue this direction further, we define quadratic cell boundings as follows.

DEFINITION 4.3—QUADRATIC CELL BOUNDING
A matrix $\bar{S}_i = \bar{S}_i^T$ is a *quadratic cell bounding* if

$$\bar{x}^T \bar{S}_i \bar{x} \geq 0 \qquad \text{for } x(t) \in X_i. \tag{4.30}$$

Furthermore, we say that $\{\bar{S}_i\}$ have the zero interpolation property if

$$\bar{S}_i = \begin{bmatrix} S_i & 0_{n\times 1} \\ 0_{1\times n} & 0 \end{bmatrix} \qquad \text{for } i \in I_0. \tag{4.31}$$

□

Now, rather than using Lemma 4.3 in the conditional analysis we use the following result.

LEMMA 4.4
Consider a piecewise quadratic function

$$V(x) = \begin{cases} x^T P_i x & x \in X_i \ i \in I_0 \\ \bar{x}^T \bar{P}_i \bar{x} & x \in X_i \ i \in I_1 \end{cases} \tag{4.32}$$

with $P_i = P_i^T$, $\bar{P}_i = \bar{P}_i^T$ and let $\bar{S}_i$ be a quadratic cell bounding satisfying (4.30) and (4.31). If there exists positive scalars $w_i \geq 0$ such that

$$P_i - w_i S_i > 0 \tag{4.33}$$
$$\bar{P}_i - w_i \bar{S}_i > 0 \tag{4.34}$$

then there exists $\alpha > 0$ such that $V(x) > \alpha \|x\|_2^2$ for all $x \in X$. □

Proof: Follows similarly to Lemma 4.3.

The following variant of Theorem 4.1 now follows directly.

PROPOSITION 4.5—PWQ STABILITY WITH QUADRATIC RELAXATION
Consider a symmetric matrix T and nonnegatvive scalars u_i and w_i such that $P_i = F_i^T T F_i$ for $i \in I_0$ and $\bar{P}_i = \bar{F}_i^T T \bar{F}_i$ for $i \in I_1$ satisfy

$$\begin{cases} 0 > A_i^T P_i + P_i A_i + u_i S_i \\ 0 < P_i - w_i S_i \end{cases} \qquad i \in I_0$$

$$\begin{cases} 0 > \bar{A}_i^T \bar{P}_i + \bar{P}_i \bar{A}_i + u_i \bar{S}_i \\ 0 < \bar{P}_i - w_i \bar{S}_i \end{cases} \qquad i \in I_1$$

Then every trajectory $x(t) \in \cup_{i \in I} X_i$ satisfying (2.3) with $u \equiv 0$ for $t \geq 0$ tends to zero exponentially. □

Proof: Follows similarly to Theorem 4.1.

This approach allows for large savings search variables, but is more conservative than the original formulation in Theorem 4.1. To be more precise, assume that $\bar{E}_i \in R^{p \times (n+1)}$. Then the polyhedral relaxations $\bar{E}_i^T U_i \bar{E}_i$ use $p(p-1)/2$ free parameters, while the quadratic formulation (4.30) uses one single parameter. The conservatism comes from the requirement that the a quadratic cell bounding has to be fixed *before* the optimization.

A natural candidate for quadratic approximation of polyhedral cells is to compute the ellipsoid with minimum volume that contains the cell. However, minimal volume has little to do with the role of the relaxation term in the LMI conditions, and in Chapter A we will be able to prove that for some important classes of partitions the use of minimal volume ellipsoids and Proposition 4.5 is always more conservative than the original formulation in Theorem 4.1. Such a proof requires some further developments, but we can already now demonstrate the arguments on a simple example.

A Comparative Example

To give a flavor of the benefits and limitations of the different formulations of piecewise quadratic stability given in Theorem 4.1, Proposition 4.4 and Proposition 4.5, we will apply them to the system shown in Figure 4.17. The system dynamics is given by

$$\dot{x} = Ax + b_1 f_1(x_1) + b_2 f_2(x_2)$$

where $A \in \mathbb{R}^{2\times 2}$, $b_1, b_2 \in \mathbb{R}^{2\times 1}$ and $f_i(x_i) = \arctan(x_i)$. We will present

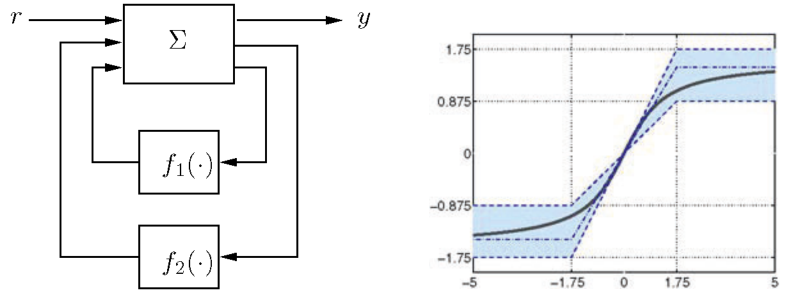

Figure 4.17 The system used as comparative example (left). The nonlinearity $f_i(x_i)$ is shown in full lines in the right figure. The dash-dotted line illustrates a piecewise linear approximation and the dashed lines show piecewise linear sector bounds.

results for both piecewise linear approximations and piecewise linear sector bounds on the nonlinearities, see Figure 4.17 (right). In both cases, the piecewise linear descriptions induce a partition of the domain $[-5, 5]\times[-5, 5]$ into nine regions.

First, we let

$$A = \begin{bmatrix} -3 & 2 \\ 1 & -3 \end{bmatrix}, \quad b_1 = \begin{bmatrix} -1 \\ 0 \end{bmatrix}, \quad b_2 = \begin{bmatrix} 0 \\ -1 \end{bmatrix}$$

and use the piecewise linear approximation of $f_i(x_i)$. In this case, all approaches succeed in verifying stability. The computational results are shown in Table 4.1. The computations were performed on a SUN Ultra 10 computer using the LMI software [62]. In the table the acronym P refers to the use of polytopic cell boundings in the analysis while Q indicates the use of quadratic cell boundings. The number 1 means that the analysis was performed in a single step (enforcing both positivity and decreasing conditions simultaneously) while 2 means that the analysis was performed in two steps (enforcing the decreasing condition during the Lyapunov function search and subsequently verifying positivity).

Table 4.1 First set-up: all approaches verify stability. Large savings in computations are obtained from the alternative formulations (P-2,Q-1,Q-2).

Approach	Time (s)	#Variables	#Constraints
P-1	1.04	117	114
P-2	0.41	69	57
Q-1	0.23	37	34
Q-2	0.11	29	17

As seen in Table 4.1, Proposition 4.4 (P-2) results in a large reduction in computation time compared with the computations required by Theorem 4.1(P-1). The computational savings are even greater when using quadratic cell boundings as in Proposition 4.5(Q-1). In this case, the quadratic cell boundings are taken as the minimal volume ellipsoids that cover each region (see Proposition A.10). By combining the two-step analysis with quadratic cell boundings (Q-2) the computational time is reduced to around 10% of what was required by the original formulation.

Using the same matrices A, b_1 and b_2, we now consider the case when the nonlinearities are described by piecewise linear sector bounds. This approach allows us to verify stability of the smooth nonlinear system in a rigorous way but it also increases the computational cost. In each region the system is now described by a differential inclusion with four extreme dynamics. As the main burden in analysis of such systems is verification of the multiple decreasing conditions, the savings of the two-step analysis procedure is somewhat reduced, see Table 4.2.

Table 4.2 Second set-up: the use of piecewise linear sector bounds decreases the benefits of the two-set analysis procedure, but good savings are still obtained.

Approach	Time (s)	#Variables	#Constraints
P-1	3.79	261	285
P-2	2.17	213	228
Q-1	0.80	61	85
Q-2	0.45	53	58

The drawback with quadratic cell boundings is that they allow very little freedom in the S-procedure-relaxation. This introduces some conservatism as can be seen by letting

$$A = \begin{bmatrix} -2 & 2 \\ 1 & -2 \end{bmatrix}, \quad b_1 = \begin{bmatrix} -1 \\ 0 \end{bmatrix}, \quad b_2 = \begin{bmatrix} 0 \\ -1 \end{bmatrix},$$

and using piecewise linear sector bounds on the nonlinearities. The computational results are shown in Figure 4.3. Stability can no longer be verified using quadratic cell boundings, while the computational savings in the use of Proposition 4.4 remain the same.

Table 4.3 Final set-up: quadratic cell boundings fail to verify stability.

Approach	Time (s)	#Variables	#Constraints
P-1	4.15	261	285
P-2	2.62	213	228
Q-1	fails	–	–
Q-2	fails	–	–

To understand the computational complexity of the different approaches, it is useful to see how different factors contribute to the total number of parameters. In this example, we have constructed the constraint matrices using the procedure given in Section A.4. This procedure gives $\bar{F}_i \in \mathbb{R}^{6\times 3}$ and $\bar{E}_i \in \mathbb{R}^{4\times 3}$. This implies that $T \in \mathbb{R}^{6\times 6}$ and that the Lyapunov function candidate $\bar{F}_i^T T \bar{F}_i$ has 21 free parameters. Each of the matrices U_i and W_i used in the polytopic S-procedure has 6 free parameters while the ellipsoidal S-procedure uses 1 parameter. As the origin lies in the interior of one cell, S-procedure relaxation is only used in 8 regions. Applied to the first set-up (Table 4.1), the approach P-1 requires $21 + 8 \cdot (1+1) \cdot 6 = 117$ parameters while P-2 uses $21 + 8 \cdot 1 \cdot 6 = 69$ parameters. For the piecewise linear sector bounds (Table 4.2), P-1 uses $21 + 8 \cdot (1+4) \cdot 6 = 261$ parameters while P-2 uses $21 + 8 \cdot 4 \cdot 6 = 213$ parameters. In this case, Q-2 uses only $21 + 8 \cdot 4 \cdot 1 = 53$ parameters.

4.10 Piecewise Linear Lyapunov Functions

There are several reasons to look for alternatives to the piecewise quadratic analysis. First, the semidefinite programming problem in Theorem 4.1 has many free search variables and analysis of large problems using these conditions may be time consuming using today's LMI software. Secondly, the

S-procedure, which was used to exploit the restriction $x \in X_i$ in the computations, can be a restrictive way to check positivity of a piecewise quadratic function on a polyhedral partition. In other words, there are systems that admit a piecewise quadratic Lyapunov function but where this function can not be found by the formulation of Theorem 4.1.

As an alternative to piecewise quadratics, we will consider Lyapunov function candidates that are continuous and piecewise linear

$$V(x) = \begin{cases} p_i^T x & x \in X_i,\ i \in I_0 \\ \bar{p}_i^T x = p_i^T \bar{x} + q_i & x \in X_i,\ i \in I_1 \end{cases} \tag{4.35}$$

Such Lyapunov functions can be computed via linear programming. Compared to LMI software, linear programming solvers have reached a high level of maturity and efficient software exists for large-scale problems that allows systems with thousands of cells to be analyzed in a matter of seconds.

Similar to the piecewise quadratic case we will use a compact parameterization of such functions that separates the free parameters from the constraints imposed by the continuity requirement. The parameterization is established in the following lemma.

LEMMA 4.5—PWL PARAMETERIZATION
Let $\{X_i\}_{i \in I}$ be a polyhedral partition, and let $\bar{F}_i \in \mathbb{R}^{p \times (n+1)}$ be continuity matrices that satisfy (4.14). Then, for each $t \in \mathbb{R}^p$, the scalar function

$$V(x) = t^T \bar{F}_i \bar{x} := \bar{p}_i \bar{x} \qquad \text{for } x \in X_i.$$

is continuous and piecewise linear. Moreover, if $\{\bar{F}_i\}$ have the zero interpolation property, there exists α and β such that

$$\alpha \|x\|_\infty \leq V(x) \leq \beta \|x\|_\infty .$$

□

Proof: Follows similarly to Lemma 4.2 and the absence of offset terms in $V(x)$ in a neighborhood around the origin.

Another attractive feature of piecewise linear Lyapunov functions is that the conditional analysis can sometimes be performed without loss. This fact is established in the following Lemma, similar in nature to Farkas' lemma [181, 221].

LEMMA 4.6
The following statements are equivalent.

1. $p^T x > 0$ for all x such that $Ex \succeq 0$, $Ex \neq 0$
2. There exists a vector $u \succ 0$ such that $p - E^T u = 0$.

□

Proof: See Section B.2.

Contrary to the standard formulation of Farkas' lemma which uses non-strict inequalities, Lemma 4.6 is formulated using strict inequalities. However, the result only considers linear forms and does not treat affine terms. The following stability theorem now follows.

THEOREM 4.3—PIECEWISE LINEAR STABILITY
Let $\{X_i\}_{i \in I} \subseteq \mathbb{R}^n$ be a polyhedral partition with continuity matrices $\bar{F}_i$, satisfying (4.14) and (4.15), and cell boundings $\bar{E}_i$, satisfying (4.19) and (4.20). Assume furthermore that $\bar{E}_i \bar{x} \neq 0$ for every $x \in X_i$ with $x \neq 0$. If there exists a vector t and non-negative vectors $u_i \succ 0$ and $w_i \succ 0$ while

$$
\begin{aligned}
p_i &= F_i^T t, && i \in I_0 \\
\bar{p}_i &= \bar{F}_i^T t, && i \in I_1
\end{aligned}
$$

satisfy

$$
\begin{cases} 0 = p_i^T A_i + u_i E_i \\ 0 = p_i^T - w_i E_i \end{cases} \qquad i \in I_0 \tag{4.36}
$$

$$
\begin{cases} 0 = \bar{p}_i^T \bar{A}_i + u_i \bar{E}_i \\ 0 = \bar{p}_i^T - w_i \bar{E}_i \end{cases} \qquad i \in I_1 \tag{4.37}
$$

then every trajectory $x(t) \in \cup_{i \in I} X_i$ satisfying (2.3) with $u \equiv 0$ for $t \geq 0$ tends to zero exponentially. □

Proof: Follows similarly to Theorem 4.1.

The search for free variables t, u_i and w_i in Theorem 4.3 is a linear programming problem. If the system does not have any attractive sliding modes a solution to this problem guarantees that

$$
V(x) = \bar{p}_i^T \bar{x} \qquad \text{for } x \in X_i, i \in I
$$

is a Lyapunov function for the system. Although the analysis conditions still use relaxation terms u_i and w_i, the number of entries in u_i and w_i has been reduced in comparison to the number of entries in the matrices U_i and W_i used in the piecewise quadratic analysis. Finally, note that the additional constraint

$$\bar{E}_i\bar{x} \neq 0 \qquad\qquad \text{for } x \in X_i \ \text{ with } \ x \neq 0$$

does not impose any further restriction. For $i \in I_0$, the assumption is violated if $\{x \mid \bar{E}_i\bar{x} \succeq 0\}$ is some linear halfspace, but $p^T x$ can not be strictly positive for all x in a closed linear halfspace. For $i \in I_1$, the situation can always be avoided by adding the additional constraint $[0_{1\times n} \quad 1]\bar{x} \geq 0$ to the cell boundings.

Piecewise Linear Lyapunov Functions on Bounded Partitions

Theorem 4.3 can be used for analysis of systems with both bounded and unbounded partitions. However, if all cells are bounded we can reduce the computations even further. More specifically, let the cells be given in vertex representation

$$X_i = \underset{k\in V(i)}{\overline{\text{co}}} \{\nu_k\}$$

where $V(i)$ are the set of indices for the vertices ν_k of cell X_i. Then, an affine function is positive on X_i if and only if it is positive on the vertices of X_i. This allows us to formulate the following result.

THEOREM 4.4
Let $\{X_i\}_{i\in I}$ be a partition of a bounded subset of $\mathbb{R}^n$ into convex polytopes with vertices ν_k, and let $\bar{F}_i$ be the associated continuity matrices satisfying (4.14) and (4.15). If there exists a vector t such that

$$\begin{aligned} p_i &= F_i^T t && \text{for } i \in I_0 \\ \bar{p}_i &= \bar{F}_i^T t && \text{for } i \in I \end{aligned}$$

satisfy

$$\begin{cases} 0 > p_i^T A_i \nu_k & i \in I_0,\ \ \nu_k \in X_i \\ 0 < p_i^T \nu_k & i \in I_0,\ \ \nu_k \in X_i \end{cases} \tag{4.38}$$

$$\begin{cases} 0 > \bar{p}_i^T \bar{A}_i \bar{\nu}_k & i \in I_1,\ \ \nu_k \in X_i \\ 0 < \bar{p}_i^T \bar{\nu}_k & i \in I_1,\ \ \nu_k \in X_i \end{cases} \tag{4.39}$$

for each $\nu_k \neq 0$, then every trajectory $x(t) \in \cup_{i \in I} X_i$ satisfying (2.3) with $u \equiv 0$ for $t \geq 0$ tends to zero exponentially. □

Proof: Follows similarly to Theorem 4.3 but where decreasing and positivity conditions are checked according to the discussion above.

Note that all the relaxation terms have vanished, and that the vector inequalities of Theorem 4.3 have been reduced to scalar inequalities.

It is possible to arrive at even simpler stability conditions if one considers partitions where each cell $X_i \subseteq \mathbb{R}^n$ has $n+1$ vertices. Such polytopes are called simplices, and are described in more detail in Chapter A. For simplex partitions, the Lyapunov function is completely determined by its values at the cell vertices, and the positivity condition can then be replaced by the requirement that all entries of the vector t should be positive, $t \succ 0$.

Polytopic Lyapunov Functions

Although Theorem 4.4 requires the analysis domain to be bounded (the cells are polytopes) it can still be used to assess global exponential stability in some cases. More precisely, if $I_1 = \emptyset$, then any piecewise linear Lyapunov function valid in some open neighborhood of the origin is also valid globally. Lyapunov functions derived in this way are often called ***polytopic Lyapunov functions***, as the level sets of such a Lyapunov function are polytopes (see [23, 147] for further details). The following example illustrates the ideas.

EXAMPLE 4.11—SELECTOR SYSTEM CONT'D

To illustrate the use of piecewise linear Lyapunov functions, we return to the simple selector system used in Section 4.4. As discussed in conjunction with Theorem 4.3, the piecewise linear Lyapunov functions cannot be used on the initial partition since the natural cells are both open linear halfspaces. Using the refined partition shown in Figure 4.18 (left), however, Theorem 4.4 returns the Lyapunov function shown in Figure 4.18 (right). Hence, global exponential stability follows from the arguments above. Note that the Lyapunov function is poorly conditioned and that the level surfaces are heavily unbalanced. By refining the partitioning further one arrives at Lyapunov functions that closely resemble the Lyapunov function used in the piecewise quadratic analysis (not shown). □

Extensions

The basic stability computations can be extended in several useful ways. One example is computation of decay rate, τ, which can be estimated from

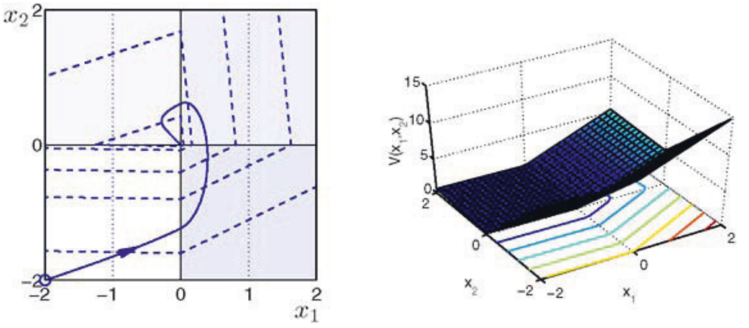

Figure 4.18 Refined partition and level surfaces of computed Lyapunov function (dashed) to the left. The computed Lyapunov function is shown to the right.

the modified Lyapunov inequality

$$\dot{V}(x) + \tau V(x) < 0 \qquad \forall x \neq 0.$$

Given a fixed value of τ, the above condition can be verified using a slight modification of the previous theorems (where A_i has been replaced by $A_i + \tau I$ in the decreasing conditions). The optimal value of τ can then be found by bisection. Another possibility is to extend the stability analysis to piecewise linear inclusions,

$$\dot{x} \in \underset{k \in K(i)}{\overline{\text{co}}} \{A_k x + a_k\} \qquad x \in X_i$$

In this case, one simply needs to verify multiple decreasing conditions in each region. Similar techniques can be used to assess stability of systems with attractive sliding modes.

4.11 A Unifying View

There is a close relationship between the parameterizations of the piecewise linear and the piecewise quadratic Lyapunov functions. In this section, we will elaborate this relationship further and establish a unifying framework for computation of globally quadratic, piecewise quadratic, polyhedral and piecewise linear Lyapunov functions.

One may view the matrix format for continuous piecewise quadratic Lyapunov functions introduced in Lemma 4.2,

$$V(x) = \bar{x}^T \bar{F}_i^T T \bar{F}_i \bar{x} \qquad x \in X_i,$$

as a quadratic form in the coordinates z obtained by the continuous piecewise linear mapping $z = \bar{F}_i x$. If one rather considers linear forms in z,

$$V(x) = t^T z = t^T \bar{F}_i x := p_i^T x \qquad\qquad x \in X_i$$

one obtains the parameterization of continuous piecewise linear functions suggested in Lemma 4.5. In fact, the piecewise linear Lyapunov functions can be seen as a direct restriction of the piecewise quadratics as follows. Let F_i be constraint matrices satisfying (4.14) and define

$$\widehat{F}_i = \begin{bmatrix} F_i & f_i \\ 0 & 1 \end{bmatrix}, \qquad T = \frac{1}{2}\begin{bmatrix} 0 & t \\ t^T & 0 \end{bmatrix}.$$

Note that $\widehat{F}_i$ also satisfies the continuity condition (4.14), and that the piecewise quadratic function $V(x)$ of Proposition 1 now evaluates to

$$x^T \bar{P}_i x = x^T \widehat{F}_i^T T \widehat{F}_i x = t^T \bar{F}_i x = p_i^T x.$$

The close relationship between the parameterizations of piecewise linear and piecewise quadratic Lyapunov functions allows us to establish a unifying view of several approaches for numerical Lyapunov function construction, see Figure 4.19.

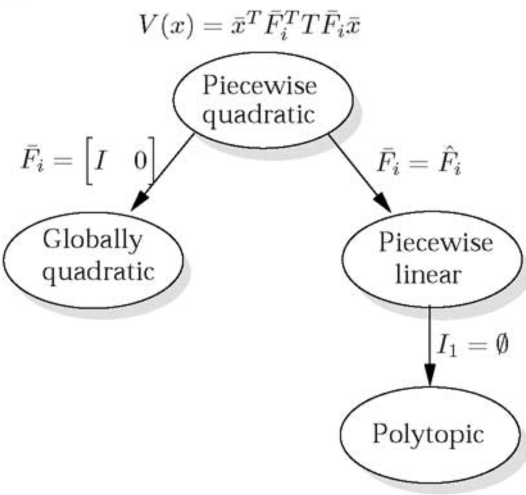

Figure 4.19 A unifying view of four classes of Lyapunov functions for piecewise linear system that can be computed via convex optimization.

Most versatile are the *piecewise quadratic Lyapunov functions* [100, 157, 72]

$$V(x) = x^T \bar{F}_i^T T \bar{F}_i x \qquad\qquad x \in X_i$$

As shown in Theorem 4.1, piecewise quadratic Lyapunov functions can be computed via convex optimization in terms of LMIs. The fact that a certain set of differential equations only describes the dynamics in a restricted region of the state space can be exploited using the S-procedure, which is a sufficient condition that appears to work very well in practice.

The *quadratic Lyapunov functions* [45, 27] are special instances of the piecewise quadratics obtained by letting $\bar{F}_i = [I_{n\times n} \quad 0_n]$. Quadratic Lyapunov functions can be computed via LMI optimization, and conditional analysis can be done using the S-procedure.

Also the *piecewise linear Lyapunov functions* [118, 96, 107]

$$V(x) = t^T \bar{F}_i \bar{x} \qquad\qquad x \in X_i$$

can be seen as a special case of the piecewise quadratics. They can be computed via linear programming as shown in Theorem 4.3 and Theorem 4.4. The conditional analysis can in some cases be formulated without loss (as established in Lemma 4.6).

Polytopic Lyapunov functions [142, 147, 23] are a special case of the piecewise linear Lyapunov functions. The polytopic Lyapunov functions can be obtained from the piecewise linear by considering partitions that consist of convex cones with base in the origin, *i.e.*, polyhedral partitions for which $I_1 = \emptyset$. The computations can be done using linear programming and the conditional analysis is performed without loss.

Choosing Lyapunov Function Class

The choice of Lyapunov function class involves many trade-offs between issues such as analytic flexibility, complexity of description, and computational requirements. For example, the quadratic Lyapunov functions have a compact description and allow for efficient computations but has limited analytic flexibility. Piecewise linear and piecewise quadratic Lyapunov functions have a high degree of flexibility but are more demanding to compute and require more parameters for their representation.

For a given partition, the linear matrix inequalities in Section 4.6 are much more demanding to solve than the linear programming problems in Section 4.10. However, as we have seen, it is often necessary to refine an initial partition in order to prove stability using a piecewise linear Lyapunov function. Partition refinements increase both the computational requirements and the number of parameters needed for representing the Lyapunov function. A particular weakness of piecewise linear Lyapunov functions is that a very fine partition is needed when the system dynamics is oscillatory. The following example illustrates this issue.

EXAMPLE 4.12—LYAPUNOV FUNCTIONS AND OSCILLATORY DYNAMICS
Consider the linear oscillator

$$\dot{x} = \begin{bmatrix} -\alpha & \beta \\ \beta & -\alpha \end{bmatrix} x \tag{4.40}$$

The system matrix has eigenvalues $\lambda = -\alpha \pm i\beta$ and the system is exponentially stable (hence, admits a quadratic Lyapunov function) for all $\alpha > 0$. The larger the value of β, the more oscillatory the dynamics and the more circular the trajectories in the phase plane. Circular trajectories require a Lyapunov function with circular level sets, and if we want to approximate these by polytopes (which is what we do when we use polytopic Lyapunov functions) the number of polygon sides might need to be very large [166]. In fact, Polański [161] proved that a polytopic Lyapunov function with a partition defined by the $2m$ vertices

$$\pm \begin{pmatrix} 1 \\ 0 \end{pmatrix}, \pm \begin{pmatrix} \cos(\pi/m) \\ \sin(\pi/m) \end{pmatrix}, \ldots, \pm \begin{pmatrix} \cos(\pi(m-1)/m) \\ \sin(\pi(m-1)/m) \end{pmatrix}$$

is a Lyapunov function for the system (4.40) if

$$m > \frac{\pi}{\arctan\left(2\alpha/\beta/(1-\alpha^2/\beta^2)\right)}$$

The number of vertices grows large when α/β grows small, see Figure 4.20 and tends to infinity as α/β tends to zero. □

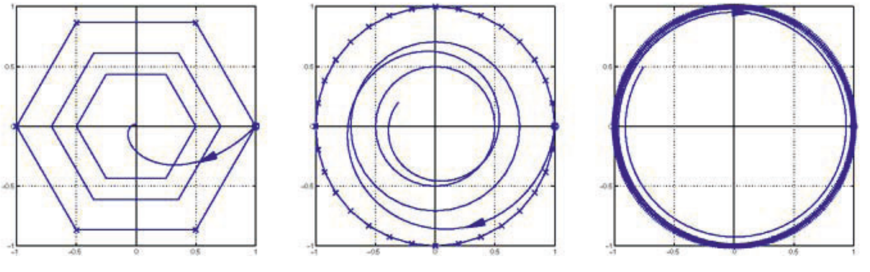

Figure 4.20 Polański's construction for $\alpha/\beta = 1$ (left) requires 6 vertices (marked with '$\times$'), $\alpha/\beta = 0.1$ requires 32, while $\alpha/\beta = 0.01$ (right) requires 316 vertices. All three systems admit a quadratic Lyapunov function that can be described by three parameters, and computed by solving a single Lyapunov equation.

The main reason for moving beyond quadratic Lyapunov functions is to increase flexibility of the Lyapunov function candidate. This flexibility is not needed for analysis of linear systems but it can be critical in the analysis of nonlinear and uncertain systems. While the level sets of quadratic Lyapunov functions are always ellipsoidal, polytopic Lyapunov functions allow level sets of arbitrary convex polyhedral shape. The piecewise linear and piecewise quadratic Lyapunov functions are even more flexible since they can be both non-convex and non-homogeneous. The following example, also used in [150, 23], demonstrates some of these issues.

EXAMPLE 4.13—ANALYTIC FLEXIBILITY
Consider the following linear uncertain system

$$\dot{x}(t) = A\{\delta(t)\}x(t) = \begin{bmatrix} 0 & 1 \\ -1+\delta(t) & -1 \end{bmatrix} x(t).$$

where $|\delta(t)| \leq d$ is an uncertain time-varying parameter. For $d > \sqrt{3}/2$ there is no quadratic Lyapunov function that can show stability for all admissible parameter variations. In [23], Blanchini reported a polyhedral Lyapunov function with 30 vertices that proves stability for $d \leq 0.98$. Using a piecewise quadratic Lyapunov function with four regions (being the four quadrants in $\mathbb{R}^2$) and Theorem 4.2 we can not only decrease the number of parameters needed to represent the Lyapunov function but also improve the bound to $d = 1 - \epsilon$ with $\epsilon = 1E - 15$. □

We believe that the piecewise quadratic Lyapunov functions strike a nice tradeoff between analytic flexibility and complexity of description: they are very versatile (as they encompass all other Lyapunov function classes discussed in this book) and they allow analysis of systems with oscillatory dynamics without the need for excessive partition refinements. However, they are computationally more demanding and the S-procedure introduces many parameters in the optimization problem. If a very fine partition is needed in order to approximate an underlying nonlinear system by a piecewise linear system and the linearized dynamics around the equilibrium point is not too oscillatory, piecewise linear Lyapunov functions might be the best choice (see also the Notes and References section at the end of this Chapter).

Another issue appears when Lyapunov-like functions are used in system analysis and optimal control problems. Different problem formulations then call for different classes of loss functions. While energy-related problems, such as computation of the induced $\mathcal{L}_2$-gain, are conveniently dealt with using quadratric or piecewise quadratic Lyapunov functions, piecewise linear and polytopic Lyapunov functions have been useful in analysis of systems with absolute constraints (*c.f.*, Section 3.2).

4.12 Comments and References

Numerical Lyapunov Function Construction

Most methods for analysis of dynamical systems are somehow related to Lyapunov functions, and a Lyapunov function appears more or less explicitly in most analysis conditions. Dissipativity analysis [212, 81], absolute stability [215, 164], and analysis based on integral quadratic constraints [139] can all be viewed as methods for Lyapunov function construction. Quadratic Lyapunov functions is the cornerstone in the analysis and design of robust linear controllers using semidefinite programming [27].

While efficient software for semidefinite programming has not appeared until quite recently, the simplex method for solving linear programming problems is more than 50 years old [47]. Researchers are since long aware of the benefits of deriving results that can be verified via linear programming. Computer algorithms for construction of piecewise linear Lyapunov functions appeared already in the late 70's, and has continued to attract a lot of attention, see *e.g.*, [33, 34, 140, 23, 142, 147, 61, 107, 93]. The focus has been on polytopic Lyapunov functions and uncertain linear systems. An important exception is the work [147] that considers polytopic Lyapunov functions for piecewise linear systems. Highly related to our approach is the stability analysis proposed in [118] in which piecewise linear Lyapunov functions (that may have affine terms and are not necessarily polytopic) were constructed using so-called facet functions.

When quadratic Lyapunov functions do not suffice, it is very natural to consider functions that are piecewise quadratic. For example, for the Lyapunov functions used in the Popov criterion are piecewise quadratic when the nonlinearity in the feedback connection is piecewise linear. The idea of "patching together" piecewise quadratic Lyapunov functions in the state space has also been used in the analysis of specific nonlinear systems, see [165]. To the best of our knowledge, this book (and the parallel work [158, 71]) is the first that presents a systematic methodology for computation of piecewise quadratic Lyapunov functions for general piecewise linear systems.

Lyapunov Function Computations in the Equality-Constrained Format

Rather than using the natural equality-constrained description of piecewise quadratic Lyapunov functions (4.13) we have introduced a special matrix format to enforce continuity of the Lyapunov function candidate. This format enables the Lyapunov function search to be carried out using widely available software for semidefinite programming and does not force the user to rely on a solver that supports equality constraints. Although this issue was critical for the early developments of the results in this book (when no equality constrained solvers were publically available) it is related to optimization technology that might change and, to some extent, already has changed.

In the equality-constrained format, continuity of the Lyapunov function is enforced by introducing the equality constraints

$$\bar{P}_i = \bar{P}_j + \bar{e}_{ij}^T \bar{t}_{ij}^T + \bar{t}_{ij}\bar{e}_{ij}^T \qquad \forall j \text{ such that } X_i \cap X_j \neq \emptyset \tag{4.41}$$

in variables $\bar{P}_i, \bar{P}_j$ and $\bar{t}_{ij}$ in the optimization problem. The ability to handle equality constraints also allows regions that contain the origin to be treated in an alternative way compared to Theorem 4.1. Let x_{eq} be an equilibrium point in the interior of cell X_i. Then, the dynamics can be written as

$$\dot{x} = A_i x + a_i = A_i(x - x_{\text{eq}}) \qquad \text{for } x \in X_i$$

and the Lyapunov function must be on the form

$$(x - x_{\text{eq}})^T P_i (x - x_{\text{eq}}) + \tilde{r}_i \qquad \text{for } x \in X_i$$

for some $\tilde{r}_i \in \mathbb{R}$. To accommodate for this in the Lyapunov function search, replace the continuity constraint (4.41) by

$$\begin{bmatrix} P_i & -P_i x_{\text{eq}} \\ -x_{\text{eq}}^T P_i & x_{\text{eq}}^T P_i x_{\text{eq}} + \tilde{r}_i \end{bmatrix} = \bar{P}_j + \bar{e}_{ij}^T \bar{t}_{ij}^T + \bar{t}_{ij}\bar{e}_{ij}^T \quad \forall j \text{ such that } X_i \cap X_j \neq \emptyset$$

and replace the Lyapunov conditions

$$\bar{P}_i - \bar{E}_i^T W_i \bar{E}_i > 0 \qquad \bar{A}_i^T \bar{P}_i + \bar{P}_i \bar{A}_i + \bar{E}_i^T U_i \bar{E}_i < 0$$

by

$$P_i - \widetilde{E}_i^T W_i \widetilde{E}_i > 0 \qquad A_i^T P_i + P_i A_i + \widetilde{E}_i^T W_i \widetilde{E}_i < 0$$

Here $\widetilde{E}_i$ is obtained from the matrix the matrix

$$\left[\begin{array}{c|c} G_i & G_i x_{\text{eq}} + g_i \end{array}\right]$$

by eliminating every row whose last entry is non-zero (this is Algorithm A.1 applied to the original cell identifiers of cell X_i). Note that the equality constraints must be eliminated in order for the analysis inequalities to admit a solution with strict inequalities. By following the above procedure, all analysis results in this book can be converted to the equality-constrained format. More details on the equality-constrained format, as well as computational experience, can be found in [72, 71] (see also [172]).

Sliding Mode Analysis and C^1 Lyapunov Functions

A drawback of using Lyapunov functions that are continuous, but not necessarily continuously differentiable, manifests itself in systems with attractive modes. In order to ensure stability of Filippov solutions, we then have to analyze a possibly large differential inclusion for each sliding set. If we restrict the Lyapunov function to be C^1 this step is no longer necessary since

$$\frac{\partial V(x,k)}{\partial x}\{A_k x + a_k\} = \frac{\partial V(x,i)}{\partial x}\{A_k x + a_k\} \qquad \forall k \in K(i)$$

The standard LMI conditions guarantee that the expression on the left-hand side is decreasing also on cell boundaries, so (4.28) is automatically satisfied.

Since quadratic functions are C^1 the existence of a globally quadratic Lyapunov function guarantees exponential stability of Filippov solutions. In addition, it is straight-forward to restrict the piecewise quadratic Lyapunov function candidates to be C^1 both in the equality-constrained format and when using the special matrix parameterization introduced in Section 4.5. In the equality-constrained setting (4.13) is replaced by

$$\bar{P}_j = \bar{P}_i + t_{ij}(\bar{h}_{ij} + \bar{h}_{ij}^T)$$

with $t_{ij} \in \mathbb{R}$. For the matrix parameterization, without loss of generality, assume that the continuity matrices are on the form

$$\bar{F}_i = \begin{bmatrix} & \bar{F}_i' \\ I_{n\times n} & 0_{n\times 1} \end{bmatrix}$$

Then, by restricting the matrix parameter T to be on the form

$$T = \begin{bmatrix} T' & 0 \\ 0 & T_0 \end{bmatrix}$$

with T' diagonal and T_0 symmetric, every function on the form (4.16) is C^1 and piecewise quadratic. However, this restriction also limits the flexibility of the Lyapunov function candidate. For example, this approach fails to establish exponential stability of the system studied in Example 4.10.

5

Dissipativity Analysis

A fundamental idea in systems and control is to view complex systems as the interconnection of simpler subsystems. Such a perspective is often helpful in bringing insight into and understanding about a dynamic system. When viewing a system as the interconnection of its components, it is natural to ask whether the analysis of a complex system can be based on the (hopefully simpler) analysis of its components. This is the idea behind input-output analysis, which has been a very successful tool in system theory. Roughly speaking, the idea is to replace detailed models of system components by input-output relationships (typically relating the energy of the input to the energy of the output) and then derive results for interconnections of such models. The most well-known results may be the small-gain and the passivity theorems. Both allow stability of a feedback interconnection to be verified from the analysis of its components. Hence, by establishing $\mathcal{L}_2$-gain or passivity properties of piecewise linear systems we can hope to establish stability of interconnections by invoking small gain and passivity theorems. This chapter will provide such tools.

An interesting aspect of this approach is that it allows us to use different tools for analyzing different components. For example, physical insight may help us to establish passivity of one subsystem and piecewise linear techniques can allow us to prove strict passivity of another subsystem. This allows us to analyze systems that combine piecewise linear subsystems with components that are not easily dealt with using piecewise linear techniques. Time delays is one example of such a component.

As we have seen in Chapter 2, several important interconnections of piecewise linear systems are themselves piecewise linear. Thus, the tools developed in this chapter will give us the choice to either analyze a complex piecewise linear system as it stands, or to analyze the subsystems in isolation and then apply small-gain and passivity results. This allows us to trade-off complexity in the computations against conservatism in the analysis.

M. Johansson: Piecewise Linear Control Systems, LNCIS 284, pp. 85-95, 2003.

5.1 Dissipativity Analysis via Convex Optimization

Dissipativity is a very useful notion in the study of performance and robustness of dynamical systems. Roughly speaking, dissipativity means that the system absorbs more energy from its environment than what it supplies. In a more abstract setting a dissipative system is defined as a system that admits a supply rate (defining "input power") and a storage function (measuring "stored energy") so that energy is always dissipated [212, 81]. Many important system properties, such as $\mathcal{L}_2$-induced norms and passivity, correspond to different supply rates.

There is a close relationship between Lyapunov functions and storage functions. In some cases, the storage function will qualify as a Lyapunov function that can be used prove system stability. As exponential stability of a linear system implies the existence of a quadratic Lyapunov function, dissipativity of a linear system with respect to a quadratic supply rate implies the existence of a quadratic storage function [212]. With the developments from the previous chapter at hand, it is natural to base a dissipativity analysis of piecewise linear systems on storage functions that are piecewise quadratic. Before giving some precise results we will illustrate the ideas on the problem of estimating the $\mathcal{L}_2$-norm of a piecewise linear system. The initial step is based on a simple and transparent Lyapunov technique developed in [212, 81, 199].

Performance Bounds from Dissipation Inequalities

Consider the problem of estimating an upper bound on the $\mathcal{L}_2$-induced gain from u to y of the system (2.3). In other words, we want to determine a constant γ such that

$$\int_0^T \|y(t)\|_2^2 \, dt \leq \gamma^2 \int_0^T \|u(t)\|_2^2 \, dt \qquad \forall u(t)$$

holds for all $T \geq 0$. We will assume that $x(0) = 0$. The inequality can be verified if we can find a non-negative storage function $V(x) \geq 0$ with $V(x(0)) = 0$ such that

$$\frac{d}{dt} V(x(t)) \leq \gamma^2 u^T u - y^T y \tag{5.1}$$

along system trajectories. Integration of this inequality gives

$$V(x(T)) - V(x(0)) \leq \gamma^2 \int_0^T \|u(t)\|_2^2 \, dt - \int_0^T \|y(t)\|_2^2 \, dt.$$

Since $V(x(0)) = 0$ and $V(x) \geq 0$, we have

$$0 \leq \gamma^2 \int_0^T \|u(t)\|_2^2 \, dt - \int_0^T \|y(t)\|_2^2 \, dt$$

and the desired bound follows.

The central difficulty in applying the technique is to find a storage function $V(x)$ that satisfies the dissipation inequality (5.1). We will consider piecewise linear systems and piecewise quadratic storage functions. This will allow us to compute estimates on the $\mathcal{L}_2$-gain using convex optimization. For a given partition a best upper bound can then be obtained by minimizing γ^2 subject to the relevant inequalities.

For linear systems, it is sufficient to consider quadratic storage functions and the exact $\mathcal{L}_2$-gain can be found using the above procedure [27]. A result of similar elegance for piecewise linear systems does not, to the best of the author's knowledge, exist. In general, the techniques developed in this chapter will only return bounds on the system performance.

Dual Bounds from Worst Case Disturbances

Since we are working with bounds rather than exact solutions, it is useful to have measures on how good the computed bounds are. For the dissipativity-like computations in this chapter, such bounds can often be obtained by constructing worst-case inputs. As the optimal value of the $\mathcal{L}_2$-gain can be obtained from the solution of the Hamilton-Jacobi-Bellman equation

$$\frac{\partial V(x)}{\partial x}(A_i x + a_i + B_i u) = \gamma u^T u - y^T y,$$

it is natural to try to construct a worst case disturbance that attains equality in (5.1). Let $\hat{V}(x)$ be a solution to (5.1) and let $\hat{\gamma}$ be the gain estimate obtained in this way. A lower bound on the $\mathcal{L}_2$-induced gain can then be obtained by maximizing the expression

$$\frac{\partial \hat{V}(x)}{\partial x}(A_i x + a_i + B_i u) + y^T y - \hat{\gamma}^2 u^T u$$

with respect to u. Simulating the piecewise linear system with this input and comparing the input and output norms then gives a lower bound on the $\mathcal{L}_2$-induced gain.

Successive Refinements via Upper and Lower Bounds

The bounds obtained by piecewise quadratic computations often give significant improvements over computations based on globally quadratic storage functions. Moreover, by refining the state-space partition, it is possible to introduce more flexibility in the piecewise quadratic storage functions. With increased flexibility, the computations can be repeated in hope of achieving better estimates. As increased flexibility comes at the price of increased computations, the upper and lower bounds can serve as an aid in the trade-off between precision in the analysis and the cost of computations.

5.2 Computation of $\mathcal{L}_2$-induced Gain

The analysis outlined above can be directly combined with the developments in Chapter 4 to give LMI conditions for $\mathcal{L}_2$-gain computations for piecewise linear systems. After verification of stability, for example using Theorem 4.1, an upper bound for the gain can be obtained as follows.

THEOREM 5.1—UPPER BOUND ON $\mathcal{L}_2$ GAIN
Suppose there exist symmetric matrices T, U_i and W_i such that U_i and W_i have non-negative entries, while $P_i = F_i^T T F_i$ and $\bar{P}_i = \bar{F}_i^T T \bar{F}_i$ satisfy

$$0 > \begin{bmatrix} P_i A_i + A_i^T P_i + C_i^T C_i + E_i^T U_i E_i & P_i B_i \\ B_i^T P_i & -\gamma^2 I \end{bmatrix} \qquad \text{for } i \in I_0$$

$$0 > \begin{bmatrix} \bar{P}_i \bar{A}_i + \bar{A}_i^T \bar{P}_i + \bar{C}_i^T \bar{C}_i + \bar{E}_i^T U_i \bar{E}_i & \bar{P}_i \bar{B}_i \\ \bar{B}_i^T \bar{P}_i & -\gamma^2 I \end{bmatrix} \qquad \text{for } i \in I_1$$

Then every trajectory $x(t)$ with $x(0) = 0$, $\int_0^\infty (\|x\|_2^2 + \|u\|_2^2)\, dt < \infty$ satisfies

$$\int_0^\infty \|y\|_2^2\, dt \leq \gamma^2 \int_0^\infty \|u\|_2^2\, dt.$$

The best upper bound on the $\mathcal{L}_2$ induced gain is achieved by minimizing γ^2 subject to the constraints defined by the inequalities. □

Proof: See Section B.3.

In analogy with the previous section, a lower bound on the gain can be computed by the construction of a worst case disturbance. For this purpose, we will consider disturbances on the form $u = \bar{L}_i \bar{x}$ obtained by maximizing the expression

$$2\bar{x}^T \bar{P}_i(\bar{A}_i \bar{x} + \bar{B}_i u) + \|\bar{C}_i \bar{x}\|_2^2 - \hat{\gamma}^2 \|u\|_2^2$$

with respect to u. The precise formulas for the resulting feedback gains $\bar{L}_i$ will be given in the next chapter and are omitted here. In the above expression, $\bar{P}_i$ and $\hat{\gamma}$ come from the upper bound computation. Simulating the system with this control law and comparing the input and output norms gives a lower bound on the $\mathcal{L}_2$ gain.

EXAMPLE 5.1—ANALYSIS OF A SATURATED CONTROL SYSTEM
Consider the control system shown in Figure 5.1. The output of the system $G_1(s)$ is subject to a unit saturation. The closed loop dynamics is piecewise linear, with three cells induced by the saturation limits $u = \pm 1$. We set $r = 0$

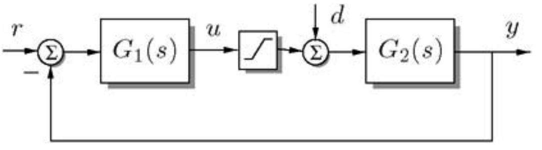

Figure 5.1 Saturated control system.

and estimate the $\mathcal{L}_2$-induced gain from the disturbance d to the output y. With the transfer functions

$$G_1(s) = \frac{s-3}{16s^2+s+2} \qquad G_2(s) = \frac{s+7}{4s^2+3s+12}$$

we obtain the results shown in Table 5.1.

Table 5.1 Various upper bounds on $\mathcal{L}_2$ gain.

Method	Gain Estimate
Quadratic Lyapunov function	No solution found
Lure function with positive η	No solution found
Lure without constraints on η	37.63
IQC for monotonic nonlinearities	5.62
Piecewise quadratic Lyapunov function	5.54

Here "Lure function" means a Lyapunov function of the form $V(x) = x^T Px + \eta \int_0^{Cx} \text{sat}(s)ds$ and "IQC for monotonic nonlinearities" means a gain estimate computed based on [218] using the toolbox [138]. A lower bound on the $\mathcal{L}_2$ gain, computed for the linear region, is equal to 5.52. □

This example is somewhat contrived, but it illustrates the differences that can be obtained from the various approaches. Apart from being useful in analysis of disturbance rejection properties, computation of $\mathcal{L}_2$-induced gain can be used for establishing robust stability in presence of norm-bound uncertainties. We will illustrate this in an example at the end of this chapter.

5.3 Estimation of Transient Energy

In order to demonstrate the use of partition refinements we will apply the central idea to the estimation of the "transient energy"

$$\int_0^\infty \bar{x}^T \bar{Q}_i \bar{x}\, dt \qquad\qquad \text{for } x(t) \in X_i, \quad i \in I$$

of a piecewise linear system. This can be seen as an alternative to simulation. The value of this integral depends on the initial value and we would like our estimate to also be a *function* of the initial value. In this way, one computation will allow us to estimate the integral for every initial state. We assume that $\bar{Q}_i = \bar{Q}_i^T$ have the zero interpolation property, *i.e.*

$$\bar{x}^T \bar{Q}_i \bar{x} = \bar{x}^T \begin{bmatrix} Q_i & 0 \\ 0 & 0 \end{bmatrix} \bar{x} = x^T Q_i x \qquad\qquad \text{for } i \in I_0$$

The desired estimates can be obtained from the following minor modification of the stability analysis in Chapter 4.

THEOREM 5.2—UPPER BOUND ON TRANSIENT ENERGY
Let $x(t) \in \cup_{i\in I} X_i$ with $x(\infty) = 0$ be a trajectory of the system (2.3) with $u \equiv 0$ for $t \geq 0$. Consider symmetric matrices T and U_i, such that U_i have non-negative entries, while $P_i = F_i^T T F_i$ and $\bar{P}_i = \bar{F}_i^T T \bar{F}_i$ satisfy

$$\begin{aligned} 0 &> P_i A_i + A_i^T P_i + Q_i + E_i^T U_i E_i & & i \in I_0, \\ 0 &> \bar{P}_i \bar{A}_i + \bar{A}_i^T \bar{P}_i + \bar{Q}_i + \bar{E}_i^T U_i \bar{E}_i & & i \in I_1. \end{aligned}$$

Then

$$\int_0^\infty \bar{x}^T \bar{Q}_i \bar{x}\, dt \leq \inf_{T, U_i} \bar{x}(0)^T \bar{P}_{i_0} \bar{x}(0). \qquad \square$$

Proof: See Section B.3.

A lower bound can be obtained similary, by replacing $\bar{Q}_i$ by $-\bar{Q}_i$ in the analysis. A solution to the resulting inequalities then implies that

$$\bar{x}(0)^T \bar{P}_{i0} \bar{x}(0) \leq \int_0^\infty \bar{x}^T \bar{Q}_i \bar{x}\, dt.$$

A best lower bound estimated in this way can be obtained by maximizing $V(x_0)$ subject to the relevant constraints. Although the computations are optimized for a specific initial value, the computed function $V(x)$ bounds the value of the integral for all initial values on the partition. Furthermore, if $\bar{Q}_i \geq 0$ for all $i \in I$, a solution to the LMIs of Theorem 5.2 also satisfies the inequalities in Proposition 4.4. Thus, if the computed $V(x)$ is positive on the partition it will also qualify as a Lyapunov function for the system.

The following example applies the results on the problem of estimating the output energy of a piecewise linear system and illustrates the use of partition refinements to obtain better and better estimates.

EXAMPLE 5.2—TRANSIENT IN FLOWER EXAMPLE
Consider again the piecewise linear system defined in Example 4.3 and introduce the output $y = x_1$, *i.e.*, let

$$C_i = \begin{bmatrix} 1 & 0 \end{bmatrix}, \qquad \forall i \in I.$$

Figure 5.2 shows a simulated trajectory (left) and the corresponding output (right). Consider the problem of estimating the "output energy",

$$\int_0^\infty \|y(t)\|_2^2 \, dt = \int_0^\infty x(t)^T C_i^T C_i x(t) \, dt$$

from a given initial value. This can be done by direct application of Theorem 5.2 by letting $Q_i = C_i^T C_i$. The output simulated from $x(0) = [1 \quad 0]$ (shown in Figure 5.2) has total energy $\int_0^\infty \|y(t)\|_2^2 \, dt = 1.88$, while the bounds obtained from Theorem 5.2 for the initial cell partition give

$$0.60 \leq \int_0^\infty \|y\|_2^2 \, dt \leq 2.50.$$

A possible reason for the gap between the bounds is that the level curves of the cost function can not be well approximated by a piecewise quadratic function on the given partition. To improve the bounds, we introduce more flexibility in the storage function by repeatedly splitting every cell in two. This simple-minded refinement procedure, illustrated in Figure 5.3, is repeated three times yielding the bounds shown in Table 5.2.

Note that the bounds on the output energy optimized for the initial state $(1, 0)$ match closely over the the whole state space, giving good estimates of the output energy also for other initial states. □

5.4 Dissipative Systems with Quadratic Supply Rates

The results of the previous sections can be generalized in a natural way to validation of more general dissipation inequalities. The same technique that

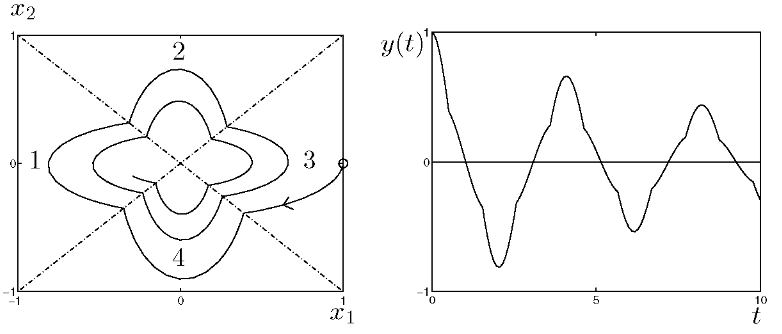

Figure 5.2 Trajectory of a simulation (left) and corresponding output (right).

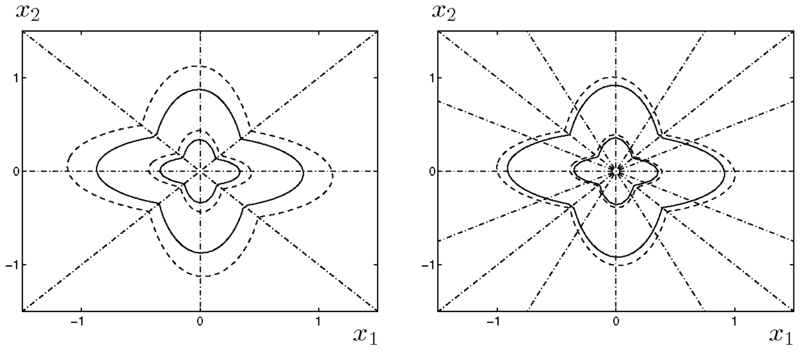

Figure 5.3 Upper (full) and lower (dashed) bounds on the storage function computed in Example 5.2. The bounds get increasingly tight when we move from 8 cells (left) to 16 cells (right).

was used in $\mathcal{L}_2$-induced gain computations can be applied to verification of dissipativity with respect to arbitrary quadratic supply functions. We give the following result.

THEOREM 5.3—VALIDATION OF DISSIPATION INEQUALITIES
Consider symmetric matrices T, U_i and W_i such that U_i and W_i have non-

Table 5.2 Lower and upper bounds for output energy estimated via Theorem 5.2.

Number of Cells	Lower bound	Upper bound
4	0.60	2.50
8	1.33	2.18
16	1.65	1.98
32	1.78	1.88

negative entries, while $P_i = F_i^T T F_i$ and $\bar{P}_i = \bar{F}_i^T T \bar{F}_i$ satisfy

$$\begin{cases} 0 < \begin{bmatrix} C_i & D_i \\ 0 & I \end{bmatrix}^T M \begin{bmatrix} C_i & D_i \\ 0 & I \end{bmatrix} - \begin{bmatrix} P_i A_i + A_i^T P_i + E_i^T U_i E_i & P_i B_i \\ B_i^T P_i & 0 \end{bmatrix} \\ 0 < P_i - E_i^T U_i E_i \end{cases}$$

for $i \in I_0$ and

$$\begin{cases} 0 < \begin{bmatrix} \bar{C}_i & \bar{D}_i \\ 0 & I \end{bmatrix}^T M \begin{bmatrix} \bar{C}_i & \bar{D}_i \\ 0 & I \end{bmatrix} - \begin{bmatrix} \bar{P}_i \bar{A}_i + \bar{A}_i^T \bar{P}_i + \bar{E}_i^T U_i \bar{E}_i & \bar{P}_i \bar{B}_i \\ \bar{B}_i^T \bar{P}_i & 0 \end{bmatrix} \\ 0 < \bar{P}_i - \bar{E}_i^T U_i \bar{E}_i. \end{cases}$$

for $i \in I_1$. Then every trajectory $x(t)$ with $x(0) = 0$ and $\int_0^t \|u(t)\|_2^2 \, dt < \infty$ satisfies

$$0 \leq \int_0^t \begin{bmatrix} y(s) \\ u(s) \end{bmatrix}^T M \begin{bmatrix} y(s) \\ u(s) \end{bmatrix} ds \qquad \forall t \geq 0$$

□

Proof: Follows similarly to Theorem 5.1.
Note that Theorem 5.1 is a special case of this result where

$$M = \begin{bmatrix} -I & 0 \\ 0 & \gamma^2 \end{bmatrix}.$$

Theorem 5.3 can be used to establish induced gain and passivity properties of piecewise linear systems that can be used in analysis based on the small gain or passivity theorems. This type of results open up many possibilities as they allow freedom in whether to incorporate nonlinearities in the system description or to replace them by energy inequalities and use interconnection results. The following example illustrates some of the ideas.

EXAMPLE 5.3—ROBUSTNESS ANALYSIS VIA THE SMALL GAIN THEOREM
Consider the system shown in Figure 5.4. This is a linear system with a dynamic uncertainty Δ and a nonlinear spring $\varphi(\cdot)$. The uncertainty block Δ is assumed to have induced $\mathcal{L}_2$-gain less than one and the spring has the nonlinear characteristic shown in Figure 5.4. Nonlinear spring arrangements of similar type can for example be found in engine control systems, see [120]. We set $u = 0$ and consider the system defined by a transfer matrix $G(s)$ with

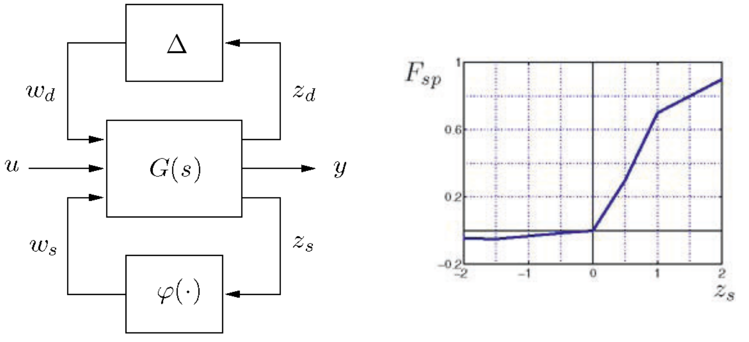

Figure 5.4 System with nonlinear spring characteristic and unmodeled dynamics (left). Detailed spring characteristic (right).

state-space realization

$$\frac{d}{dt}\begin{bmatrix} x_1 \\ x_2 \\ x_3 \end{bmatrix} = \begin{bmatrix} -3 & 0 & -1 \\ 4 & -1 & 0 \\ 0 & 2 & -1 \end{bmatrix}\begin{bmatrix} x_1 \\ x_2 \\ x_3 \end{bmatrix} + \begin{bmatrix} 0 & -5 \\ 0 & 0 \\ 1 & 0 \end{bmatrix}\begin{bmatrix} w_d \\ w_s \end{bmatrix}$$

and outputs $z_d = x_1$, $z_s = x_2$.

The tools derived so far give a large flexibility in how to analyze stability of this system. A first crude approximation is to use a norm bounds on both the Δ-block and on the spring characteristic and then apply the small gain theorem. However, this approach fails for the suggested example since the H_∞ norm of the linear system exceeds one (the H_∞ norm is 5.73). Another approach is to consider the feedback interconnection of the linear system and the spring as a piecewise linear system and only treat the Δ-block as uncertain. We may then start by using global sector bounds on the spring nonlinearity and estimate the $\mathcal{L}_2$-gain from w_d to z_d (see Figure 2.11). This approach estimates the $\mathcal{L}_2$-gain to 1.12 and stability can not be established. Using the piecewise linear sector bounds in Figure 2.11 (middle), Theorem 5.1 verifies that the gain from w_d to z_d is less than 0.25 and closed loop stability follows. □

This example demonstrates how induced $\mathcal{L}_2$-gain computations can be used for robustness analysis of piecewise linear uncertain systems, and how partition refinements are useful for obtaining sufficient accuracy in the analysis.

5.5 Comments and References

Piecewise Linear Systems and Integral Quadratic Constraints

The verification of dissipation inequalities could easily be extended to treat more general integral quadratic constraints (IQCs). For example, integral quadratic constraints with a frequency dependent weight rather than a constant matrix M could be verified using Theorem 5.3 by first introducing a state space realization of the weight and then include this dynamics in the system description. Once a certain integral quadratic constraint has been verified for a piecewise linear component it can be used in the general framework for IQC-based system analysis developed in [139]. A more straightforward approach would be to perform an IQC-based analysis directly in the piecewise linear framework. The analysis of piecewise linear systems interconnected with components described by IQCs could potentially be very useful. A good starting point for a stability analysis based on piecewise quadratic Lyapunov functions could be the Lyapunov approach outlined in [106, Section 1.7].

Nonlinear H_∞ Control

Interpreted in time domain, the linear H_∞ problem is concerned with attenuation of the $\mathcal{L}_2$-induced gain from disturbances to outputs. Nonlinear H_∞ refers to the extensions of these techniques to nonlinear systems, see [90]. In this context, $\mathcal{L}_2$-induced gains are often estimated using finite difference discretization of the dissipation inequalities [91].

Incorporation of Hard Bounds

In some cases we know that the disturbances, in addition to having bounded energy, satisfy hard amplitude constraints. It is straight-forward to modify Theorem 5.1 so as to account for this information. If we describe the input constraints via

$$G_i x + H_i u \geq 0 \text{ for } i \in I_0 \qquad \bar{G}_i \bar{x} + \bar{H}_i u \geq 0 \text{ for } i \in I$$

the first inequality condition in Theorem 5.1 becomes

$$0 < \begin{bmatrix} P_i A_i + A_i^T P_i + C_i C_i^T & P_i B_i \\ B_i^T P_i & -\gamma^T I \end{bmatrix} - \begin{bmatrix} E_i & 0 \\ G_i & H_i \end{bmatrix}^T U_i \begin{bmatrix} E_i & 0 \\ G_i & H_i \end{bmatrix}$$

and the second is analogous.

6

Controller Design

So far, we have focused on deriving methods for stability and performance analysis of piecewise linear systems. At the very least such methods can be used in control design procedures that iterate between design and analysis steps. In this chapter, we will proceed by extending the piecewise quadratic techniques to design of feedback control laws.

We will start out by showing how the problem of finding a globally linear state feedback that stabilizes a given piecewise linear system can be cast as a convex optimization problem. This approach is elegant, but restrictive in at least two ways: it is based on globally quadratic Lyapunov functions and it generates discontinuous feedback laws. When we try to alleviate these shortcomings, however, we will find that it is not so easy to use piecewise quadratic Lyapunov functions as the basis for control design while keeping convexity in the computations. We will present an approach to optimal control of piecewise linear systems with piecewise quadratic loss functions. Feedback laws can then be derived from the solution to the associated Hamilton-Jacobi-Bellman equation. By considering Hamilton-Jacobi-Bellman *inequalities* rather than equations, we will show how convex optimization and piecewise quadratic functions can be used to compute bounds on the optimal performance. In particular, we will show how a lower bound on the cost that can be achieved using *any* control can be computed via semi-definite programming. The computations also suggest a natural piecewise linear feedback law that tries to achieve this cost. The performance of this control law can be evaluated using the dual Hamilton-Jacobi-Bellman inequality, yielding an upper bound on the achievable cost. The dual inequality can also be used for control design. However, the resulting matrix inequalities are bilinear and the associated design problem can only be solved locally. In an example, we show how the upper and lower bounds can be combined and a continuous piecewise linear state feedback with tight bounds on the guaranteed performance can be designed.

M. Johansson: Piecewise Linear Control Systems, LNCIS 284, pp. 96-106, 2003.

6.1 Quadratic Stabilization of Piecewise Linear Systems

We have already discussed how piecewise linear systems can be conservatively analyzed as linear differential inclusions using quadratic Lyapunov functions. The same approach can also be used to formulate a number of central feedback control problems in terms of linear matrix inequalities [27, 180]. However, this approach is very restrictive since it does not allow for bias terms in the system dynamics and it does not use any partition information in the analysis. In this section, we will describe an approach by Hassibi and Boyd [72] that alleviates both these shortcomings.

Consider the piecewise linear system (2.3) under linear state feedback

$$u = -Lx.$$

This results in the closed loop system

$$\dot{x}(t) = (A_i - B_i L)x(t) + a_i \qquad x \in X_i \quad i \in I. \tag{6.1}$$

The ***quadratic stabilization*** problem ammounts to finding a feedback gain L so that the closed-loop system (6.1) admits a quadratic Lyapunov function

$$V(x) = x^T P x$$

Assume that we use ellipsoidal cell boundings, *i.e.*, that we for each cell X_i have determined matrices S_i and s_i such that

$$\|S_i x + s_i\|_2 \leq 1 \qquad \forall x \in X_i$$

Then the closed-loop system is quadratically stable if we can find a postive definite matrix $P = P^T \geq 0$ and positive scalars $u_i \geq 0$ such that

$$\begin{cases} 0 > (A_i - B_i L)^T P + P(A_i - B_i L) & i \in I_0 \\ 0 > \begin{bmatrix} (A_i - B_i L)^T P + P(A_i - B_i L) & Pa_i \\ a_i^T P & 0 \end{bmatrix} + u_i \begin{bmatrix} -S_i^T S_i & -S_i^T s_i \\ -s_i S_i & 1 - s_i^2 \end{bmatrix} & i \in I_1 \end{cases}$$

These conditions are not jointly convex in the variables L, P and u_i, but convexity can be recovered using the following result.

LEMMA 6.1
There exists a solution $P = P^T > 0$ and $u \geq 0$ to the matrix inequality

$$0 > \begin{bmatrix} A^T P + PA - uC^T C & PB - uC^T D \\ (PB - uC^T D)^T & u(I - D^T D) \end{bmatrix}$$

if and only if there exists a solution $Q = Q^T > 0$ and $v \geq 0$ to

$$0 > \begin{bmatrix} AQ + QA^T - vBB^T & -vBD^T + QC^T \\ (-vBD^T + QC^T)^T & v(I - DD^T) \end{bmatrix}$$

Moreover, the soutions are related via $Q = P^{-1}$ and $v = u^{-1}$. □

Proof: See [27, Section 5.1]).

Using the above result, and introducing the variable Y via $Y = LQ$, we arrive at the following result [72].

THEOREM 6.1—QUADRATIC STABILIZATION
If there exists a positive definite matrix $Q = Q^T > 0$, positive scalars $v_i \geq 0$, and a matrix Y such that

$$\begin{cases} 0 > QA_i^T + A_iQ - Y^TB_i^T - B_iY & i \in I_0 \\ 0 > \begin{bmatrix} QA_i^T + A_iQ - Y^TB_i^T - B_iY - v_ia_ia_i^T & QS_i^T - v_ia_is_i^T \\ (QS_i^T - v_ia_is_i^T)^T & v_i(I - s_is_i^T) \end{bmatrix} & i \in I_1 \end{cases}$$

Then, the feedback $u = -Lx$ with $L = YQ^{-1}$ renders the piecewise linear system (2.3) exponentially stable. □

The above result extends directly to the design of piecewise linear state feedback laws on the form

$$u = -L_ix \qquad\qquad x \in X_i.$$

One then simply replaces the common matrix Y in the above conditions by separate variables Y_i for each region. This feedback law is typically discontinuous and might introduce attractive sliding modes in the closed-loop system. However, according to the discussion in Section 4.12 the existence of a common quadratic Lyapunov function guarantees that all potential Fillipov solutions tend to zero exponentially.

The reader who is familiar with the work on LMI-based analysis and design of linear uncertain systems might recognize the techniques from analysis of norm-bound LDIs (see, *e.g.*, [27, Section 5.1]). Indeed, all results developed for norm-bound LDIs can be used for analysis and design of piecewise linear systems along the lines of the discussion above.

6.2 Controller Synthesis based on Piecewise Quadratics

The quadratic stabilization approach is elegant and gives a significant decrease in conservatism compared to an approach that models the piecewise linear elements as a polytopic uncertainty (compare Corollary 4.1). Still, with the powerful machinery developed in the previous chapters it is natural to attempt to derive synthesis procedures based on piecewise quadratic Lyapunov functions. Unfortunately, there does not appear to be any simple analogue to the change-of-variables $Q = P^{-1}$ when we base our analysis on piecewise quadratics and it does not seem to be possible to find a convex formulation of the design problem.

In this section, we will investigate two approaches that allow us to design controllers based on piecewise quadratic Lyapunov functions. We will focus on optimal control problems with piecewise quadratic costs. The first approach formulates the design problems as an optimization problem over bilinear matrix inequalities (BMIs). These problems are not convex and one cannot hope to find efficient algorithms that are guaranteed to find the globally optimal solution (or even a feasible solution) for all problem instances. However, there are many heuristic algorithms for solving BMIs that appear to work reasonably well in practice. The second approach, first suggested in [169, 170], uses convex optimization to compute a lower bound on the objective that can be achieved by *any* control and suggests a natural piecewise linear control law that tries to achieve this cost. The control law gives an upper bound on the cost. If the upper and lower bounds obtained in this way are not sufficiently tight, one can use this control law as a starting point for the BMI-based design procedure. When combined, the upper and lower bound computations allow us to design piecewise linear state feedbacks with guaranteed (and often quite tight) performance bounds.

Optimal Control and Hamilton-Jacobi-Bellman Inequalities

Consider the following general form of optimal control problem

$$\begin{array}{ll} \text{minimize} & \int_0^\infty L(x,u)dt \\ \text{subject to} & \begin{cases} \dot{x}(t) = f(x(t),u(t)) \\ x(0) = x_0 \end{cases} \end{array}$$

It is well known that solutions of this problem can be characterized in terms of the Hamilton—Jacobi—Bellman (H-J-B) equation

$$0 = \inf_u \left(\frac{\partial V}{\partial x} f(x,u) + L(x,u) \right). \tag{6.2}$$

In fact, by integrating the inequality

$$0 \leq \frac{\partial V}{\partial x} f(x,u) + L(x,u) \qquad \forall x, u \tag{6.3}$$

and assuming that $x(\infty) = 0$, we get

$$V(x_0) - V(0) = -\int_0^\infty \frac{\partial V}{\partial x} f(x,u)dt \leq \int_0^\infty L(x,u)dt.$$

Hence, every V that satisfies (6.3) gives a lower bound on the optimal value of the loss function. Similarly, for a given control law $u = l(x)$, the inequality

$$0 \geq \frac{\partial V}{\partial x} f(x, l(x)) + L(x, l(x)) \qquad \forall x \tag{6.4}$$

guarantees that

$$V(x_0) - V(0) \geq \int_0^\infty L(x, l(x))\, dt$$

and any V that satisfies (6.4) gives an upper bound on the cost. In particular, V has then decay rate given by $-L(x, l(x))$, which is typically negative, so V may serve as a Lyapunov function to prove that the control law is stabilizing.

We will consider the case where f is piecewise linear and L is piecewise quadratic. The control objective is then to bring the system (2.3) from a given initial state $x(0) = x_0$ to rest at $x(\infty) = 0$ while limiting the cost

$$J(x_0, u) = \int_0^\infty \left(\bar{x}(t)^T \bar{Q}_{i(t)} \bar{x}(t) + u(t)^T R_{i(t)} u(t)\right) dt. \tag{6.5}$$

Here $i(t)$ is defined so that $x(t) \in X_{i(t)}$. We will assume that

$$\bar{Q}_i = \begin{bmatrix} Q_i & 0 \\ 0 & 0 \end{bmatrix} \qquad \text{for } i \in I_0 \tag{6.6}$$

and that Q_i and R_i are positive definite.

Upper Bounds via Bilinear Matrix Optimization

Consider the piecewise linear system (2.3) under piecewise linear feedback

$$u = -L_i x - l_i = -\bar{L}_i \bar{x} \qquad x \in X_i, \quad i \in I \tag{6.7}$$

with $l_i = 0$ for $i \in I_0$. Then, an upper bound on the associated loss function (6.5) can be computed via (6.4) in analogy with Theorem 5.2.

THEOREM 6.2—UPPER BOUND ON OPTIMAL COST
Assume existence of symmetric matrices T and U_i, such that U_i have non-negative entries, while $P_i = F_i^T T F_i$ and $\bar{P}_i = \bar{F}_i^T T \bar{F}_i$ satisfy

$$0 > \begin{bmatrix} (A_i - B_i L_i)^T P_i + P_i(A_i - B_i L_i) + Q_i + E_i^T U_i E_i & L_i^T \\ L_i & -R_i^{-1} \end{bmatrix} \qquad i \in I_0$$

$$0 > \begin{bmatrix} (\bar{A}_i - \bar{B}_i \bar{L}_i)^T \bar{P}_i + \bar{P}_i(\bar{A}_i - \bar{B}_i \bar{L}_i) + \bar{Q}_i + \bar{E}_i^T U_i \bar{E}_i & \bar{L}_i^T \\ \bar{L}_i & -R_i^{-1} \end{bmatrix} \qquad i \in I_1$$

Then, every trajectory $x(t)$ of (2.3) under the control (6.7) such that $x(t) \in \cup_{i \in I} X_i$, $x(\infty) = 0$ and $x(0) = x_0 \in X_{i_0}$ satisfies

$$J(x_0, u) \leq \inf_{T, U_i} \bar{x}_0^T \bar{P}_{i_0} \bar{x}_0 \tag{6.8}$$

□

Proof: Similar to Theorem 5.2 via the Schur complement (Proposition A.2).

When the L_i's are fixed, the matrix inequalities are linear in P_i and an upper bound on the control performance can be obtained via semidefinite programming. The formulation can be used for controller design if we consider both P_i and L_i as variables. However, in this case the inequalities contain bilinear forms $\bar{P}_i \bar{B}_i \bar{L}_i$. Optimization problems involving bilinear matrix inequalities are non-convex in general, but a number of heuristic methods for solving such problems have been proposed (see, *e.g.*, [64, 66, 74, 196]). One of the simplest methods is the V-K iteration, which sequentially fixes one set of variables (say, the value function V) and optimizes over the others (typically, the controller gains), then fixes the second set of variables and optimizes over the first. The procedure is repeated until no further performance improvements can be made.

Unfortunately, the V-K iteration is not easily adopted to solving the BMIs in Theorem 6.2 since the objective (6.8) does not depend on L_i. Instead, we will use the linearization method suggested in [74]. The basic idea of this approach is to linearize the design inequalities around an initial solution (P_i^0, L_i^0), by letting $P_i = P_i^0 + \delta P_i$, $L_i = L_i^0 + \delta L_i$ and ignoring higher-order terms. Thus, the expressions

$$(A_i - B_i L_i)^T P_i + P_i(A_i - B_i L_i)$$

in the inequalities of Theorem 6.2 are replaced by

$$(A_{ic}^0)^T P_i^0 + P_i^0 A_{ic}^0 + (A_{ic}^0)^T \delta P_i + \delta P_i A_{ic}^0 - P_i^0 B_i \delta L_i - (\delta L_i)^T B_i^T P_i^0$$

where $A_{ic} = A_i - B_i L_i^0$, L_i is replaced by $L_i^0 + \delta L_i$, and the other entries of the design inequalities remain unchanged. This approximates the inequalities in Theorem 6.2 by linear matrix inequalities in δP_i and δL_i. To guarantee that the linearization is valid, it is useful to add a trust region constraint such as

$$\|\delta P_i\| \leq \alpha \|P_i^0\|$$

Finally, rather than minimizing the right-hand side of (6.8) we minimize the quantity $x_0^T(\delta P_{i0})x_0$.

An interesting feature of the BMI-based design approach is that it is easy to include additional constraints, such as continuity and boundedness of the control law (see, *e.g.*, [171]). The following example illustrates the techniques.

EXAMPLE 6.1
Consider the following simple model of an inverted pendulum

$$\begin{aligned} \dot{x}_1 &= x_2 \\ \dot{x}_2 &= -0.1x_2 + \sin(x_1) + u \end{aligned} \tag{6.9}$$

We are interested in applying the proposed techniques to find a feedback control that brings the pendulum from rest at the stable equilibrium $(\pi, 0)$ to the upright position $(0, 0)$ while minimizing the criteria

$$J(x, u) = \int_{t=0}^{\infty} 4x_1^2(\tau) + 4x_2^2(\tau) + u^2(\tau)\, d\tau.$$

A piecewise linear model of the system (6.9) can be constructed by finding piecewise affine bounds on the system nonlinearity $\sin(x_1)$. For the purpose of this example, we divide the interval $[-4, 4]$ into five segments and compute the bounds illustrated in Figure 6.1 (left).

The equilibrium point $(0, 0)$ is unstable, but the system is quadratically stabilizable and Theorem 6.1 returns the stabilizing control law

$$u = -Lx = -1.20x_1 - 1.15x_2$$

Theorem 6.2 estimates the performance of this control law to be

$$J(x_0, -Lx) \leq 90.68$$

This control law can be used as starting point for the linearization method outlined above. To illustrate how additional constraints can be incorporated in the design procedure, we will require that the control law is continuous.

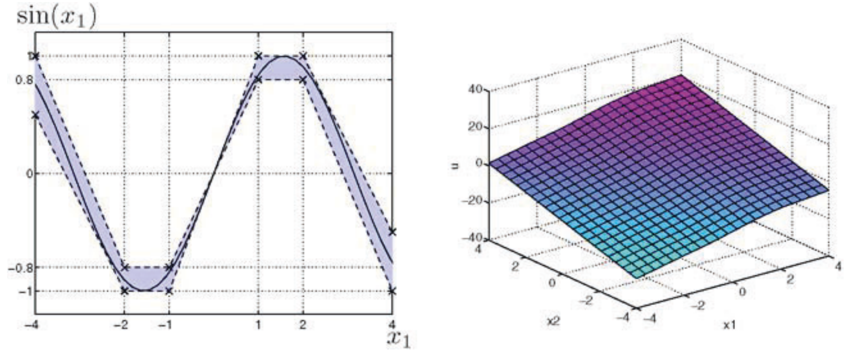

Figure 6.1 The left figure shows bounds on the system nonlinearity. The right figure shows the synthesized continuous and piecewise linear state feedback law.

We use the format for continuous piecewise linear functions proposed in Section 4.10, *i.e.*, we will let $\bar{L}_i$ be on the form

$$\bar{L}_i = L^T \bar{F}_i \qquad i \in I \tag{6.10}$$

Here, L is the parameter vector and $\bar{F}_i$ are the same continuity matrices that are used to parameterize the Lyapunov function candidate. A couple of iterations of the linearization procedure gives a continuous piecewise linear feedback shown in Figure 6.1 (right) with estimated performance 58.75. □

Lower Bounds via Convex Optimization

The non-convexity of the control design problem in the general case is somewhat discomforting. When the iterations cease to make progress we have no way of telling if the associated solution is close to optimal or not. In this section, we will use the alternative Hamilton-Jacobi-Bellman inequality (6.3) to derive a lower bound on the objective that can be achieved by *any* control. This bound can be computed via convex optimization. The computations also give a natural piecewise linear state feedback that tries to achieve this cost. The method can be used by itself or together with the design methods described above. The following result shows how the lower bound computation can be cast as a semidefinite programming problem.

THEOREM 6.3—LOWER BOUND ON OPTIMAL COST
Assume existence of symmetric matrices T and U_i, such that U_i have non-

negative entries, while $P_i = F_i^T T F_i$ and $\bar{P}_i = \bar{F}_i^T T \bar{F}_i$ satisfy

$$0 < \begin{bmatrix} P_i A_i + A_i^T P_i + Q_i - E_i^T U_i E_i & P_i B_i \\ B_i^T P_i & R_i \end{bmatrix} \qquad i \in I_0$$

$$0 < \begin{bmatrix} \bar{P}_i \bar{A}_i + \bar{A}_i^T \bar{P}_i + \bar{Q}_i - \bar{E}_i^T U_i \bar{E}_i & \bar{P}_i \bar{B}_i \\ \bar{B}_i^T \bar{P}_i & R_i \end{bmatrix} \qquad i \in I_1$$

Then, every trajectory $x(t)$ of (2.3) with $x(t) \in X$, $x(\infty) = 0$ and $x(0) = x_0 \in X_{i_0}$ satisfies

$$J(x_0, u) \geq \sup_{T, U_i} \bar{x}_0^T \bar{P}_{i_0} \bar{x}_0$$

□

Proof: See Appendix A.

Theorem 6.3 gives a lower bound on the minimal value of the cost function J that can be achieved by any control. Upper bounds are obtained by studying specific control laws, such as the one obtained by the minimization

$$\min_u \left(\frac{\partial V}{\partial x} f(x, u) + L(x, u) \right). \tag{6.11}$$

If the H-J-B equation (6.2) holds, then every minimizing control law is optimal. However, if only the inequality (6.3) holds (for example as a result of solving the matrix inequalities in Theorem 6.3) then there is no guarantee that the control law minimizing (6.11) is even stabilizing. Still, the minimization problem can be used as the starting point for definition of control laws that will be used in our further analysis.

Exact minimization of the expression (6.11) can be done analytically in analogy with ordinary linear quadratic control, using the notation

$$\begin{aligned} L_i &= R_i^{-1} B_i^T P_i, & \bar{L}_i &= R_i^{-1} \bar{B}_i^T \bar{P}_i, \\ \mathcal{A}_i &= A_i - B_i L_i, & \bar{\mathcal{A}}_i &= \bar{A}_i - \bar{B}_i \bar{L}_i, \\ \mathcal{Q}_i &= Q_i + P_i B_i R_i^{-1} B_i^T P_i, & \bar{\mathcal{Q}}_i &= \bar{Q}_i + \bar{P}_i \bar{B}_i R_i^{-1} \bar{B}_i^T \bar{P}_i. \end{aligned} \tag{6.12}$$

The minimizing control law can then be written as

$$u(t) = -\bar{L}_i \bar{x} \qquad x \in X_i.$$

If the control law is stabilizing, an upper bound on the optimal cost can be obtained from Theorem 6.2.

This control law is simple but may be discontinuous and give rise to attractive sliding modes (which are disregarded in Theorem 6.3). A procedure for constructing continuous feedback laws was suggested in [170]. In addition, one can always use the value function computed in Theorem 6.3 to initialize the BMI approach. It is then easy to enforce continuity of the control law using, for example, the techniques from Example 6.1. The following example illustrates the use of the lower bound computations.

EXAMPLE 6.2—CONTROL OF INVERTED PENDULUM (CONTINUED)
Consider again the control of the inverted pendulum described in Example 6.1. A direct application of Theorem 6.3 gives the lower bound

$$54.23 \leq J(x_0, u)$$

Thus, the contol law computed in Example 6.1 is close to optimal. It is easy to verify that the control law (6.12) obtained from the lower bound computation results in a stable closed-loop system with no attractive sliding modes. An evaluation of the performance of this control law using Theorem 6.2 gives the upper bound $J(x_0, u) \leq 59.64$. This is slightly worse than what was achieved by the (computationally more intensive) BMI-approach. We conclude that the control law computed in Example 6.1 satisfies

$$54.23 \leq J(x_0, u) \leq 58.75.$$

Note that although the bounds are optimized for one particular initial value, the computed functions bound the performance for all initial values that result in trajectories that remain in the partition. The level surfaces of the upper and lower bounds on the value function are shown in Figure 6.2 (left). In addition, the computed control law is evaluated on the pendulum model (6.9) by simulation. The value of the loss function computed in this way is $J(x_0, u) = 54.49$. □

6.3 Comments and References

BMI-Based Controller Design

The use of the matrix inequalities in Theorem 6.2 for control design is, to the best of the author's knowledge, new. However, BMI-based control design procedures for piecewise linear systems have been suggested before. Slupphaug [190] derived BMI conditions for quadratic stabilizability of discrete-time piecewise linear systems, Rodrigues *et.al.* have developed a number

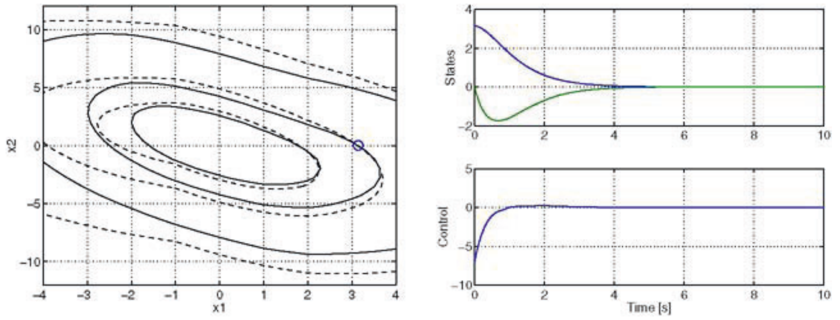

Figure 6.2 The left figure shows lower (dashed) and upper (solid) bounds on the optimal costs. Although the bounds are optimized for the initial value $x_0 = (\pi,\ 0)$, the bounds match well over the full partition. The right figure shows a simulation of the computed control law.

of BMI-based techniques for stabilization of piecewise linear systems with multiple equilibria, and Mulder and Kothare [143] used piecewise quadratic Lyapunov functions and BMI-optimization to design anti-windup control systems. The description of the BMI-based design procedure in this book is very short and the interested reader is urged to seek out the above references for more details and alternative formulations.

Optimal Control and the Hamilton-Jacobi-Bellman Inequality

Trajectory optimization and design of optimal feedback laws are important problems in science and engineering, and a wide variety of numerical methods for solving optimal control problems have been developed (see, *e.g.*, [12, 37, 185]). We have considered an alternative approach based on Hamilton-Jacobi-Bellman inequalities and convex optimization. These ideas have been further developed in [168]. We also note that the H-J-B inequality has a long history in optimal control of systems with discrete states, see, *e.g.*, [20].

Piecewise Linear Quadratic Control

Work related to the term piecewise linear quadratic control has appeared in [11, 213]. In [11], linear quadratic control problems for piecewise linear systems were addressed by solving Riccati differential equations and the optimum had to be recomputed for each new final state. The reference [213] treats control design for linear systems with bounded controls. A piecewise linear control law is obtained by scheduling a set of state feedback controllers designed via linear quadratic theory.

7

Selected Topics

The analysis procedures developed so far can be extended in many useful ways. In this chapter, we present four specific extensions.

Our first extension is to demonstrate how piecewise quadratic Lyapunov functions can be used to estimate regions of attractions. For systems with finite stability regions, the analysis conditions derived in Chapter 4 cannot be verified globally and the techniques cannot be immediately applied. We propose a simple solution to this problem that addresses the central issues of how to restrict the analysis region and optimize the size of the estimated stability domain. We observe that this approach yields significantly better estimates than recent methods based on the circle and Popov criteria.

We then investigate how piecewise linear system approximations and piecewise quadratic Lyapunov functions can be used for rigorous analysis of smooth nonlinear systems. We show how approximation errors can be accounted for so that a successful stability analysis of the piecewise linear approximation also guarantees stability of the underlying smooth system. In addition, we establish a converse theorem stating that, in principle, whenever the underlying system is exponentially stable we can compute a piecewise quadratic Lyapunov function that proves it.

It is often necessary to refine an initial partition in order to achieve sufficient accuracy in the piecewise linear approximation and adequate flexibility in the piecewise quadratic Lyapunov function candidate. It is then natural to ask how such partition refinements can be made efficiently and automatically. As a third extension we devise a simple method for automatic partition refinements. The algorithm uses linear programming duality in an attempt to improve flexibility and accuracy where it is needed the most.

Our final extension is to show how fuzzy systems can be viewed as piecewise linear differential inclusions and analyzed using piecewise quadratic Lyapunov functions. This allows an important class of fuzzy control systems to be analyzed using substantially more powerful methods than was previously available.

M. Johansson: Piecewise Linear Control Systems, LNCIS 284, pp. 107-128, 2003.

7.1 Estimation of Regions of Attraction

In many cases, a local stability analysis of an equilibrium point cannot be extended globally. This occurs when the equilibrium point has a finite region of attraction (so that trajectories that start outside this region never converge to the equilibrium point) but can also happen for other reasons. The following example illustrates an interesting situation.

EXAMPLE 7.1—LYAPUNOV ANALYSIS OF SATURATED SYSTEM
Consider again the double integrator under bounded linear feedback

$$\begin{aligned}\dot{x}_1 &= x_2\\ \dot{x}_2 &= -\mathrm{sat}(2x_1 + 3x_2)\end{aligned}$$

We know from Example 4.1 that the origin is locally stable and that a (relatively small) region of attraction can be estimated using Proposition 4.1. Although an attempt to establish global stability using Theorem 4.1 fails, it is easy to verify that the piecewise quadratic Lyapunov function

$$V(x_1, x_2) = \frac{1}{2}x_1^2 + \frac{1}{2}\int_0^{2x_1+3x_2} \mathrm{sat}(z)\, dz \tag{7.1}$$

proves global asymptotic stability of the origin. The failure of Theorem 4.1 can be understood by noting that the convergence is not exponential in the saturated regions and that the Lyapunov function (7.1) cannot be bounded in the sense of Lemma 4.1 (the Lyapunov function grows quadratically in the x_1-direction, but only linearly in the x_2-direction). □

Even if the stability conditions developed in Chapter 4 fail to hold on the natural partition of the piecewise linear system one can still hope to find a larger stability domain than the one resulting from a purely linear analysis. A simple way to extend the local analysis is to try to verify the stability conditions on some ellipsoid $\mathcal{E}_A(r) = \{x \mid x^T P x \le r^2\} \subseteq X$. By gradually increasing the radius r of the ellipsoid, one increases the analysis domain, and hopefully also the resulting domain of attraction. Let

$$\bar{S}_A(r) = \begin{bmatrix} -P & 0 \\ 0 & r^2 \end{bmatrix} \tag{7.2}$$

and express $\mathcal{E}_A(r)$ as

$$\mathcal{E}_A(r) = \left\{x \mid \bar{x}^T \bar{S}_A(r) \bar{x} \ge 0\right\}$$

Stability analysis on $X \cap \mathcal{E}_A(r)$ can then be carried out by adding the relaxation term $u_i \bar{S}_A(r)$ to the LMI conditions of Theorem 4.1. This leads to the following straight-forward but useful extension.

PROPOSITION 7.1
Consider positive scalars u_i and w_i and symmetric matrices T, U_i and W_i such that U_i and W_i have nonnegative entries, while $P_i = F_i^T T F_i$ and $\bar{P}_i = \bar{F}_i^T T \bar{F}_i$ satisfy

$$\begin{cases} 0 > A_i^T P_i + P_i A_i + E_i^T U_i E_i \\ 0 < P_i - E_i^T W_i E_i \end{cases} \qquad i \in I_0$$

$$\begin{cases} 0 > \bar{A}_i^T \bar{P}_i + \bar{P}_i \bar{A}_i + \bar{E}_i^T U_i \bar{E}_i + u_i \bar{S}_A(r) \\ 0 < \bar{P}_i - \bar{E}_i^T W_i \bar{E}_i - w_i \bar{S}_A(r) \end{cases} \qquad i \in I_1$$

Then, every level set

$$\mathcal{D}_\alpha = \{x \mid \bar{x}^T \bar{P}_i \bar{x} \leq \alpha \quad x \in X_i,\ i \in I\}$$

such that $\mathcal{D}_\alpha \subseteq \mathcal{E}_A(r)$ is a domain of attraction of the origin for the system (2.3) in the sense that all trajectories of (2.3) with $u \equiv 0$ and $x(0) \in \mathcal{D}_\alpha$ tend to the origin exponentially. □

Since there might be several solutions to the conditions of Proposition 7.1, it is natural to try to maximize the "size" of the computed level sets. However, determining the volume of a convex body (even if it is restricted to be a convex polyhedron) is computationally hard in general [69] and a formula that allows direct optimization of the volume of $\mathcal{D}_\alpha$ appears out of reach. For quadratic Lyapunov functions, $V(x) = x^T P x$, one alternative to maximizing the volume of $\mathcal{D}_\alpha$ is to minimize the trace of P (see Section A.2). Inspired by this criterion, we suggest to minimize the sum of traces of the matrices P_i that describe the Lyapunov function in each region. Hence, we propose to solve the convex optimization problem

$$\text{minimize} \sum_{i \in I} \mathbf{Tr} P_i \tag{7.3}$$

subject to the conditions in Proposition 7.1. This is only a heuristic criterion, but it appears to work very well in practice.

It makes intuitive sense to apply Proposition 7.1 iteratively. By restricting the analysis region to some ellipsoid $\mathcal{E}_A(r)$ we can compute a piecewise quadratic Lyapunov function $V(x) = \bar{x}^T \bar{P}_i^0 \bar{x}$ and an associated estimate of the region of attraction. This estimate often captures the shape of the actual region of attraction better than the initial ellipsoid and an improved estimate can be obtained by restricting the analysis region to a scaled version of this domain. This can be done by replacing $\bar{S}_A(r)$ with

$$\begin{bmatrix} 0 & 0 \\ 0 & r^2 \end{bmatrix} - \bar{P}_i^{(0)}$$

in Proposition 7.1 and sweeping r to find the largest value for which the revised analysis conditions admit a solution.

To extract the best region of attraction that can be estimated using Proposition 7.1 we need to find the largest level set of $V(x)$ contained in the analysis region. A good estimate can often be obtained as follows:

PROPOSITION 7.2
For every $i \in I$, let $\alpha_i^\star$ be the largest α_i such that

$$\bar{S}_A(r) > w_i \left(\begin{bmatrix} 0 & 0 \\ 0 & \alpha_i \end{bmatrix} - \bar{P}_i \right) + \bar{G}_i^T W_i \bar{G}_i$$

has a feasible solution $W_i \succeq 0$, $w_i \geq 0$. Then

$$\mathcal{D}_\alpha \subseteq \mathcal{E}_A(r)$$

for all $\alpha < \min_{i \in I} \alpha_i^\star$. □

Proof: For $x \in \mathcal{D}_\alpha$, the inequality implies $\bar{x}^T \bar{S}_A(r) \bar{x} \geq 0$, and hence $x \in \mathcal{E}_A(r)$.

The following example demonstrates how Propositions 7.1 and 7.2 can be used to compute significantly better estimates of the region of attraction for the saturated system than what can be obtained from Proposition 4.1.

EXAMPLE 7.2—EXTENDED ROA ESTIMATION FOR SATURATED SYSTEM
By restricting the analysis to a ball ($P = I$) and gradually increasing the analysis radius r, exponential stability can be established for a very large radius (in the order or $r = 1E4$). The level surfaces of the computed Lyapunov function are shown in Figure 7.1. Note that this is a drastic improvement over the linear analysis suggested in Example 4.1.

We can understand the improved results by noting that even if the Lyapunov function (7.1) cannot be bounded by quadratic functions globally it can be bounded by quadratics on any compact domain. Numerical precision appears to limit how far the analysis domain can be extended. □

The choice of initial analysis ellipsoid is crucial for obtaining good results using Proposition 7.1. A simple choice is to use the ellipsoid obtained by the linear analysis of Proposition 4.1 but better analysis ellipsoids can be

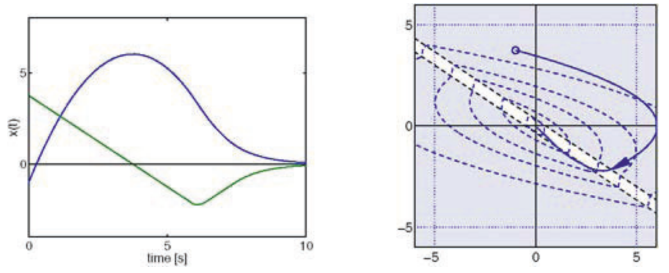

Figure 7.1 Although the system trajectories do not have uniform global exponential decay in the saturated regions (left), it is still possible to find a piecewise quadratic Lyapunov function that verifies stability for a very large set of initial values.

obtained for particular classes of systems. In the rest of this section we will focus on linear systems with saturation. We will show how the resulting approach gives significant improvements over alternative methods and yields estimates close to the true regions of attraction.

Estimating Regions of Attraction for Saturated Linear Systems

Consider a linear system under saturated linear feedback

$$\dot{x}(t) = Ax(t) + b\,\mathrm{sat}(k^T x) \qquad x(0) = x_0 \tag{7.4}$$

where sat$(\cdot)$ denotes the unit saturation. For simplicity, we will focus on the case of a single saturation nonlinearity (the multiple saturation case can be dealt with using similar ideas). A piecewise linear description for this system has been worked out in Examples 2.1, 4.5 and 4.4.

In Example 4.1, we illustrated how a simple estimate of the region of attraction can be computed using a linear analysis restricted to the non-saturated region. However, as shown in [160, 82], it is possible to obtain much better estimates at a slight increase in computations. By modelling the saturation as a locally sector-bounded element

$$q/r \leq \mathrm{sat}(q) \leq q \qquad \text{for } |q| \leq r$$

(see Figure 7.2) we obtain a polytopic model of the system dynamics

$$\dot{x}(t) \in \overline{\mathrm{co}}\left\{(A + bk^T)x(t), (A + r^{-1}bk^T)x(t)\right\}$$

This model is valid for all trajectories $x(t)$ of (7.4) that satisfy

$$|k^T x(t)| \leq r \qquad \forall t \geq 0$$

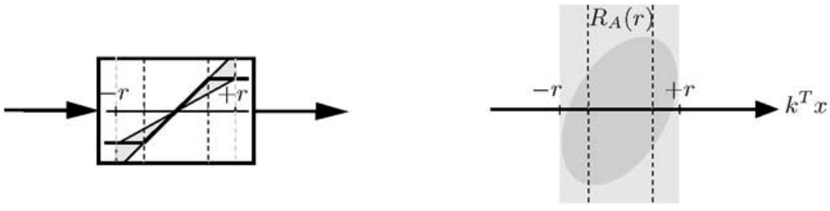

Figure 7.2 Modeling the saturation nonlinearity as a sector-bounded element (left) and the associated analysis region $R_A(r)$ in the state space (right).

An estimate of the domain of attraction can be found by searching for a simultaneous Lyapunov function for the extreme systems of the polytopic model (similarly to Proposition 4.2). Since the model is only valid within the analysis region

$$R_A(r) = \{x \mid -r \leq k^T x \leq r\}$$

any level set of $V(x)$ contained within $R_A(r)$ is a domain of attraction of the system (7.4). The following result shows how to find the simultaneous Lyapunov function with largest level set (in terms of trace) fully contained in the analysis region (*cf.* [82, 160])

PROPOSITION 7.3—ELLIPSOIDAL RoA FOR SATURATED LINEAR SYSTEM
A solution $P = P^T$ to the convex optimization problem

$$\begin{array}{lll} \text{minimize} & \mathbf{Tr} P & \\ \text{subject to} & (A + bk^T)^T P + P(A + bk^T) & < 0 \\ & (A + r^{-1}bk^T)^T P + P(A + r^{-1}bk^T) & < 0 \\ & \begin{bmatrix} r^2 & k^T \\ k & P \end{bmatrix} & > 0 \end{array} \tag{7.5}$$

guarantees that $\mathcal{D}_r = \left\{x \mid x^T P x \leq 1\right\}$ is a region of attraction for (7.4). □

To find the largest domain of attraction that can be estimated using the formulation above, we need to do a search over the parameter r. The resulting estimate is often substantially better than what can be obtained using a purely linear analysis. Moreover, since the estimated region of attraction typically captures the rough shape of the true stability domain it is natural to use $\mathcal{D}_r$ as analysis ellipsoid in the piecewise quadratic approach. Thus, we propose to first apply Proposition 7.3, use the optimal solution P to define the matrices $\bar{S}_A$ in (7.2), and then apply Proposition 7.1.

Finally, when we restrict the analysis domain to the ellipsoid $\mathcal{E}_A(r)$ we can also refine the cell boundings to reflect the relevant parts of the saturated regions. Since $x \in \mathcal{E}_A(r)$ implies that $|k^T x| \leq r$, we can replace the cell boundings suggested in Example 4.5 by

$$\bar{E}_1 = \begin{bmatrix} -k^T & -1 \\ k^T & r \end{bmatrix} \qquad \bar{E}_3 = \begin{bmatrix} k^T & -1 \\ -k^T & r \end{bmatrix}$$

Our proposed methodology for finding a piecewise quadratic estimate of the domain of attraction for the linear system with saturation (7.4) can now be summarized as follows:

ALGORITHM 7.1—ROA ESTIMATE FOR SATURATED LINEAR SYSTEM

1. Compute an initial estimate of the domain of attraction using the robust approach described in Proposition 7.3.
2. Use this quadratic estimate to define an initial analysis ellipsoid via (7.2) and to refine the cell boundings for the saturated regions.
3. Compute a piecewise quadratic estimate by minimizing the objective function (7.3) subject to the conditions in Proposition 7.1. Extract the estimated region of attraction using Proposition 7.2.
4. If desired, use the piecewise quadratic estimate to redefine the analysis region and go to step 3.

□

The follwing two examples illustrate the approach.

EXAMPLE 7.3—[160]
Consider the saturated linear system (7.4) defined by

$$A = \begin{bmatrix} 0 & 1 \\ 1 & 0 \end{bmatrix} \quad b = \begin{bmatrix} 0 \\ -5 \end{bmatrix} \quad k = \begin{bmatrix} 2 \\ 1 \end{bmatrix}$$

The domain of attraction estimated by the various methods are shown in Figure 7.3. Note that the piecewise quadratic Lyapunov function matches the actual region of attraction very closely and that dynamics in the saturated regions have unstable equilibrium points in $\pm\begin{pmatrix} 5 & 0 \end{pmatrix}$. In fact, the level sets of the computed Lyapunov function are parabolic rather than ellipsoidal in the saturated regions (the matrices P_1 and P_3 both have one negative eigenvalue). □

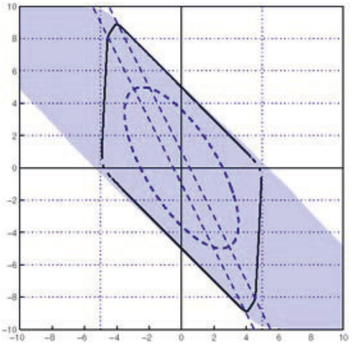

Figure 7.3 Domain of attraction estimated by Proposition 7.3 (dashed) and Proposition 7.1 (full). The shaded region is the true region of attraction (obtained via simulation).

EXAMPLE 7.4
As a second example, consider (7.4) with

$$A = \begin{bmatrix} 0 & 1 \\ 0 & 0.1 \end{bmatrix} \quad b = \begin{bmatrix} 0 \\ -1 \end{bmatrix} \quad k = \begin{bmatrix} 2 \\ 3 \end{bmatrix}$$

In this example, we apply the iterative procedure where the initial piecewise quadratic estimate is used to define the analysis region in the second pass. We find the piecewise quadratic estimate shown in Figure 7.4 (full line). Again, the result is significantly larger than what is produced by Proposition 7.3 and matches the true region of attraction very well. □

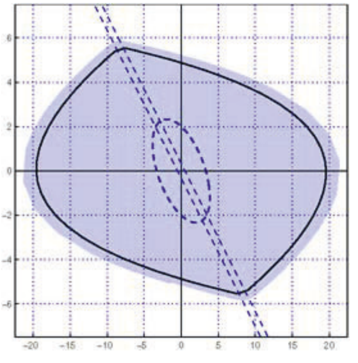

Figure 7.4 The domain of attraction can be improved substantially using the iterative procedure (full line).

7.2 Rigorous Analysis of Smooth Nonlinear Systems

In this section, we will study how the piecewise linear techniques developed in Chapter 4 can be used to analyze smooth nonlinear systems. We will consider an approach where the smooth nonlinear system is approximated by a piecewise linear system and show how approximation errors can be accounted for in the analysis to yield rigorous results for the underlying smooth system. In addition, we will formulate a converse theorem which states that whenever the smooth system is exponentially stable, we can compute a piecewise quadratic Lyapunov function that proves it.

Intuitively, if a piecewise linear approximation of a smooth nonlinear system is "accurate enough" and the approximation admits a piecewise quadratic Lyapunov function, this Lyapunov function should also be valid for the underlying smooth system. To transfer this intuition into a formal statement we must take the approximation errors between the piecewise linear model and the smooth system in account. One way of doing so is to use piecewise linear differential inclusions (*c.f.* Section 4.7). Another alternative is to use a norm bound of the approximation error as follows.

THEOREM 7.1—NORM BOUND APPROXIMATION ERRORS
Let $x(t)$ be a piecewise $\mathcal{C}^1$ trajectory of the system $\dot{x} = f(x)$ and assume that

$$\|f(x) - A_i x - a_i\|_2 \leq \epsilon_i \|x\|_2 \qquad\qquad x \in X_i, i \in I.$$

If there exists numbers $\gamma_i > 0$, symmetric matrices U_i and W_i with non-negative entries, and a symmetric matrix T such that $P_i = F_i^T T F_i$ and $\bar{P}_i = \bar{F}_i^T T \bar{F}_i$ satisfy

$$-2\epsilon_i \gamma_i I > A_i^T P_i + P_i A_i + E_i^T U_i E_i \tag{7.6}$$

$$E_i^T W_i E_i < P_i < \gamma_i I \tag{7.7}$$

for $i \in I_0$ and

$$-2\epsilon_i \gamma_i I > \bar{A}_i^T \bar{P}_i + \bar{P}_i \bar{A}_i + \bar{E}_i^T U_i \bar{E}_i \tag{7.8}$$

$$\bar{E}_i^T W_i \bar{E}_i < \bar{P}_i < \gamma_i I \tag{7.9}$$

for $i \in I_1$, then $x(t)$ tends to zero exponentially. □

Proof: See Section B.5.

In the introductory examples, we used a particularly simple approach for constructing a piecewise linear approximation of a smooth nonlinear function. A compact and convex subset $X \subseteq \mathbb{R}^n$ is partitioned into simplicies by specifying a number of grid points ν_k (vertices of the simplices). A piecewise linear approximation is then constructed by matching the smooth function at the grid points, $f(\nu_k) = A_i\nu_k + a_i$, and interpolating linearly between these points. The approximation error induced by this scheme depends on the smoothness of the function f and the size of the simplices (see [151] for a precise statement). Hence, if no solution to the matrix inequalities in Theorem 7.1 can be found, it makes sense to refine the partition by introducing new grid points (that decrease the size of the simplices) and to try again. Such subdivisions simultaneously reduce the approximation error and increase the flexibility of the Lyapunov function candidate.

It is natural to ask how restrictive this approach is compared to a theorem based on arbitrary continuous Lyapunov functions. The answer is given by the following result which demonstrates that, in priciple, whenever a Lyapunov function exists there also exists a norm-bound piecewise linear approximation and a piecewise quadratic Lyapunov function that satisfies the relevant matrix inequalities of Theorem 7.1.

THEOREM 7.2—A CONVERSE THEOREM
Let $f \in \mathcal{C}^1(X)$ where X is a bounded invariant polytope for the system $\dot{x} = f(x)$. If the system is globally exponentially stable on X, then for every sufficiently refined simplex partition X with corresponding matrices $\bar{E}_i$ and $\bar{F}_i$ defined Proposition A.12 and with $\bar{A}_i$ satisfying $\bar{A}_i\bar{\nu}_i = f(\nu_i)$, there exists a solution $\gamma_i, U_i, \bar{U}_i, W_i, \bar{W}_i$ and T to the inequalities in Theorem 7.1. □

Proof: See Section B.5.

The partition refinements decrease the approximation error and increase the flexibility of the Lyapunov function candidates, but introduce additional matrix inequalities in the analysis problem. For such an approach to be useful in practice, it is important to have support for partition refinements so that increased flexibility is introduced only where it is needed. The problem of automated partition refinements is studied next.

7.3 Automated Partition Refinements

When analyzing a piecewise linear system with a given partition it is natural to use the same partition for the Lyapunov function. However, this is not a definitive choice: some systems admit globally quadratic Lyapunov functions while other systems require repeated partition refinements before the Lyapunov function candidate becomes flexible enough. For example, the initial partition for the dynamics in Example 4.11 had two cells but the Lyapunov function needed a refined partition of four cells before a solution to the analysis inequalities could be found. To verify stability of the smooth nonlinear system in Example 4.8 it was necessary to refine a (globally) linear differential inclusion into a piecewise linear differential inclusion. In Chapter 5, we illustrated how tighter performance bounds could be obtained by refining the partition in order to increase the flexibility of the piecewise quadratic storage function. The approach for analysis of smooth nonlinear systems described in the previous section relies on repeated partition refinements to decrease approximation errors and increase flexibility of the Lyapunov function candidate.

For simple systems, the partition refinements can often be made in an ad-hoc manner. For more complex systems, however, it is important to have tools that indicate where partition refinements are needed the most. In this section we will show how linear programming duality can be used for automated partition refinements in the stability analysis based on piecewise linear Lyapunov functions.

Introducing Flexibility Where Needed

To illustrate the ideas, consider the problem of finding a piecewise linear Lyapunov function on a polytopic partition. Rather than solving the linear programming problem as it stands in Theorem 4.4, we consider the following slight modification

$$\begin{array}{ll} \text{minimize} & \tau \\ \text{subject to} & \tau > p_i^T A_i \nu_k \quad i \in I_0, \ \nu_k \in X_i \\ & \tau > \bar{p}_i^T \bar{A}_i \bar{\nu}_k \quad i \in I_1, \ \nu_k \in X_i \end{array} \tag{7.10}$$

In this formulation, exponential stability according to Theorem 4.4 is obtained when $\tau < 0$. If the optimal value of the linear program is positive, no piecewise linear Lyapunov function exists on the current partition. It is then reasonable to find the cell which imposes the strongest constraint on the optimization problem and to subdivide this cell in order to increase the flexibility of the Lyapunov function candidate. The computations can then be repeated, proving stability or suggesting further partition refinements.

The sensitivity information about which constraints restrict the optimal value τ can be obtained from the solution to the associated dual problem (see, *e.g.*, [21]). Since there are many constraints (*i.e.*, many dual variables) associated to each cell, we propose to compute the "total constraint cost" for each cell as the sum of the dual variables associated to it. The cell with the largest constraint cost can then be subdivided, and an iterative refinement procedure can proceed along the following steps.

ALGORITHM 7.2—AUTOMATED PARTITION REFINEMENTS

1. Solve the linear program from Theorem 4.4, modified as in (7.10).

2. If $\tau < 0$, the procedure has terminated and asymptotic stability has been proven. Otherwise, refine the cell with the highest constraint cost and return to 1.

□

Cell Splitting

After deciding *which* cell to subdivide, one must also decide *how* this subdivision should be done. This appears to be a delicate issue, since not every splitting operation increases the flexibility of the Lyapunov function. The simple idea of splitting a cell by introducing a new vertex in its center has the disadvantage that the boundaries of the cells are never refined (see Figure 7.5a). We therefore suggest to split a cell by introducing a new vertex

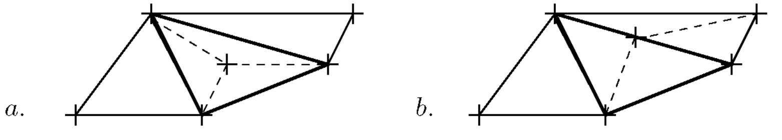

Figure 7.5 Procedures for subdividing a simplex; insertion of a new vertex in the center of a cell (left), or at the center of the longest edge.

in the center of its longest edge (see Figure 7.5b). Note that this operation induces a subdivision also of the neighboring cells. Since the vector field in cells containing the origin is homogeneous, we propose to split these cells by introducing a new vertex in the largest edge of the facet that does not contain the origin.

The following example illustrates the proposed approach.

Example 7.5
Consider the following system

$$\begin{cases} \dot{x}_1 = x_2 \\ \dot{x}_2 = -5x_1 - x_2 - \text{sat}(x_1 + x_2) \end{cases} \tag{7.11}$$

where sat(·) denotes the unit saturation. This system is piecewise linear and has oscillatory dynamics in both the linear and the saturated operating regions. We know from Chapter 4 that piecewise linear Lyapunov functions may require a rather fine partition of the state space in order to prove stability of oscillatory systems. Indeed, for the coarse initial partition shown in Figure 7.6 (left), no piecewise linear Lyapunov function can be found. Based on this initial partition the automatic refinement procedure terminates with the partition shown in Figure 7.6 (right). The corresponding Lyapunov function, shown to the left in Figure 7.7, guarantees exponential decay of all trajectories within the estimated region of attraction, shown as the outermost level set in Figure 7.7 (right).

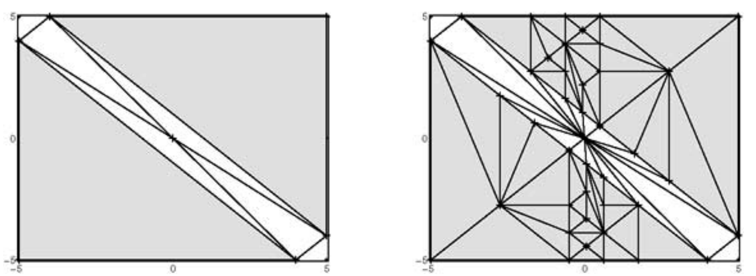

Figure 7.6 Initial partition (left) and automatically refined partition (right).

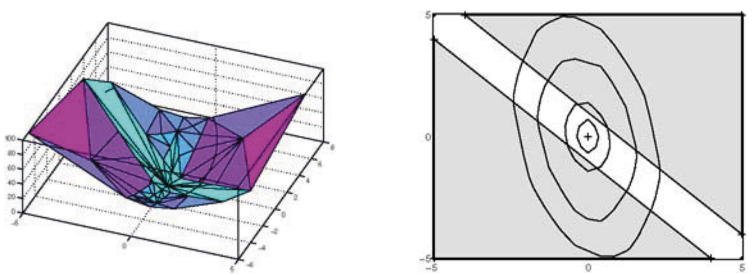

Figure 7.7 Lyapunov function (left) and guaranteed region attraction (right).

□

7.4 Fuzzy Logic Systems

While fuzzy control was quickly embraced by industry, its acceptance in academia has been slow. One reason for this is the evident lack of systematic methods for analysis and design of fuzzy control systems. In this section, we will demonstrate how an important class of fuzzy systems can be modeled and analyzed as piecewise linear differential inclusions, and show how the pwLDI description can be constructed systematically from a given fuzzy rule base. This allows an important class of fuzzy systems to be analyzed using substantially more powerful methods than was previously available.

Takagi-Sugeno Fuzzy Systems

A large amount of work in fuzzy systems literature has been devoted to analysis of Takagi-Sugeno systems [194]. The behavior of these systems are described by a set of rules on the form

$$\begin{aligned} R_i: \quad & \text{IF } x_1 \text{ is } F_{i,1} \text{ AND } \ldots \text{ AND } x_n \text{ is } F_{i,n} \\ & \text{THEN } \dot{x} = A_i x + a_i, \qquad\qquad i = 1, \ldots, L. \end{aligned} \tag{7.12}$$

Normally, the fuzzy sets $F_{i,k}$ (describing the kth input variable in the ith rule) are labeled using linguistic terms such as "Small", "Hot" or "Saturated". Contrary to classical logic, where a proposition such as "x_k is $F_{i,k}$" can only take on values 0 or 1, fuzzy logic allows propositions to be fulfilled to any degree in the interval $[0, 1]$. To support this, one introduces membership functions

$$\mu_{i,k}(x_k) : \mathbb{R} \mapsto [0, 1],$$

that to each x_k assigns a degree of validity of the proposition "x_k is $F_{i,k}$". Using extensions of the inference and compositional rules of classical logic, fuzzy logic provides a framework for reasoning using linguistic rules and information described by fuzzy sets. In particular, given a set of linguistic rules on the form (7.12) and a numerical observation x, fuzzy logic can be used to infer a numerical value of $\dot{x}$. This allows us to specify dynamic system models using a set of linguistic rules, the associated membership functions and some inference parameters (see [50, 209, 7] for further details). By the appropriate restrictions of the fuzzy inference parameters [194, 195, 209] the dynamics infered from the rules (7.12) can be written as

$$\dot{x} = \sum_{i=1}^{L} \mu_i(x) \{A_i x + a_i\} \tag{7.13}$$

where $\mu_i(x)$ are normalized membership functions defined as

$$\begin{cases} \widetilde{\mu}_i(x) = \prod_{k=1}^{n} \mu_{i,k}(x) \\ \mu_i(x) = \dfrac{\widetilde{\mu}_i(x)}{\sum_{i=1}^{L} \widetilde{\mu}_i(x)} \end{cases} \tag{7.14}$$

The normalization implies that $\mu_i(x)$ satisfy $0 \leq \mu_i(x) \leq 1$, $\sum_i \mu_i(x) = 1$.

Drawing upon the work on quadratic stability and quadratic stabilization, the formulation (7.13) has been used as a basis for solve analysis and control problems for fuzzy systems using LMI computations, see *e.g.*, [219, 195]. Although a major breakthrough in the analysis of fuzzy system, these methods view the fuzzy system (7.13) as a linear differential inclusion and are subject to the same criticism as the quadratic stability analysis of piecewise linear systems. First, they disregard the partition information encoded in the membership functions and the premises of the fuzzy rules. Second, they do not admit affine terms in the consequent dynamics. This is a major shortcoming, since many applications use affine Takagi-Sugeno systems (see, *e.g.*, [192, 10]) and the function approximation capabilities of Takagi-Sugeno systems are significantly improved when offset terms are allowed [53]. Finally, they use a very restricted Lyapunov function class (quadratics).

It is thus natural to extend the piecewise quadratic analysis to fuzzy systems. Such an extension would allow fuzzy systems with affine consequent dynamics to be analyzed using very powerful Lyapunov functions in a way that accounts for the structural information expressed by the linguistic rules.

A Piecewise Linear Perspective

In order to clarify the link between fuzzy systems and the piecewise linear systems considered in this book, it is fruitful to consider fuzzy systems as a particular instance of operating regime based models [94, 144]. Operating regime based modeling is a common name for techniques that construct a globally valid model of the system dynamics by combining simple local models, each valid within a certain operating regime. In this context, the special feature of fuzzy systems is that prior knowledge of operating regimes and locally valid dynamics is encoded using fuzzy rules. Each rule premise defines an operating regime and the associated rule consequent specifies the local model valid within this region:

$$\begin{aligned} R_i : \quad & \underbrace{\text{IF } x_1 \text{ is } F_{i,1} \text{ AND } \ldots \text{ AND } x_n \text{ is } F_{i,n}}_{\text{operating regime specification}} \\ & \text{THEN } \underbrace{\dot{x} = A_i x + a_i}_{\text{local dynamics}}, \qquad i = 1, \ldots, L \end{aligned}$$

From the representation (7.13) we see that in regions where $\mu_i(x) = 1$ for some i, all other normalized membership functions evaluate to zero and the dynamics of the system is given by $\dot{x} = A_i x + a_i$. We will call this region the *operating regime* of model i. Between operating regimes there are regions where $0 < \mu_i(x) < 1$. In these regions, the system dynamics is given by a convex combination of several affine systems. We will call these regions *interpolation regimes*. As we will see next, the partitioning into operating and interpolation regimes is often polyhedral and can derived directly from the fuzzy rule base.

The Geometry of Fuzzy Partitions

There is more structure in fuzzy system partitions than what is directly visible in the formulation (7.13). Consider for simplicity the case when the model scheduling is governed by one variable, say, x_k:

$$R_i : \text{IF } x_k \text{ is } F_i \text{ THEN } \dot{x} = A_i x + a_i \qquad i = 1, \ldots, L. \tag{7.15}$$

The operating regimes where $\mu_{i,k}(x_k) = 1$ induce intervals in the scheduling space and parallelotopes in the state space. An example of membership functions and the associated partitioning is shown in Figure 7.8.

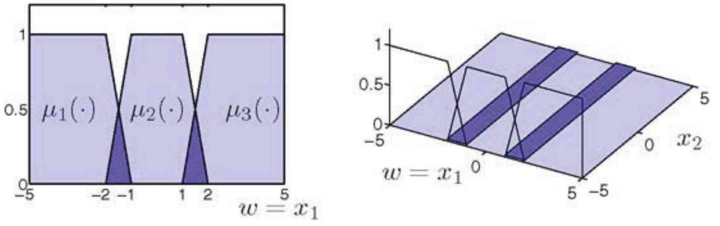

Figure 7.8 The normalized membership functions (left) and the resulting partition of the state space into operating and interpolation regimes (right).

A similar partition structure results when rules are formed using the AND connective in a higher dimensional scheduling space. The rules then take the form (7.12), and the normalized membership functions are obtained as in (7.14). Since $\mu_i(x) = 1$ in operating regime i, we must have $\mu_{i,k}(x_k) = 1$ for all $k = 1, \ldots, n$. Hence, operating regime i is given by the intersection of the cells induced by the fuzzy sets that describe each propositional variable

$$X_i = \{x \mid \mu_i(x) = 1\} = \bigcap_{m=1}^{n} \{x \mid \mu_{i,k}(x_k) = 1\}$$

This allows us to view the partition resulting from rules formed with the AND connective as the composition of several simple partitions, see Figure 7.9. The induced operating and interpolation regimes are also in this case parallelotopes and their description can be obtained directly from the membership function of the simple propositions.

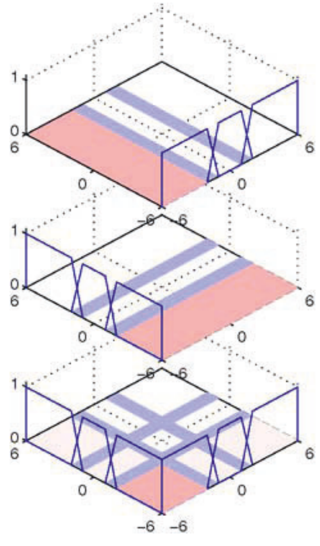

Figure 7.9 The fuzzy partition with scheduling in two variables (bottom) can be derived from the intersection of simple partitions induced by each propositional variable (top and center).

Fuzzy Systems as Piecewise Linear Differential Inclusions

The discussion above establishes that affine Takagi-Sugeno systems can be modeled as piecewise linear differential inclusions. The fuzzy rules (7.12) induce a partitioning of the state space into convex polyhedral sets that act as operation or interpolation regimes. Within each cell, the dynamics is given by a state-dependent convex combination of affine dynamical systems

$$\dot{x} = \sum_{k \in K(i)} \mu_k(x) \{A_k x + a_k\} \qquad\qquad x \in X_i$$

where $0 \leq \mu_k(x) \leq 1$, $\sum_{k \in K(i)} \mu_k(x) = 1$, and

$$K(i) = \{k \mid \mu_k(x) > 0 \text{ for some } x \in X_i\}.$$

In particular, if X_i is an operating regime, then $K(i)$ contains only one element. By disregarding the state dependence of the membership functions within each cell, we can embed these systems into the class of pwLDIs

$$\dot{\bar{x}} \in \overline{\text{co}}_{k\in K(i)} \{\bar{A}_k \bar{x}\} \qquad\qquad x \in X_i$$

and Theorem 4.2 applies directly. This allows an important class of fuzzy systems to be analyzed using much more powerful methods than was previously available.

If the associated LMI problem has too many variables, one might consider alternative formulations based on solving the analysis problem in two steps or the use of quadratic cell boundings (compare Section 4.9). Since the cells are often parallelotopes, quadratic cell boundings of minimal volume can be computed efficiently using Proposition A.10.

An Example

In order to demonstrate the feasibility of the approach to problems of realistic size, this section presents a piecewise quadratic stability analysis of a 25-region fuzzy system. The system dynamics is given by the nine rules in Table 7.1. The membership functions of the fuzzy propositions "x_i is $F_{l,i}$"

Table 7.1 Rule base for 25 region fuzzy system.

IF	x_1 is negative	AND	x_2 is positive	THEN	$\dot{x} = A_1x + a_1$
IF	x_1 is zero	AND	x_2 is positive	THEN	$\dot{x} = A_2x + a_2$
IF	x_1 is positive	AND	x_2 is positive	THEN	$\dot{x} = A_3x + a_3$
IF	x_1 is negative	AND	x_2 is zero	THEN	$\dot{x} = A_4x + a_4$
IF	x_1 is zero	AND	x_2 is zero	THEN	$\dot{x} = A_5x + a_5$
IF	x_1 is positive	AND	x_2 is zero	THEN	$\dot{x} = A_6x + a_6$
IF	x_1 is negative	AND	x_2 is negative	THEN	$\dot{x} = A_7x + a_7$
IF	x_1 is zero	AND	x_2 is negative	THEN	$\dot{x} = A_8x + a_8$
IF	x_1 is positive	AND	x_2 is negative	THEN	$\dot{x} = A_9x + a_9$

are trapezoidal as shown in Figure 7.8, and the resulting partitioning of the state space into operating and interpolation regimes is shown in Figure 7.10. Note that the dynamics have bias terms in all regions that do not contain the origin, and that the system matrices associated to some of the operating regions are non-Hurwitz (these operating regimes, given by the two last rules of the rule base, are slightly shaded in Figure 7.10). Hence, the standard conditions for quadratic stability cannot be applied.

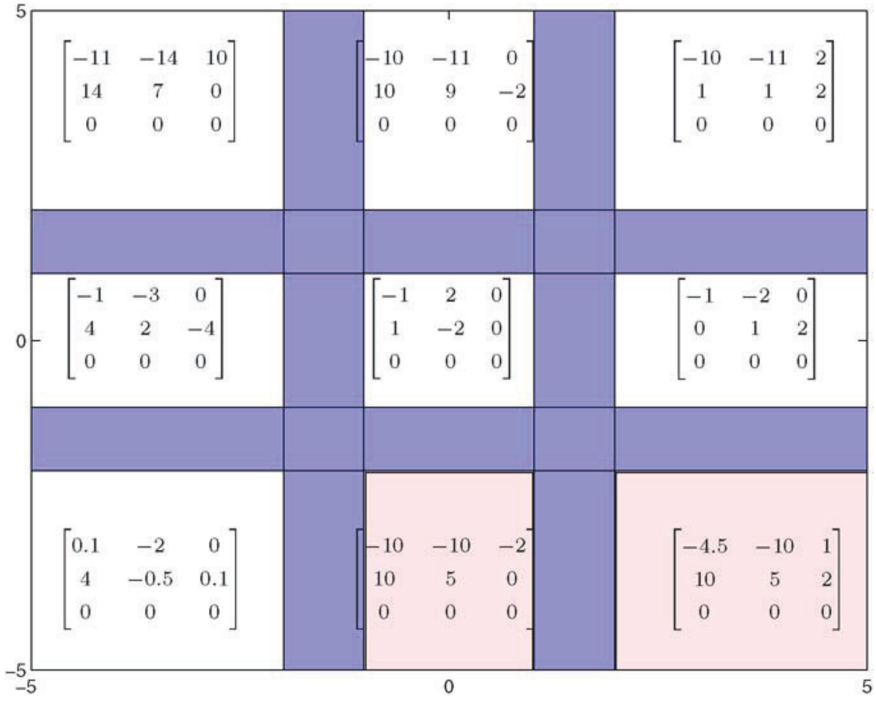

Figure 7.10 Partition of the fuzzy system defined by the rules in Table 7.1 into operating regimes and interpolation regimes. The matrices $\bar{A}_i$ defining the dynamics in each operating regime are also shown.

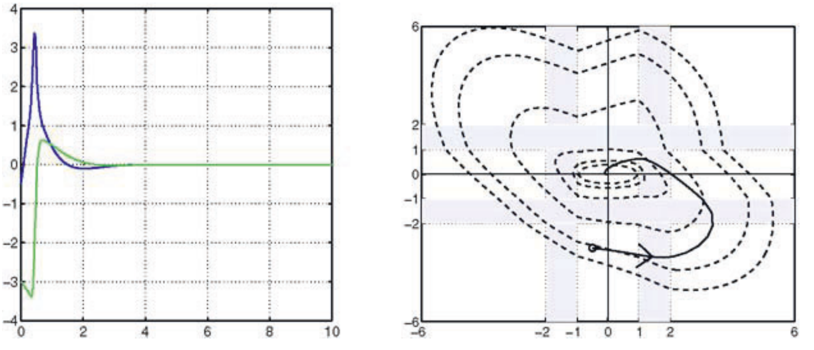

Figure 7.11 System response from a typical initial condition (left), and level surfaces of the computed Lyapunov function (right).

As shown in Figure 7.11(left), simulations reveal a highly nonlinear behavior but suggest that the system is stable. The linear matrix inequalities of Theorem 4.2 have a feasible solution proving exponential stability of the origin. The level surfaces of the computed Lyapunov function are indicated by dashed lines in Figure 7.11(right). We conclude asymptotic stability of the origin with a guaranteed region of attraction indicated by the outermost level set shown in Figure 7.11.

7.5 Comments and References

Estimating Regions of Attraction

The problem of determining regions of attraction for nonlinear systems has a long history and a wealth of techniques have been developed in the literature (see, for example, the survey papers [63, 24]). The problem is not only theoretically challenging, but also very relevant in practice. In many safety-critical systems (such as power systems, aerospace applications, and process control systems [152, 17, 179, 1]) it is essential to be able to determine the region of safe operation. In addition, many high-performance controllers (*e.g.*, [137, 217]) use time-optimal control for state transfer and a dynamic controller for regulation around a set-point. To be able to do safe switching between the controller modes, it is important to know when the system state has entered the region of attraction of the dynamic controller (see [136] for more details). Although our approach applies to general piecewise linear systems, we have focused on linear systems with saturation for which both computational techniques and theoretical tools are more complete (see, *e.g.*, [82, 160, 85, 174, 148, 65, 178, 86]). Techniques closely related to ours can be found in [82, 160, 85].

Establishing Convergence to a Set

Some systems have equilibrium sets (multiple equilibrium points, limit cycles, etc.) rather than a single equilibrium point. Although the results developed so far do not apply to this situation it is often possible to prove convergence to a set using a dual approach to the technique used for estimating regions of attraction. Let $\mathcal{E}_A(r)$ be an ellipsoid. If we can find a Lyapunov function $V(x)$ that satisfies the Lyapunov inequalities on $X \backslash \mathcal{E}_A(r)$ (*i.e.*, on the partition with $\mathcal{E}_A(r)$ removed) then any trajectory starting within the largest level set of $V(x)$ contained in X converges to the smallest level set of $V(x)$ that contains $\mathcal{E}_A(r)$. If $\mathcal{E}_A(r)$ contains the origin, the Lyapunov function search leads to similar matrix inequalities as in Proposition 7.1 but with $\bar{S}_A(r)$ replaced by $-\bar{S}_A(r)$.

Stability Analysis of Fuzzy Systems

The fuzzy community may have been first in using LMI computations for design and analysis of nonlinear control laws [219, 195] and the need to move beyond quadratic Lyapunov functions was recognized early [118]. In fact, the use of *discontinuous* piecewise quadratic Lyapunov functions has also been used in the independent work [54]. In comparison with these results, an application of Theorem 4.2 to fuzzy systems constitutes a number of significant improvements. This includes the use of the S-procedure to exploit structural information and the ability to handle affine Takagi-Sugeno systems. Moreover, although [54] give procedures for computing different Lyapunov function expressions for each region, one must subsequently verify certain boundary conditions to guarantee system stability. It is suggested that these boundary conditions could be verified by simulation. The approach taken in this chapter avoids this non-trivial step by parameterizing the Lyapunov function candidate to be continuous across cell boundaries.

It should be noted, however, that when the normalized membership functions have global support (*i.e.*, $\mu_i(x) > 0$ for all $x \in X$) there is no clear partition of the state-space into operating and interpolation regimes, and the procedure described in Section 7.4 results in operating regimes where all consequent dynamics are active. An alternative approach for dealing with this class of systems has been proposed by Feng and Harris [55]. Inspired by the use of operating and interpolation regimes we can, for example, define cell X_i as

$$X_i = \bigcap_k \{x \mid \mu_{i,k}(x_k) \geq \mu_{l,k}(x_k) \quad \forall l\}$$

Although rule R_i dominates in X_i, all rules are active. Rather than using a differential inclusion that involves all consequent dynamics, Feng and Harris propose to re-write the dynamics as

$$\dot{x} = \sum_{i=1}^{L} \mu_i(x)\,\{A_i x + a_i\} = A_i x + a_i + \sum_{j=1}^{L} \mu_j(x)\,\{\Delta A_{ij} x + \Delta a_{ij}\} \quad x \in X_i$$

where $\Delta A_{ij} = A_j - A_i$ and $\Delta a_{ij} = a_j - a_i$. Now, the derivative of the Lyapunov function $V(x) = \bar{x}^T \bar{P}_i \bar{x}$ along trajectories of the fuzzy system in cell X_i can be estimated as

$$\begin{aligned}\frac{d}{dt}V(x(t)) &= 2\bar{x}^T \bar{P}_i \left(\bar{A}_i + \sum_{j=1}^{L} \mu_j(x)\overline{\Delta A}_{ij} \right) \bar{x} \\ &\leq \bar{x}^T \left(\bar{A}_i^T \bar{P}_i + \bar{P}_i \bar{A}_i + 2\sum_{j=1}^{L} \zeta_j \bar{P}_i \right) \bar{x} \qquad (7.16)\end{aligned}$$

where $\zeta_{ij} = \|\overline{\Delta A_{ij}}\|_2 \sup_{x \in X_i} \mu_j(x)$. The scalars ζ_{ij} are readily computed, and the search for a piecewise quadratic Lyapunov function whose derivative is negative can be formulated using the techniques from Chapter 4.

Finally, we have only considered fuzzy systems of the Takagi-Sugeno type. Stability conditions for Mamdani-type fuzzy systems based on piecewise quadratic Lyapunov functions can be found in [119].

8

Linear Hybrid Dynamical Systems

Hybrid dynamical systems are systems that combine continuous dynamics and discrete events. In practice, hybrid systems arise when some parts of a physical system can be modeled by differential equations while other parts are more conveniently described by logic or discrete-event systems. A simple example is a continuous process controlled by switching logic (implemented by, say, a programmable logic controller). Although the piecewise linear systems considered so far can be regarded as hybrid systems (the cell index can be seen as a discrete state variable whose value changes when the continuous state crosses a cell boundary) the discrete state has a very passive role in this case, and this model class exhibits few behaviors that cannot be understood using standard nonlinear systems theory.

In this chapter we will consider linear hybrid dynamical systems, a class of piecewise linear systems with a more prominent hybrid nature. In contrast to the piecewise linear systems studied so far, the discrete state is no longer directly determined by the continuous state. The discrete dynamics is described by a finite automoton whose state changes when the continuous state vector enters certain transition sets. Hence, the transition rules for the discrete dynamics depend on both the continuous and the discrete state. This model is simple enough to allow us to develop computational analysis tools yet rich enough to capture the essentials of many practical hybrid systems. In relation to the piecewise linear systems we can view this hybrid extension as piecewise linear systems with overlapping cells in $\mathbb{R}^n$.

We will describe two computational approaches for stability analysis of linear hybrid dynamical systems. One is based on piecewise quadratic Lyapunov functions that are discontinuous but decrease in value at every switching instant, while the other approach uses Lyapunov functionals.

M. Johansson: Piecewise Linear Control Systems, LNCIS 284, pp. 129-141, 2003.

8.1 Linear Hybrid Dynamical Systems

A *linear hybrid dynamical system* can be represented as

$$\begin{cases} \dot{x}(t) = f(x(t), i(t)) & = A_{i(t)}x(t) + a_{i(t)} \\ i(t) = \nu(x(t), i(t^-)) \end{cases} \tag{8.1}$$

Here $x(t) \in \mathbb{R}^n$ is the continuous state vector and $i(t) \in I \subset \mathbb{Z}$ is the discrete state variable. The differential equations describe the continuous dynamics while the algebraic equation models the discrete dynamics. The model associates one affine vector field for the continuous state to each value of the discrete state. The discrete dynamics is described by a finite automoton, whose state changes when the continuous state vector enters certain transition sets. More precisely, a transition from the discrete state j to the discrete state k occurs when the continuous state $x(t)$ enters the *transition surface*

$$\mathcal{S}_{jk} = \{x \mid \bar{f}_{jk}^T \bar{x} = 0\} \tag{8.2}$$

In this way, the discrete state variable $i(t)$ becomes a piecewise constant function of time, and the notation t^- in (8.1) indicates that $i(t)$ is piecewise continuous from the right. A *trajectory* of the system (8.1) on $[t_0, t_f]$ is a pair $(x(t), i(t))$, where $i(t)$ is piecewise constant and $x(t)$ is absolutely continuous, that satisfies the model equations for almost all $t \in [t_0, t_f]$.

In our analysis procedures we need to keep track of the feasible transitions in the discrete state. We represent each feasible transition $j \to k$ by an ordered pair (j, k) and denote the set of all feasible transitions T. In addition we allow affine *mode invariants* $\bar{E}_j$ to be specified for each discrete state. These play the role of cell boundings in the piecewise linear systems model and it is assumed that $\bar{E}_j\bar{x}(t) \succeq 0$ whenever $i(t) = j$. Similarly to the piecewise linear case, the mode invariants do not influence the dynamics but are introduced to reduce conservatism of the analysis. The mode invariants can be derived from the transition surfaces and other invariance considerations.

Linear hybrid dynamical systems can be conveniently visualized as directed graphs which we will call *transition diagrams*, see Figure 8.1. Nodes in the transition diagram correspond to discrete states and arcs describe possible transitions between discrete states. There is an affine dynamics and a mode invariant associated to each node and a transition surface associated to each arc. We identify nodes by the corresponding value of the discrete state and represent arcs as ordered pairs (j, k) of nodes. The leftmost arrow in Figure 8.1 indicates the initial state.

The following example illustrates the model class and the need to extend the piecewise quadratic analysis developed in Chapter 4.

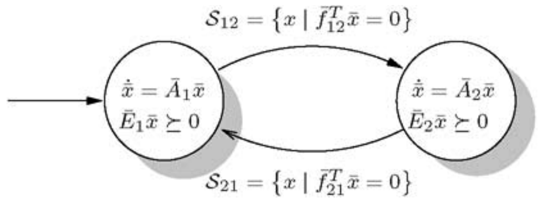

Figure 8.1 Transition diagram of linear hybrid dynamical system in Example 8.1.

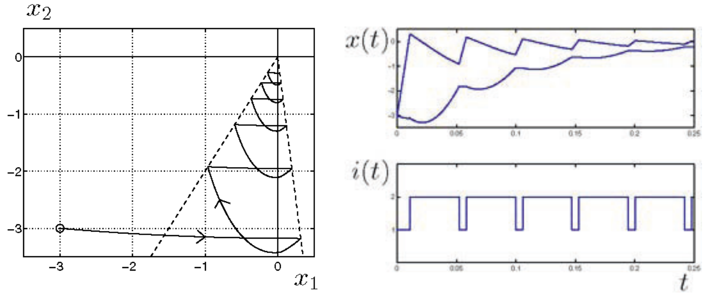

Figure 8.2 Sample trajectory of the hybrid system projected onto the continuous state space (left) and corresponding time responses (right).

EXAMPLE 8.1

Figure 8.2 (left) shows a simulation of the system $\dot{x}(t) = A_{i(t)}x(t)$

$$i(t) = \begin{cases} 2, & \text{if } i(t^-) = 1 \text{ and } f_{12}^T x(t) = 0 \\ 1, & \text{if } i(t^-) = 2 \text{ and } f_{21}^T x(t) = 0 \end{cases} \tag{8.3}$$

with $i(0) = 1$, switching boundaries

$$f_{12} = \begin{bmatrix} -10 & -1 \end{bmatrix}^T, \qquad f_{21} = \begin{bmatrix} 2 & -1 \end{bmatrix}^T$$

and system matrices

$$A_1 = \begin{bmatrix} -1 & -100 \\ 10 & -1 \end{bmatrix}, \qquad A_2 = \begin{bmatrix} 1 & 10 \\ -100 & 1 \end{bmatrix}.$$

The simulations shown in Figure 8.2 indicate that the system is asymptotically stable. From the simulated trajectory it is also clear that the system cannot be analyzed using a Lyapunov function that disregards the influence of the discrete state. □

The state space of the model (8.1), $\mathbb{R}^n \times \mathbb{Z}$, can be thought of as a set of enumerated copies of $\mathbb{R}^n$. From this perspective, a transition in the discrete state can be seen as the transfer from one copy of $\mathbb{R}^n$ to the other, see Figure 8.3. The simulation in Figure 8.2 is the projection of this trajectory onto $\mathbb{R}^n$.

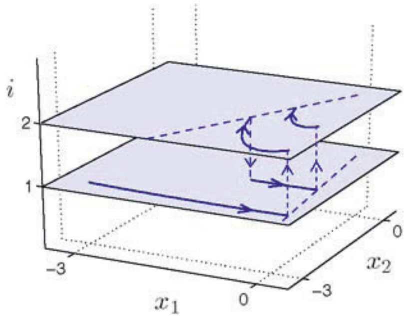

Figure 8.3 State space of hybrid system illustrated as a number of enumerated copies of $\mathbb{R}^n$. Changes in the discrete state transfers the state from one copy to the other.

8.2 Analysis Using Discontinuous Lyapunov Functions

The analysis procedures that we have developed for piecewise linear systems have all been based on continuous Lyapunov functions. When we try to analyze the more complex linear hybrid dynamical systems, however, additional flexibility is often needed. One way of increasing the analytic flexibility is to consider Lyapunov functions that are discontinuous, but whose value decreases every time there is a change in the discrete state. As the following simple argument shows, such Lyapunov functions can also be found by semidefinite programming.

Let the Lyapunov function candidate be $V(x, i) = \bar{x}^T \bar{P}_i \bar{x}$ and assume that the discrete state initially have the value j. Consider the transition from discrete state j to k, which occurs when the continuous state enters the transition surface $\mathcal{S}_{jk}$. The requirement that the Lyapunov function be decreasing at the discrete state change can be expressed as

$$\bar{x}^T \bar{P}_j \bar{x} \geq \bar{x}^T \bar{P}_k \bar{x} \qquad \text{for } x \in \mathcal{S}_{jk} = \{x \mid \bar{f}_{jk}^T \bar{x} = 0\}$$

which is equivalent to the following LMI in $\bar{P}_j, \bar{P}_k$ and $\bar{t}_{jk}$

$$\bar{P}_j - \bar{P}_k + \bar{f}_{jk}\bar{t}_{jk}^T + \bar{t}_{jk}\bar{f}_{jk}^T \geq 0.$$

To formalize these ideas, we consider the problem of establishing exponential stability of the equilibium point $x = 0$. Let $I_0 \subseteq I$ be the non-empty set of discrete states for which $x(t) \equiv 0$ is admissible, and let $I_1 = I \backslash I_0$. For each $i \in I$, assume that the mode invariants are on the form

$$E_i x \succeq 0 \qquad i \in I_0, \qquad\qquad \bar{E}_i \bar{x} \succeq 0 \qquad i \in I_1$$

To obtain strict inequalities in our analysis computations, we define

$$f_{jk} = \begin{cases} \begin{bmatrix} I & 0 \end{bmatrix} \bar{f}_{jk} & \text{if } 0 \in \mathcal{S}_{jk} \\ 0 & \text{otherwise} \end{cases} \tag{8.4}$$

and let $\bar{P}_i = [I \quad 0]^T P_i [I \quad 0]$ for $i \in I_0$. We then have the following result.

THEOREM 8.1
Consider symmetric matrices U_i and W_i with non-negative entries, symmetric matrices P_i and $\bar{P}_i$, and vectors t_{jk} and $\bar{t}_{jk}$ such that

$$\begin{cases} 0 > A_i^T P_i + P_i A_i + E_i^T U_i E_i \\ 0 < P_i - E_i^T W_i E_i \end{cases} \qquad i \in I_0 \tag{8.5}$$

$$\begin{cases} 0 > \bar{A}_i^T \bar{P}_i + \bar{P}_i \bar{A}_i + \bar{E}_i^T U_i \bar{E}_i \\ 0 < \bar{P}_i - \bar{E}_i^T W_i \bar{E}_i \end{cases} \qquad i \in I_1 \tag{8.6}$$

$$0 < \bar{P}_j - \bar{P}_k + \bar{f}_{jk} \bar{t}_{jk}^T + \bar{t}_{jk} \bar{f}_{jk}^T \qquad (j,k) \in T, \quad j \in I_1 \text{ or } k \in I_1 \tag{8.7}$$

$$0 < P_j - P_k + f_{jk} t_{jk}^T + t_{jk} f_{jk}^T \qquad (j,k) \in T, \quad j,k \in I_0 \tag{8.8}$$

then $x(t)$ tends to zero exponentially for every trajectory of (8.1). □

There is a strong relation between Theorem 8.1 and Theorem 4.1. By allowing non-strict inequalities in (8.7) and (8.8), Theorem 4.1 can be seen as a special case of Theorem 8.1 where $\bar{f}_{jk} = \bar{f}_{ji} \; \forall\, i,j \in I$. However, a formulation with non-strict inequalities is numerically very sensitive and most LMI solvers can not treat non-strict inequalities as they stand. Inherent algebraic constraints must first be eliminated. Theorem 4.1 can be seen as the outcome of such an elimination.

Theorem 8.1 can be applied directly to the system of Example 8.1.

EXAMPLE 8.2
Consider again the switching system (8.3). To illustrate the use of mode invariants, we let

$$E_1 = \begin{bmatrix} 0 & 0 \\ 0 & 0 \end{bmatrix}, \qquad E_2 = \begin{bmatrix} -10 & -1 \\ 2 & -1 \end{bmatrix}.$$

The LMI conditions of Theorem 8.1 have a feasible solution

$$P_1 = \begin{bmatrix} 17.9 & -0.89 \\ -0.89 & 179 \end{bmatrix}, \quad P_2 = \begin{bmatrix} 739 & -38.1 \\ -38.1 & 91.8 \end{bmatrix}.$$

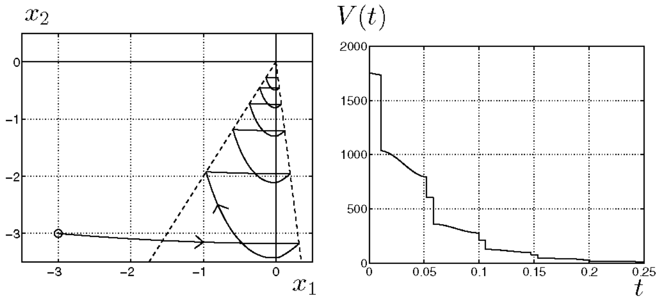

Figure 8.4 Sample trajectory of the hybrid system (left) and the corresponding value of the Lyapunov function (right).

A simulated trajectory of the system and the corresponding value of the computed Lyapunov function are shown in Figure 8.4. The discontinuities in the Lyapunov function concur with changes in the discrete state. □

Extensions

Several useful extension can be made to the above results. It is, for example, straight-forward to allow for nonlinear or uncertain dynamics by conisdering differential inclusions in each mode. Similarly to before, this results in multiple decreasing conditions (one for each extreme system defining the dynamics in each mode).

It is also easy to extend the approach from considering global transition surfaces to allowing for polyhedral transition sets

$$\mathcal{S}_{jk} = \left\{ x \mid \bar{f}_{jk}^T \bar{x} = 0 \ \wedge \ \bar{G}_{jk}\bar{x} \succeq 0 \right\}$$

In this case, (8.7) is replaced by

$$0 < \bar{P}_j - \bar{P}_k + \bar{f}_{jk}\bar{t}_{jk}^T + \bar{t}_{jk}\bar{f}_{jk}^T - \bar{G}_{jk}^T Z_{jk} \bar{G}_{jk}$$

where Z_{jk} has non-negative entries. The other inequalities follow similarly. The same approach can also be used for modeling uncertain transition surfaces, since a solution to the inequality

$$0 < \bar{P}_j - \bar{P}_k - \bar{G}_{jk}^T Z_{jk} \bar{G}_{jk}$$

guarantees that $V(x, j) > V(x, k)$ for all x with $\bar{G}_{jk}\bar{x} \succeq 0$ (see, *e.g.*, [158]).

Finally, it is possible to consider systems that allow for jumps in the continuous state at discrete transitions. In particular, assume that we have affine jump-maps

$$x(t) = \bar{H}_{i(t^-)i(t)}\bar{x}(t^-) \qquad \forall t$$

with $\bar{H}_{ii} = 0$. Then, the condition $\bar{x}^T(t)\bar{P}_j\bar{x}(t) < \bar{x}^T(t^-)\bar{P}_i\bar{x}(t^-)$ can be expressed as

$$0 < \bar{P}_i - \bar{H}_{jk}^T\bar{P}_j\bar{H}_{jk} + \bar{f}_{jk}\bar{t}_{jk}^T + \bar{t}_{jk}\bar{f}_{jk}^T$$

and the other inequalities follow similarly (note, however, that we need to require that the jump maps are linear when $i, j \in I_0$ in order to have strict inequalities in our formulation).

8.3 Stability Analysis Using Lyapunov Functionals

An alternative approach to analysis of linear hybrid dynamical systems has been suggested by Hassibi, Boyd and How [73]. The approach is much more involved than the method presented in Section 8.2 and we will not present it in its fullest generality or detail here. Rather, we aim at giving the flavour of the approach, illustrate how it differs from the analysis based on piecewise quadratic Lyapunov functions, and demonstrate how it can be applied to the analysis of a simple hybrid system. More details can be found in [73, 71].

Lagrange Stability and a Lyapunov Functional Class

Contrary to the analysis procedures derived so far, which consider exponential stability, the analysis procedure described in this section is concerned with Lagrange stability. Recall that a dynamical system with state x is called *Lagrange stable* if $\|x(t)\|$ remains bounded for any given initial state $x(0) = x_0$ [123]. The stability analysis conditions are based on the following result.

PROPOSITION 8.1—[71]
Suppose that the functional $V : (x, i) \mapsto \mathbb{R}$ is such that $V(x, i) \to \infty$ as $\|x\| \to \infty$. Suppose furthermore that V is bounded below, *i.e.*, that there exists $\beta \geq 0$ such that $V \geq -\beta$. Along trajectories of the dynamical system $V(t) = V(x(t), i(t))$ becomes a function of time t. If $V(t)$ is a decreasing function of t, then the system is Lagrange stable. □

To make constructive use of Proposition 8.1, Hassbi *et. al.*, propose a flexible class of Lyapunov functionals that can be computed via convex optimization. To simplify the presentation, we will describe the approach for a systems whose transition surfaces are parallell to each other

$$\mathcal{S}_{jk} = \{x \mid f^T x - g_{jk} = 0\} \tag{8.9}$$

In this case, the stability analysis is based on the Lyapunov functional

$$V(t) = \bar{x}(t)^T\bar{P}_{i(t)}\bar{x}(t) + 2\int_0^t (\alpha(s)f^T x(s) + \beta(s))f^T \frac{d}{ds}x(s)\, ds \tag{8.10}$$

Here, the matrices $\bar{P}_i$ describe a continuous piecewise quadratic Lyapunov function (like the ones we have used in Chapter 4). The parameters of the integral term, $\alpha(t)$ and $\beta(t)$, are piecewise constant and change values when a discrete state transition takes place, *i.e.*,

$$\alpha(t) = \begin{cases} \alpha_{jk} & \text{if } i(t^-) = j \text{ and } i(t) = k \\ \alpha(t^-) & \text{otherwise} \end{cases}$$

and

$$\beta(t) = \begin{cases} \beta_{jk} & \text{if } i(t^-) = j \text{ and } i(t) = k \\ \beta(t^-) & \text{otherwise} \end{cases}$$

In other words, there is one set of parameters $(\alpha_{jk}, \beta_{jk})$ associated to each arc of the transition diagram. Note that the value of $V(t)$ is not uniquely given by $x(t)$ and $i(t)$ but depends on the full history of the trajectory. This contrasts the approach presented in Section 8.2, where $V(t)$ is an explicit function of $(x(t), i(t))$.

Computing Lyapunov Functionals via Convex Optimization

We will now show how the conditions in Proposition 8.1 can be converted into constraints on the parameters of the Lyapunov functional (8.10). To simplify the presentation even further, we will assume that the Lyapunov function part is globally quadratic, *i.e.*, $\bar{P}_i = [I \quad 0]^T P [I \quad 0]$ for all modes.

It is convenient to the Lyapunov function part be positive definite. To guarantee that the Lyapunov functional (8.10) is bounded below, it is then sufficient to require that

1. The integral term remains bounded from below for each fixed $i(t) = i$.
2. The net ammount of the integral term around any cycle of the transition diagram is non-negative.

To deal with the first requirement, assume that there is a transition from mode j to mode k at time t_k. Then, for every $t > t_k$ such that the system remains in mode k we have

$$\int_{t_k}^{t} (\alpha(s) f^T x(s) + \beta(s)) f^T \frac{d}{ds} x(s)\, ds =$$
$$\alpha_{jk}(x(t)^T f f^T x(t) - g_{jk}^2)/2 + \beta_{jk}(f^T x(t) - g_{jk})$$

If $|f^T x|$ can become unbounded in mode k, we must require that $\alpha_{jk} \geq 0$. To this end, we let $I_u \subseteq I$ be the set of modes for which $|f^T x|$ can become unbouded and require that

$$\alpha_{jk} \geq 0 \qquad\qquad \forall k \in I_u \tag{8.11}$$

To satisfy the second requirement, suppose that $x(t)$ hits the transition surface $\mathcal{S}_{jk}$ at time t_k and subsequently hits $\mathcal{S}_{kl}$ at time t_l. Then,

$$\begin{aligned}\int_{t_k}^{t_l} (\alpha(s) f^T x(s) + \beta(s)) f^T \frac{d}{ds} x(s)\, ds &= \int_{g_{jk}}^{g_{kl}} (\alpha_{jk}\sigma + \beta_{jk})\, d\sigma \\ &= \alpha_{jk}(g_{kl}^2 - g_{jk}^2)/2 + \beta_{jk}(g_{kl} - g_{jk})\end{aligned}$$

which is a linear expression in the parameters α_{jk} and β_{jk}. For any cycle in the transition diagram, we can evaluate the net ammount of the integral term similarly. Let $(k_1, k_2, \ldots, k_L, k_1)$ be a sequence of discrete modes that constitute a cycle in the transition diagram. Then, the condition that the ammount of integral around the cycle be non-negative reads

$$\sum_{i=1}^{L} \alpha_{k_i k_{i+1}} \frac{g_{k_{i+1}k_{i+2}}^2 - g_{k_i k_{i+1}}^2}{2} + \beta_{k_i k_{i+1}} (g_{k_{i+1}k_{i+2}} - g_{k_i k_{i+1}}) \geq 0 \tag{8.12}$$

In this summation, subindices should be taken modulo L, *i.e.*, k_{L+1} should be understood as k_1 and k_{L+2} should be interpreted as k_2.

Finally, consider the requirement that $V(t)$ should be decreasing with time. For fixed discrete state $i(t) = k$ and associated parameters $\alpha(t) = \alpha_{jk}$ and $\beta(t) = \beta_{jk}$, the time derivative of the Lyapunov functional is

$$\frac{d}{dt} V(t) = 2x(t)^T P(A_k x(t) + a_k) + \tag{8.13}$$

$$+ 2(\alpha_{jk} f^T x(t) + \beta_{jk}) f^T (A_k x(t) + a_k) \tag{8.14}$$

Here, j denotes the previous discrete state. The time-derivative is quadratic in $x(t)$, and we can use the S-procedure to derive conditions for its negativity for all x that satisfy the mode invariant (similar to what was done in Chapter 4). This condition has to be imposed for all admissible pairs (j, k). We summarize the developments in the following result, which is a simplified version of the results in [73, 71] adopted to the notation of this book.

PROPOSITION 8.2—LAGRANGE STABILITY OF SIMPLE LHDS
Consider the linear hybrid dynamical system (8.1) with parallel transition surfaces (8.9). For each admissible discrete transition $j \to k$, define

$$\bar{P}_{jk} = \begin{bmatrix} I & 0 \end{bmatrix}^T P \begin{bmatrix} I & 0 \end{bmatrix} + \begin{bmatrix} \alpha_{jk} f f^T & \beta_{jk} f \\ \beta_{jk} f^T & 0 \end{bmatrix}$$

If there exists $P = P^T$, $W_{jk} \succeq 0$, α_{jk} and β_{jk} such that

$$P > 0$$

$$\bar{A}_k^T \bar{P}_{jk} + \bar{P}_{jk}\bar{A}_k + \bar{E}_k^T W_{jk} \bar{E}_k < 0 \qquad \forall (j,k) \in T$$

and α_{jk}, β_{jk} satisfy (8.12) and (8.11) then the system is Lagrange stable. □

Note that the above formulation does not single out modes that contain equilibrium points and that the Lyapunov functional have affine terms in all modes. In order to verify the analysis conditions one thus needs to eliminate inherent equality constraints using the technique described in Section 4.12 and solve the resulting optimization problem using a solver that supports equality constraints.

The requirement that the integral term should be non-negative around *every* cycle of the transition diagram can first appear overwhelming since even very simple transition diagrams can admit a huge number of cycles. However, a fundamental result from graph theory (see, *e.g.*, [68, Chapter 4]) states that every cycle can be expressed as the sum of disjoint elementary cycles[1]. Thus, we only need to impose (8.12) for elementary cycles.

The following example, taken from [71], illustrates the approach on a simple system that cannot be analyzed using Theorem 8.1.

EXAMPLE 8.3—LAGRANGE STABILITY OF HYSTERESIS SYSTEM

Consider a linear system in a feedback connection with a hysteresis element as shown in Figure 8.5. Note that the hysteresis element is non-standard, in the sense that the hysteresis loop is clock-wise. We use the numerical values

$$A = \begin{bmatrix} -0.1 & -1 \\ 0 & -0.2 \end{bmatrix} \qquad B = \begin{bmatrix} 0.2 \\ 1 \end{bmatrix} \qquad C = \begin{bmatrix} 1 \\ 0 \end{bmatrix} x$$

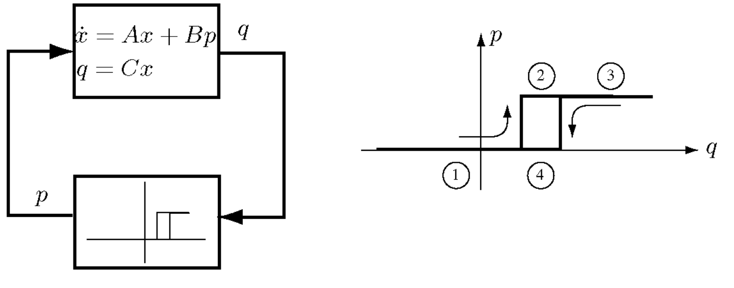

Figure 8.5 Linear system in feedback interconnection with hystersis element.

[1] An elementary cycle is a cycle that does not visit any node (except for the initial and terminal nodes) more than once. The elementary cycles of a directed graph can be computed in polynomial time using, for example, the algorithm described in [156].

The transition diagram for the linear hybrid dynamical system is shown in Figure 8.6, where we have introduced

$$A_1 = A_4 = A \qquad \bar{A}_2 = \bar{A}_3 = \begin{bmatrix} A & B \end{bmatrix}$$
$$\bar{E}_1 = \begin{bmatrix} -C & 1 \end{bmatrix} \qquad \bar{E}_2 = \bar{E}_4 = \begin{bmatrix} C & -1 \\ -C & 2 \end{bmatrix} \qquad \bar{E}_3 = \begin{bmatrix} C & -2 \end{bmatrix}$$

Since $|f^T x|$ can become unbounded in modes 1 and 3, we require that

$$\alpha_{21} \geq 0 \qquad \alpha_{41} \geq 0 \qquad \alpha_{23} \geq 0 \qquad \alpha_{43} \geq 0$$

The transition diagram shows three fundamental cycles:

$$\mathcal{L}_1 = (1, 2, 1) \qquad \mathcal{L}_2 = (3, 4, 3) \qquad \mathcal{L}_3 = (1, 2, 3, 4, 1)$$

However, since $g_{12} = g_{21}$ and $g_{34} = g_{43}$, the net amount of integral term is zero around the first two cycles. For the third cycle, noting that $g_{23} = g_{34}$ and $g_{41} = g_{12}$, the condition that the net amount of integral around the cycle should be non-negative can be simplified to

$$1.5(\alpha_{34} - \alpha_{12}) + (\beta_{34} - \beta_{12}) \geq 0$$

The LMI conditions of Theorem 8.1 have a feasible solution

$$P = \begin{bmatrix} 1.1663 & -1.4149 \\ -1.4149 & 13.7400 \end{bmatrix}$$

and

$$\alpha_{21} = \alpha_{41} = \alpha_{23} = \alpha_{43} = 0.0359 \qquad \alpha_{12} = -0.4922 \qquad \alpha_{34} = -0.1925$$
$$\beta_{21} = \beta_{41} = 11.4197 \qquad \beta_{23} = \beta_{43} = 0 \qquad \beta_{12} = 0.0152 \qquad \beta_{34} = 12.6413$$

which guarantees Lagrange stability of the system. □

8.4 Comments and References

Analysis of Linear Hybrid Dynamical Systems

The area of hybrid systems has attracted a large interest over the last couple of years, and many tools and techniques for analysis and design of hybrid

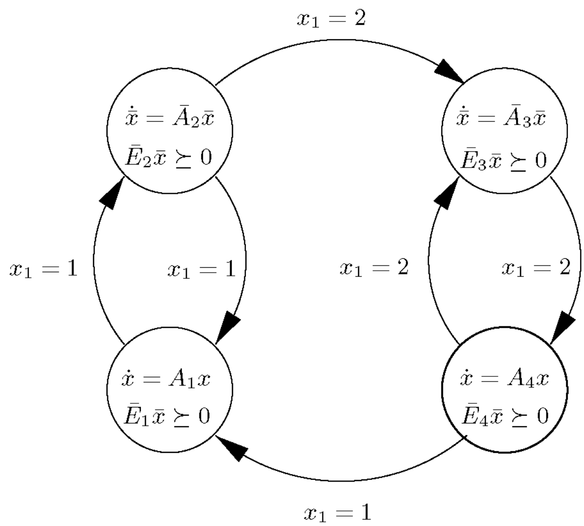

Figure 8.6 Transition diagram for linear system with hysteresis component.

systems have appeared alongside with strong theoretical developments. A complete survey of the field is beyond the scope of this book, but relatively broad expositions can be found in, for example, [201, 135, 158, 52, 4, 5, 121]

We have focused on stability analysis of a particular class of hybrid systems, which we call linear hybrid dynamical systems. In the computer science literature, a linear hybrid system usually refers to a hybrid dynamical system in which *trajectories* of the continuous state in every mode are linear (the continuous dynamics is described by integrators). Our definition is much more general.

Linear hybrid dynamical systems have been studied by several research groups, see *e.g.*, [100, 157, 76, 92]. Our main contribution has been to show how convex optimization can be used to construct piecewise quadratic Lyapunov functions for such systems. This allows computationally efficient analysis of an important class of hybrid systems. The results presented in this chapter first appeared in [100, 102] and similar ideas have been suggested in the independent work [157]. The Lyapunov functional approach was introduced in [73, 71].

LHDS as Hybrid Automota

A general framework for representing autonomous hybrid systems that has gained widespread acceptance is the hybrid automoton, see, *e.g.*, [201]. Many variations of the basic model exist, but the following definition is useful to enable comparisons between linear hybrid dynamical systems and other hybrid system models. A ***hybrid automaton*** H is a collection

$$H = (X, I, f, \text{inv}, \text{jump}, \text{init})$$

where

X is the finite ordered set $X = \{x_1, \dots, x_n\}$ of continuous state variables.

I is the finite set of discrete modes.

f is a function $f : \mathbb{R}^n \times I \mapsto \mathbb{R}^n$ that defines the continuous flow in each discrete mode $i \in I$ through a differential equation $\dot{x} = f(x, i)$.

inv is a set, $\text{inv} \subset \mathbb{R}^n \times I$, called the ***invariant condition*** that describes the possible states (z, i) of the hybrid automaton. For each discrete mode i, the set $\text{inv}(i) = \{z \mid (z, i) \in \text{inv}\}$ is called the mode invariant.

jump is a set-valued function $\text{jump} : \mathbb{R}^n \times I \mapsto P(\mathbb{R}^n \times I)$ called ***the jump condition***. Here $P(\Omega)$ denotes the power set of Ω, *i.e.*, the set of all subsets of Ω. The jump condition specifies if a transition from one discrete mode to another is possible, and what new value sould be assigned to the continuous variable after the jump. It is convenient to separate the jump map into guard conditions

$$G(i(t^-), i(t)) = \{z(t^-) \in \mathbb{R}^n \mid \exists z(t) \in \mathbb{R}^n, (i(t), z(t)) \in \text{jump}(z(t^-), i(t^-))\}$$

and associated jump maps

$$J(i(t^-), i(t), z(t^-)) = \{z(t) \in \mathbb{R}^n \mid (z(t), i(t)) \in \text{jump}(z(t^-), i(t^-))\}$$

init is a set $\text{init} \subset \mathbb{R}^n \times I$, called ***the initial condition***, that defines the possible initial states of H.

We can now discern several features of linear hybrid dynamical systems. First, in each mode i the vector fields are affine in the continuous state vector x. Second, the mode invariants are polyhedral regions in the continuous state space. Third, the jump maps do not alter the continuous state, *i.e.*, $J(i(t^-), i(t), z(t^-)) = z$, and the guards are hyperplanes in the continuous state space.

9

Concluding Remarks

This book has treated analysis and design of piecewise linear control systems. The developments contain two important ingredients: a powerful systems class and a set of computationally efficient tools for system analysis and controller design.

Piecewise linear systems is a natural extension of linear systems and a powerful model class for approximating smooth nonlinear systems. Many of the most common nonlinearities in engineering systems, such as saturations and relays, are piecewise linear. Although a large body of literature exists on analysis of linear systems interconnected with specific components, almost no results exist for general piecewise linear systems. Research in the circuit and systems community has been focused on efficient simulation and static analysis, but have left analysis of the dynamics largely unattended. We have tried to take a broad view of piecewise linear dynamical systems and derived computational analysis tools that are generally applicable.

Our description of piecewise linear systems draws from many sources but it also contains many new developments. We presented a simple matrix representation of polyhedral piecewise linear systems that is convenient for computations. We defined solution concepts and discussed issues related to attractive sliding modes. We extended uncertainty models for linear systems to piecewise linear systems and demonstrated how this allows for less conservative analysis of uncertain nonlinear systems. We also showed how series, parallel, and feedback interconnections of piecewise linear systems are themselves piecewise linear systems. Such properties allow us to construct complex piecewise linear systems from simpler components and open up many interesting possibilities for input-output analysis of piecewise linear systems. Finally, we reviewed memory-efficient representations of piecewise linear systems with continuous right-hand side.

We have provided a wide variety of analysis and design tools that are applicable to general piecewise linear systems. This includes simple procedures for computing equilibrium points equilibrium points and verifying in-

M. Johansson: Piecewise Linear Control Systems, LNCIS 284, pp. 142-143, 2003.

variant sets, but also sophisticated methods for stability analysis, gain computations, and controller design. The main contribution of the book has been to show how piecewise quadratic Lyapunov functions can be computed via convex optimization. This is a novel idea that can be implemented using very efficient computations. The approach performs strictly better than analysis procedures based on the Popov criterion but its main attraction is that it easily deals with multi-variable nonlinearities. Moreover,the piecewise quadratic Lyapunov functions can also be used in dissipativity analysis and the design of optimal control laws. An important feature of the analysis and design procedures in this book is that they provide simultaneous upper and lower bounds on the estimated performance. These bounds can be used to judge the quality of the performance estimate and can also be useful in guiding partition refinements that aim at increasing the flexibility of the Lyapunov function candidate. When the piecewise linear system comes from the approximation of an asymptotically stable smooth nonlinear system, we have shown that such partition refinements will eventually allow us to compute a Lyapunov function using the suggested techniques.

The basic analysis techniques have been extended in many directions. We have shown how smooth nonlinear systems and fuzzy logic systems can be analyzed rigorously in the piecewise linear framework and derived specialized procedures for estimating regions of attractions. We also considered piecewise linear Lyapunov functions, showed how these can be computed via linear programming and suggested a procedure for automatic partition refinements based on linear programming duality. Finally, we extended the stability analysis procedures to a class of hybrid systems with piecewise linear dynamics. These systems, which we have called linear hybrid dynamical systems, can be viewed as piecewise linear systems whose cells overlap on $\mathbb{R}^n$. Changes in the cell index are no longer determined directly by the continuous state, but have to be specified via a set of transition rules that depend on both the current cell index and the continuous state vector.

Although this book has made significant progress towards a useful theory for piecewise linear systems, many problems remain open and many techniques can be improved. One of the strengths of this book is that it does not constrain the class of piecewise linear systems (*e.g.*, to have continuous right-hand side) but presents procedures that are generally applicable. At the same time, this generality is also one of its weaknesses: it is hard to analyze well-posedness, controllability, observability, etc. for general piecewise linear systems. The results presented here would benefit from a more complete system-theoretic understanding, even in a simplified and restricted setting. In addition, we believe that there is much to do on the computational side. By exploiting problem structure and developing specialized optimization methods, we believe that it would be possible to leverage the tools to allow analysis of complex systems with large state-spaces and partitions.

A

Computational Issues

The results derived in the previous chapters allow analysis and design of piecewise linear control systems based on numerical computations. For clarity of presentation, detailed discussions about computational issues have been postponed to this chapter.

While most readers of this book probably have a good knowledge about linear and nonlinear systems theory [110, 176, 189, 116] they may be less familiar with convex sets and convex optimization. Since these concepts play a central role in our approach, we will begin this chapter by an elementary overview of the material on convex sets and convex optimization that is used in this book. The presentation is inspired by the excellent survey [92, Chapter 11] but has been both restricted and extended to suit our purposes.

Our computational analysis procedures have made heavy use of the constraint matrices $\bar{G}_i$, $\bar{E}_i$ and $\bar{F}_i$ without actually going into details of how these can be determined for a given partition. Using the results presented in the first part of this chapter we will show how these matrices can be computed for two important classes of partitions. In both cases, the constraint matrices can be computed efficiently using simple manipulations. We will also demonstrate how constraint matrices for complex partitions can sometimes be computed from the descriptions of simpler partitions.

The S-procedure has played an important role in many computations and the conservatism of our approach is largely dependent on the conservatism of the S-procedure. Our final effort will be to provide some further insight into the role of the S-procedure and to derive two interesting results. Both consider simplex partitions. The first result states that analysis using the polyhedral S-procedure is always less conservative than the use of minimum volume ellipsoids. The second result establishes non-conservatism of the polyhedral S-procedure for simplex cells in $\mathbb{R}^n$ with $n \leq 3$.

M. Johansson: Piecewise Linear Control Systems, LNCIS 284, pp. 144-170, 2003.

A.1 Linear and Semidefinite Programming

Convex optimization is the problem of minimizing a convex function over a convex set. Such problems have many desirable properties (*e.g.*, locally optimal solutions are also globally optimal) and admit an extensive and useful theory. Formulating design problems as convex optimization problems is also practically appealing since these problems can be solved numerically with great efficiency. For many classes of convex optimization problems such as linear programming, semidefinite-programming, etc., public and commercial solvers exist that can exploit problem structure and solve large problem instances very efficiently.

Very little of the general theory for convex optimization is needed in order to understand and apply the results of this book. All problems can be formulated as linear or semidefinite programming problems using classical linear algebra techniques and a handful of key results that are summarized below. Excellent presentations of the general theory and algorithms for convex optimization can be found in, *e.g.*, [204, 210, 19, 28].

Linear Programming

A linear program is a special class of convex optimization problems where the objective function and the constraints are linear

$$\begin{array}{ll} \text{minimize} & c^T x \\ \text{subject to} & a_i^T x \leq b_i \qquad i = 1, \ldots, m. \end{array}$$

The field of linear programming is well-developed, and large-scale linear programs can be solved very efficiently using a variety of public and commercial codes (*e.g.*, [46, 177, 6]). The theoretical aspects of linear programming are also well understood (see, *e.g.*, [182, 21]). The only result that we will need, however, is Farkas' lemma, which allows us to verify that a set of linear inequalities does not admit any solution.

PROPOSITION A.1—FARKAS' LEMMA
Either there exists a vector x such that

$$Ax \preceq b$$

or there exists a vector $y \succeq 0$ such that

$$y^T A = 0 \qquad\qquad y^T b < 0$$

but not both. □

Semidefinite Programming

A semidefinite program is a convex optimization problem with a linear objective and constraints specified in terms of linear matrix inequalities. A ***linear matrix inequality (LMI)*** is an inequality on the form

$$F(x) = F_0 + \sum_{i=1}^{m} x_i F_i \geq 0 \tag{A.1}$$

where $x = (x_1, \ldots, x_m)$ is the variable, $F_i = F_i^T \in \mathbb{R}^{n \times n}$ are given symmetric matrices and the matrix inequality $F(x) \geq 0$ means that $F(x)$ is positive semidefinite. Hence, a ***semidefinite programming (SDP) problem*** takes the form

$$\begin{array}{ll} \text{minimize} & c^T x \\ \text{subject to} & F(x) \geq 0 \end{array}$$

In this book, we will never write LMIs on the standard form (A.1). Rather, we will phrase LMI constraints directly using matrix variables. For example, the constraint that the symmetric matrix variable $X = X^T \in \mathbb{R}^{2\times 2}$ be positive semidefinite can be written in standard form via

$$X = \begin{bmatrix} x_{11} & x_{12} \\ x_{12} & x_{22} \end{bmatrix} = x_{11} \begin{bmatrix} 1 & 0 \\ 0 & 0 \end{bmatrix} + x_{12} \begin{bmatrix} 0 & 1 \\ 1 & 0 \end{bmatrix} + x_{22} \begin{bmatrix} 0 & 0 \\ 0 & 1 \end{bmatrix} \geq 0$$

Clearly, any expression on the form

$$A_0 + \sum_j \sum_i A_{ij}^T X_j B_{ij} + B_{ij}^T X_j A_{ij} \geq 0$$

in an LMI in the symmetric matrix variables X_j and can be put in standard form by first expanding the matrix variables as above, and then pre- and post-multiply the basis matrices with the data matrices A_{ij} and B_{ij}. Today, most semidefinite programming solvers (*e.g.*, [62, 29, 122]) have good interfaces that allow the user to specify LMIs directly in terms of matrix variables.

A useful extension of SDP problems are the *max-det* problems

$$\begin{array}{ll} \text{minimize} & c^T x + \log\det G(x)^{-1} \\ \text{subject to} & G(x) > 0 \\ & F(x) \geq 0 \end{array}$$

which we will encounter when computing optimal ellipsoidal approximations of polytopes. As of today, there is only a few codes (*e.g.*, [206]) that can solve max-det problems.

The following results are useful when formulating and manipulating linear matrix inequalities (see, *e.g.*, [27]).

PROPOSITION A.2—SCHUR COMPLEMENT
Let $Q(x) = Q(x)^T$, $R(x) = R(x)^T$ and $S(x)$ be matrices whose entries depend affinely on the vector x. Then, the LMI

$$\begin{bmatrix} Q(x) & S(x) \\ S(x)^T & R(x) \end{bmatrix} > 0$$

is equivalent to

$$R(x) > 0, \qquad Q(x) - S(x)R(x)^{-1}S(x) > 0$$

□

PROPOSITION A.3—S-PROCEDURE [216, 27]
Let $Q_0, \ldots, Q_p$ be quadratic functions of $x \in \mathbb{R}^n$,

$$Q_i(x) = x^T A_i x + 2b_i^T x + c_i, \qquad i = 0, \ldots, p \tag{A.2}$$

where $A_i = A_i^T$. Consider the following condition

$$Q_0(x) \geq 0 \qquad \text{for all } x \text{ such that } Q_i(x) \geq 0, \quad i = 1, \ldots, p \tag{A.3}$$

A sufficient condition for (A.3) to hold is that there exist positive scalars $\tau_i \geq 0$ such that

$$Q_0(x) \geq \sum_{i=1}^{p} \tau_i Q_i(x) \tag{A.4}$$

Moreover, if $p = 1$ and there exists an x_0 such that $Q_0(x_0) > 0$, then condition (A.4) is also necessary. □

When using the S-procedure in this book, we will re-write the quadratic inequalities (A.2) in matrix format

$$Q_i(x) = \begin{bmatrix} x \\ 1 \end{bmatrix}^T \begin{bmatrix} A_i & b_i \\ b_i^T & c_i \end{bmatrix} \begin{bmatrix} x \\ 1 \end{bmatrix}$$

and then convert (A.4) into an LMI condition using the following result.

PROPOSITION A.4
Let $A_i = A_i^T \in \mathbb{R}^{n\times n}$, $b_i \in \mathbb{R}^n$ and $c_i \in \mathbb{R}$. Then,

$$\begin{bmatrix} x \\ 1 \end{bmatrix}^T \begin{bmatrix} A_i & b_i \\ b_i^T & c_i \end{bmatrix} \begin{bmatrix} x \\ 1 \end{bmatrix} \geq 0 \qquad \forall x \in \mathbb{R}^n \tag{A.5}$$

if and only if

$$\begin{bmatrix} A_i & b_i \\ b_i^T & c_i \end{bmatrix} \geq 0 \tag{A.6}$$

□

Note that the when we replace the non-strict inequalities in Proposition A.3 and Proposition A.4 by strict inequalities, Condition (A.4) is only sufficient for (A.3) and Condition (A.6) is only sufficient for for (A.5). For example, the inequality

$$1 = \begin{bmatrix} x \\ 1 \end{bmatrix}^T \begin{bmatrix} 0 & 0 \\ 0 & 1 \end{bmatrix} \begin{bmatrix} x \\ 1 \end{bmatrix} > 0 \qquad \forall x \in \mathbb{R}^n$$

cannot be verified using an analogue of Proposition A.4 that uses strict inequalities, since the matrix

$$\begin{bmatrix} 0 & 0 \\ 0 & 1 \end{bmatrix}$$

is only positive semidefinite. However, in our experience, the conversion from a strict quadratic inequality to a strict LMI and the use of the strict S-procedure appears to work very well in practice. A more detailed discussion about the specific way in which the S-procedure is used in this book will be given in Section A.5.

A.2 Polyhedra, Polytopes, and Ellipsoids

As stressed in Chapter 2, any analysis procedure for piecewise linear systems must adequately account for both the partition and the dynamics. In this section, we will review the necessary background material on describing and manipulating polyhedra, polytopes and ellipsoids.

The notation in this section is standard with (perhaps) a few exceptions: for a matrix M, $M_\perp$ denotes any full rank matrix such that $M_\perp M = 0$; $M_\mathcal{N}$ is a full rank matrix whose columns form a basis for the null space of M; and $M^\dagger$ denotes the generalized (or Moore-Penrose) inverse of M.

Convex Sets and Their Representations

Convex sets can be represented in many ways. In this book, we make use of two different representations: the *constraint representation*

$$\mathcal{C} = \{x \in \mathbb{R}^n \mid g(x) \leq 0 \wedge h(x) = 0\}$$

and the *constrained parameter representation*

$$\mathcal{C} = \{x = f(\theta) \mid g(\theta) \leq 0 \wedge h(\theta) = 0 \quad \theta \in \mathbb{R}^m\}$$

where $g(\cdot)$ is convex and $h(\cdot)$ is linear.

Hyperplanes and Halfspaces

Definition A.1—Hyperplane
A *hyperplane* in $\mathbb{R}^n$ is a set on the form

$$\partial\mathcal{H} = \left\{x \in \mathbb{R}^n \mid a^T(x - x_0) = 0\right\} \tag{A.7}$$

It can be equivalently represented as

$$\partial\mathcal{H} = \left\{x = x_0 + A\theta \mid \theta \in \mathbb{R}^{n-1}\right\} \tag{A.8}$$

□

Geometrically, the parameter a is the normal vector of the hyperplane, and x_0 is an arbitrary point on the hyperplane, see Figure A.1(left).

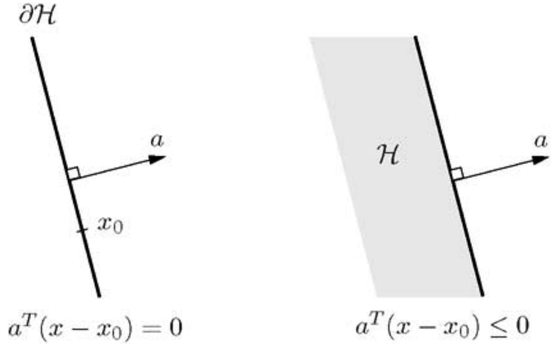

Figure A.1 Hyperplane (left) and halfspace (right).

To convert from the constraint representation (A.7) to the constrained parameter representation (A.8) we let $A = a_{\mathcal{N}}^T$; to pass from (A.8) to (A.7) we let $a^T = A_\perp$. In some cases, the hyperplanes will be given on the form

$$\partial\mathcal{H} = \{x \in \mathbb{R}^n \mid a^T x = b\}$$

We can convert from this representation to (A.7) by setting $x_0 = (a^T)^\dagger b$.

DEFINITION A.2—HALFSPACE
A *halfspace* is a set on the form

$$\mathcal{H} = \big\{x \in \mathbb{R}^n \mid a^T(x - x_0) \leq 0\big\} \tag{A.9}$$

It can be equivalently represented as

$$\mathcal{H} = \big\{x = x_0 + A\theta + at \mid \theta \in \mathbb{R}^{n-1},\ t \geq 0\big\} \tag{A.10}$$

□

To pass from (A.9) to (A.10) we let $A = a_{\mathcal{N}}^T$. To convert from the representation (A.10) to (A.9) we let $a^T = -\mathrm{sign}(A_\perp a)A_\perp$.

Polyhedra and Polytopes

DEFINITION A.3—POLYHEDRON
A *polyhedron* is a set on the form

$$\mathcal{P} = \big\{x \in \mathbb{R}^n \mid a_i^T x \leq b_i,\ i = 1, \ldots, m\big\} = \{x \in \mathbb{R}^n \mid Ax \preceq b\} \tag{A.11}$$

It can be equivalently represented as

$$\mathcal{P} = \{x = V\lambda + W\mu \mid \sum_i \lambda_i = 1,\ \lambda \succeq 0,\ \mu \succeq 0\} \tag{A.12}$$

□

The representation (A.11) describes the polyhedron as the intersection of a finite number of halfspaces while the formulation (A.12) represents the polyhedron as the set addition (Minkowski sum) of the convex hull of the columns of the matrix V and the conic hull of the columns of the matrix W. The columns of V are called the *vertices* of the polyhedron, while the columns of W are called *extreme rays*.

DEFINITION A.4—POLYTOPE
A *polytope* is a bounded polyhedron. It can be represented as

$$\mathcal{P} = \{x \mid Ax \preceq b\} \tag{A.13}$$

or, equivalently,

$$\mathcal{P} = \{x = V\lambda \mid \sum_i \lambda_i = 1,\ \lambda \succeq 0\} \tag{A.14}$$

□

The representation (A.13) is sometimes referred to as the ***halfspace representation***, while (A.14) is called the ***vertex representation***. The conversion between the two representations (A.13) and (A.14) is conceptually simple but computationally hard (see, *e.g.*, [9]). If scalability and generality of an algorithm is important it is usually advised to use only one of the representations and not introduce steps that require the conversion between the two. For small- to moderate-sized problems, the conversion can be made using a variety of publically available codes, see [41, 9] and the references therein.

The ***dimension*** of a polyhedron is the dimension of its affine hull. For example, the dimension of a singleton $\{v\}$ is 0, the dimension of a line segment is 1, etc.

DEFINITION A.5—FACES, FACETS, VERTICES AND EDGES
Let $\mathcal{P}$ be a polyhedron and let $\mathcal{H}$ be a halfspace such that $\mathcal{P} \subset \mathcal{H}$ and $\mathcal{P}_F = \mathcal{P} \cap \mathcal{H} \neq \emptyset$. The polyhedron $\mathcal{P}_F$ is called a *face* of $\mathcal{P}$. Faces of dimension 0 are called *vertices*, faces of dimension 1 are called *edges*, and faces of $\mathcal{P}$ of dimension $\dim(\mathcal{P}) - 1$ are called *facets*, see Figure A.2. □

We note that polytopes defined by few halfspaces might have very many vertices and vice versa (see, *e.g.*, [9]). As a simple example, note that a unit cube in $\mathbb{R}^n$ is defined by $2n$ halfspaces but has 2^n vertices.

Two particular families of polytopes, simplices and parallelotopes, will appear repeatedly in this book. They are defined as follows.

EXAMPLE A.1—SIMPLEX
An *r-simplex* in $\mathbb{R}^n$ is a polytope that can be expressed as

$$\mathcal{P} = \left\{ x = \sum_{i=1}^{r+1} \lambda_i v_i,\ \sum_i \lambda_i = 1,\ \lambda_i \right\}$$

for affinely independent vectors $v_1, \ldots, v_r$. □

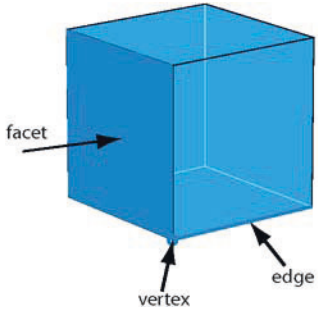

Figure A.2 Facets, edges, and vertices of a polytope.

EXAMPLE A.2—PARALLELOTOPE
An *r-parallelotope* in $\mathbb{R}^n$ is a polyhedron that can be expressed as

$$\mathcal{P} = \left\{x \in \mathbb{R}^n \mid |a_i^T x - b_i| \leq 1, \quad i = 1, \ldots, r\right\}$$

for linearly independent vectors $a_1, \ldots, a_r$. □

Quadratic Sets and Ellipsoids

A natural extension of polyhedra, which are defined by linear inequalities, is to consider sets defined by quadratic inequalities in the following way.

DEFINITION A.6—QUADRATIC SET
A *quadratic set* is a set on the form

$$Q = \left\{x \in \mathbb{R}^n \mid x^T A x + 2b^T x + c \leq 0\right\} \tag{A.15}$$

□

It is often convenient to parameterize the quadratic polynomials as

$$x^T A x + 2b^T x + c = \begin{bmatrix} x \\ 1 \end{bmatrix}^T \begin{bmatrix} A & b \\ b^T & c \end{bmatrix} \begin{bmatrix} x \\ 1 \end{bmatrix}$$

where $A = A^T \in \mathbb{R}^{n \times n}$, $b \in \mathbb{R}^n$ and $c \in \mathbb{R}$.

Quadratic sets can be convex or non-convex, bounded or unbounded, connected or disconnected (see, *e.g.*, [92]). Of particular interest are ellipsoids since they define bounded, connected and convex sets.

DEFINITION A.7—ELLIPSOID
An *ellipsoid* is a set on the form

$$\mathcal{E} = \left\{x \mid (x - x_0)^T P^{-1}(x - x_0) \leq 1\right\} \tag{A.16}$$

with $P = P^T \geq 0$. It can be equivalently represented as

$$\mathcal{E} = \{x = Q\theta + x_0 \mid \|\theta\|_2 \leq 1\} \tag{A.17}$$

□

Geometrically, x_0 is the center of the ellipsoid while the matrix P determines its shape. To be more specific, let $P = U\Lambda U^T$ be an orthonormal eigenvalue decomposition of P, where $U = [u_1 \ \dots \ u_n]$ and $\Lambda = \mathrm{diag}(\lambda_1, \dots, \lambda_n)$ with $\lambda_i \geq 0$ (such a decomposition is always possible when P is positive definite). Then, the semi-axes of $\mathcal{E}$ are given by u_i and their respective lengths are $\sqrt{\lambda_i}$, see Figure A.3.

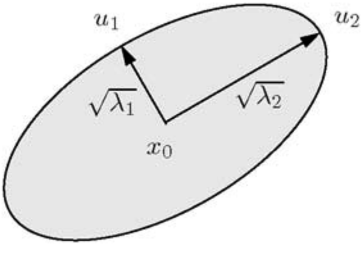

Figure A.3 Center, semi-axes, and semi-axes lengths for an ellipsoid.

We can convert from the representation (A.16) to (A.17) by letting $Q = P^{1/2}$. If the ellipsoid is defined by a set on the form (4.30), then we can pass to the representation (A.16) by letting $P = (b^T A^{-1} b - c)A^{-1}$, $x_0 = -A^{-1}b$. We will also encounter ellipsoids parameterized as

$$\mathcal{E} = \{x \in \mathbb{R}^n \mid \|Cx + d\|_2 \leq 1\}$$

We can pass from the representation (A.17) to this representation by letting $C = Q^{-1}$ and $d = -Q^{-1}x_0$.

In many cases, it is desirable to optimize the "size" of an ellipsoid subject to constraints. A natural measure of size is the volume of the ellipsoid,

$$\operatorname{vol}(\mathcal{E}) = \nu_n \sqrt{\det P}$$

where ν_n is the volume of the unit sphere in $\mathbb{R}^n$. Other measures of size includes the trace of P (which measures the sum of squared semi-axes lengths) and the maximum eigenvalue of P (which measures the maximum semi-axis length).

Containment

A fundamental problem that arises on several occasions in this book (*e.g.*, Section 7.1) is to determine if a convex set contains another convex set. The following two results are then useful.

Proposition A.5—Ellipsoid in Halfspace
The ellipsoid (A.16) is contained in the halfspace (A.9) if and only if

$$a^T x_0 + \sqrt{a^T P a} \leq b \tag{A.18}$$

If the ellipsoid is represented as (A.17), the containment condition is

$$a^T x_0 + \|Qa\|_2 \leq b$$

□

To verify that an ellipsoid $\mathcal{E}$ is contained in a polyhedron $\mathcal{P}$, the containment condition (A.18) must be satisfied for all halfspaces that define $\mathcal{P}$.

Proposition A.6—Quadratic Set in Quadratic Set
Let

$$\mathcal{Q}_i = \left\{ x \in \mathbb{R}^n \mid x^T A_i x + 2b_i^T x + c_i \leq 0 \right\} \qquad i = 1, 2.$$

be two quadratic sets and assume that $\mathcal{Q}_2 \neq \emptyset$. Then $\mathcal{Q}_1 \subset \mathcal{Q}_2$ if and only if

$$\begin{bmatrix} A_2 & b_2 \\ b_2^T & c_2 \end{bmatrix} - \tau \begin{bmatrix} A_1 & b_1 \\ b_1^T & c_1 \end{bmatrix} \leq 0$$

for some positive scalar $\tau \geq 0$. □

Ellipsoidal Approximation of Polytopes

Although we consider polyhedral piecewise linear systems, we have seen that it can sometimes can be useful to use (approximate) ellipsoidal descriptions of the polyhedral cells. For example, in Section 4.9 we demonstrated how ellipsoidal cell boundings allow for faster computations of piecewise quadratic Lyapunov functions, and in Section 6.1 we showed how the use of ellipsoidal cell descriptions enables a convex formulation of the quadratic stabilizability problem for piecewise linear systems. The following results demonstrate how optimal ellipsoidal approximations of polytopes can be computed using convex optimization.

PROPOSITION A.7—ELLIPSOIDAL APPROXIMATION OF A POLYTOPE
Consider the polytope

$$\mathcal{P} = \mathrm{co}\,\{v_1, \ldots, v_m\}$$

The parameters (C, d) that specify the minimum volume ellipsoid

$$\mathcal{E}_{\mathrm{mve}} = \{x \in \mathbb{R}^n \mid \|Cx + d\|_2 \leq 1\}$$

that contains $\mathcal{P}$ can be obtained by solving the max-det problem

$$\begin{array}{ll} \text{minimize} & \log\det C^{-1} \\ \text{subject to} & \begin{bmatrix} I & Cv_i + d \\ v_i^T C^T + d^T & 1 \end{bmatrix} \geq 0 \qquad i = 1, \ldots, m. \\ & C = C^T > 0 \end{array}$$

Moreover, the ellipsoid

$$\mathcal{E}' = \{x \in \mathbb{R}^n \mid \|n(Cx + d)\|_2 \leq 1\}$$

is contained in $\mathcal{P}$. □

The inner ellipsoid obtained by scaling the minimum volume ellipsoid is often called the Löwner-John ellipsoid and the scale factor n can be improved to $\sqrt{n}$ if the polytope is symmetric around its center [105]. When $\mathcal{P}$ is a simplex, we can obtain the minimum volume ellipsoid directly.

PROPOSITION A.8—ELLIPSOIDAL APPROXIMATION OF A SIMPLEX
Let X be an n-simplex in $\mathbb{R}^n$ with vertices v_i, and let $\bar{V} = [\bar{v}_1, \ldots, \bar{v}_{n+1}]$. Then, the minimum volume ellipsoid that contains X is given by

$$\mathcal{E}_{\mathrm{mve}} = \left\{x \in \mathbb{R}^n \;\middle|\; \bar{x}^T(\bar{V}\bar{V}^T)^{-1}\bar{x} \leq 1\right\}$$

□

The analogue result of Proposition A.7 for polytopes in halfspace representation is the following.

PROPOSITION A.9—ELLIPSOIDAL APPROXIMATION OF A POLYTOPE II
Consider the polytope

$$\mathcal{P} = \left\{ x \in \mathbb{R}^n \mid a_i^T x \leq b_i, i = 1, \ldots, m \right\}$$

The parameters (Q, x_0) that specify the maximum volume ellipsoid

$$\mathcal{E}_{\text{MVE}} = \{ x = Qu + x_0 \mid \|u\|_2 \leq 1 \}$$

contained in $\mathcal{P}$ are obtained by solving the max-det problem

$$\begin{array}{ll} \text{minimize} & \log\det Q^{-1} \\ \text{subject to} & \begin{bmatrix} (b_i - a_i^T x_0) I & Q a_i \\ (Q a_i)^T & b_i - a_i^T x_0 \end{bmatrix} \geq 0 \qquad i = 1, \ldots, m. \\ & Q = Q^T > 0 \end{array}$$

Moreover, the ellipsoid

$$\mathcal{E}' = \{ x = nQu + x_0 \mid \|u\|_2 \leq 1 \}$$

contains $\mathcal{P}$. □

Similar to above, the factor n can be replaced by $\sqrt{n}$ if the polytope is symmetric around its center. A drawback with this formulation is that the optimized ellipsoid is *contained* in $\mathcal{P}$ and that the scaled ellipsoid that contains $\mathcal{P}$ is not necessarily very tight.

For the special case of parallelotopes, we can obtain an explicit expression for the minimum volume ellipsoid that contains $\mathcal{P}$.

PROPOSITION A.10—ELLIPSOIDAL APPROXIMATION OF PARALLELOTOPE
Let X be an n-parallelotope in $\mathbb{R}^n$,

$$X = \left\{ x \in \mathbb{R}^n \mid |a_i^T x - b_i| \leq 1, \quad i = 1, \ldots, n \right\}$$

and define

$$\bar{H} = \begin{bmatrix} a_1^T & -b_1 \\ \vdots & \vdots \\ a_n^T & -b_n \end{bmatrix}$$

Then, the minimum volume ellipsoid that contains X is

$$\mathcal{E}_{\text{mve}} = \left\{ x \in \mathbb{R}^n \;\middle|\; \bar{x}^T \bar{H}^T \bar{H} \bar{x} \leq n \right\}$$

□

A.3 Polyhedral Partitions

More complex geometrical structures can be constructed by "gluing" together simple polyhedra, see Figure A.4. In computational geometry and combinatorics, the resulting objects are called ***polyhedral complexes*** (see, *e.g.*, [221]). In our setting it is more natural to adopt a dual view, since the complexes arise from the subdivision of a given set into convex polyhedra. We have called these objects polyhedral partitions, and defined them as follows:

DEFINITION A.8—POLYHEDRAL PARTITION
A ***polyhedral partition*** $X \subseteq \mathbb{R}^n$ is a collection of closed n-dimensional convex polyhedra X_i such that

1. $\cup_{i \in I} X_i = X$
2. the polyhedra have disjoint interior, $\text{int}(X_i) \cap \text{int}(X_j) = \emptyset$ if $i \neq j$
3. the polyhedra only share their common boundaries. In other words, if $X_i \cap X_j \neq \emptyset$, then $X_i \cap X_j$ is a common face of X_i and X_j.

□

In other fields of science, similar objects have been defined under the names ***piecewise linear manifolds*** [2] and, if all polyhedra have the same shape, ***meshes*** (see, *e.g.*, [18]).

In order to represent a polyhedral partition we need to represent the individual polyhedra as well as their topology. The development of efficient data structures for polyhedral partitions is far from trivial and the complexity of the data structure depends on what information we need to be able to access quickly. For example, in some situations we only need to represent the n-dimensional polyhedra and their adjacency relations while in other cases we might need to access definitions and adjacency information of all cell faces (down to edges and vertices). Data structures for efficient representation of polyhedral partitions can be found in, for example, [159, 36, 130].

As we have seen in Section A.2, convex polytopes admit two equivalent representations: they can either be represented as the convex hull of a finite number of points or as the intersection of a finite number of halfspaces. From these two descriptions, two classes of partitions appear particularly natural: one class is the partitions induced by a number of hyperplanes and the other is the partitions induced by a number of points.

Hyperplane Partitions

A ***hyperplane partition*** is a partition which is induced by a number of global hyperplanes. The cells of a hyperplane partition are convex polyhedra that have these hyperplanes as boundaries. Given a set of convex polyhedra, an associated hyperplane partition can be obtained by extending the cell boundaries globally. This extension of boundaries may induce new cells, see Figure A.4. Hence, a partition obtained in this way may have more cells than the number of polyhedra that generated it.

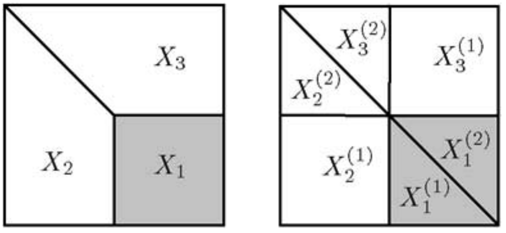

Figure A.4 A hyperplane partition generated from an initial set of polyhedra by extending their boundaries globally.

Simplex Partitions

A *simplex partition* is a partition induced by a number of grid points. Given a set of grid points in $\mathbb{R}^n$, we can form a simplex partition by creating n-simplices that contain exactly $n + 1$ grid points and form a partition. Note that a set of points in $\mathbb{R}^n$ can be combined into many different simplex partitions, see Figure A.5. In other words, a set of vertices does not induce a unique simplex partition (see [124] for further details).

Every convex polytope can be partitioned into simplices by the possible insertion of new vertices. Thus, given some initial polytopic partition, it can always be refined into a simplex partition. A simplex partition derived in this way may then have more cells than the original (non-simplex) partition that generated it, see Figure A.5.

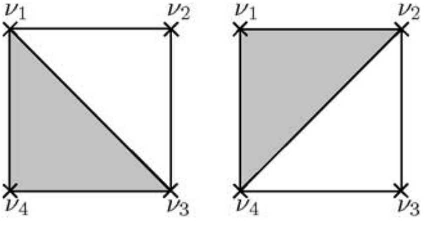

Figure A.5 Two simplex partitions induced by the four vertices ν_k of a square.

A.4 Constraint Matrices

The analysis procedures developed in this book are not restricted to any particular partition type but their formulation do require that some key properties of the partition are expressed in the specific matrix format defined in Section 4.5. The matrices used in different computations are the cell identifiers, $\bar{G}_i$, the cell boundings, $\bar{E}_i$, and the continuity matrices, $\bar{F}_i$. For this parameterization to be useful we need to be able to compute these matrices for a given partition. In this section, we will show how this can be done for hyperplane and simplex partitions.

Cell Identifiers and Cell Boundings

The cell identifiers $\bar{G}_i$ and cell boundings $\bar{E}_i$ are closely related. In fact, the only reason that the cell identifiers cannot be used in the Lyapunov function computations is that they typically do not satisfy the zero interpolation property which is critical for formulating the Lyapunov function search using strict LMIs. The following procedure shows how cell boundings with the zero interpolation property can be computed from the corresponding cell identifiers.

ALGORITHM A.1—FROM CELL IDENTIFIER TO CELL BOUNDING
Let $\{X_i\}_{i\in I}$ be a polyhedral partition with associated cell identifiers $\bar{G}_i$. The corresponding cell boundings can be computed as follows:

if $i \in I_0$, then $\bar{E}_i$ is obtained by deleting all rows of $\bar{G}_i$ whose last entry is non-zero.

if $i \in I_1$ and X_i is unbounded, then $\bar{E}_i$ is obtained by augmenting $\bar{G}_i$ with the row $[0_{1\times n}\ 1]$, otherwise $\bar{E}_i = \bar{G}_i$.

□

It is natural to ask if there is any loss in using cell boundings rather than cell identifiers in conditional analysis of piecewise quadratic functions. The following lemma shows that this is not the case.

LEMMA A.1
Consider the piecewise quadratic function $V(x)$ constructed in Lemma 4.2 and let $\bar{E}_i$ be cell boundings constructed using Algorithm A.1. Then $\bar{E}_i$ have the zero interpolation property, and

$$V(x) > 0 \qquad \text{for } x \in X_i \tag{A.19}$$

if and only if

$$V(x) > 0 \qquad \text{for } \{x \mid \bar{E}_i\bar{x} \succeq 0\} \tag{A.20}$$

□

Proof: See Section B.6.

Since the cell boundings can be computed from the cell identifiers without introducing any conservatism we only need to derive procedures for computing cell identifiers and continuity matrices. We will now show how this can be done for hyperplane and simplex partitions.

Constraint Matrices for Hyperplane Partitions

A hyperplane partition is a partition induced by K hyperplanes,

$$\partial\mathcal{H}_k = \{x \mid h_k^T x + g_k = 0\} \qquad\qquad k = 1, \ldots, K.$$

The partition induced by a saturated linear state feedback, illustrated in Figure 2.1, is a typical example. For convenient representation, we collect all hyperplane data in a hyperplane matrix $\bar{H}$:

$$\bar{H} = \begin{bmatrix} h_1^T & g_1 \\ \vdots & \vdots \\ h_K^T & g_K \end{bmatrix}.$$

We adopt the convention that every hyperplane is defined with $g_k \leq 0$. Each hyperplane induces two closed halfspaces,

$$\begin{aligned} \mathcal{H}_k^+ &= \{x \mid h_k^T x + g_k \geq 0\} \\ \mathcal{H}_k^- &= \{x \mid h_k^T x + g_k \leq 0\} \end{aligned}$$

which we will call the positive and negative induced halfspace of $\partial\mathcal{H}_k$, respectively. The convention $g_k \leq 0$ then implies that $0 \in \mathcal{H}_k^-$ for all k.

Every cell of the partition can be specified by stating whether it belongs to the positive or negative induced halfspace of each hyperplane. Hence, a cell identifier $\bar{G}_i$ for cell X_i can be obtained by multiplying the kth row of $\bar{H}$ with -1 if $X_i \subseteq \mathcal{H}_k^-$ and with $+1$ if $X_i \subseteq \mathcal{H}_k^+$. Note that the resulting cell identifier might have many redundant constraints.

Continuity matrices $\bar{F}_i$ can be computed as follows. Let the kth row of $\bar{F}_i$ be equal to the kth row of $\bar{H}$ if $X_i \subseteq \mathcal{H}_k^+$ and equal to the zero vector otherwise. Since $0 \in \mathcal{H}_k^-$ for all k, this assures that

$$\bar{F}_i \bar{x} = \max\left\{\bar{H}\bar{x}, 0\right\} \qquad\qquad x \in X_i,$$

where $\max(z, v)$ denotes element-wise maximum. This implies that the matrices $\bar{F}_i$ have the zero interpolation property. We summarize the development in the following proposition.

PROPOSITION
A.11—CONSTRAINT MATRICES FOR HYPERPLANE PARTITIONS
Let $\{X_i\}_{i\in I}$ be a hyperplane partition. The matrices $\bar{G}_i$ and $\bar{F}_i$ constructed as above satisfy the conditions (2.4) and (4.14), respectively. Moreover, the matrices $\bar{F}_i$ have the zero interpolation property. □

In order to give the continuity matrices full column rank, we can augment them according to

$$\bar{F}_i = \begin{bmatrix} F_i & f_i \\ I & 0 \end{bmatrix}. \tag{A.21}$$

The constraint matrices for the saturated system given in Example 2.3, Example 4.4 and Example 4.5 were computed using the procedure outlined above and augmented as in (A.21). The following example illustrates the use of the hyperplane matrix when computing the cell identifier for one of the regions.

EXAMPLE A.3—CONSTRAINT MATRICES FOR SATURATED SYSTEM
Consider again the linear system with actuator saturation,

$$\dot{x} = Ax + b\,\mathsf{sat}(k^T x)$$

The hyperplanes induced by the saturation give the hyperplane matrix

$$\bar{H} = \begin{bmatrix} h_1^T & g_1 \\ h_2^T & g_2 \end{bmatrix} = \begin{bmatrix} k^T & -1 \\ -k^T & -1 \end{bmatrix}.$$

Note that $g_k \le 0$ for all k. Consider the cell X_3 corresponding to positive saturation ($k^T x \ge 1$). Since $X_3 \subseteq \mathcal{H}_1^+$ and $X_3 \subseteq \mathcal{H}_2^-$ we can obtain a cell identifier by multiplying the second row of $\bar{H}$ with -1. This gives

$$\widetilde{G}_3 = \begin{bmatrix} k^T & -1 \\ k^T & 1 \end{bmatrix}.$$

As only $\partial\mathcal{H}_1$ is a boundary of X_3, we delete the second row and arrive at

$$\bar{G}_3 = \begin{bmatrix} k^T & -1 \end{bmatrix},$$

which was the cell identifier given in Example 2.3. □

Constraint Matrices for Simplex Partitions

A simplex partition $X \subseteq \mathbb{R}^n$ is induced by a set of points $\{\nu_0, \dots, \nu_K\}$. We will assume that the origin is one of the vertices and, without loss of generality, let $\nu_0 = 0$. Each cell X_i is defined as the convex hull of $n+1$ affinely independent points from this set in such a way that $\{X_i\}_{i \in I}$ form a polyhedral partition of $\overline{\text{co}}\{\nu_0, \dots, \nu_K\}$, see Figure A.6.

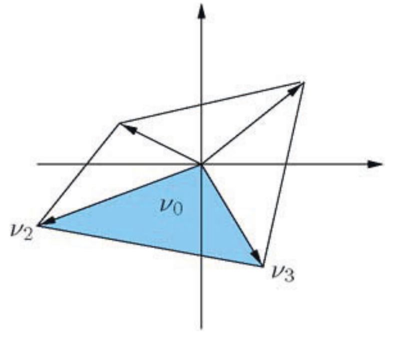

Figure A.6 Simplex partition of state space.

Since cells are represented by the convex hull of their vertices, each $x \in X_i$ can be represented as

$$x = \sum_{k\,:\,\nu_k \in X_i} z_k \nu_k \qquad x \in X_i \tag{A.22}$$

with $z_k \geq 0$, $\sum_k z_k = 1$. The numbers z_k are sometimes called the ***Barycentric coordinates*** of X_i. Since each cell has $n+1$ affinely independent vertices, the Barycentric coordinates are unique and can be obtained by solving

$$\begin{cases} x &= \sum_k \nu_k z_k \\ 1 &= \sum_k z_k \end{cases}$$

If the decomposition (A.22) is used for $x \notin X_i$ then at least one of the Barycentric coordinates will be negative. This indicates that the affine mapping from x to the Barycentric coordinates of X_i qualifies as cell identifier (this is indeed what we will use later).

Similarly, each $x \in X$ can be uniquely represented by a convex combination of *all* vertices of the partition

$$x = \sum_{k=0}^{K} z_k \nu_k \tag{A.23}$$

by letting $z_k = 0$ if $\nu_k \notin X_i$. Clearly, $z_k \geq 0$ for all k and $\sum_k z_k = 1$. Since the partition coordinates are unique for each $x \in X$, the affine mapping from x to $z = [z_0 \ \ldots \ z_K]$ is continuous and can be used for constructing continuity matrices.

To describe the computations we introduce an *extraction matrix* $\mathcal{E}_i \in \mathbb{R}^{(K+1)\times(n+1)}$ as follows: the kth row of $\mathcal{E}_i$ is zero for all k such that $\nu_k \notin X_i$ and the non-zero rows of $\mathcal{E}_i$ are equal to the rows of an identity matrix. The extraction matrix has the property that

$$z(x) = \mathcal{E}_i \tilde{z}_i(x) \qquad\qquad x \in X_i$$

where $\tilde{z}_i$ is the vector of Barycentric coordinates of $x \in X_i$ (the precise ordering of the components of $\tilde{z}_i$ depends on the choice of extraction matrix). Also introduce

$$\bar{\mathcal{V}} = \begin{bmatrix} \nu_0 & \ldots & \nu_K \\ 1 & \ldots & 1 \end{bmatrix}, \tag{A.24}$$

Then, we have

$$\begin{aligned} \bar{x} &= \bar{\mathcal{V}} z = \bar{\mathcal{V}} \mathcal{E}_i \tilde{z}_i \\ z &= \mathcal{E}_i \tilde{z}_i = \mathcal{E}_i (\bar{V} \mathcal{E}_i)^{-1} \bar{x} \end{aligned}$$

The matrix $\bar{\mathcal{V}}\mathcal{E}_i$ is invertible since the vertices of each simplex cell are affinely independent. It turns out that continuity matrices constructed from the mapping $\bar{x} \mapsto z$ does not have the zero interpolation property. However, such matrices can be constructed by simply disregarding the partition coordinate z_0 in the mapping. Thus, we propose to use

$$\bar{F}_i = \begin{bmatrix} 0 & I_K \end{bmatrix} \mathcal{E}_i (\bar{V} \mathcal{E}_i)^{-1} \tag{A.25}$$

which guarantees that

$$\bar{F}_i \bar{x} = \begin{bmatrix} 0 & I_K \end{bmatrix} z = \begin{bmatrix} z_1 & \ldots & z_K \end{bmatrix}^T$$

Since the origin corresponds to $z_0 = 1$ and $z_i = 0$, $i = 1, \ldots, K$ in (A.23), we have $\bar{F}_i [0 \quad 1]^T = 0$ so these matrices do indeed have the zero interpolation property. Cell boundings with the zero interpolation property can be constructed as

$$\bar{E}_i = \mathcal{E}_i^T \begin{bmatrix} 0 \\ \bar{F}_i \end{bmatrix} \tag{A.26}$$

We have the following result.

PROPOSITION A.12—CONSTRAINT MATRICES FOR SIMPLEX PARTITIONS
Let $\{X_i\}_{i\in I}$ be a simplex partition. The matrices $\bar{F}_i$ and $\bar{E}_i$ constructed as in (A.25) and (A.26) have the zero interpolation property and satisfy the conditions (4.14 and (4.19), respectively. □

It can be verified that the cell boundings computed above are equivalent to the ones that are obtained by first computing cell identifiers

$$\bar{G}_i = (\bar{V}\mathcal{E}_i)^{-1}$$

and then applying Algorithm A.1.

The above construction extends straightforwardly to unbounded polyhedra by considering simplices that have vertices "at infinity". In this case every $x \in X_i$ can be written as

$$x = \sum_{k=0}^{q} z_k \nu_k + \sum_{k=q+1}^{K} z_k w_k$$

where $z_k \geq 0$ and $\sum_{k=0}^{q} z_k = 1$. The vectors $\nu_1, \ldots, \nu_q$ are vertices of the polytope, while $w_{q+1}, \ldots, w_K$ define extreme rays. The computations of constraint matrices remain the same and statements above hold true also in this case, provided that each cell has at least one vertex and that we define

$$\bar{\mathcal{V}} = \begin{bmatrix} \nu_0 & \ldots & \nu_q & w_{q+1} & \ldots & w_p \\ 1 & \ldots & 1 & 0 & \ldots & 0 \end{bmatrix}.$$

Building Complex Partitions from Simple Partitions

In the computations above we assumed that the dimension of the partition was the same as the dimension of the state space, *i.e.*, that the partitioning has been done with respect to all state variables. However, when significant nonlinearities are confined to a subset of the states (as in the min-max selector system described in Section 4.6) it can be natural to concentrate the flexibility of the Lyapunov function candidate to these states.

Partitioning a Subset of the State Let $x \in \mathbb{R}^n$ and assume that the partitioning has been performed on the subspace

$$Z = \{z \in \mathbb{R}^q \mid z = Cx\}$$

Then, constraint matrices for the corresponding partition in $\mathbb{R}^n$ can then be constructed by post-multiplying the matrices constructed in $\mathbb{R}^q$ by

$$\bar{N} = \begin{bmatrix} C & 0 \\ 0 & 1 \end{bmatrix}$$

That is, let $\bar{F}_{Zi}$, $\bar{E}_{Zi}$ and $\bar{G}_{Zi}$ be constraint matrices for a polyhedral partition in $\mathbb{R}^q$, let $C \in \mathbb{R}^{q\times(n+1)}$, and let N be defined as above. Then,

$$\bar{F}_i = \bar{F}_{Zi}\bar{N}, \qquad \bar{E}_i = \bar{E}_{Zi}\bar{N}, \qquad \bar{G}_i = \bar{G}_{Zi}\bar{N},$$

are constraint matrices for the corresponding cells in $\mathbb{R}^n$. Moreover, if $\bar{F}_{Zi}$ and $\bar{E}_{Zi}$ have the zero interpolation property, then so have $\bar{F}_i$ and $\bar{E}_i$. This approach was used to construct constraint matrices for the min-max selector system analyzed in Chapter 4. If the constructed continuity matrix does not have full row rank, this can be achieved by the augmentation (A.21).

Creating Cells by Intersecting Partitions Another issue appears when we interconnect two piecewise linear systems for which we have already computed constraint matrices. Let S_x be a piecewise linear component with state vector $x \in \mathbb{R}^{n_x}$ and partition $\{X_i\}_{i\in I}$, and let S_z be a piecewise linear component with state vector $z \in \mathbb{R}^{n_z}$ and partition $\{Z_j\}_{j\in J}$. The interconnected system can then be realized with a state vector $v \in \mathbb{R}^{n_x+n_z}$. The partition of the interconnected system is obtained as the product between the partitions of the components

$$\{X_i\}_{i\in I} \times \{Z_j\}_{j\in J} = \{V_{ij} \mid i \in I, j \in J\}$$

where

$$V_{ij} = \{(x,z) \mid x \in X_i, z \in Z_j\}$$

The corresponding constraint matrices can be constructed by first extending the constraint matrices for the subsystems into $\mathbb{R}^{n_x} \times \mathbb{R}^{n_z}$ (using the technique described above) and then stacking them on top of each other (creating the intersection). Similar to above, if the constraint matrices of the individual components have the zero interpolation property then so have the matrices describing the product partition. This approach was used to construct constraint matrices for the fuzzy system example in Section 7.4.

A.5 On the S-Procedure in Piecewise Quadratic Analysis

The S-procedure plays a crucial role in the piecewise quadratic analysis, as it allows us to verify conditions on the form

$$\bar{x}^T\bar{P}_i\bar{x} > 0 \qquad\qquad \text{for } x \in X_i$$

using semidefinite programming. The conservatism of our approach depends to a large extent on the conservatism of the S-procedure.

The S-procedure has been studied in depth by Yakubovich in the early 70's [216]. To review his key results, let

$$V(x) = \bar{x}^T \bar{P} \bar{x}$$

be a quadratic function, and let

$$\mathcal{E}_i = \{x \mid \bar{x}^T \bar{S}_i \bar{x} \geq 0\} \qquad i = 1, \ldots, m$$

be quadratic sets. Yakubovich established that the condition

$$V(x) \geq 0 \qquad \forall x \in \mathcal{E}_i$$

holds if and only if there exists a non-negative scalar u_i such that

$$\bar{P} - u_i \bar{S}_i \geq 0$$

Clearly, if there exist positive scalars u_i such that

$$\bar{P} - \sum_{i=1}^{m} u_i \bar{S}_i \geq 0 \tag{A.27}$$

then

$$V(x) \geq 0 \qquad \forall x \in \cap_{i=1}^{m} \mathcal{E}_i \tag{A.28}$$

By a simple example Yakubovich proved that the converse is, in general, not true. In other words, there exist quadratic functions $V(x)$ and quadratic sets $\mathcal{E}_i$ such that (A.28) holds but where no solution $u_i \geq 0$ to the LMI (A.27) can be found. Hence, while the S-procedure is a necessary and sufficient condition for positivity of a quadratic function on a quadratic set it is only sufficient for verifying positivity on the intersection of several quadratic sets.

To understand the implications for our approach, let $\bar{e}_{ik}^T$ denote the kth row of $\bar{E}_i$. Then, our use of the S-procedure is a special case of (A.27) since

$$\bar{P} - \bar{E}_i^T U_i \bar{E}_i = \bar{P} - \sum_{j,k} u_{jk} \bar{e}_{ij} \bar{e}_{ik}^T > 0 \tag{A.29}$$

This indicates that the S-procedure is only a sufficient condition for verifying positivity of a quadratic function on a polyhedron. In this section, we will show that our use of the S-procedure is conservative in general, but that no conservatism is introduced for simplex partitions in $\mathbb{R}^n$ with $n \leq 3$.

It is easy to come to the premature conclusion that it is more conservative to use polyhedral cell boundings (for which our use of the S-procedure is only sufficient) than to fix a quadratic cell bounding of the polyhedral region and use this in the LMI computations (so that the S-procedure step itself becomes lossless). We will show that this is, in general, not true. For some important classes of partitions we will be able to prove that the polytopic relaxation is always stronger than quadratic relaxations.

Copositivity and Non-conservatism of the S-Procedure

The problem of verifying positivity of a quadratic form on a polyhedron has a long history with numerous applications in optimization (see, *e.g.*, [48, 167, 89]). Most of the work has been concerned with verification of matrix copositivity. A matrix C is said to be ***copositive*** if $x^T Cx \geq 0$ for all $x \in \mathbb{R}^n_+$. For some time it was conjectured that if C is copositive, then it can be written as the sum of two matrices

$$C = P + N \tag{A.30}$$

where P is positive semidefinite and N has non-negative entries. The following result was proven in [48] (see also [89]).

PROPOSITION A.13—DECOMPOSITION OF COPOSITIVE MATRICES
For dimensions $n \leq 4$, every copositive matrix C can be decomposed as in (A.30). However, indecomposable copositive matrices exist for $n \geq 5$. □

The decomposition (A.30) suggests an immediate test for copositivity: if, for a given matrix C, there exists a matrix N with non-negative entries such that

$$C - N \geq 0 \tag{A.31}$$

then C is copositive. However, as stated in Proposition A.13, this test is only sufficient and there exist copositive matrices for which the test fails. To see the relation to our approach, consider the problem of verifying positivity of $x^T P_i x$ on the positive orthant, for which $\bar{G}_i = [I \quad 0]$ and $E_i = I$. Then, the positivity condition (A.29) reduces to

$$P_i - W_i \geq 0$$

which is identical to (A.31). Hence, by Proposition A.13, there exist quadratic functions that are positive on polyhedra but where this fact cannot be verified using our approach.

Proposition A.13 can also be used to prove that our approach is non-conservative in some cases. In what follows, let X_i be a simplex in $\mathbb{R}^n$ with associated continuity matrix $\bar{F}_i$ and cell bounding $\bar{E}_i$ computed as in Section A.4. Assume that $i \in I_1$ and consider verification of the inequality

$$\bar{x}^T \bar{F}_i^T T \bar{F}_i \bar{x} \geq 0 \qquad\qquad x \in X_i \tag{A.32}$$

Since $i \in I_1$, we have $\bar{E}_i = \bar{G}_i = (\bar{V}\mathcal{E}_i)^{-1}$ and $\tilde{z}_i = \bar{G}_i \bar{x}$ are the Barycentric coordinates of $x \in X_i$. Condition (A.32)is equivalent to

$$\tilde{z}_i^T \mathcal{E}_i^T \begin{bmatrix} 0 & I_K \end{bmatrix}^T T \begin{bmatrix} 0 & I_K \end{bmatrix} \mathcal{E}_i \tilde{z}_i \geq 0 \qquad\qquad \forall\, \tilde{z}_i \in \mathbb{R}_+^{(n+1)} \tag{A.33}$$

i.e., verification of copositivity of $T_i = \mathcal{E}_i^T [0 \;\; I_K]^T T [0 \;\; I_K] \mathcal{E}_i$ (the restriction $\mathbf{1}^T \tilde{z}_i = 1$ can be disregarded due to homogeneity). Proposition A.13 states that for $n \leq 4$, T_i is copositive if and only if there exists a $W_i \succeq 0$ such that

$$T_i - W_i \geq 0. \tag{A.34}$$

This inequality holds if and only if

$$(\bar{V}\mathcal{E}_i)^{-T} T_i (\bar{V}\mathcal{E}_i)^{-1} - (\bar{V}\mathcal{E}_i)^{-T} W_i (\bar{V}\mathcal{E}_i)^{-1} \geq 0$$

which can be reformulated as

$$\bar{F}_i^T T \bar{F}_i - \bar{E}_i^T W_i \bar{E}_i \geq 0.$$

This is a non-strict version of the LMI condition in Theorem 4.1. The following proposition extends the result to strict inequalities and the exact formulation used in Theorem 4.1.

PROPOSITION A.14—NON-CONSERVATISM OF THE S-PROCEDURE
Let $\{X_i\}_{i \in I}$ be a simplex partition in $\mathbb{R}^n$ with $n \leq 3$, and with constraint matrices $\bar{E}_i$ and $\bar{F}_i$ computed as in Section A.4. Then

$$V(x) = \bar{x}^T \bar{F}_i^T T \bar{F}_i \bar{x} > 0 \qquad\qquad \text{for } x \in X_i \backslash \{0\},\ i \in I$$

if and only if there exists matrices W_i with positive entries such that

$$\begin{aligned} F_i^T T F_i - E_i^T W_i E_i &> 0 \qquad\qquad \text{for } i \in I_0 \\ \bar{F}_i^T T \bar{F}_i - \bar{E}_i^T W_i \bar{E}_i &> 0 \qquad\qquad \text{for } i \in I_1 \end{aligned}$$

□

Proof: See Section B.6.

Polyhedral Relaxation is Stronger than Ellipsoidal

In Section 4.9, we illustrated by a simple example how the use of quadratic cell boundings can allow for significant computational savings compared to a formulation based on polyhedral cell boundings. However, as the same example demonstrated, these savings come at the price of increased conservatism in the analysis. The developments in Section A.4 will now allow us to be more precise: we will show that if the piecewise quadratic computations that use the quadratic cell boundings of minimum volume have a solution then so do the computations based on polyhedral cell boundings, while the opposite is not true. This is contrary to a statement in [72, Section 4.1] where it was indicated that computations using ellipsoidal cell boundings would be less conservative than those using polyhedral relaxations since the S-procedure may be lossy when several quadratic terms are used. We have the following result.

PROPOSITION
A.15—POLYHEDRAL RELAXATION IS STRONGER THAN ELLIPSOIDAL
Let X_i be a simplex with associated cell bounding $\bar{E}_i$ (computed as described in Proposition A.12 and Algorithm A.1), and let $\bar{S}_i$ describe the minimal volume ellipsoidal bounding computed using Proposition A.8. Then, if the LMI

$$\bar{P}_i - \tau_i \bar{S}_i > 0 \tag{A.35}$$

has a solution then so has the LMI

$$\bar{P}_i - \bar{E}_i^T W_i \bar{E}_i > 0, \tag{A.36}$$

but there are cases when (A.36) admits a solution while (A.35) does not. □

Proof: See Appendix B.6.

To understand this result better, note that the role of the S-procedure in the verification of the constraint

$$V(x) = \bar{x}^T \bar{P}_i \bar{x} > 0 \qquad\qquad x \in X_i \tag{A.37}$$

is to compute a quadratic set that contains X_i but does not intersect the set $V_i^- = \{x \mid \bar{x}^T \bar{P}_i \bar{x} \leq 0\}$. Clearly, the volume of the covering ellipsoid might have very little to do with this separation. Figure A.7 illustrates this for the specific counter-example used in the proof of Proposition A.15. Here, the minimum volume ellipsoid that contains X_i intersects the set V^- and can therefore not be used to verify the desired inequality. The polyhedral

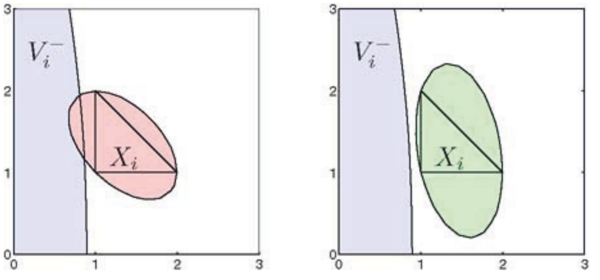

Figure A.7 The counter example in Proposition A.15. The minimal volume ellipsoid fails to separate X_i from V_i^- (left), while optimizing over the covering ellipsoids using the polyhedral formulation easily finds a separating supset.

relaxation, on the other hand, allows a lot of freedom in the optimization and separation can easily be established, see Figure A.7(right).

We conclude this section by stressing that even if the S-procedure is only sufficient when there is more than one quadratic constraint, adding new constraints can never make the inequalities harder to satisfy. On the contrary, adding new terms may allow separations that would otherwise not be possible.

A.6 Comments and References

Computational Tests for Copositivity

We have used the S-procedure to enforce positivity of quadratic functions on polyhedra. It appears that this technique was first used by Shor in the late 80's [187] and similar ideas appear in, for example, [162, 167].

Recently, Parrilo [154] has proposed a set of computational tests for copositivity based on the sums-of-squares decomposition of multivariable polynomials. These tests are formulated in terms of linear matrix inequalities and are strictly stronger than the simple decomposition results used here (for example, the approach can be used to establish copositivity of the matrix used in [48] to prove that the decomposition (A.30) breaks down in $\mathbb{R}^5$). These procedures could potentially be used to formulate stronger, but computationally more demanding, stability tests than the ones developed in this book.

B

Proofs

B.1 Proofs from Chapter 2

PROOF B.1—PROPOSITION 2.1
Consider two polyhedral piecewise linear systems

$$\Sigma_1 : \begin{cases} \dot{x} &= A_i x + a_i + B_i u_1 \\ y_1 &= C_i x + c_i + D_i u_1 \end{cases} \qquad x \in X_i \quad i \in I$$
$$\Sigma_2 : \begin{cases} \dot{z} &= A_j z + a_j + B_j u_2 \\ y_2 &= C_j z + c_j + D_j u_2 \end{cases} \qquad z \in Z_j \quad j \in J$$

where X_i and Z_j denote polyhedral sets, represented as

$$X_i = \{x \mid G_i x + g_i \succeq 0\} \qquad\qquad Z_j = \{z \mid G_j z + g_j \succeq 0\}$$

When we interconnect the systems, we will obtain a partition with cells

$$\widetilde{X}_{ij} = \{(x, z) \mid x \in X_i \wedge z \in Z_j\}$$

which can be represented as

$$\widetilde{X}_{ij} = \left\{ \begin{bmatrix} x \\ z \end{bmatrix} \;\middle|\; \begin{bmatrix} G_i & 0 & g_i \\ 0 & G_j & g_j \end{bmatrix} \begin{bmatrix} x \\ z \\ 1 \end{bmatrix} \succeq 0 \right\} \qquad i \in I, \quad j \in J$$

This gives rise to a partition with $|I| \times |J|$ cells. Within each cell, the dynamics of each subsystem is linear and the dynamics of the interconnected system can be constructed using standard operations for linear systems.

M. Johansson: Piecewise Linear Control Systems, LNCIS 284, pp. 171-184, 2003.

For the series connection, we let $u_2 = y_1$ and obtain

$$\begin{bmatrix} \dot{x} \\ \dot{z} \end{bmatrix} = \left[\begin{array}{c|c|c} A_i & 0 & a_i \\ B_j C_i & A_j & a_j + B_j c_i \end{array}\right] \begin{bmatrix} x \\ z \\ 1 \end{bmatrix} + \begin{bmatrix} B_i \\ B_j D_i \end{bmatrix} u_1 \qquad \begin{bmatrix} x \\ z \end{bmatrix} \in \widetilde{X}_{ij}$$

$$y_2 = \left[\begin{array}{c|c|c} D_j C_i & C_j & c_j + D_j c_i \end{array}\right] \begin{bmatrix} x \\ z \\ 1 \end{bmatrix} + D_j D_i u_1 \qquad \begin{bmatrix} x \\ z \end{bmatrix} \in \widetilde{X}_{ij}$$

The parallel and feedback interconnections follow similarly. □

B.2 Proofs from Chapter 4

PROOF B.2—LEMMA 4.1
The following formula for evaluating a piecewise smooth function $W(t)$ will be useful. Let $W(t)$ be a piecewise smooth function, and let t_k denote the points of discontinuity of $W(t)$. Then,

$$W(t^-) = W(0) + \int_0^t \frac{d}{ds} W(s)\, ds + \sum_{k:t_k<t} \Delta W(t_k) \tag{B.1}$$

where $\Delta W(t_k) = W(t_k^+) - W(t_-^+)$. Obviously, if $W(t)$ is non-increasing, then $\Delta W(t_k) \leq 0$ for all k and we have

$$W(t^-) \leq W(0) + \int_0^t \frac{d}{ds} W(s)\, ds.$$

Let us first consider the case $\alpha > 0$. The inequalities (4.1) and (4.2) imply

$$\frac{d}{dt} V(t) \leq -\gamma \|x(t)\|^p \leq -\frac{\gamma}{\beta} V(t) \qquad \text{a.e.}$$

and multiplication with the positive function $e^{\gamma t/\beta}$ gives

$$e^{\gamma t/\beta}\left(\frac{d}{dt} V(t) + \frac{\gamma}{\beta} V(t)\right) = \frac{d}{dt}\left(e^{\gamma t/\beta} V(t)\right) \leq 0 \qquad \text{a.e.}$$

Letting $W(t) = e^{\gamma t/\beta} V(t)$ and noting that $W(t)$ is non-increasing we have

$$V(t^-)e^{\gamma t/\beta} \leq V(0) + \int_0^t \frac{d}{ds} V(s) e^{\gamma s/\beta}\, ds.$$

The inequality (4.1) and the fact that $V(t)$ is non-negative implies

$$V(t^-)e^{\gamma t/\beta} \leq V(0) - \frac{\gamma}{\beta} \int_0^t V(s) e^{\gamma s/\beta}\, ds \leq V(0)$$

Estimating $V(t^-)$ and $V(0)$ using the lower and upper bounds in (4.2) gives

$$\|x(t)\|^p \leq \frac{\beta}{\alpha} \|x(0)\|^p e^{-\gamma t/\beta}$$

which establishes exponential convergence.
Now, let the maximal α that satisfies (4.2) be negative. This implies that there is a time $t = t_0$ such that $V(t_0) = \alpha \|x(t_0)\| < 0$. Similarly to above, we have

$$V(t^-) \leq V(t_0) + \int_{t_0}^t \frac{d}{ds} V(s)\, ds \leq V(t_0) + \frac{\gamma}{|\alpha|} \int_{t_0}^t V(s)\, ds.$$

Since $V(t)$ is nonincreasing, we have $V(t) \leq V(t_0)$ for $t \geq t_0$ and

$$V(t) \leq \left(1 + (t - t_0)\frac{\gamma}{|\alpha|}\right) V(t_0).$$

Thus, $V(t) \to -\infty$ as $t \to \infty$ and by (4.2) it follows that $\|x(t)\|^p \to \infty$.

□

PROOF B.3—PROPOSITION 4.2

Consider the Lyapunov function candidate $V(x) = x^T P x$. Since P is positive definite, $V(x)$ can be bounded in the sense of Lemma 4.1, Equation (4.2). A solution to the strict inequalities (4.6) implies the existence of a $\gamma > 0$ such that

$$A_i^T P + P A_i + \gamma I \leq 0 \qquad i = 1, \ldots, L.$$

Now, consider the representation (4.5) of the differential inclusion (4.4). For the suggested Lyapunov function, $V(x) = x^T P x$, we have

$$\begin{aligned} \frac{d}{dt} V(x(t)) &= \sum_{i=1}^{L} \lambda_i(t) x(t)^T (A_i^T P + P A_i) x(t) \leq \\ &\leq \sum_{i}^{L} \lambda_i(t)(-\gamma \|x(t)\|_2^2) = -\gamma \|x(t)\|_2^2. \end{aligned}$$

The desired result now follows from Lemma 4.1 by letting the vector norm $\|\cdot\|$ be the two-norm $\|\cdot\|_2$ and by setting $p = 2$. $\square$

PROOF B.4—COROLLARY 4.1

Note that we can write the system (2.3) on the form (4.5) for almost all t by setting $\lambda_i(t) = 1$ if x is in the interior of cell X_i and $\lambda_i(t) = 0$ otherwise. Since trajectories in the sense of Definition 2.1 do not remain on the boundary for any time interval, we do not need to define the dynamics on the cell boundaries. Continuity of $V(x)$ and $x(t)$ implies that $V(t) = V(x(t))$ is continuous for all t. The result now follows from Lemma 4.1.

$\square$

PROOF B.5—PROPOSITION 4.3

If there exist R_i that solve the above inequalities, then for every $P > 0$

$$0 < \text{Tr}\,[P\sum_i (R_i A_i^T + A_i R_i)] = \sum_i \text{Tr}\,[R_i(A_i^T P + P A_i)]$$

Hence, $0 < \text{Tr}\,[R_i(A_i^T P + P A_i)]$ for some i, so $A_i^T P + P A_i$ cannot be negative definite. $\square$

PROOF B.6—LEMMA 4.2

Clearly, $V(x)$ is piecewise quadratic. Continuity of $V(x)$ follows from (4.14). The only obstacle in establishing (4.17) can occur around the origin. However, the zero interpolation property guarantees that $V(x)$ has no affine terms in regions that contain origin, *i.e.*,

$$V(x) = \bar{x}^T \bar{P}_i \bar{x} = \bar{x}^T \bar{F}_i^T T \bar{F}_i \bar{x} = x^T F_i^T T F_i x = x^T P_i x \qquad x \in X_i$$

and the desired result follows. $\square$

PROOF B.7—LEMMA 4.3

A solution to (4.23) guarantees that there exist $\epsilon_i > 0$ such that

$$z^T(\bar{P}_i - \bar{E}_i^T W_i \bar{E}_i)z \geq \epsilon_i z^T z$$

for all $z \in \mathbb{R}^{n+1}$. In particular, for all $\bar{x}$ with $x \in X_i$, a solution implies that

$$V(x) = \bar{x}^T \bar{P}_i \bar{x} \geq \bar{x}^T \bar{E}_i^T W_i \bar{E}_i \bar{x} + \epsilon_i \bar{x}^T \bar{x} > 0 \qquad x \in X_i$$

The last inequality follows from the fact that $\bar{E}_i\bar{x} \succeq 0$ for $x \in X_i$ and that W_i has non-negative entries. Similarly, a solution to (4.22) guarantees that

$$V(x) = x^T P_i x \geq \epsilon_i x^T x \qquad\qquad x \in X_i$$

Thus,

$$\alpha = \inf_{x \neq 0} \frac{V(x)}{\|x\|_2^2}$$

is positive and finite, and satisfies $V(x) \geq \alpha \|x\|_2^2$. □

PROOF B.8—THEOREM 4.1
Consider the Lyapunov function candidate $V(t) = V(x(t))$ defined by (4.24). Since trajectories $x(t)$ in the sense of Definition 2.1 are continuous and piecewise $\mathcal{C}^1$, Lemma 4.2 implies that $V(t)$ constructed in this way is continuous and piecewise $\mathcal{C}^1$. Moreover, according to Lemma 4.2, there exists $\beta > 0$ such that the upper bound of (4.2) in Lemma 4.1 holds. A solution to the inequalities above implies that there exists $\alpha > 0$ and $\gamma > 0$ such that $\alpha\|x(t)\|_2^2 < V(t)$ and $dV(t)/dt < -\gamma\|x(t)\|_2^2$. Hence, exponential convergence follows from Lemma 4.1 with $\|\cdot\| = \|\cdot\|_2$ and $p = 2$. □

PROOF B.9—LEMMA 4.6
We will first prove the following lemma.

LEMMA B.1
The following statements are equivalent

1. $p^T x > 0$ for all x such that $Ex \succeq 0$ and $x \neq 0$.
2. $p \in \mathrm{Int}(\mathcal{K}_E)$ where $\mathcal{K}_E = \{y \mid y = E^T u,\ u \succeq 0\}$
3. There exists a vector $u \succ 0$ such that $p - E^T u = 0$.

□

Proof: Let $\mathcal{K}_E^o$ denote the polar cone of $\mathcal{K}_E$, *i.e.*,

$$\mathcal{K}_E^o = \{x \mid x^T y \leq 0,\ \forall y \in \mathcal{K}_E\}$$

and let $\mathcal{B}$ denote the ball $\mathcal{B} = \{x \mid \|x\| = 1\}$ Then, equivalence of Claim 1 and Claim 2 follows from

$$\begin{aligned}
1 \Leftrightarrow & \; p^T x > 0 && \forall x \in -\mathcal{K}_E^o \backslash \{0\} \\
\Leftrightarrow & \; p^T \frac{x}{\|x\|} && \forall x \in -\mathcal{K}_E^o \backslash \{0\} \\
\Leftrightarrow & \; p^T x > 0 && \forall x \in -\mathcal{K}_E^o \cap \mathcal{B} \\
\Leftrightarrow & \; \exists \epsilon > 0,\, p^T x > \epsilon && \forall x \in -\mathcal{K}_E^o \cap \mathcal{B} \\
\Leftrightarrow & \; p^T x \geq \epsilon \|x\| && \forall x \in -\mathcal{K}_E^o \\
\Leftrightarrow & \; p^T x \geq \epsilon y^T x && \forall x \in -\mathcal{K}_E^o, \forall y \in \mathcal{B} \\
\Leftrightarrow & \; (p - \epsilon y)^T x \geq 0 && \forall x \in -\mathcal{K}_E^o, \forall y \in \mathcal{B}
\end{aligned}$$

Hence, by Farkas' lemma, $p - \epsilon y \in \mathcal{K}_E \; \forall y \in \mathcal{B}$ which implies

$$\Leftrightarrow p \in \mathrm{Int}(\mathcal{K}_E) \qquad\qquad \Leftrightarrow 2.$$

We prove equivalence of Claim 2 and Claim 3 in two steps. First

$$2 \Leftrightarrow p - \epsilon y \in \mathcal{K}_E, \qquad\qquad \forall y \in \mathcal{B}$$

Let $\mathbf{1} = \begin{bmatrix} 1 & \dots & 1 \end{bmatrix}^T$. Then, the statement above implies

$$\begin{aligned}
\Rightarrow & \; p - \epsilon \frac{E^T \mathbf{1}}{\|E^T \mathbf{1}\|} \in \mathcal{K}_E \\
\Leftrightarrow & \; \exists u_0 \geq 0, p - \epsilon \frac{E^T \mathbf{1}}{\|E^T \mathbf{1}\|} = E^T u_0 \\
\Leftrightarrow & \; p = E^T \left(u_0 + \epsilon \frac{\mathbf{1}}{\|E^T \mathbf{1}\|} \right) := E^T u \Leftrightarrow 3
\end{aligned}$$

where $u \succ 0$. Hence Claim 2 implies Claim 3. Conversely,

$$\begin{aligned}
3 \Leftrightarrow & p = E^T u, u \succ 0 \\
\Leftrightarrow & \exists \epsilon > 0, u + \epsilon v \succeq 0 && \forall v \in \mathcal{B} \\
\Leftrightarrow & \exists \epsilon > 0, p + \epsilon E^T v \in \mathcal{K}_E \\
\Leftrightarrow & p + \epsilon E^T v \in \mathcal{K}_E
\end{aligned}$$

and, if E has full column rank,

$$\Rightarrow p \in \mathrm{Int}(\mathcal{K}_E) \Leftrightarrow 2$$

We can now proceed to prove Lemma 4.6. Note that Claim 2 implies Claim 1 trivially, since

$$p^T x = u^T E x \geq 0$$

for $u \succ 0$ and all x with $Ex \neq 0$.

Consider the converse statement. If E has full column rank, then 1⇒ 2 by Lemma B.1. When E does not have full column rank then we can, without loss of generality, assume that E is on the form

$$E = \begin{bmatrix} E_+ & 0 \end{bmatrix}.$$

where E_+ has full column rank. Now, Claim 1 implies that p must be on the form

$$p = \begin{bmatrix} p_+^T & 0 \end{bmatrix}^T.$$

Let $x = \begin{bmatrix} x_+ & x_0 \end{bmatrix}$. Then, we have

$$p_+^T x_+ > 0 \qquad \forall x_+ \text{ with } E_+ x_+ \geq 0,\ x_+ \neq 0$$

and, by Lemma B.1, there exists $u_+ \succ 0$ such that

$$p_+ - E_+^T u_+ = 0$$

Hence Claim 2 follows with $u = \begin{bmatrix} u_+^T & u_0^T \end{bmatrix}^T \succ 0$, with arbitrary but $u_0 \succ 0$.

□

B.3 Proofs from Chapter 5

PROOF B.10—THEOREM 5.1

Let $i(t)$ be chosen so that $x(t) \in X_i$, and let $\bar{P}_i = [\,I \quad 0\,]^T P_i\,[\,I \quad 0\,]$ for $i \in I_0$. It then follows from the matrix inequalities in Theorem 5.1 that

$$0 \geq \begin{bmatrix} \bar{P}_i \bar{A}_i + \bar{A}_i^T \bar{P}_i + \bar{C}_i^T \bar{C}_i + \bar{E}_i^T U_i \bar{E}_i & \bar{P}_i \bar{B}_i \\ \bar{B}_i^T \bar{P}_i & -\gamma^2 I \end{bmatrix} \qquad \forall i \in I.$$

Multiplying from the left and right with $\begin{bmatrix}\bar{x}^T & u\end{bmatrix}$ and removing the non-negative terms $\bar{x}^T\bar{E}_i^T U_i \bar{E}_i \bar{x}$ gives

$$\begin{aligned} 0 &\geq 2\bar{x}^T\bar{P}_i(\bar{A}_i\bar{x}+\bar{B}_iu)+\bar{x}^T\bar{C}_i^T\bar{C}_i\bar{x}-\gamma^2u^Tu = \\ &= \frac{d}{dt}\left(\bar{x}^T\bar{P}_i\bar{x}\right)+\|y\|_2^2-\gamma^2\|u\|_2^2 \end{aligned}$$

Integration from 0 to ∞ gives the desired inequality. □

PROOF B.11—THEOREM 5.2
It follows directly from the two inequalities that

$$0 \geq \bar{P}_i\bar{A}_i+\bar{A}_i^T\bar{P}_i+\bar{Q}_i+\bar{E}_i^TU_i\bar{E}_i, \qquad i\in I.$$

Let $i(t)$ be chosen so that $x(t)\in X_i$. Then, multiplying the above inequality from left and right by $\bar{x}$ and removing nonnegative terms gives

$$0 \geq \frac{d}{dt}(\bar{x}^T\bar{P}_i\bar{x})+\bar{x}(t)^T\bar{Q}_i\bar{x}(t).$$

Integration from $t=0$ to $t=\infty$ gives the desired result.

□

B.4 Proofs from Chapter 6

PROOF B.12—THEOREM 6.3
It follows directly from the matrix inequalities in Theorem 6.3 that

$$0 \leq \begin{bmatrix}\bar{P}_i\bar{A}_i+\bar{A}_i^T\bar{P}_i+\bar{Q}_i-\bar{E}_i^TU_i\bar{E}_i & \bar{P}_i\bar{B}_i \\ \bar{B}_i^T\bar{P}_i & R_i\end{bmatrix} \qquad i\in I$$

Multiplying from left and right by $(\bar{x},u)$ and removing the nonnegative terms including U_i gives

$$\begin{aligned} 0 &\leq 2\bar{x}^T\bar{P}_i(\bar{A}_i\bar{x}+\bar{B}_iu)+\bar{x}^T\bar{Q}_i\bar{x}+u^TR_iu \\ &= \frac{d}{dt}\left(\bar{x}^T\bar{P}_i\bar{x}\right)+\bar{x}^T\bar{Q}_i\bar{x}+u^TR_iu \end{aligned}$$

Integration from 0 to ∞ gives the desired result. □

B.5 Proofs from Chapter 7

PROOF B.13—THEOREM 7.1
Define the function

$$\bar{V}(x) = \bar{p}_i^T \bar{x} \qquad\qquad x \in X_i, \qquad i \in I.$$

Recall that by the construction of the matrices $\bar{F}_i$ for simplex partitions, the entries of t specify the values of $\bar{V}$ at the vertices. More precisely, we have $\bar{V}(0) = 0$ and $\bar{V}(\nu_k) = t_k$. The condtion $0 \prec t \prec 1$ implies that

$$c_1 \|x\|_\infty \leq \bar{V}(x) \leq c_2 \|x\|_\infty$$

for some positive scalars $c_1, c_2 > 0$. Denote the approximation error by

$$\widetilde{a}_i(x) = \begin{bmatrix} f(x) - A_i x - a_i \\ 0 \end{bmatrix} \qquad\qquad x \in X_i, \qquad i \in I.$$

We have

$$\begin{aligned}\frac{d}{dt}\bar{V}(x) &= \bar{p}_i^T f(x) \\ &= \bar{p}_i(\bar{A}_i \bar{x} + \widetilde{a}_i(x)) \\ &< -(\epsilon_i + \delta)\|x\|_\infty + \|t\|_\infty \cdot \|\widetilde{a}_i(x)\|_\infty \\ &\leq -\delta \|x\|_\infty \leq -\delta \bar{V}(x)/c_2.\end{aligned}$$

for some $\delta > 0$. Exponential stability follows. □

PROOF B.14—THEOREM 7.2
By a standard converse Lyapunov theorem, such as Theorem 3.12 in [116], there exists a $\mathcal{C}^1$ Lyapunov function $V(x)$ that satisfies

$$c_1 \|x\|_2^2 \leq V(x) \leq c_2 \|x\|_2^2 \tag{B.2}$$

$$\frac{\partial V}{\partial x} f(x) \leq -c_3 \|x\|_2^2 \tag{B.3}$$

$$\left\| \frac{\partial V}{\partial x} \right\|_2 \leq c_4 \|x\|_2$$

for some positive constants c_1, c_2, c_3 and c_4. The function $V(x)$ can be approximated by a function $\bar{V}$ on the form

$$\bar{V}(x) = \bar{x}^T \bar{P}_i \bar{x} \qquad\qquad x \in X_i, \quad i \in I$$

by letting $\bar{P}_i = \bar{F}_i^T T \bar{F}_i$ with $\bar{F}_i$ computed using Proposition A.12 and

$$T = \begin{bmatrix}1 & \dots & 1\end{bmatrix}^T \begin{bmatrix}V(\nu_1) & \dots & V(\nu_p)\end{bmatrix}/2 + \\ + \begin{bmatrix}V(\nu_1) & \dots & V(\nu_p)\end{bmatrix}^T \begin{bmatrix}1 & \dots & 1\end{bmatrix}/2$$

Then,

$$\bar{V}(\nu_i) = T_{ii} := V(\nu_i) \qquad\qquad i = 1, \dots, p.$$

and $\bar{V}$ and $\partial\bar{V}/\partial x$ become arbitrarily accurate approximations of V and $\partial V/\partial x$ as the partition is refined. Let γ_i be defined by the size of V. For sufficiently small approximation errors ϵ_i inequalities (B.2) and (B.3) imply

$$c_1\|x\|_2^2/2 \le \bar{x}^T \bar{P}_i \bar{x} \le c_2\|x\|_2^2$$
$$\bar{x}^T(\bar{A}_i^T \bar{P}_i + \bar{P}_i \bar{A}_i)\bar{x} \le -2\epsilon_i\gamma_i\|x\|_2^2$$

What remains is to find U_i and W_i with non-negative entries such that (7.6)-(7.9) hold. By the $\mathcal{C}^1$ condition on f it can be assumed without restriction that V and $\bar{V}$ are quadratic and positive definite in a neighbourhood of the origin. Hence, U_i and W_i are not needed and can be put to zero. In the regions that do not contain the origin, $\bar{V}$ is linear, so U_i and W_i exist by Farkas' lemma. □

B.6 Proofs from Chapter A

PROOF B.15—PROPOSITION A.8
We will first establish the following results.

LEMMA B.2
Let $x, z \in \mathbb{R}^n$ and let $x = \bar{\mathcal{T}}\bar{z} = \mathcal{T}z + t$ be an affine bijective map. If

$$\mathcal{E}(\bar{S}_i) = \{z \mid \bar{z}^T \bar{S}_i \bar{z} \le 1\}$$

is the minimal volume ellipsoid that contains the set Z_i, then

$$\mathcal{E}(\bar{\mathcal{T}}^T \bar{S}_i \bar{\mathcal{T}}) = \{x \mid \bar{x}^T \bar{\mathcal{T}}^T \bar{S}_i \bar{\mathcal{T}} \bar{x} \le 1\}$$

is the minimum volume ellipsoid that contains the set

$$X_i = \{x = \bar{\mathcal{T}}\bar{z} \mid z \in Z_i\}.$$

□

Proof: Since the mapping $x = \bar{\mathcal{T}}\bar{z}$, is affine and bijective,

$$\mathcal{E}(\bar{S}_i) \supseteq Z_i \Leftrightarrow \mathcal{E}(\bar{\mathcal{T}}^T\bar{S}_i\bar{\mathcal{T}}) \supseteq X_i.$$

Moreover, if $\mathcal{E}(\bar{S}_i)$ describes an ellipsoid, it can be written as

$$\mathcal{E}(\bar{S}_i) = \{z \mid (z - z_0)^T P^{-1}(z - z_0) \leq 1\}$$

for some x_0 and some $P = P^T > 0$. The volume of $\mathcal{E}(\bar{S}_i)$ is then

$$vol(\mathcal{E}(\bar{S}_i)) = \sqrt{\det P} \cdot V_n$$

where V_n denotes the volume of a unit sphere in $\mathbb{R}^n$. Let

$$\bar{\mathcal{T}} = \begin{bmatrix}\mathcal{T} & \tau\end{bmatrix}.$$

Then, the volume of the transformed ellipsoid is

$$vol(\mathcal{E}(\bar{\mathcal{T}}^T\bar{S}_i\bar{\mathcal{T}})) = \det\mathcal{T}\sqrt{\det P} \cdot V_n.$$

Hence, for a given mapping $\bar{\mathcal{T}}$ the volume is proportional to $\det P$, and the circumscribing ellipsoid of minimal volume can be obtained by optimizing the volume of either $\mathcal{E}(\bar{S}_i)$ or $\mathcal{E}(\bar{\mathcal{T}}^T\bar{S}_i\bar{\mathcal{T}})$.

LEMMA B.3
The minimum volume ellipsoid containing the standard simplex,

$$X_i = \{x \in \mathbb{R}^{n+1} \mid x_k \geq 0, \sum_{k=1}^{n+1} x_k = 1\}$$

is the ball

$$\mathcal{E}^* = \{x \mid x^T x \leq 1, \sum_{k=1}^{n+1} x_k = 1\} \tag{B.4}$$

□

Proof See [98].

Proposition A.8 now follows trivially, since the map $x \mapsto z$ defined by

$$z = \bar{G}_i \bar{x}$$

is a bijective affine map, that transforms an arbitrary simplex in $\mathbb{R}^n$ into a regular simplex in the constraint hyperplane. $\sum_{k=1}^{n+1} z_k = 1$. By virtue of Lemma B.3, the circumscribing ellipsoid with minimal ellipsoid is then the ball (B.4). By virtue of Lemma B.2, the minimal ellipsoid that contains an arbitrary simplex in $\mathbb{R}^n$ is given by

$$\mathcal{E}^* = \left\{ x \mid \bar{x}^T \bar{G}_i^T \bar{G}_i \bar{x} \leq 1 \right\}.$$

This concludes the proof.

□

PROOF B.16—PROPOSITION A.10

Since the minimum volume n-dimensional ellipsoid containing the unit cube

$$X_i = \{x \in \mathbb{R}^n \mid \|x\|_\infty \leq 1\}$$

is the ball $\{x \in \mathbb{R}^n \mid x^T x \leq n\}$, the results follows by direct application of Lemma B.2. □

PROOF B.17—LEMMA A.1

Consider a cell X_i with cell identifier $\bar{G}_i$ partitioned as

$$\bar{G}_i = \begin{bmatrix} G_i & 0 \\ H_i & h_i \end{bmatrix} \tag{B.5}$$

First, consider $i \in I_0$. By deleting all rows whose last entry is non-zero we find the cell identifer

$$\bar{E}_i = \begin{bmatrix} G_i & 0 \end{bmatrix}$$

which clearly has the zero interpolation property. This proves the first claim. Now consider the second claim. The implication (A.20) $\Rightarrow$ (A.19) is immediate since $X_i \subseteq \{x \mid \bar{E}_i \bar{x} \succeq 0\}$. To prove the converse, (A.19) $\Rightarrow$ (A.20), note that since $0 \in X_i$ we must have $h_i \succ 0$ in (B.5). Hence, for every

$x \in \{x \mid \bar{E}_i \bar{x} \succeq 0\}$ there exists some $\epsilon > 0$ such that $\epsilon x \in X_i$. Since V is quadratic we have

$$V(x) > 0 \Rightarrow V(tx) > 0 \qquad \forall t \neq 0$$

In particular, since $V(\epsilon x) > 0$ we have $V(x) > 0$. This proves the second claim. For $i \in I_1$ we simply note that the added constraint $[0 \quad 1]\bar{x} \geq 0$ is satisfied for all $x \in \mathbb{R}^n$ so $X_i = \{x \mid \bar{E}_i \bar{x} \succeq 0\}$ and, hence, (A.19) $\Leftrightarrow$ (A.20). This concludes the proof. □

PROOF B.18—PROPOSITION A.14

As discussed in the text, $V(x) > 0$ for $x \in X_i,\ i \in I$ is equivalent to

$$\widetilde{z}_i^T T_i \widetilde{z}_i > 0 \qquad \widetilde{z}_i \succeq 0 \tag{B.6}$$

where $\widetilde{z}_i = \bar{G}_i \bar{x}$ are the Barycentric coordinates of $x \in X_i$. Let O be a matrix where every entry is unity. Then, this inequality implies that there exists an $\epsilon_i > 0$ such that

$$\widetilde{z}_i^T (T_i - \epsilon_i (I + O)) \widetilde{z}_i \geq 0 \qquad \widetilde{z}_i \succeq 0. \tag{B.7}$$

In fact, since $\widetilde{z}_i^T (O + I) \widetilde{z}_i \geq 0$ on the domain of interest, ϵ_i can be taken as the minimal ϵ_i that satisfies (B.7) on the compact set

$$\{\widetilde{z}_i \mid \|\widetilde{z}_i\|_2 = 1,\ \widetilde{z}_i \succeq 0\}$$

This implies that $T_i - \epsilon_i(I + O)$ is copositive and, by Proposition A.13, there exists $\widetilde{U}_i \succeq 0$ such that

$$T_i - \widetilde{U}_i - \epsilon_i O - \epsilon I \geq 0$$

Let $W_i = \widetilde{U}_i + \epsilon_i O$. Then $W_i \succ 0$, and

$$T_i - W_i \geq \epsilon_i I > 0$$

Pre- and post-multiplication with the full rank matrix $\bar{E}_i$ and invoking the identity $\bar{E}_i^T T_i \bar{E}_i = \bar{F}_i^T T \bar{F}_i$ gives

$$\bar{F}_i^T T \bar{F}_i - \bar{E}_i^T W_i \bar{E}_i > 0$$

For $i \in I_0$, we can follow the lines of Lemma A.1 and establish a similar identity to (B.6) in terms of $\widetilde{z}_i = E_i x$ (the partition coordinates for the non-zero vertices of X_i). The proof then follows similarly.

□

PROOF B.19—PROPOSITION A.15

According to Proposition A.8, the ellipsoidal bounding of a simplex that has minimal volume is given by

$$\bar{S}_i = \begin{bmatrix} 0_{n\times n} & 0 \\ 0_{1\times n} & 1 \end{bmatrix} - \bar{E}_i^T \bar{E}_i$$

Let $\bar{0} = \begin{bmatrix} 0_{1\times n} & 1 \end{bmatrix}$ and $\bar{1} = \begin{bmatrix} 1_{1\times n} & 1 \end{bmatrix}$. From the definition of $\bar{E}_i$ we have

$$\bar{1}^T \bar{E}_i = \bar{0}$$

and thus

$$u_i \bar{S}_i = u_i \bar{E}_i^T (\bar{1}\bar{1}^T - I)\bar{E}_i = \bar{E}_i^T u_i (\bar{1}\bar{1}^T - I)\bar{E}_i$$

which is on the form $\bar{E}_i^T U_i \bar{E}_i$ with $u_{ij} = u_i$ if $i \neq j$ and 0 otherwise. This concludes the first part of the proof. For the second part of the proof, consider the simplex

$$X_i = \left\{ x \,|\, x \in \overline{\text{co}}(\begin{bmatrix} 1 \\ 1 \end{bmatrix}, \begin{bmatrix} 2 \\ 1 \end{bmatrix}, \begin{bmatrix} 1 \\ 2 \end{bmatrix}) \right\}$$

for which we have

$$\bar{E}_i = \begin{bmatrix} -1 & -1 & 3 \\ 1 & 0 & -1 \\ 0 & 1 & -1 \end{bmatrix}, \qquad \bar{S}_i = \begin{bmatrix} 2 & 1 & -4 \\ 1 & 2 & -4 \\ -4 & -4 & 10 \end{bmatrix}.$$

Let

$$\bar{P}_i = \begin{bmatrix} 20 & 0 & 5 \\ 0 & 1 & 0 \\ 5 & 0 & -25 \end{bmatrix}$$

Pre- and postmultiplying the LMI (A.35) by $\bar{z} = \begin{bmatrix} 3 & 6 & 4 \end{bmatrix}^T$ we obtain $-64 - 2u_i$, which is negative for all admissible values of u_i ($u_i \geq 0$). Hence, there is no solution to this LMI. However, for the formulation (A.36), it is straightforward to verify that the choice

$$U_i = \begin{bmatrix} 0 & 20 & 5 \\ 20 & 0 & 20 \\ 5 & 20 & 0 \end{bmatrix}$$

solves the LMI. □

C

Bibliography

[1] J. Åkesson and K. J. Åström. Safe manual control of the Furuta pendulum. In *Proceedings of the IEEE International Conference on Control Applications*, pages 890–895, Mexico City, Mexico, 2001.

[2] E. L. Allgower and K. Georg. Piecewise linear methods for nonlinear equations and optimization. *Journal of Computational and Applied Mathematics*, 124(1–2):245–261, December 2000.

[3] A. A. Andronov and C. E. Chaikin. *Theory of Oscillations.* Princeton University Press, Princeton, NJ, 1949.

[4] P. Antsaklis, editor. *Proceedings of the IEEE, Special Issue on Hybrid Systems: Theory and Applications*, volume 88, 2000.

[5] P. Antsaklis and A. Nerode, editors. *IEEE Transactions on Automatic Control, Special Issue on Hybrid Control Systems*, volume 43, 1998.

[6] EKA Consulting ApS. *The MOSEK Optimization Toolbox for MATLAB: User's guide and reference manual*, 2nd edition, 2001.

[7] K.-E. Årzén, M. Johansson, and R. Babuška. A survey on fuzzy control. Technical report, Esprit LTR project FAMIMO Deliverable D1.1B, 1998.

[8] K. J Åström and T. Hägglund. *PID Controllers: Theory, Design, and Tuning.* Instrument Society of America, Research Triangle Park, NC, 1995.

[9] D. Avis, D. Bremner, and R. Seidel. How good are convex hull algorithms. *Computational Geometry: Theory and Applications*, 7:265–301, 1997.

[10] R. Babuška, H. A. B. te Braake A. J. Krijgsman, and H. B. Verbruggen. Comparison of intelligent control schemes for real-time pressure control. *Control Engineering Practice*, 4(11):1585–1592, 1996.

M. Johansson: Piecewise Linear Control Systems, LNCIS 284, pp. 185-202, 2003.

[11] S. P. Banks and S. A. Khathur. Structure and control of piecewise-linear systems. *International Journal of Control*, 50(2):667–686, 1989.

[12] R. Beard, G. Saridis, and J. Wen. Approximate solutions to the time-invariant Hamilton-Jacobi-bellman equation. *Journal of Optimization Theory and Applications*, 96(3):589–626, 1998.

[13] R. Bellman. *Dynamic Programming*. Princeton University Press, NJ, 1957.

[14] R. Bellman and K. Fan. On systems of linear inequalities in hermitian matrix variables. In V. L. Klee, editor, *Convexity (Volume 7 of Proceedings of Symposia in Pure Mathematics)*, volume 7, pages 1–11. American Mathematical Society, 1963.

[15] A. Bemporad and M. Morari. Control of systems integrating logic, dynamics, and constraints. *Automatica*, 35(3):407–427, March 1999.

[16] A. Bemporad, M. Morari, V. Dua, and E. N. Pistikopoulos. The explicit linear quadratic regulator for constrained systems. *Automatica*, 38(1):3–20, 2002.

[17] M. Berezowski. Method for analyzing global stability of pseudohomogeneous chemical reactors with recycle. *Chemical Engineering Science*, 46(7):1781–1785, 1991.

[18] M. Bern and P. M. Plassmann. Mesh generation. In *Handbook of Computational Geometry*, chapter 6, pages 291–332. Elsevier, 2000.

[19] D. Bertsekas. *Nonlinear Programming*. Athena Scientific, 2nd edition, 1999.

[20] D. P. Bertsekas and J. Tsitsiklis. *Neuro-Dynamic Programming*. Athena Scientific, 1996.

[21] D. Bertsimas and J. Tsitsiklis. *Introduction to Linear Optimization*. Athena Scientific, 1997.

[22] S. A. Billings and W. S. F. Voon. Piecewise linear identification of non-linear systems. *International Journal of Control*, 46:215–235, 1987.

[23] F. Blanchini. Nonquadratic Lyapunov functions for robust control. *Automatica*, 31(3):451–461, 1995.

[24] F. Blanchini. Set invariance in control – a survey. *Automatica*, 35(11):1747–1768, 1999.

[25] F. Blanchini and M. Sznaier. Persistent disturbance rejection via static state feedback. *IEEE Transactions on Automatic Control*, 40(6):1127–1131, 1995.

[26] V. D. Blondel, O. Bournez, P. Koiran, and J. N. Tsitsiklis. The stability of saturated linear systems is undecidable. *Journal of Computer and System Sciences*, 62:442–462, 2001.

[27] S. Boyd, L. El Ghaoui, E. Feron, and V. Balakrishnan. *Linear Matrix Inequalities in System and Control Theory*. SIAM Studies in Applied Mathematics, 1994.

[28] S. Boyd and L. Vandenberghe. Convex optimization with engineering applications. Lecture Notes, Information Systems Laboratory. Stanford University, 2001. `http://www.stanford.edu/class/ee364`.

[29] S. Boyd and S.-P. Wu. *SDPSOL: A Parser/Solver for Semidefinite Programs with Matrix Structure. User's Guide, Version Alpha.* Stanford University, March 1995.

[30] S. Boyd and Q. Yang. Structured and simultaneous Lyapunov functions for system stability problems. 49(6):2215–2240, 1989.

[31] M. S. Branicky. Analysis of continuous switching systems: Theory and examples. In *Proc. American Control Conference*, pages 3110–3114, Baltimore, MD, 1994.

[32] M. S. Branicky. *Studies in Hybrid Systems: Modeling, Analysis and Control.* PhD thesis, Department of Electrical Engineering and Computer Science, M.I.T., Cambridge, MA, 1995.

[33] R. K. Brayton and C. H. Tong. Stability of dynamical systems: A constructive approach. *IEEE Transaction on Circuits and Systems*, 26:224–234, 1979.

[34] R. K. Brayton and C. H. Tong. Constructive stability and asymptotic stability of dynamical systems. *IEEE Transactions on Circuits and Systems*, 27:1121–1130, 1980.

[35] L. Breiman. Hinging hyperplanes for regression, classification, and function approximation. *IEEE Transactions on Information Theory*, 39(3):999–1013, 1993.

[36] E. Brisson. Representing geometric structures in d dimensions: Topology and order. *Discrete and Computational Geometry*, 9:387–426, 1993.

[37] A. E. Bryson. Optimal control – 1950 to 1985. *IEEE Control Systems*, 16(3):26–33, 1996.

[38] H. W. Buurman. *From Circuit to Signal – Development of a Piecewise Linear Simulator*. PhD thesis, Eindhoven University of Technology, Eindhoven, the Netherlands, 1993.

[39] E. B. Castelan and J.-C. Hennet. On invariant polyhedra of continuous-time linear systems. *IEEE Transactions on Automatic Control*, 38:1680–1685, 1993.

[40] M. J. Chien and E. S. Kuh. Solving nonlinear resistive networks using piecewise-linear analysis and simplicial subdivision. *IEEE Trans. Circuits and Systems*, CAS-24:305–317, 1977.

[41] T. Christof and A. Löbel. PORTA: Polyhedron representation transformation algorithm (version 1.3.1). Technical report, Zib, 1997. Available from `http://www.zib.de/Optimization/Software/Porta/`.

[42] L. O. Chua. Section-wise piecewise linear functions. Canonical representation, properties and applications. *Proceedings of the IEEE*, 65:915–929, 1977.

[43] L. O. Chua, C. A. Desoer, and E. S. Kuh. *Linear and Nonlinear Circuits*. McGraw-Hill, New-York, 1987.

[44] L. O. Chua and R. L. P. Ying. Finding all solutions of piecewise-linear circuits. *Circuit Theory and Applications*, 10:201–229, 1982.

[45] M. Corless. Robust stability analysis and controller design with quadratic Lyapunov functions. In Alan S. I. Zinober, editor, *Variable Structure and Lyapunov Control*, Lecture notes in Control and Information Sciences, chapter 9, pages 181–203. Springer Verlag, 1994.

[46] J. Czyzyk, S. Mehrotra, M. Wagner, and S. J. Wright. Pcx user guide (version 1.1). Technical Report OTC 96/01, Optimization Technology Center, 1997.

[47] G. B. Dantzig. Maximizing a linear function of variables subject to linear inequalities. In Tj. C. Koopmans, editor, *Activity Analysis of Production and Allocation*, pages 339–347. Wiley, New York, 1951.

[48] P. H. Diananda. On non-negative forms in real variables some or all which are non-negative. *Proceedings of the Cambridge Philosophical Society*, 58:17–25, 1962.

[49] C. E. T. Dórea and J.-C. Hennet. (A,B)-invariance conditions of polyhedral domains for continuous-time systems. In *Proceedings of the European Control Conference*, 1997.

[50] D. Driankov, H. Hellendoorn, and M. Reinfrank. *An Introduction to Fuzzy Control*. Springer Verlag, 2nd edition, 1996.

[51] V. Einarsson. *Model Checking Methods for Mode Switching Systems*. PhD thesis, Department of Electrical Engineering, Linköping University, Sweden, 2000.

[52] R. J. Evans and A. V. Savkin, editors. *Systems and Control Letters, Special Issue on Hybrid Control Systems*, volume 38, October 1999.

[53] C. Fantuzzi and R. Rovatti. On the approximation capabilities of the homogeneous Takagi-Sugeno model. In *Proceedings of the Fifth IEEE International Conference on Fuzzy Systems*, pages 1067–1072, New Orleans, USA, 1996.

[54] G. Feng, S. G. Cao, N. W. Rees, and C.M. Cheng. Analysis and design of model based fuzzy control systems. In *Proceedings of the sixth IEEE Conference on Fuzzy Systems*, pages 901–906, 1997.

[55] M. Feng and C. J. Harris. Piecewise Lyapunov stability conditions of fuzzy systems. *IEEE Transactions on Systems, Man, and Cybernatics – Part B*, 31(2):259–262, 2001.

[56] G. Ferrari-Trecate, F. A. Cuzzola, D. Mignone, and M. Morari. Analysis and control with performance of piecewise affine and hybrid systems. In *Proceedings of the American Control Conference*, volume 1, pages 200–205, Arlington, Virginia, June 2001.

[57] A. F. Filippov. *Differential Equations with Discontinuous Righthand Sides*. Kluwer Academic Publishers, 1988.

[58] I. Flügge-Lotz. *Discontinuous and Optimal Control*. McGraw-Hill, New York, 1968.

[59] A. M. Foss. Criterion to assess stability of a 'lowest wins' control strategy. *IEEE Proceedings Part D*, 128(1):1–8, 1981.

[60] L. Fridman and A. Levant. Sliding modes of higher order as a natural phenomenon in control theory. In F. Garofalo and L. Glielmo, editors, *Robust Control via Variable Structure & Lyapunov Techniques*, volume 217 of *Lecture Notes in Control and Information Science*, pages 107–133. Springer-Verlag, 1996.

[61] P. Gahinet, P. Apkarian, and M. Chilali. Affine parameter-dependent Lyapunov functions and real parametric uncertainty. *IEEE Transactions on Automatic Control*, 41(3):436–442, 1996.

[62] P. Gahinet, A. Nemirovski, A. J. Laub, and M. Chilali. *LMI Control Toolbox for use with Matlab*. The Mathworks Inc., 1995.

[63] R. Genesio, M. Tartaglia, and A. Vicino. On the estimation of asymptotic stability regions: state of the art and new proposals. *IEEE Transactions on Automatic Control*, 30(8):747–755, 1985.

[64] L. El Ghaoui and V. Balakrishnan. Synthesis of fixed-structure controllers via numerical optimization. In *Proceedings of the 33rd IEEE Conference on Decision and Control*, pages 2678–2683, Lake Buena Vista, FL, 1994.

[65] E. G. Gilbert and K. T. Tan. Linear systems with state and control constraints: the theory and application of maximal output admissible sets. *IEEE Transaction on Automatic Control*, 36(9):1008–1020, 1991.

[66] K. C. Goh, L. Turan, M. G. Safonov, P.Papavassilopoulos, and J. H. Ly. Bi-affine matrix inequality properties and computational methods. In *Proceedings of the American Control Conference*, pages 850–855, Baltimore, MD, 1994.

[67] J. Goncalves. *Constructive Global Analysis of Hybrid Systems*. PhD thesis, Massachusetts Institute of Technology, Cambridge, MA, 2000.

[68] M. Gondran, M. Minoux, and S. Vajda. *Graphs and Algorithms*. John Wiley & Sons, 1984.

[69] P. Gritzmann and V. Klee. On the complexity of some basic problems in computational convexity: II. volume and mixed volumes. Technical Report TR: 94-31, Center for Discrete Mathematics and Theoretical Computer Science (DIMACS), Rutgers University, NJ, 1994.

[70] G. Güzelis and I. Göknar. A canonical representation for piecewise linear affine maps and its application to circuit analysis. *IEEE Trans. Circ. and Syst.*, 38:1342–1354, 1991.

[71] A. Hassibi. *Lyapunov Methods in the Analysis of Complex Dynamical Systems*. PhD thesis, Stanford University, Stanford, California, 2000.

[72] A. Hassibi and S. Boyd. Quadratic stabilization and control of piecewise-linear systems. In *Proceedings of the American Control Conference*, pages 3659–3664, Philadelphia, PA, 1998.

[73] A. Hassibi, S. Boyd, and J. How. A class of Lyapunov functionals for analyzing hybrid dynamical systems. In *Proceedings of the American Control Conference*, pages 2455–2460, San Diego, CA, 1999.

[74] A. Hassibi, J. How, and S. Boyd. A path-following method for solving BMI problems in control. In *Proceedgins of the American Control Conference*, pages 1385–1389, San Diego, CA, 1999.

[75] J. T. Hawkins. Automatic regulators for heating apparatus. *Trans. American Society of Mechanical Engineers*, 9:432, 1887.

[76] K. X. He and M. D. Lemmon. Lyapunov stability of continuous valued systems under the supervision of discrete event transition systems. In *Proceedings of Hybrid Systems: Control and Computation*, volume 1386 of *Lecture Notes in Computer Science*. Springer Verlag, 1998.

[77] S. Hedlund and M. Johansson. A toolbox for computational analysis of piecewise linear systems. In *Proceedings of the European Control Conference*, 1999.

[78] W. P. M. H. Heemels. *Linear Complementary Systems: A Study in Hybrid Dynamics*. PhD thesis, Eindhoven University of Technology, 1999.

[79] W. P. M. H. Heemels, J. M. Schumacher, and S. Weiland. Linear complementarity systems. *SIAM Journal of Applied Mathematics*, 60:1234–1269, 2000.

[80] W. P. M. H. Heemels, B. De Schutter, and A. Bemporad. Equivalence of hybrid dynamical models. *Automatica*, 37(7):1085–1091, 2001.

[81] D. Hill and P. Moylan. The stability of nonlinear dissipative systems. *IEEE Transactions on Automatic Control*, 21:708–711, 1976.

[82] H. Hindi and S. Boyd. Analysis of linear systems with saturation using convex optimization. In *Proceedings of the 37th IEEE Conference on Decision and Control*, volume 1, pages 903–908, 1998.

[83] A. P. Horisberger and P. R. Bélanger. Regulators for linear, time invariant plants with uncertain parameters. *IEEE Transactions on Automatic Control*, 21:705–708, 1976.

[84] C. S. Hsu. A theory of cell to cell mapping of dynamical systems. *Journal of Applied Mechanics*, 47, 1980.

[85] T. Hu, Z. Lin, and B. M. Chen. An analysis and design method for linear systems subject to actuator saturation and disturbance. In *Proceedings of the American Control Conference*, pages 725–729, Chicago, IL, 2000.

[86] T. Hu, L. Qiu, and Z. Lin. Stabilization of LTI systems with planar anti-stable dynamics using saturated linear feedback. In *Proceedings of the 37th IEEE Conference on Decision and Control*, pages 389–394, Tampa, FL, 1998.

[87] J.-I. Imura and A. van der Schaft. Characterization of well-posedness of piecewise linear systems. *IEEE Transactions on Automatic Control*, 45(9):1600–1619, 2000.

[88] M. Iri. A method of multi-dimensional linear interpolation. *J. Inform. Processing Soc. of Japan*, pages 211–215, 1967.

[89] D. H. Jacobson. *Extensions of Linear-Quadratic Control Theory*. Springer Verlag, 1980.

[90] M. R. James. Recent developments in nonlinear H_∞ control. In *Proceeding of the IFAC Symposium on Nonlinear Control System Design, NOLCOS'95*, Lake Tahoe, 1995.

[91] M. R. James and S. Yuliar. Numerical approximation of the H_∞ norm for nonlinear systems. *Automatica*, 31(8):1075–1086, 1995.

[92] M. Jirstrand. *Constructive Methods for Inequality Constraints in Control*. PhD thesis, Department of Electrical Engineering, Linköping University, Sweden, 1998.

[93] T. A. Johansen. Computation of Lyapunov functions for smooth nonlinear systems using convex optimization. *Automatica*, 36(11):1617–1626, 2000.

[94] T. A. Johansen and B. A. Foss. Operating regime based process modeling and identification. *Computers and Chemical Engineering*, 21:159–176, 1997.

[95] K. H. Johansson. *Relay feedback and multivariable control*. PhD thesis, Department of Automatic Control, Lund Institute of Technology, Sweden, 1997.

[96] M. Johansson. Analysis of piecewise linear systems via convex optimization – a unifying approach. In *Proceedings of the 1999 IFAC World Congress*, Beijing, China, 1999.

[97] M. Johansson. *Piecewise Linear Control Systems*. PhD thesis, Department of Automatic Control, Lund Institute of Technology, Sweden, 1999.

[98] M. Johansson, A. Ghulchak, and A. Rantzer. Improving efficiency in the computation of piecewise quadratic Lyapunov functions. In *Proceedings of the 7th IEEE Mediterranean Conference in Control and Automation*, Haifa, Israel, June 1999.

[99] M. Johansson, J. Malmborg, A. Rantzer, B. Bernhardsson, and K.-E. Årzén. Modeling and control of fuzzy, heterogeneous and hybrid systems. In *Proceedings of the SiCiCa 1997*, Annecy, France, June 1997.

[100] M. Johansson and A. Rantzer. Computation of piecewise quadratic Lyapunov functions for hybrid systems. Technical Report ISRN-TFRT-7459, Department of Automatic Control, Lund Institute of Technology, Sweden, June 1996.

[101] M. Johansson and A. Rantzer. Computation of piecewise quadratic Lyapunov functions for hybrid systems. In *Proceedings of the 1997 European Control Conference*, Brussels, Belgium, July 1997.

[102] M. Johansson and A. Rantzer. Computation of piecewise quadratic Lyapunov functions for hybrid systems. *IEEE Transactions on Automatic Control*, 43(4):555–559, April 1998. Special issue on Hybrid Systems.

[103] M. Johansson, A. Rantzer, and K.-E. Årzén. Piecewise quadratic stability of affine sugeno systems. In *Proceedings of the 7th IEEE Initernational Conference on Fuzzy Systems, Fuzz-IEEE*, Anchorage, USA, May 1998.

[104] M. Johansson, A. Rantzer, and K.-E. Årzén. Piecewise quadratic stability of fuzzy systems. *IEEE Transactions on Fuzzy Systems*, 1999.

[105] F. John. Extremum problems with inequalities as subsidary conditions. In *Studies and Essays presented to R. Courant on his 60th birthday, January 8, 1948*, pages 187–204. Interscience Publ. Inc., New York, 1948.

[106] U. Jönsson. *Robustness Analysis of Uncertain and Nonlinear Systems.* PhD thesis, Department of Automatic Control, Lund Institute of Technology, Sweden, 1996.

[107] P. Julián. *A High Level Canonical Piecewise Linear Representation: Theory and Applications.* PhD thesis, Universidad Nacional del Sur, Bahia Blanca, Argentina, 1999.

[108] P. Julián, M. Jordan, and A. Desages. Canonical piecewise-linear approximation of smooth functions. *IEEE Transactions on Circuits and Systems – I: Fundamental Theory and Applications*, 45(5):567–571, May 1998.

[109] C. Kahlert and L. O. Chua. A generalized canonical piecewise linear representation. *IEEE Trans. Circ. Syst.*, 37:373–382, 1990.

[110] T. Kailath. *Linear Systems.* Prentice-Hall, Englewood Cliffs, N.J., 1980.

[111] R. E. Kalman. Phase-plane analysis of automatic control systems with nonlinear gain elements. *Trans. AIEE Part II: Applications and Industry*, 73:383–390, 1954.

[112] R. E. Kalman. Contributions to the theory of optimal control. *Bol. de Soc. Math. Mexicana*, page 102, 1960.

[113] M. Kantner. Robust stability of piecewise linear discrete time systems. In *Proceedings of the American Control Conference*, 1997.

[114] N. Karmarkar. A new polynomial-time algorithm for linear programming. *Combinatorics*, 4:373–395, 1984.

[115] T. A. M. Kevenaar, D. M. W. Leenaerts, and W. M. G. van Bokhoven. Extensions to Chua's explicit piecewise-linear function descriptions. *IEEE Transactions on Circuits and Systems*, 41:308–314, 1994.

[116] H. K. Khalil. *Nonlinear Systems.* Prentice Hall, Upper Saddle River, N.J., second edition, 1996.

[117] H. Kiendl. Calculation of the maximum absolute values of dynamical variables in linear control systems. *IEEE Transactions on Automatic Control*, 27(1), 1980.

[118] H. Kiendl and J. J. Rüger. Stability analysis of fuzzy control systems using facet functions. *Fuzzy Sets and Systems*, 70:275–285, 1995.

[119] E. Kim. A new approach to numerical stability analysis of fuzzy control systems. *IEEE Transactions on Systems, Man, and Cybernetics – Part C*, 31(1):107–113, 2001.

[120] A. Kitahara, A. Sato, M. Hoshino, N. Kurihara, and S. Shin. LQG based electronic throttle control with a two degree of freedom structure. In *Proceedings of the 35th IEEE Conference on Decision and Control*, Kobe, Japan, 1996.

[121] H. Kwakernaak, S. Morse, C. Pantelides, S. Sastry, and H. Schumacher, editors. *Automatica, Special Issue on Hybrid Systems*, volume 35, April 1999.

[122] Y. Labit, D. Peaucelle, and D. Henrion. SeDuMi interface 1.02: a tool for solving LMI problems with SeDuMi. Technical Report 01616, LAAS, Toulouse, France, 2001.

[123] J. P. LaSalle. Some extensions of Liapunov's second method. *IRE Transactions on Circuit Theory*, CT-7(4):520–527, 1960.

[124] C. W. Lee. Subdivisions and triangulations of polytopes. In Jacob E. Goodman and Joseph O'Rourke, editors, *Handbook of Discrete and Computational Geometry*, chapter 14, pages 271–290. CRC Press LLC, 1997.

[125] K. K. Lee and A. Arapostathis. On the controllability of piecewise-linear hypersurface systems. *System & Control Letters*, 9:89–96, 1987.

[126] D. M. W. Leenaerts. Further extensions to Chua's explicit piecewise linear function descriptions. *International Journal Circuit Theory and Application*, 24:621–633, 1996.

[127] D. M. W. Leenaerts and W. M. G. Bokhoven. *Piecewise Linear Modeling and Analysis.* Kluwer, Dordrecht, The Netherlands, 1998.

[128] C. A. Lehalle and R. Azencott. Piecewise affine neural networks and nonlinear control. In *Proceedings of the 8th International Conference on Neural Networks*, volume 2, pages 633–638, 1998.

[129] B. Lenze. On constructive one-sided spline approximation. In C. K. Chui, L. L. Schumaker, and J. D. Ward, editors, *Approximation Theory VI*, volume 2, pages 383–386. Academic Press, 1989.

[130] P. Lienhardt. Subdivisions of n-dimensional spaces and n-dimensional generalized maps. In *Proceedings of the fifth annual symposium on Computatoinal geometry*, pages 228–236, Saarbruchen, West Germany, June 1989.

[131] P. Lötstedt. Mechanical systems of rigid bodies subject to unilateral constraints. *SIAM Journal on Applied Mathetmatics*, 42:281–296, 1982.

[132] A. Lure and V. Postnikov. On the theory of stability of control systems. *Prikl. Mat. i Mekh*, pages 3–13, 1944.

[133] A. M. Lyapunov. *The general problem of the stability of motion (in Russian)*, volume Collected Works II. Kharkov Mathematical Society, 1892.

[134] A. M. Lyapunov. The general problem of the stability of motion (translated into English by A. T. Fuller). *Int. Journal of Control*, 55:531–773, 1992. Also published as a book by Taylor & Francis, London.

[135] J. Lygeros, G. Pappas, and S. Sastry. An introduction to hybrid systems modeling, analysis and control. In *Preprints of the First Nonlinear Control Network Pedagogical School*, pages 307–329, Athens, Greece, 1999.

[136] J. Malmborg. *Analysis and Design of Hybrid Control Systems.* PhD thesis, Department of Automatic Control, Lund Institute of Technology, Sweden, 1998.

[137] J. Malmborg and J. Eker. Design and implementation of a hybrid control strategy. *IEEE Control Systems Magazine*, 19(4):12–21, 1999.

[138] A. Megretski, C.-Y. Kao, U. Jönsson, and A. Rantzer. IQCβ: A collection of Matlab routines for robustness analysis. Available from http://www.mit.edu/people/ameg.

[139] A. Megretski and A. Rantzer. System analysis via integral quadratic constraints. *IEEE Transactions on Automatic Control*, 47(6):819–830, 1997.

[140] A. N. Michel, B. H. Nam, and V. Vittal. Computer generated Lyapunov functions for interconnected systems: Improved results with application to power systems. *IEEE Transactions on Circuits and Systems*, 31:189–198, 1984.

[141] D. Mignone, G. Ferrari-Trecate, and M. Morari. Stability and stabilization of piecewise affine and hybrid systems: An LMI approach. In *Proceedings of the 39th IEEE Conference on Decision and Control*, volume 1, pages 504–509, Sydney, Australia, December 2000.

[142] A. P. Molchanov and E. S. Pyatnitskii. Lyapunov functions that specify necessary and sufficient conditions for absolute stability of nonlinear systems III. *Automation and Remote Control*, 47:620–630, 1986.

[143] E. F. Mulder and M. V. Kothare. Synthesis of stabilizing anti-windup controllers using piecewise quadratic Lyapunov functions. In *Proceedings of the American Control Conference*, pages 3249–3243, Chicago, Il, 2000.

[144] R. Murray-Smith and T. A. Johansen (Eds.). *Multiple Model Approaches to Modelling and Control.* Taylor and Francis, London, 1997.

[145] A. Nakamura and N. Hamada. Nonlinear dynamical system identification by piecewise-linear system. In *Proceedings of the 1990 IEEE International Symposium on Circuits and Systems*, pages 1454–1457. IEEE, 1990.

[146] Y. Nesterov and A. Nemirovski. *Interior point polynomial methods in convex programming*, volume 13 of *Studies in Applied Mathematics.* SIAM, Philadelphia, 1993.

[147] Y. Ohta, H. Imanishi, L. Gong, and H. Haneda. Computer generated Lyapunov functions for a class of nonlinear systems. *IEEE Transactions on Circuits and Systems – I*, 40(5):343–354, 1993.

[148] Y. Ohta, T. Nonomura, H. Imanishi, and H. Haneda. Computer generation of Lyapunov functions and estimation of stability region. *Electronics and Communications in Japan, Part 3: Fundamental Electronic Science*, 77(4):44–54, 1994.

[149] T. Ohtsuki and N. Yoshida. DC analysis of nonlinear networks based on generalized piecewise-linear characterization. *IEEE Tran. Circuit Theory*, CT-18:146–151, 1971.

[150] A. Olas. On robustness of systems with structured uncertainties. In *Proc. 4th Workshop on Control Mechanics*, University of Southern California, 1991.

[151] S. M. Omohundro. The Delauney triangulation and function learning. Technical report, International Computer Science Institute, Berkeley, CA, 1990.

[152] M. A. Pai and C. L. Narayana. Finite regions of attraction for multi-nonlinear systems and its application to power-system stability problem. *IEEE Transactions on Automatic Control*, 21(5):716–721, 1976.

[153] P. Painlevé. Sur les lois du frottemont de glissement. *C. R. Acad. Sci.*, 121:112–115, 1895.

[154] P. Parrilo. *Structured Semidefinite Programs and Semialgebraic Geometry Methods in Robustness and Optimization.* PhD thesis, California Institute of Technology, Pasadena, California, 2000.

[155] S. Pastore and A. Premoli. Polyhedral elements: A new algorithm for capturing all the equilibrium points of piecewise-linear circuits. *IEEE Trans. Circuits. Syst.*, 40:124–131, 1993.

[156] K. Paton. An algorithm for finding a fundamental set of cycles of a graph. *Comm. ACM*, 12(9):514–518, 1969.

[157] S. Pettersson. *Modelling, Control and Stability Analysis of Hybrid Systems.* Licentiate thesis, Chalmers University of Technology, 1996.

[158] S. Pettersson. *Analysis and Design of Hybrid Systems.* PhD thesis, Department of Signals and Systems, Chalmers University of Technology, Gothenburg, Sweden, 1999.

[159] N. B. O. L. Pettit. *Analysis of Piecewise Linear Dynamical Systems.* Research Studies Press Ltd. / John Wiley & Sons Limited, 1995.

[160] C. Pittet, S. Tarbouriech, and C. Burgat. Stability regions for linear systems with saturating controls via circle and Popov criteria. In *Proceedings of the 36th IEEE Conference on Decision and Control*, volume 5, pages 4518–4523, 1997.

[161] A. Polański. On infinity norms as Lyapunov functions for linear systems. *IEEE Transactions on Automatic Control*, 40(7):1270–1274, 1995.

[162] S. Poljak, F. Rendl, and H. Wolkowicz. A recipe for best semidefinite relaxation for $(0,1)$-quadratic programming. Technical Report CORR 94-7, University of Waterloo, 1994.

[163] V. M. Popov. Absolute stability of nonlinear systems of automatic control. *Automation and Remote Control*, 22:857–875, 1962. Russian original in August 1961.

[164] V. M. Popov. *Hyperstability of Control Systems.* Springer Verlag, New York, 1973.

[165] H. M. Power and A. C. Tsoi. Improving the predictions of the circle criterion by combining quadratic forms. *IEEE Transactions on Automatic Control*, 18(1):65–67, 1973.

[166] E. S. Pyatnitskii and V. I. Skorodinskii. Numerical methods of Lyapunov function construction and their application to the absolute stability problem. *System. Control Letters*, 2(2):130–135, 1982.

[167] A. J. Quist, E. De Klerk, C. Roos, and T. Terlaky. Copositive relaxation for general quadratic programming. *Optimization methods and software*, 9:185–208, 1998.

[168] A. Rantzer. Dynamic programming via convex optimization. In *Preprints of the 14th World Congress of IFAC*, volume D, pages 491–496, Beijing, P. R. China, 1999.

[169] A. Rantzer and M. Johansson. Piecewise linear-quadratic optimal control. In *Proceedings of the American Control Conference*, Albaquerque, NM, 1997.

[170] A. Rantzer and M. Johansson. Piecewise linear-quadratic optimal control. *IEEE Transactions on Automatic Control*, 45(4):629–637, 2000.

[171] L. Rodrigues, A. Hassibi, and J. P. How. Stability and control of piecewise-affine systems with multiple equilibria. Research report, Stanford University, September 1999.

[172] L. Rodrigues, A. Hassibi, and J. P How. Output feedback controller synthesis for piecewise-affine systems with multiple equilibria. In *Proceedings of the American Control Conference*, pages 1784–1789, Chicago, Il, 2000.

[173] J. Roll. Robust verification and identification of piecewise affine systems. Licentiate thesis, Deparmtent of Electrical Engineering, Linköping University, Sweden, 2001.

[174] B. G. Romanchuk. Computing regions of attraction with polytopes: planar case. *Automatica*, 32(12):1727–1732, 1996.

[175] W. Rudin. *Principles of Mathematical Analysis*. McGraw-Hill, 3rd edition, 1976.

[176] W. J. Rugh. *Linear System Theory*. Prentice-Hall, Englewood Cliffs, N.J., 1993.

[177] ILOG SA. *ILOG Cplex 7.0, User's Manual*, 2000.

[178] A. Saberi, Z. Lin, and A. R. Teel. Control of linear systems with saturating actuators. *IEEE Transactions on Automatic Control*, 41(3):368–378, 1996.

[179] A. Saraf, G. Deodhare, and D. Ghose. Synthesis of nonlinear controller to recover an unstable aircraft from poststall regime. *Journal of Guidance Control and Dynamics*, 22(5):710–717, 1999.

[180] C. Scherer and S. Weiland. Linear matrix inequalities in control. DISC (Dutch graduate school in control) Lecture Notes, 1997.

[181] A. Schrijver. *Theory of Integer and Linear Programming*. Wiley, Chichester, 1986.

[182] A. Schrijver. *Theory of Linear and Integer Programming*. Wiley, 1986.

[183] B. De Schutter and T. van den Boom. On model predictive control for max-min-plus-scaling discrete event systems. *Automatica*, 37(7):1049–1056, 2001.

[184] J. W. Schwartz. Piecewise linear servomechanisms. *AIEE Transactions*, 72:401–405, 1953.

[185] A. L. Schwarz. *Theory and Implementation of Numerical Methods Based on Runge-Kutta Integration for Solving Optimal Control Problems*. PhD thesis, University of California at Berkeley, 1996.

[186] J. Shamma. Optimization of the l^∞-induced norm under full state feedback. *IEEE Transaction of Automatic Control*, 41(4):533–544, 1996.

[187] N. Z. Shor. Quadratic optimization problems. *Soviet Journal of Computer and Systems Sciences*, 25(6):1–11, 1987.

[188] A. Skeppstedt, L. Ljung, and M. Millnert. Construction of composite models from observed data. *International Journal of Control*, 55:141–152, 1992.

[189] J.-J. Slotine and W. Li. *Applied Nonlinear Control*. Prentice-Hall, Englewood Cliffs, N.J., 1991.

[190] O. Slupphaug. *On Robust Constrained Nonlinear Control and Hybrid Control: BMI and MPC-based State-Feedback Schemes*. PhD thesis, Department of Engineering Cybernetics, Norwegian University of Science and Technology, Trondheim, Norway, October 1998.

[191] E. D. Sontag. Nonlinear regulation: The piecewise linear approach. *IEEE Transactions on Automatic Control*, 26:346–358, 1981.

[192] J. M. Sousa, R. Babuška, and H. B. Verbruggen. Fuzzy predictive control applied to an air-conditioning system. *Control Engineering Practice*, 5(10):1395–1406, 1997.

[193] D. D. Sworder. Feedback control of a class of linear systems with jump parameters. *IEEE Transactions on Automatic Control*, 14(1):9–14, 1969.

[194] T. Takagi and M. Sugeno. Fuzzy identification of systems and its applications to modeling and control. *IEEE Transactions on Systems, Man and Cybernetics*, 15(1):116–132, 1985.

[195] K. Tanaka, T. Ikeda, and H. O. Wang. Robust stabilization of a class of uncertain nonlinear systems via fuzzy control: quadratic stabilizability, H_∞ control theory and linear matrix inequalities. *IEEE Transactions on Fuzzy Systems*, 4(1):1–13, 1996.

[196] H. D. Tuan, P. Apkarian, S. Hosoe, and H. Tuy. D.C. optimization in robust control: fesibility problems. *International Journal of Control*, (73):89–104, 2000.

[197] V. I. Utkin. *Sliding Modes in Control and Optimization*. Springer-Verlag, 1992.

[198] W. M. G. van Bokhoven. *Piecewise Linear Modelling and Analysis*. Kluwer Techische boeken, Deventer, the Netherlands, 1981.

[199] A. J. van der Schaft. L_2-gain analysis of nonlinear systems and nonlinear state feedback H_∞ control. *IEEE Transactions on Automatic Control*, 37(6), 1992.

[200] A. J. van der Schaft and H. Schumacher. Complementary modeling of hybrid systems. *IEEE Transactions on Automatic Control*, 43(3):483–490, 1998.

[201] A. J van der Schaft and H. Schumacher. *An Introduction to Hybrid Dynamical Systems*. Number 251 in Lecture Notes in Control and Information Sciences. Springer Verlag, 2000.

[202] A. J. van der Schaft and J. M. Schumacher. The complementary-slackness class of hybrid systems. *Mathematics of Control, Signals and Systems*, 9:266–301, 1996.

[203] J. H. van Schuppen. A sufficient condition for controllability of a class of hybrid systems. In T. A. Henzinger and S. Sastry, editors, *Hybrid systems: computation and control*, number 1386 in Lecture Notes in Computer Science, pages 374–383. Springer Verlag, 1998.

[204] J van Tiel. *Convex Anaysis: An Introductory Text*. John Wiley & Sons, 1984.

[205] L. Vandenberghe and S. Boyd. A polynomial-time algorithm for determining quadratic Lyapunov functions for nonlinear systems. In *Proceedings of the European Conference of Circuit Theory and Design*, pages 1065–1068, Davos, Switzerland, August 1993.

[206] L. Vandenberghe, S. Boyd, and S.-P. Wu. Determinant maximization with linear matrix inequality constraints. *SIAM Journal on Matrix Analysis and Applications*, 19(2):499–533, 1998.

[207] L. Vandenberghe, B. L. De Moor, and J. Vanderwalle. The generalized linear complementarity problem appliced to the complete analysis of resistive piecewise-linear circuits. *IEEE Trans. Circuits. Syst.*, 36:1382–1391, 1989.

[208] V. M. Veliov and M. I. Krastanov. Controllability of piecewise linear systems. *System & Control Letters*, 7:335–341, 1986.

[209] L.-X. Wang. *Adaptive Fuzzy Systems and Control*. Prentice Hall, 1994.

[210] R. Webster. *Convexity*. Oxford Science Publications, 1994.

[211] J. C. Willems. The least squares stationary optimal control and the algebraic Riccati equation. *IEEE Transactions on Automatic Control*, 16(6):621–634, 1971.

[212] J. C. Willems. Dissipative dynamical systems, part I: General theory; part II: Linear systems with quadratic supply rates. *Arch. Rational Mechanics and Analysis*, 45(5):321–393, 1972.

[213] G. F. Wredenhagen and P. R. Belanger. Piecewise-linear LQ control for systems with input constraints. *Automatica*, 30(3):403–416, 1994.

[214] S.-P. Wu and S. Boyd. Design and implementation of a parser/solver for SDPs with matrix structure. In *Proc. of IEEE Conf. on Computer Aided Control System Design*, 1996.

[215] V. A. Yakubovich. The method of matrix inequalities in the theory of stability of nonlinear control systems, Part I-III. *Avtomatika i Telemechanika*, 1964. 25(7):1017-1029, 26(4):577-599, 1964, 26(5): 753-763, 1965, (English translation in Autom. Remote Control).

[216] V. A. Yakubovich. S-procedure in nonlinear control theory. *Vestnik Leningrad University*, pages 62–77, 1971. (English translation in Vestnik Leningrad Univ. 4:73-93, 1977).

[217] T. Yamaguchi, K. Shishida, S. Tohyama, and H. Hiari. Mode switching control design with initial value compensation and its application to head positioning control on magnetic disk drives. *IEEE Transactions on Industrial Electronics*, 43(1):65–73, 1996.

[218] G. Zames and P. L. Falb. Stability conditions for systems with monotone and slope-restricted nonlinearities. *SIAM Journal of Control*, 6(1):89–108, 1968.

[219] J. Zhao. *System Modeling, Identification and Control using Fuzzy Logic.* PhD thesis, Université Catholique de Louvain, Belgium, 1995.

[220] K. Zhou, K. Glover, and J.C. Doyle. *Robust and Optimal Control.* Prentice Hall, NJ, 1995.

[221] G. M. Ziegler. *Lectures on Polytopes.* Springer-Verlag, 1994.